MEASUREMENT OF RADIATION DAMAGE IN CERAMICS AND ITS APPLICATION TO AGE DETERMINATION.

An Abstract of a Thesis submitted for the Degree of Doctor of Philosophy in the University of Oxford.

BODLEIAN LIBRARY OXFORD
DEPOSITED
THESIS
30.IV.66

Hilary Term, 1965

Michael Stanley Tite,
Christ Church.

ABSTRACT

The effects of high energy radiation on ancient ceramics, as observed through the measurement of the resulting thermoluminescence, is reported and the possibility of using thermoluminescence measurements to determine the age of the ceramics is investigated.

The radiation effects considered are the filling of existing electron and hole traps and the creation of new traps since a knowledge of the relative importance of these two effects is essential for age determination. Trap filling and trap creation are investigated principally by means of rate curves (i.e. the plot of the thermoluminescence acquired versus the radiation dose). Evidence for trap creation is forthcoming in the case of X-rays and alpha particles but not in the case of beta particles.

The fact that the X-ray rate curves can be resolved into saturating and linearly increasing components provides the first indication that X-rays create new electron and hole traps in addition to filling those already present. However this result is not conclusive since a linearly increasing component can arise from the filling of traps with a very low capture cross-section. The increase in the saturation level observed for samples, which are pre-irradiated with X-rays and then thermally bleached, provides more conclusive evidence for trap creation by X-rays. It is shown that the measurement of the saturation level after pre-irradiation and thermal bleaching is necessary since the susceptibility to small X-ray doses is increased as a result of competition phenomena, in addition to any increase occurring as a result of trap creation.

The competition phenomena are investigated in more detail using beta particles. A model involving high temperature traps, which are not bleached by heating to 600°C and which have a high capture cross-section compared to traps associated with the 20-500°C range, is proposed to explain these competition phenomena. This model also provides an explanation for the non-linearity of the beta particle rate curves observed for small radiation doses.

The alpha particle rate curves can, in some temperature regions, be resolved into saturating and linearly increasing components while, in other regions, the thermoluminescence reaches a maximum value and with further irradiation decreases continuously. Again the form of the rate curves does not, by itself, prove that trap creation is occurring but conclusive evidence is provided, as in the case of X-rays, by pre-irradiation experiments. On the basis of the simple model which is proposed, approximate quantitative agreement is obtained between the pre-irradiation experiments and the alpha particle rate curves.

By comparing the slope of the linearly increasing component of the alpha particle rate curves with the saturation level, it is shown that, for typical pottery, the number of new traps created since firing, by the natural radioactivity of the sherd, is small compared to the number of traps already existing. In addition there is no obvious method of distinguishing these newly-created traps from the remainder since annealing also produces changes in the luminescence efficiency of the material. Hence it is seen that age determination, based on the number of traps created since firing, is not

practical and that the only approach available is through the measurement of the number of traps filled since firing.

In determining the age of the pottery from the number of traps filled, the susceptibility (i.e. the number of traps filled per unit of absorbed energy) of the sherd to alpha, beta and gamma radiation must be measured. Since the filled traps cannot be emptied without changing the luminescence efficiency of the sherd, measurements are made on the untreated sherd. The resulting inaccuracies introduced into the value obtained for the susceptibility, because of the non-linearity of the rate curves, are discussed. Because of the short range of the alpha particles, it is difficult to obtain a value for the relative susceptibility to alpha and beta particles. Irradiations using a solution of Ra^{224} in alcohol show that the alpha particle susceptibility is less than that for the beta particles by a factor of approximately 10. Further evidence for this low alpha particle susceptibility is provided by the age determination results themselves.

It is noted that for successful age determination measurements, based on the number of traps filled, the glow curves (i.e. the plot of the thermoluminescence emitted versus temperature) must be measured in nitrogen otherwise spurious thermoluminescence, not due to radiation-filled traps, appears. It is further noted that, after grinding, the sample must not be exposed to light otherwise the thermoluminescence is bleached. This method of age determination also depends on the fact that the high temperature traps, at least, have not been thermally bleached during the centuries of burial. It is shown by trap depth measurements and thermal bleaching experiments on

artificially irradiated samples that this assumption is justified for traps associated with the 350-500°C range.

An age determination programme using seven groups of sherds of known archaeological age is described. The beta particle susceptibility is measured and on the basis of the Ra^{224} results, the alpha particle susceptibility is assumed to be one tenth of this. This assumption provides an absolute age for the sherds in approximate agreement with the archaeological age whereas, if the alpha and beta particle susceptibilities are assumed equal, the absolute age obtained is approximately one fifth of the archaeological age. These results show that thermoluminescence measurements, based on the number of traps filled since firing, provide an essentially valid method of age determination and considering the possible sources of error, the agreement obtained is remarkable. However it appears, at the moment, that the non-uniform rate of acquisition of thermoluminescence constitutes an insuperable barrier to more precise age determination by this technique.

MEASUREMENT OF RADIATION DAMAGE IN CERAMICS AND ITS APPLICATION TO AGE DETERMINATION

A Thesis submitted for the Degree of Doctor of Philosophy in the University of Oxford.

Hilary Term, 1965

Michael Stanley Tite,
Christ Church.

TABLE OF CONTENTS

		Page No.
INTRODUCTION		1
PART I		
CHAPTER 1	PRELIMINARY RESULTS	6
1.1.	Natural thermoluminescence	6
1.1.1.	Correction for grinding and gas adsorption	9
1.2.	Susceptibility	10
1.3.	Radiation dose	11
1.4.	Specific thermoluminescence	11
CHAPTER 2	APPARATUS	15
2.1.	Heating system	15
2.1.1.	Temperature lags	16
2.1.2.	Servo-system for fast heating apparatus	18
2.1.3.	Slow heating apparatus	19
2.2.	Measurement of light output	21
2.2.1.	Reduction of black body radiation	22
2.2.2.	Theoretical value for black body radiation	23
2.2.3.	Accuracy of light measurements	25
2.2.4.	Linearity of response of the photomultiplier	29
CHAPTER 3	GLOW CURVE THEORY	31
3.1.	Glow curve theory	32
3.1.1.	Monomolecular process	33
3.1.2.	Bimolecular process	34
3.2.	Trap depths and half-lives	35
3.2.1.	"Initial rise" method	36
3.2.2.	"Peak shift" method	38
3.3.	Wavelength of thermoluminescence	40
3.3.1.	Measurement of optical spectrum	41
3.4.	Nature of traps	43
3.4.1.	Limestone	48
3.4.2.	Quartz	50
3.5.	Conclusions	51
PART II		
CHAPTER 4	RADIATION EFFECTS - REVIEW	52
4.1.	Theory for production of atomic displacements	53
4.1.1.	Interaction of incident particles	55
4.1.2.	Behaviour of primary recoils	57
4.1.3.	Total number of displacements	57

		Page No.
4.1.4.	Displacements due to natural radioactivity	59
4.1.5.	Displacements due to alpha sources	59
4.2.	Changes in physical properties	61
4.2.1.	Structural changes	61
4.2.2.	Electronic changes	63
4.2.3.	Annealing experiments	66
4.3.	Thermoluminescence measurements	67
4.3.1.	Rate curve theory	68
4.3.2.	Comparison of thermoluminescence and optical absorption	71
4.4.	Thermoluminescence from ceramics	72
CHAPTER 5	MEASUREMENT OF RADIATION DAMAGE TRAPS	75
5.1.	Determination of trap concentration	75
5.1.1.	X-irradiation	75
5.1.2.	Ultra-violet light	77
5.1.3.	Beta-irradiation	78
5.2.	Annealing experiments	79
5.2.1.	Annealing to 600°C in air and nitrogen	81
5.2.2.	Annealing to 900°C in air	82
5.2.3.	Thermally stable samples of sherd r	84
5.3.	Conclusions	85
CHAPTER 6	X-IRRADIATION	86
6.1.	Thermal bleaching of X-irradiated sherds	88
6.1.1.	Comparison with X-ray rate curves	89
6.2.	Rate curves for thermally stable samples of sherd r	92
6.3.	Optical bleaching experiment	94
6.4.	Conclusions	95
CHAPTER 7	BETA IRRADIATION	97
7.1.	Non-linearity of beta particle rate curves	98
7.2.	Thermal bleaching - "Forman effect"	99
7.3.	Age determination	102
7.3.1.	Thermal bleaching to 170°C	104
CHAPTER 8	ALPHA IRRADIATION	106
8.1.	Preliminary results	107
8.2.	Radiation bleaching	109
8.3.	Comparison of rate curves	114
8.4.	Thermal and optical bleaching	117
8.4.1.	Sherd r	117
8.4.2.	Limestone extraction from sherd k	119

Page No.

8.5. Thermal bleaching of stabilised samples of sherd r 122
8.6. Use of Ra^{224} solution 125
8.7. Dependence on the strength of the alpha sources 126
8.8. Conclusions 128
8.1.1. Comparison with X-rays 130
8.1.2. Age determination 131

CHAPTER 9 COMPARISON OF TRAP FILLING BY DIFFERENT TYPES OF RADIATION 134
9.1. Comparison of alpha and beta particle glow curves 134
9.1.1. Surface traps 135
9.1.2. Optical absorption 136
9.1.3. Change in shape with radiation dose 137
9.2. Relative trap filling efficiency 138
9.2.1. Radiation doses 139
9.2.2. Comparison of alpha (Po^{210} source) and beta radiation 142
9.2.3. Comparison of alpha (Ra^{224} soln.) and beta radiation 143
9.2.4. Comparison of gamma and beta radiation 145
9.2.5. Age determination 146

PART III

CHAPTER 10 SPURIOUS THERMOLUMINESCENCE 148
10.1. Glow curves in air - preliminary measurements 148
10.1.1. Triboluminescence 149
10.1.2. Gas adsorption 150
10.1.3. Chemiluminescence 150
10.1.4. Discussion 151
10.2. Measurements at a reduced pressure 152
10.3. Glow curves in nitrogen 154
10.3.1. Glow curves in nitrogen - effect of cooling conditions 155
10.3.2. Discussion 157
10.4. Age determination 159
10.4.1. Spurious thermoluminescence in nitrogen 160
10.4.2. Effect of grinding 161

CHAPTER 11 THERMAL AND OPTICAL BLEACHING 164
11.1. Thermal bleaching 164
11.1.1. Thermal bleaching at 135°C and 195°C 165
11.2. Optical bleaching 167

		Page No.
CHAPTER 12	AGE DETERMINATION RESULTS	170
12.1.	Depth studies	172
12.2.	Technique	175
	12.2.1. Preparation of sample	175
	12.2.2. Measurement of thermoluminescence	176
	12.2.3. Susceptibility	177
	12.2.4. Natural radiation dose	179
12.3.	Specific thermoluminescence	182
	12.3.1. Absolute age	188
12.4.	Conclusions	188
APPENDIX 1	Activity of alpha sources	192
APPENDIX 2	Archaeological notes	193
APPENDIX 3	Radioactive impurities in the pottery	195
ACKNOWLEDGEMENTS		197
REFERENCES		198

LIST OF ILLUSTRATIONS

Figure No.		Facing Page
1/1	Fast heating apparatus	7
1/2	Heating circuit for fast heating apparatus	9
1/3	Dynode resistor chain for photomultiplier	9
1/4	Glow curves in air - sherd r	10
1/5	Ratio of natural thermoluminescence to Ra^{224} thermoluminescence versus temperature	12
1/6	Specific thermoluminescence (air) versus age	13
2/1	Typical heating-rate curves	16
2/2	Voltage across graphite plate versus heating rate	16
2/3	Black body radiation (graphite plate) for different heating rates	17
2/4	Temperature for standard black body radiation (graphite plate) versus heating rate	17
2/5	Temperature for standard black body radiation (Cotswold limestone) versus heating rate	17
2/6	Servo-system for fast heating apparatus	19
2/7	Peak position (Tarquinia limestone) versus weight	20
2/8	Slow heating apparatus	20
2/9	Quantum efficiency of photomultipliers versus wavelength	22
2/10	Percentage transmission of filters versus wavelength	23
2/11	Anode current/Dark current versus E.H.T. voltage	27
2/12	Linearity of photomultiplier type 6255S	30
3/1	Model for production of thermoluminescence	32
3/2	Theoretical values T_g and δ versus heating rate	35
3/3	Glow curves - sherd f	36
3/4	Log I versus 1/T - sherd f	37
3/5	Energy levels versus configuration coordinate	41
3/6	Percentage transmission of filters versus wavelength	42
3/7	Glow curves - sherd k (limestone extraction)	50
3/8	Glow curves - sherd 6b4 (quartz extraction)	51
4/1	Theoretical rate curves for "single centre" model	70
5/1	X-ray rate curves - sherd r	77
5/2	Glow curve (X-irradiation) - sherd r	77
5/3	Components of X-ray rate curve	77
5/4	Log $(L_s - L_t)$ versus radiation time (X-rays) - sherd r	77
5/5	Rate curves for ultra-violet light - sherd r	78
5/6	Glow curves: bleach with ultra-violet light - sherd r	79
5/7	Beta particle rate curves - sherd r	79

Figure No.		Facing Page
5/8	Log ($L_s - L_t$) versus radiation time (beta particles) - sherd r	80
5/9	Glow curves: effect of annealing - sherd k	83
5/10	Glow curves: effect of annealing - sherd 6b4	83
6/1	Glow curves: pre-irradiation with X-rays - sherd r	89
6/2	L_x versus pre-irradiation time - sherds i and r	89
6/3	X-ray rate curves: pre-irradiation and thermal bleaching - sherd r (thermally stabilized)	93
6/4	X-ray rate curves: pre-irradiation and optical bleaching - sherd r	95
7/1	Beta particle rate curves: initial portion - sherd r	99
7/2	Theoretical rate curves for E_1 type traps	100
7/3	Beta particle rate curves: pre-irradiation and thermal bleaching - sherd r	100
7/4	Glow curves: pre-irradiation with beta particles - sherd r	101
8/1	Alpha particle rate curves - sherd i	108
8/2	Alpha particle rate curves - sherd r	110
8/3	Alpha particle rate curves - sherd k (limestone extraction)	116
8/4	Glow curves: pre-irradiation with alpha particles - sherd r	119
8/5	Glow curves: pre-irradiation with alpha particles - sherd k (limestone extraction)	121
8/6	Thermal bleaching experiments - sherd r	125
8/7	Rate curves for Ra^{224} solution - sherd r	127
8/8	Variation of τ, k and R with source strength - sherd r	128
9/1	Alpha and beta particle glow curves - sherd a4	135
9/2	Alpha and beta particle glow curves - sherd r	135
9/3	Alpha and beta particle glow curves - sherd k (limestone extraction)	135
9/4	Alpha and beta particle glow curves: mixing and variation of sample weight - sherd a4	138
9/5	L_1/I_4 for alpha and beta particle glow curves versus radiation time - sherd a4	138
10/1	Glow curves (air): respreading - sherd c and Tarquinia limestone	149
10/2	Glow curves: cool in vacuum - Tarquinia limestone	154
10/3	Light output when vacuum released - Tarquinia limestone	154

Figure No.		Facing Page
10/4	Glow curves (air and nitrogen) - Boston M/2 and Tarquinia limestone	155
10/5	Glow curves (nitrogen): effect of oxygen content - sherd 4g1	155
10/6	Glow curves (nitrogen): effect of cooling conditions - sherd 4g1	156
10/7	Glow curves (air) - sherd 4g1	157
11/1	Glow curves: thermal bleaching - sherd 4b2	165
11/2	Glow curves: thermal bleaching - sherd b3	167
11/3	Glow curves: optical bleaching - sherd A/Ash	168
11/4	Optical bleaching by fluorescent light - sherd r	168
11/5	Glow curves: optical bleaching through filters - sherd r	169
12/1	Ratio of natural thermoluminescence to beta thermoluminescence versus temperature	179
12/2	Specific thermoluminescence ($k = 1$) versus age	184
12/3	Specific thermoluminescence ($k = 0.1$) versus age	184
12/4	Specific thermoluminescence ($k = 0.02$) versus age	184

INTRODUCTION

This thesis will describe the effects of high energy radiation on ancient ceramics as observed through the measurement of the resulting thermoluminescence, together with the application of this technique to the age determination of ceramics.

The interaction of high energy radiation with matter can be divided into two classes; elastic collisions in which the radiation interacts with an atom of the target material imparting some energy to the latter and losing a like amount of energy itself, and inelastic collisions in which energy is lost through electronic excitation. The former can result in the displacement of atoms from their lattice sites and thus the creation of electron energy levels situated, in the case of non-conducting materials, between the conduction and valence bands. These energy levels act as electron and hole traps. Inelastic collisions result in ionisation and the filling of these newly created traps, as well as the filling of existing traps. If, after being subjected to high energy radiation, the material is heated these traps are emptied and the electrons and holes return to their ground state with the emission of light. This phenomena is known as thermoluminescence.

The effects of high energy radiation on a large number of materials, including the alkali halides, magnesium oxide, crystalline and fused quartz, has been studied by means of thermoluminescence measurements (Chapter 4) while measurement of the intensity of the thermoluminescence from lithium fluoride crystals has provided an extremely sensitive and linear radiation

dosimeter (Cameron et al., 1961).

In addition it was discovered as early as 1705 (Oldenburg,1705) that when naturally occurring minerals are heated, light is emitted in many cases. This arises from the action of the radioactive impurities, such as uranium, thorium and potassium, which are present in small quantities in the minerals. Daniels (1953) suggested that thermoluminescence measurements could be used to determine the age of limestones and ancient ceramics. In the case of limestones, the amount of thermoluminescence depends on the time that has elapsed since crystallisation and the method has been applied by Zeller et al. (1954, 1957 and 1962) and by Johnson (1963) with varying degrees of success.

Houtermans et al. (1957) made measurements on meteorites to determine how long they had been exposed to cosmic radiation in interplanetary space and in addition applied the method to ancient ceramics to determine their date of firing (Houtermans et al., 1960). After the clay is fired, it retains no thermoluminescence below the temperature of firing and subsequently the natural thermoluminescence is thought to build up linearly with time. Kennedy and Knopff (1960) extended the work on ceramics, applying the method to sixteen dated sherds of Greek pottery, ranging in age from 1000 B.C. to 400 A.D., and obtained highly encouraging results. However it is understood that their work has now been discontinued. Finally Sabels (1962) used thermoluminescence measurements for determining the age of basaltic lava flows. He found that for young lavas (up to 10,000 years) the amount of thermoluminescence was age dependent but that the results for older lavas were unsatisfactory because a saturation level for the thermoluminescence had been reached.

If an accuracy of better than ± 10% could be achieved for the age determination of ancient ceramics by means of thermoluminescence, then it would provide an extremely valuable tool for archaeologists, particularly for prehistoric periods. Its application would be far greater than that of magnetic dating (Aitken, 1961) since the latter method requires fired clay structures, such as kilns and hearths, found in situ and also necessitates the establishment of detailed calibration curves using structures of known age. Thermoluminescent dating would also provide a valuable check for radiocarbon dating (Libby, 1952) and would have the advantage of dating the pottery itself, rather than dating the associated organic remains.

There are two possible criteria on which age determination by means of thermoluminescence can be based. On the one hand the number of new electron and hole traps created, since firing, by the high energy particles from the radioactive impurities can be determined. In this case the effect of the alpha particles and their associated recoil nuclei predominate. Alternatively it is assumed that the majority of the traps are already present due to imperfections in the crystal lattice, such as impurity atoms, and the number of traps filled, as a result of the radioactive impurities, is measured. The work described in Chapter 5 established that, for the temperature and wavelength range used, the former approach was impractical in the case of ceramics, because of the inability to distinguish between the newly created damage traps and those already existing in the ceramic when firing was terminated.

The adoption of the concept that the number of filled traps is age

dependent implies that to date a sherd of pottery, three basic measurements must be made - the natural thermoluminescence (L_n), the thermoluminescence resulting from a standard dose of radiation (L_s) and the radiation dose received per gram per year (R). The specific thermoluminescence (S) is given by:

$$S = \frac{L_n}{L_s \; R}$$

and should vary linearly with the age of the ceramic.

Chapter 1 contains the results of a preliminary test of the above hypothesis carried out with eighteen pottery sherds of known date. These results are not in agreement with the above theory but further work (Aitken, Tite and Reid, 1964) established that, if the thermoluminescence measurements are made in nitrogen instead of air, an essentially linear relationship between the specific thermoluminescence and age is obtained.

The limitations of and subsequent improvements made to the apparatus used for the measurement of the thermoluminescence, are discussed in Chapter 2. The theory of thermoluminescent glow curves, the determination of trap depths and the measurement of the spectral composition of the light emitted, together with the work done to establish the minerals present in the pottery which are responsible for the thermoluminescence, are described in Chapter 3.

The second part of this thesis contains the results of measurements of the thermoluminescence induced using artificial sources of high energy radiation. The initial aim of this work was to establish a method for determining the number of traps created by the high energy radiation from the

radioactive impurities, since the pottery was fired (Chapter 5). This however proved to be impractical and the work was extended to establish the number of new traps created by X-rays (Chapter 6), beta particles (Chapter 7) and alpha particles (Chapter 8). The initial rate at which traps were filled was studied in detail for the beta particles (Chapter 7) and in addition, the effect of the previous radiation history of the sherd on the rate of trap filling was investigated. Finally an attempt was made to determine the relative efficiency of alpha, beta, gamma and X-irradiation with respect to trap filling (Chapter 9).

In the third part of the thesis further factors relevant to the age determination of ceramics, by measurement of the number of traps filled since firing, are discussed. The contribution made to the natural thermoluminescence by other than radiation-filled traps was investigated (Chapter 10) and the stability of the filled traps, when subjected to thermal and optical bleaching, was studied (Chapter 11). Finally the results of a third and more comprehensive age determination programme, again using samples of known age, are given in Chapter 12.

PART I

CHAPTER 1 PRELIMINARY RESULTS

Initial work on the effects of X-irradiation (Chapter 5) suggested that the determination of the number of electron traps created by radioactive impurities since the pottery was fired was impractical. Consequently, following the successful results obtained by Kennedy and Knopff (1960) from a group of Greek pottery, a more general test of the criterion that the number of traps filled with electrons, since firing, is age dependent, was performed. For this purpose a varied selection of pottery, ranging in provenance from Egypt to England and in age from 6000 B C. to 1300 A.D., was collected (Table 1/1). The values obtained for the specific thermoluminescence are shown in fig. 1/6 plotted against the archaeological age.

1.1. Natural thermoluminescence

The pottery was ground with a pestle and mortar so that it all passed through a 120 mesh sieve (less than 130 microns). 40 mgms. of the powder was spread evenly over the central portion (area = 1.54 cm.^{2}) of a graphite plate (10 x 5 x 0 .25 cm.^{3}) using a paint brush (Rowney no. 6). The graphite plate was mounted on four pyrophillite supports, its ends were coated with Leitsilber silver paint to provide satisfactory electrical contact and were connected to braided copper leads by means of four copper blocks (fig. 1/1 shows the final form of the fast heating apparatus). The braided copper leads (length = 15 cm. cross-section = 2.5 x 0.25 cm.^{2}) allowed for the expansion of the graphite and prevented it from breaking

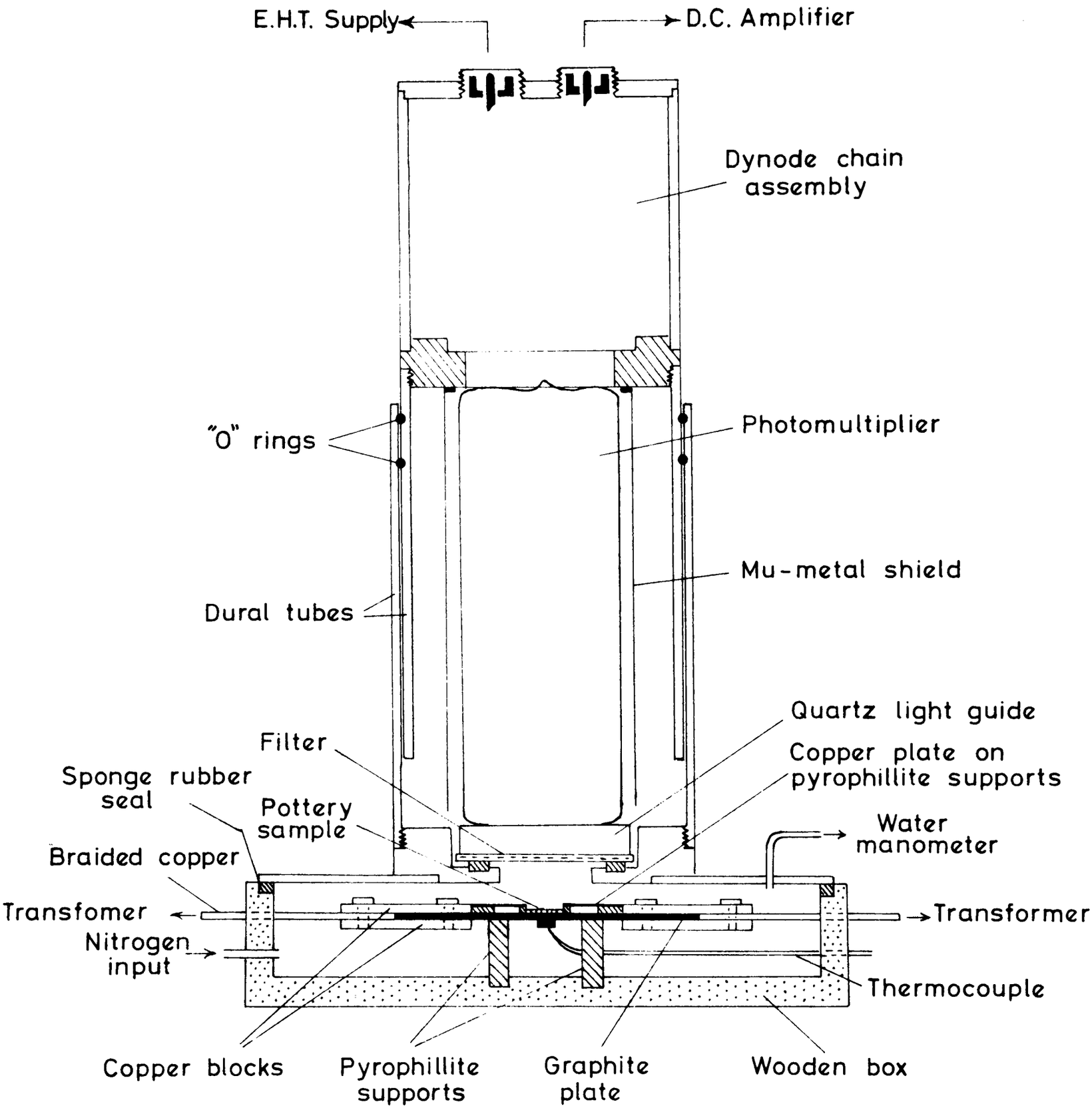

E.H.T. Supply
D.C. Amplifier
Dynode chain assembly
"O" rings
Photomultiplier
Mu-metal shield
Dural tubes
Quartz light guide
Filter
Copper plate on pyrophillite supports
Sponge rubber seal
Pottery sample
Water manometer
Braided copper
Transfomer
Transformer
Nitrogen input
Thermocouple
Copper blocks
Pyrophillite supports
Graphite plate
Wooden box

Fig 1/1

Table 1/1
List of Sherds

Sherd	Provenance			Archaeological age	
b	Mersin	:	Turkey	Neolithic	C. 5500 B.C.
c	Mersin	:	Turkey	Chalcolithic	C. 5000 B.C.
d	Arpachiyn	:	Iraq	Chalcolithic	C. 4500 B.C.
e	Mersin	:	Turkey	Chalcolithic	C. 3500 B.C.
f	Jericho	:	Jordan	Bronze Age	C. 3000 B.C.
g	Duweir	:	Israel	Bronze Age	C. 1500 B.C.
h	Sinai	:	Egypt	XIX Dynasty	C. 1300 B.C.
i	Sybaris	:	Italy	Greek	C. 500 B.C.
j	Sybaris	:	Italy	Greek	C. 400 B.C.
k	Provence	:	France	Roman	C. 200 B.C.
p	Sybaris	:	Italy	Roman	C. 100 B.C.
m	Wroxeter	:	England	Roman	C. 200 A.D.
n	Wroxeter	:	England	Roman	C. 200 A.D.
o	Wroxeter	:	England	Roman	C. 300 A.D.
q	Hira	:	Iraq	Byzantine	C. 800 A.D.
r	Thetford	:	England	Saxon	C 1000 A.D.
s	Brill	:	England	Mediaeval	C. 1300 A.D.
t	Oxford	:	England	Mediaeval	C. 1300 A.D.

when heated; they were connected to a 10 KVA transformer (Harmsworth Townley Ltd..,) by means of copper strips of cross-section 1.25 x 0.25 cm.^{2}. The remainder of the graphite was shielded from the photomultiplier by means of a copper plate supported on strips of pyrophillite; the temperature of the metal lagged behind that of the graphite by approximately 200°C and therefore contributed negligible black body radiation.

The sample was heated in air to 400°C in approximately 25 seconds by passing an alternating current of several hundred amps. at a 2 volt R.M.S. potential through the graphite plate; the heating circuit used is shown in fig. 1/2. The temperature of the sample was measured using a T1 - T2 thermocouple (British Driver - Harris Co. Ltd.) inserted in a protrusion under the graphite plate; the second thermocouple junction being held at 0°C by means of melting ice. The resulting voltage was fed to the X axis of a X - Y recorder (Moseley Autograph, Model 135).

The thermoluminescence was measured using a photomultiplier (E.M.I. type 6097) placed just above the sample and the whole assembly was made light-tight by means of a sponge rubber seal coated with Edwards silicone grease. A lucite light guide, length 1 cm. and diameter 5 cm., was attached to the front of the photomultiplier in order to improve the light-collecting efficiency of the system and to prevent heating-up of the photo-multiplier cathode. In addition the photomultiplier was protected from the effect of magnetic fields by means of a mu-metal shield. The dynode resistor chain for the photomultiplier is shown in fig. 1/3; the minus 1100 volts applied at the cathode was supplied from a Fluke E.H.T. unit

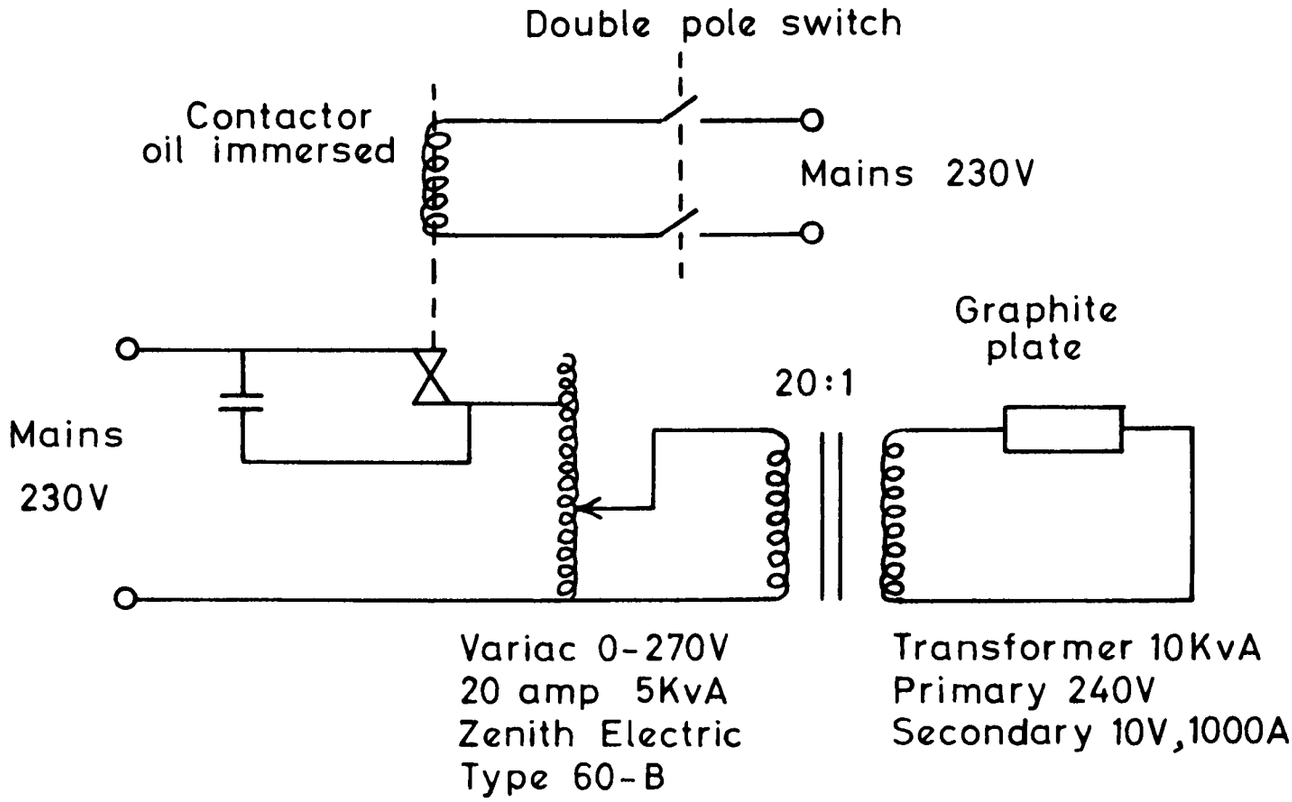

Double pole switch
Contactor
oil immersed
Mains 230V
Graphite
plate
20:1
Mains
230V
Variac 0-270V
20 amp 5KvA
Zenith Electric
Type 60-B
Transformer 10KvA
Primary 240V
Secondary 10V,1000A

Fig 1/2.

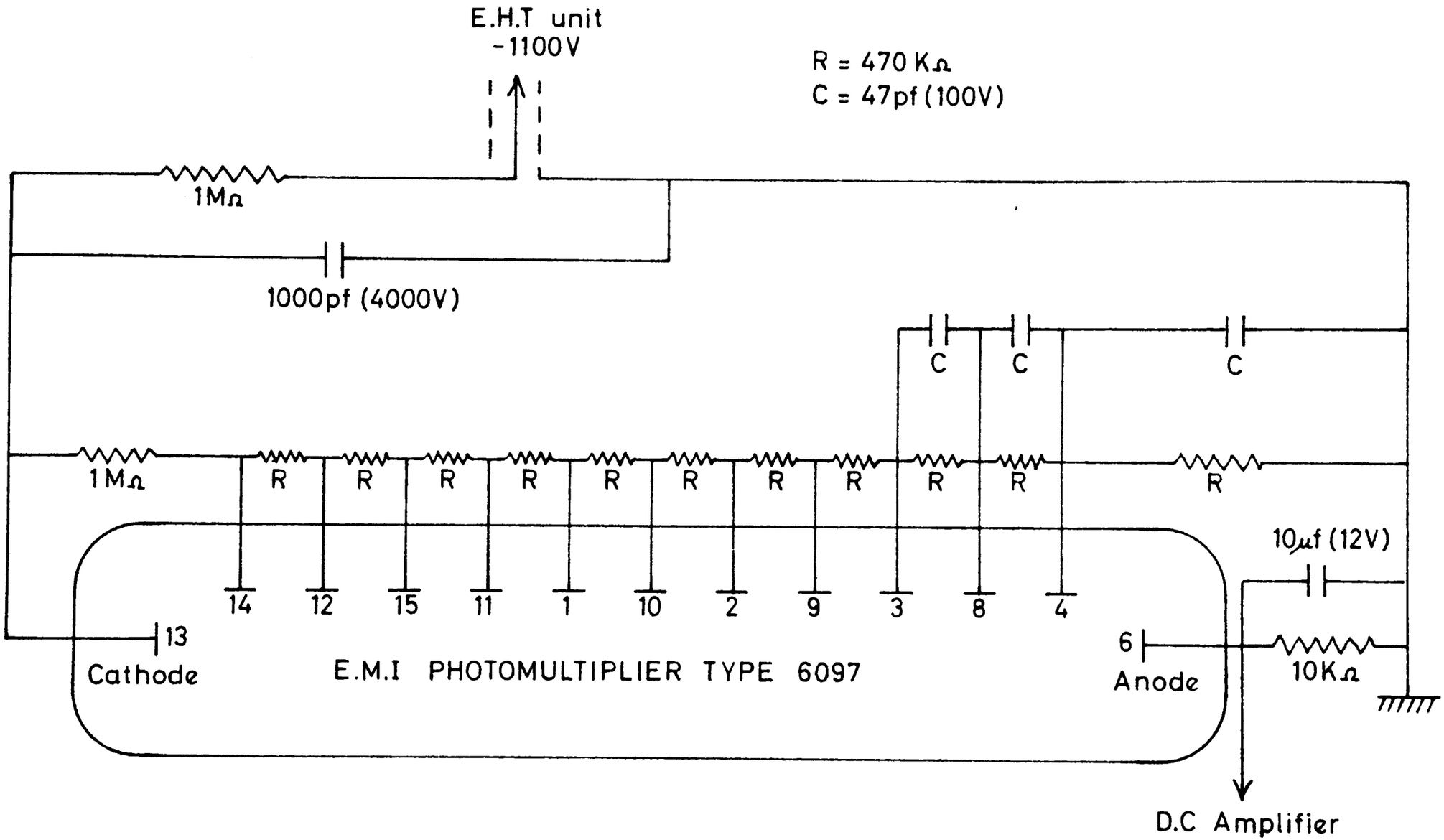

E.H.T unit
-1100V
R = 470 KΩ
C = 47pf (100V)
1MΩ
1000pf (4000V)
C
C
C
1MΩ
R
R
R
R
R
R
R
R
R
R
R
R
10μf (12V)
14
12
15
11
1
10
2
9
3
8
4
13
Cathode
E.M.I PHOTOMULTIPLIER TYPE 6097
6
Anode
10KΩ
D.C Amplifier

Fig 1/3

(Model no. 412 A/AJ). The voltage at the output of the photomultiplier was amplified by a high gain, low noise d.c. amplifier (Honeywell Brown Accudata III) and fed to the Y axis of the X - Y recorder.

Hence, on heating, a graph of light output plotted against temperature was obtained; this is referred to as the natural glow curve (fig. 1/4). The same sample was then heated a second time in order to determine the light due to black body radiation.

The area between the two curves was measured in the temperature range 200 - 400°C using a planimeter. This area was then corrected for changes in heating rate, the time taken for the temperature of the plate to increase from 200°C to 400°C having been measured with a stop-watch, and for changes in the overall gain of the photomultiplier and electronic apparatus by means of a standard light source. This had an intensity of 0.24 microlumens and consisted of a zinc sulphide phosphor activated by Sr^{90} (Brandhurst Co. Ltd.).

1.1.1. Correction for grinding and gas adsorption

Under these conditions of measurement it was found that thermoluminescence was obtained from modern brick and from refired ancient pottery. At this stage in the work, this thermoluminescence was attributed to the grinding process and to the adsorption of gas at the grain surfaces (Chapter 10). An attempt to correct for the contribution of these effects to the natural thermoluminescence was made by heating ground and unground portions of the ceramics in a furnace at 800°C for one hour. After cooling, the latter were ground and the measurement of the thermoluminescence was repeated for both portions, thus providing values for the grinding plus gas adsorption

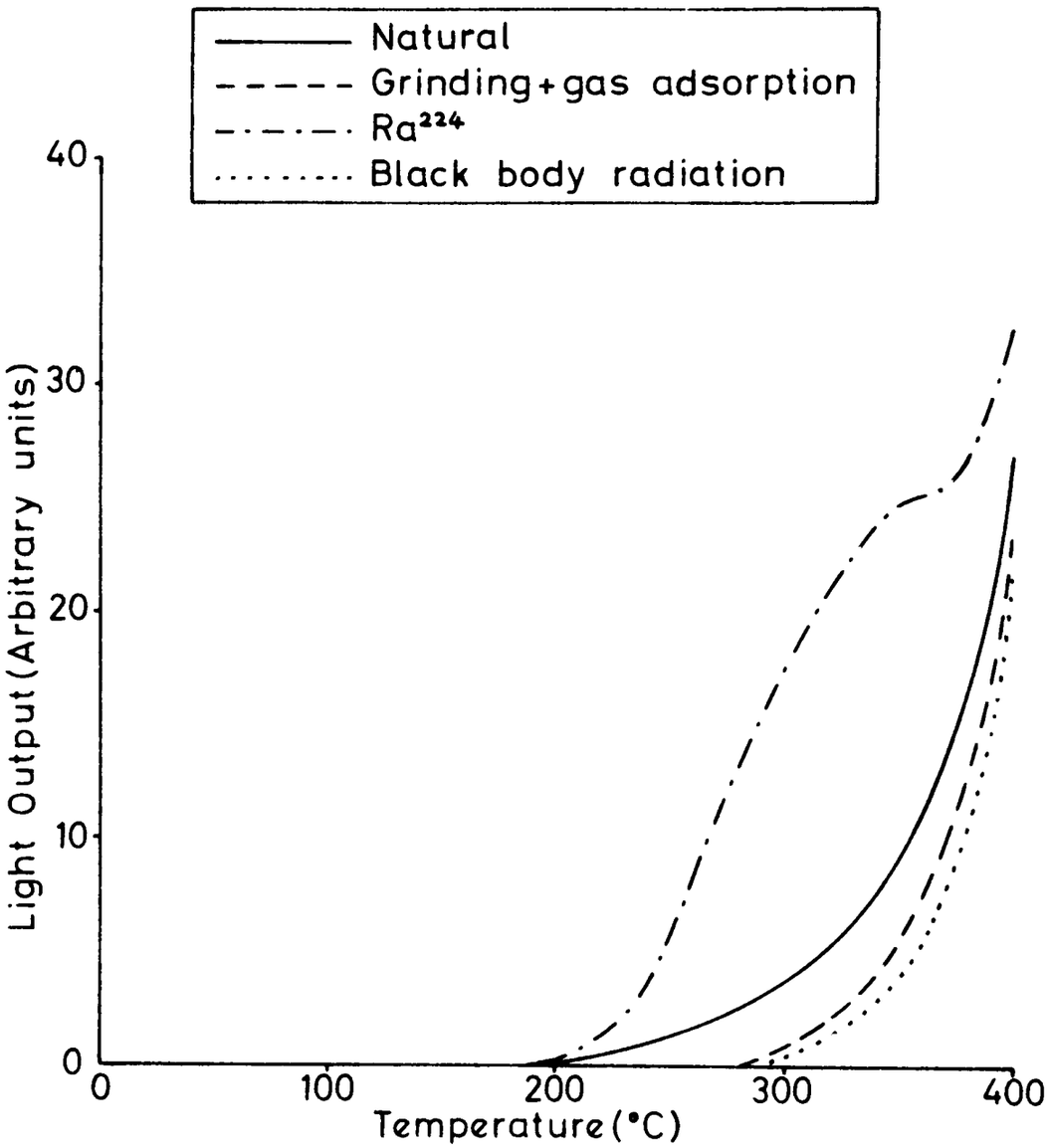

Natural
Grinding + gas adsorption
Ra224
Black body radiation
Light Output (Arbitrary units)
0
10
20
30
40
0
100
200
300
400
Temperature (°C)

Fig 1/4

correction and the gas adsorption correction by itself (Table 1/2).

1.2. Susceptibility

The susceptibility of the pottery to radiation was measured using a solution of Ra^{224} (ThX) in alcohol. Ra^{224} decays with the emission of alpha particles and it was therefore hoped that its effects would be directly comparable with those produced by the radioactive impurities.

Ground-up samples of the pottery were first heated to 500°C on the graphite plate to remove the natural thermoluminescence and 0.125 ccs. of the Ra^{224} solution was then added to 120 mgm. samples using a micro-pipette. Three samples from each sherd were dosed in this manner, the activity of the solutions used being in the ratio 1 : 2 : 3. The activity of the strongest solution, when added, was approximately 30 microcuries per cc. Since the half-life of Ra^{224} was 3.64 days after three weeks the activity remaining was such that the samples could be safely handled.

In the natural glow curve, no thermoluminescence was observed below 200°C indicating that all the traps associated with these low temperatures had been completely bleached, while some bleaching had undoubtedly occurred above 200°C. In order to make some allowance for this, the samples dosed with Ra^{224} solution were thermally bleached in an oven at 140°C for four hours before measuring their thermoluminescence (fig.1/4).

After making a correction for gas adsorption, the thermoluminescence from the three samples was proportional to the radiation dose to within ± 15%. Therefore the average value, obtained from the three samples for the thermoluminescence per unit dose, was used to calculate the specific thermo-

luminescence and also provided a correction for the different wavelengths emitted by different ceramics.

The ratio of the natural thermoluminescence, after correction for grinding plus gas adsorption, to the Ra^{224} thermoluminescence, after correction for gas adsorption, was plotted against temperature for all the sherds. Ideally if equivalent amounts of thermal bleaching had occurred for both the natural and the Ra^{224} thermoluminescence and if the correction for grinding plus gas adsorption was valid, the ratio should be constant at all temperatures above 200°C. In practice a constant value was not obtained (fig. 1/5) and the specific thermoluminescence was calculated from the glow curve areas in the 200 - 400°C range.

1.3. Radiation dose

The radiation dose received by the pottery came almost entirely from the radioactive impurities present in the pottery, i.e. uranium, thorium and potassium. A measure of the total uranium and thorium content was obtained by measuring the alpha activity using a scintillation counter (Tite and Waine, 1962) and from this the roentgen dose per gram per year was calculated. To this was added the roentgen dose arising from the decay of the K^{40} isotope, the total potassium content being measured by means of a flame photometer.

1.4. Specific thermoluminescence

The three measurements described above provide a figure for the specific thermoluminescence which should, according to the simple theory propounded

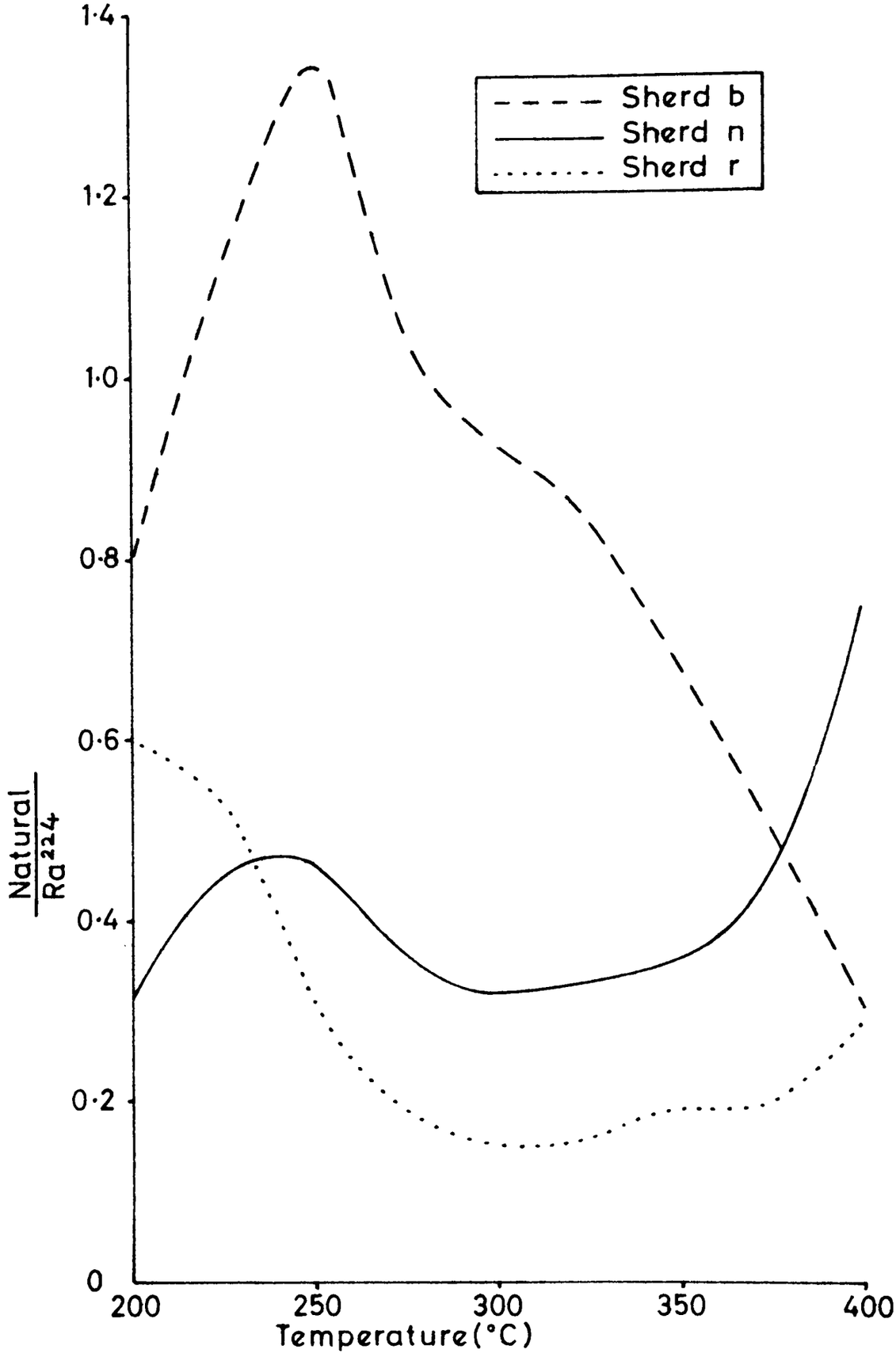

1·4
1·2
1·0
0·8
0·6
0·4
0·2
0
Natural / Ra^224
Sherd b
Sherd n
Sherd r
200
250
300
350
400
Temperature (°C)

Fig 1/5

in the introduction, be proportional to the age of the ceramic.

Table 1/2 contains the results for the pottery on which this trial experiment was carried out, the specific thermoluminescence was calculated from the corrected and uncorrected values for the natural thermoluminescence. Fig. 1/6 shows the specific thermoluminescence plotted against the archaeological age for sixteen of the eighteen sherds used.

These results were extremely discouraging since, even after correcting for grinding plus gas adsorption, the points could not be fitted to the straight line through the origin which had been hoped for on the basis of Kennedy's results. Furthermore the experimental errors, which in all cases were estimated to be less than $\pm$ 20%, were insufficient to account for this dispersion.

The fundamental difficulty associated with the technique described above was the uncertainty introduced by making a correction for grinding plus gas adsorption since, in heating the sample to remove the radiation-induced thermoluminescence, changes in the crystalline structure of the sherd were likely to have occurred. However it was found that if the thermoluminescence was measured in nitrogen instead of air, there was a radical reduction in the natural thermoluminescence and in addition, zero thermoluminescence was obtained from a sherd of modern pottery (Boston M/2) and from the majority of the sherds of refired ancient pottery (Chapter 10). Because of this a second programme, using known-age samples, was carried out (Aitken, Tite and Reid, 1963) in which all the measurements were made under nitrogen and in which the ground-up samples were exposed to as little light as possible

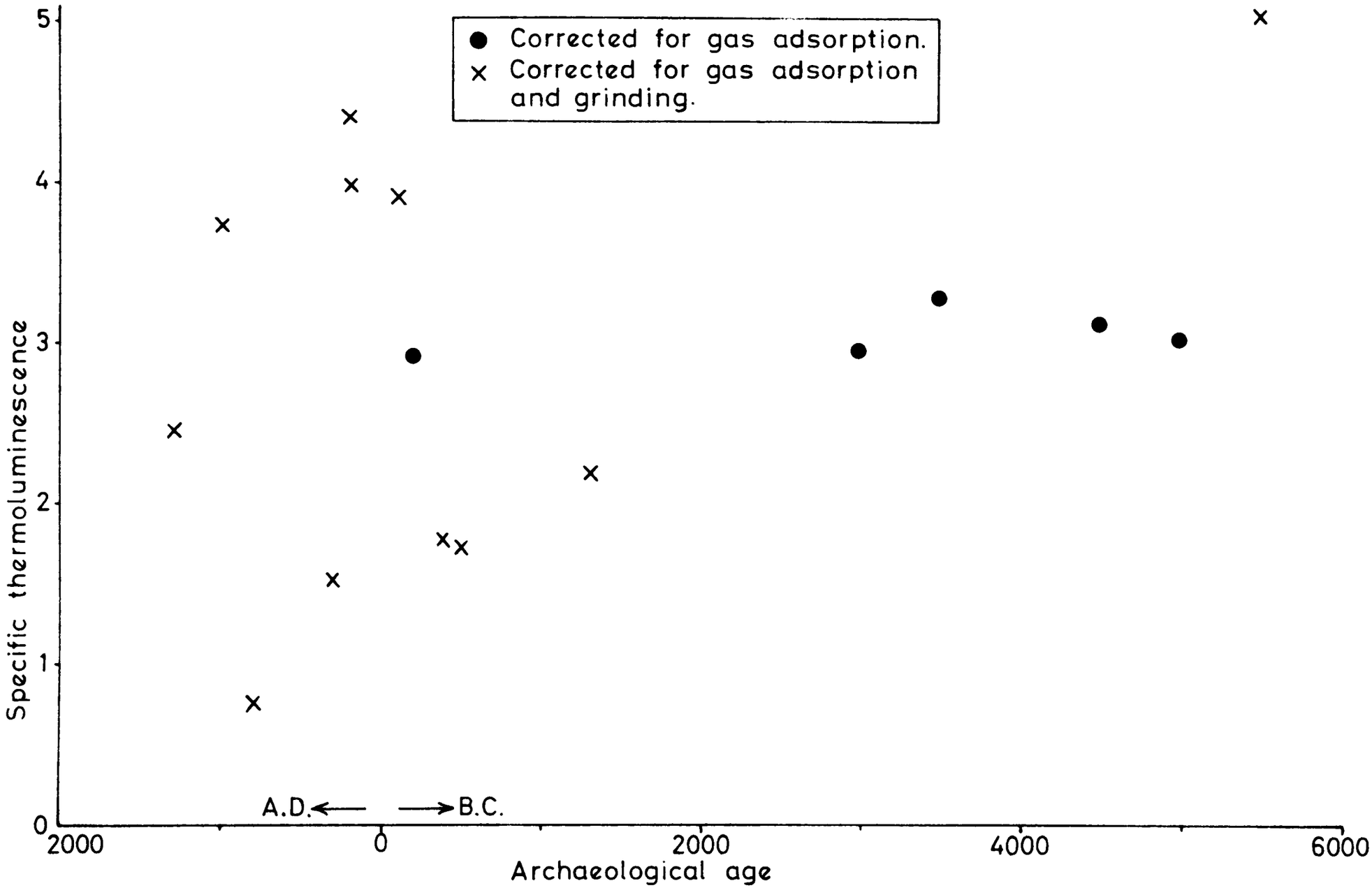

Corrected for gas adsorption.
Corrected for gas adsorption and grinding.
Specific thermoluminescence
0
1
2
3
4
5
A.D.
B.C.
2000
0
2000
4000
6000
Archaeological age

Fig 1/6

(Chapter 11). These results satisfactorily established that within the limits of experimental accuracy the specific thermoluminescence depends on the age of the ceramic. The results of a third and more comprehensive age determination programme are given in Chapter 12.

TABLE 1/2

PRELIMINARY RESULTS

Sherd	Natural t-l	Grinding + gas adsorption	Gas adsn.	Ra^{224} Solution t-l	Roentgen dose per gm per year	Specific Thermoluminescence		
						Uncorrected	Grinding + gas adsn.	Gas adsorption
b	420	25	0	223	3.69	5.10	5.06	5.10
c	531	-	226	513	1.97	5.25	-	3.02
d	319	-	155	273	1.95	5.99	-	3.12
e	916	-	216	1140	1.88	4.82	-	3.29
f.	1720	-	394	1690	2.61	3.90	-	2.96
g	618	-	620	250	1.65	15.00	-	-
h	371	340	145	540	0.26	26.40	2.21	16.10
i	184	90	0	238	2.27	3.40	1.74	3.40
j	181	51	35	270	2.75	2.44	1.75	1.96
k	1283	2650	350	460	6.94	4.02	-	2.92
p	329	120	4	230	2.32	6.17	3.92	6.09
m	454	176	52	392	1.60	7.24	4.43	6.41
n	200	46	8	142	2.71	5.19	4.00	4.99
o	352	200	20	325	3.05	3.54	1.53	3.35
q	279	170	67	900	1.55	2.00	0.78	1.52
r	242	60	0	320	2.02	3.74	2.82	3.74
s	268	144	11	345	3.02	2.57	1.19	2.47
t	415	43	18	70	2.50	23.70	21.30	22.70

Natural t-l, Ra^{224} t-l and specific t-l are given in arbitary units.

CHAPTER 2 APPARATUS

The basic details of the apparatus first used for thermoluminescence measurements have been given in section 1.1. The difficulties associated with and the modifications made to the heating and light measurement systems are now described (Sections 2.1 and 2.2 respectively).

2.1. Heating system

The integrated light output (I), which is proportional to the total number of filled traps associated with the temperature range T1 to T2, is given by:

$$I = \int_{T_1}^{T_2} \frac{I_T}{H_T} \, dT$$

where I_T = instantaneous light output at temperature, T and $H_T = \left(\frac{dT}{dt}\right)_T$, the heating rate at temperature, T.

The major source of error associated with the heating system, described in section 1.1., was that the heating rate was not constant throughout the temperature range 20-500°C; for a typical glow curve measurement, the heating rate varied from 20°C/sec. at 100°C to 7°C/sec at 500°C (fig.2/1). Furthermore the heating rate for a particular temperature range changed by approximately ± 10% for successive glow curves.

For a fixed variac setting, the voltages across the graphite plate (excluding the copper contacts) ranged from 1.81 - 1.88 volts R.M.S. for a series of heatings (1-17) and these changes in voltage could be correlated with the observed change in heating rate (fig. 2/2). No corresponding changes in the mains voltage supplied to the variac were observed but on the other hand, tightening the screws clamping the graphite plate to the copper leads produced a 20% increase in the heating rate and a 10% increase in the

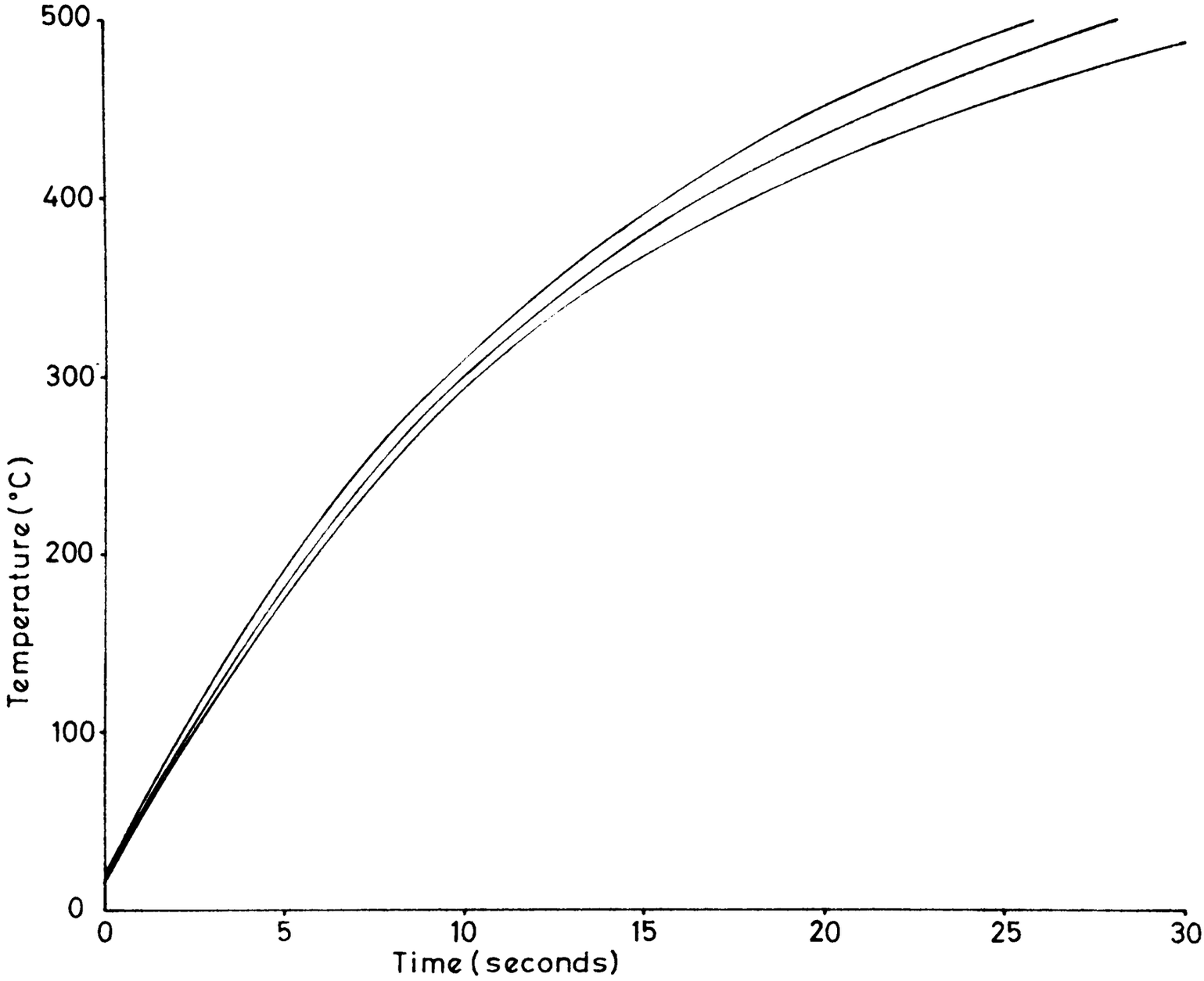

500
400
300
200
100
0
Temperature (°C)
0
5
10
15
20
25
30
Time (seconds)

Fig 2/1

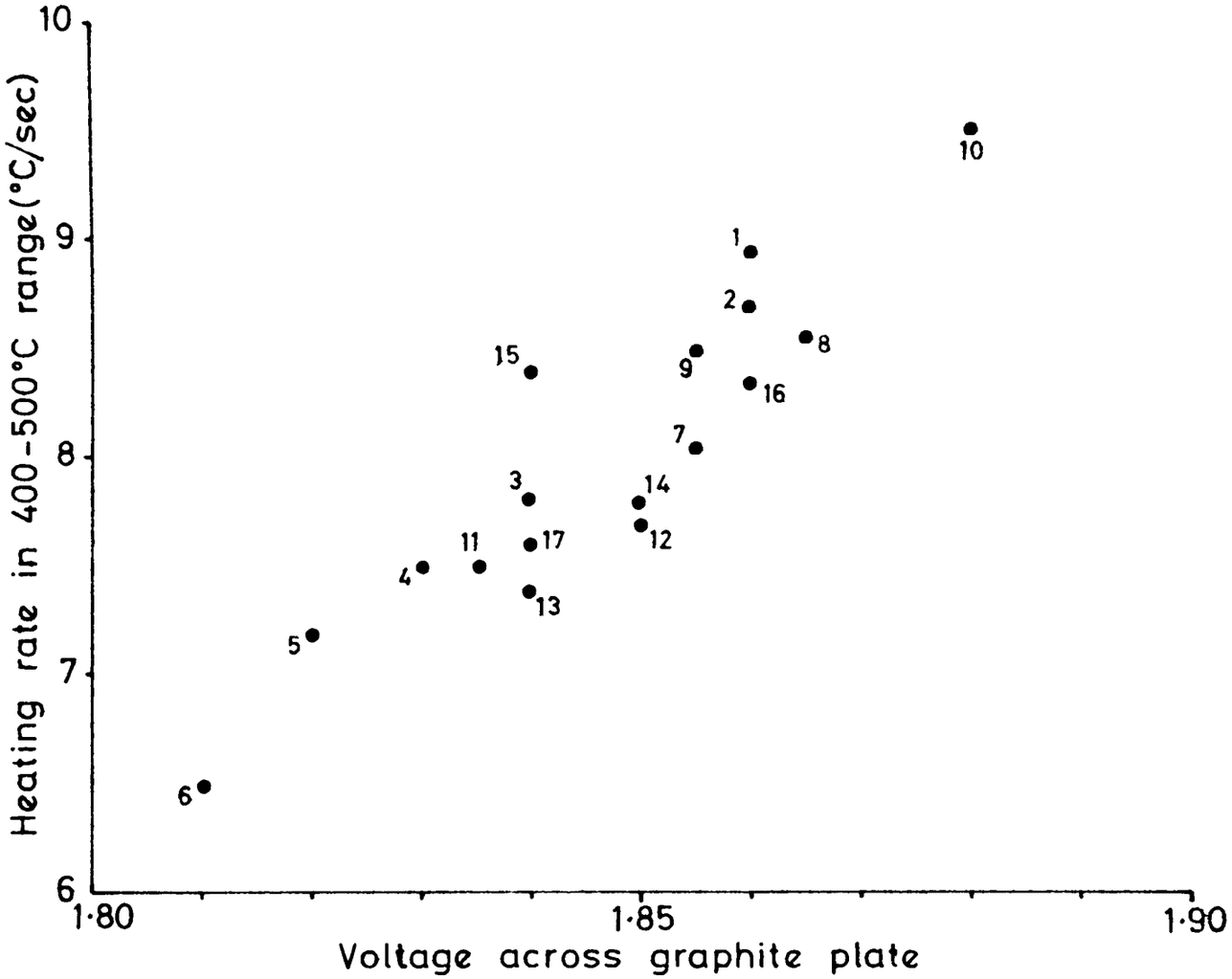

10
9
8
7
6
Heating rate in 400-500°C range(°C/sec)
1·80
1·85
1·90
Voltage across graphite plate
1
2
3
4
5
6
7
8
9
10
11
12
13
14
15
16
17

Fig 2/2

voltage across the plate. It thus appeared that the variation in heating rate was due to changes in the contact resistance between the graphite plate and the copper leads.

Although measurement with a stop-watch, of the time taken for the heating up, provided an approximate correction for these variations in heating rate, it was not possible to correct for the change in temperature lag between the thermocouple and the surface of the sample by this means.

2.1.1. Temperature lags

An indication of the extent to which the temperature recorded by the thermocouple lagged behind the temperature of the surface of the graphite plate, was obtained by measuring the black body radiation of the plate at a series of heating rates. With increasing heating rate, achieved by changing the variac setting, the black body curve moved to a lower thermocouple temperature (fig. 2/3) and by extrapolating to zero heating rate, it was estimated that, for an average heating rate of 40°C/sec. in the 400-500°C range, the thermocouple temperature was 400°C when the temperature of the surface of the plate was approximately 455°C (fig. 2/4).

The changes in the overall temperature lag between the surface of a sample of Cotswold limestone and the thermocouple, with heating rate, were also determined by measurement of the shift in the black body radiation. Fig. 2/5 shows the temperature for a standard intensity of black body radiation plotted against the average heating rate in the 400-500°C range, for sample weights of 40, 80 and 120 mgms. spread over an area of 1.54 cm^2. The change in slope of the lines indicated that for a 40 mgm. and a 80 mgm.

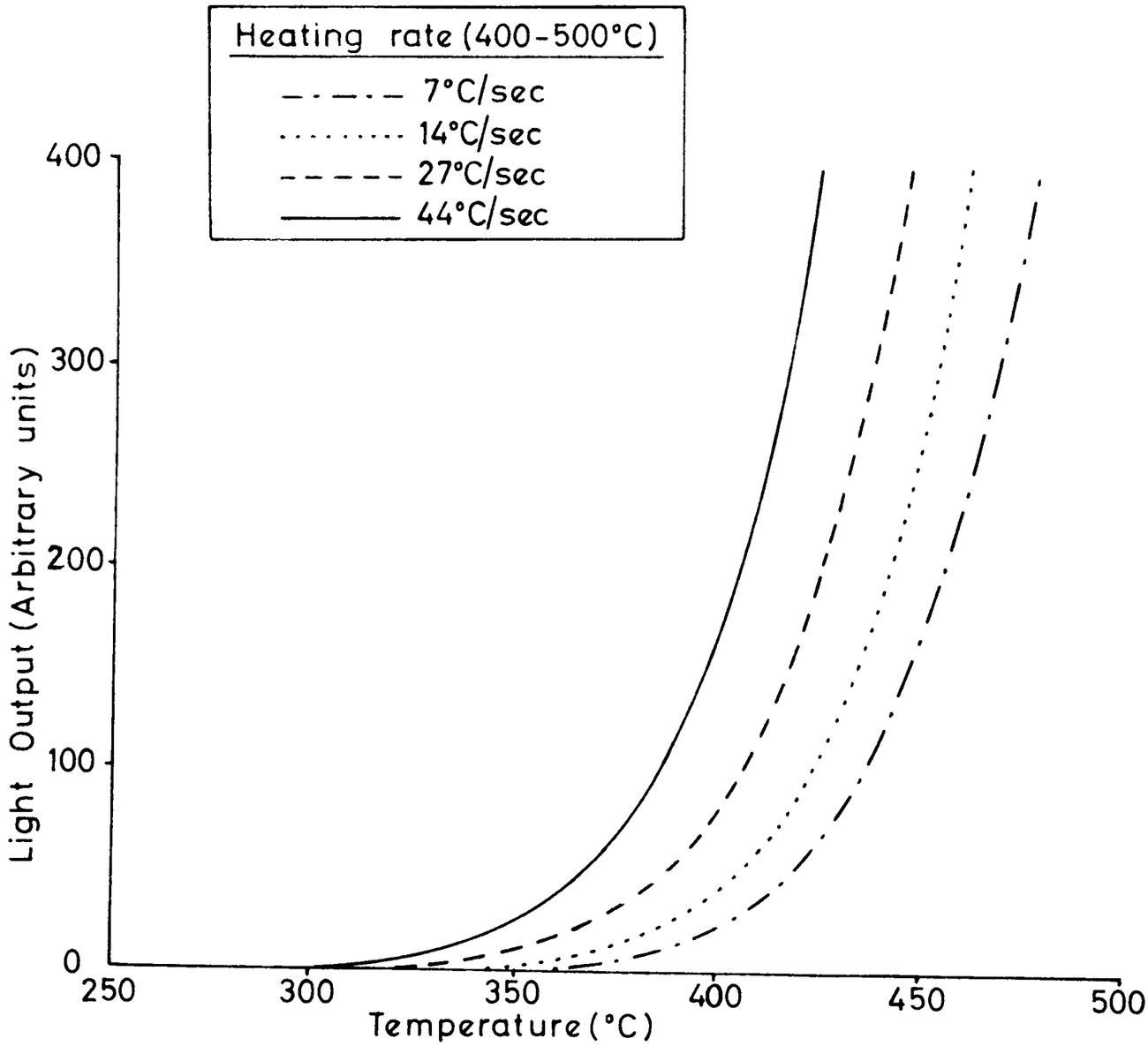

Heating rate (400-500°C)
7°C/sec
14°C/sec
27°C/sec
44°C/sec
Light Output (Arbitrary units)
400
300
200
100
0
250
300
350
400
450
500
Temperature (°C)

Fig 2/3

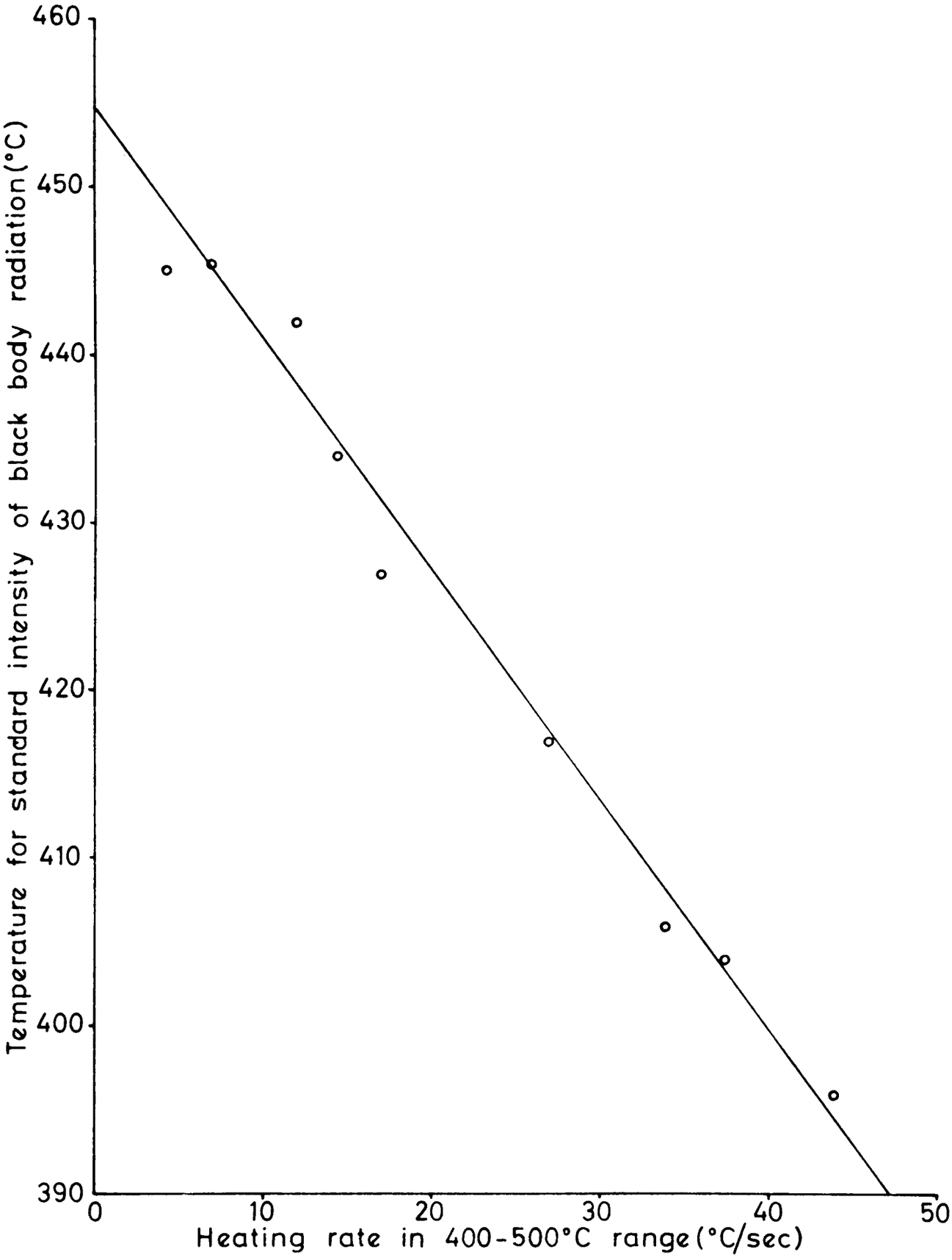

460
450
440
430
420
410
400
390
Temperature for standard intensity of black body radiation (°C)
0
10
20
30
40
50
Heating rate in 400-500°C range (°C/sec)

Fig 2/4

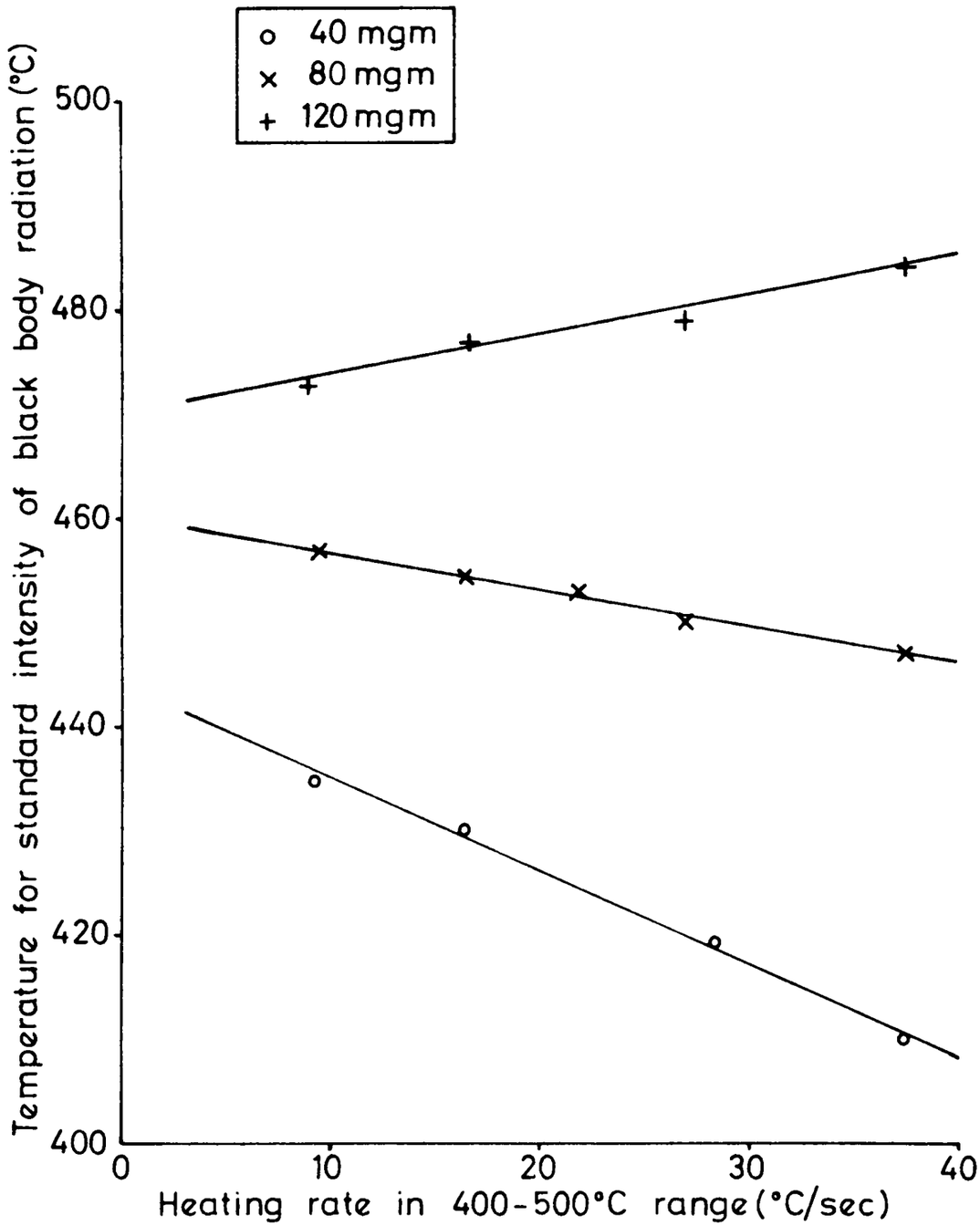

o 40 mgm
× 80 mgm
+ 120 mgm
Temperature for standard intensity of black body radiation (°C)
500
480
460
440
420
400
0
10
20
30
40
Heating rate in 400-500°C range (°C/sec)

Fig 2/5

sample the thermocouple temperature lagged behind the temperature of the sample surface while for a 120 mgm. sample the thermocouple temperature was ahead.

The results indicate that the variations in heating rate, observed for the same variac setting, could produce changes in the temperature lag of approximately ± 5°C for a 40 mgm. sample and a nominal heating rate of 25°C/sec. in the 400-500°C range. For a typical sherd the natural thermoluminescence plus black body radiation in the 400-500°C range equalled 100 units while the black body radiation, assuming changes in temperature lag of ± 5°C, equalled 25 ± 8 units. Hence the natural thermoluminescence equalled 75± 8 units, a possible error of ± 10% arising from the variation in heating rates.

Consequently it was decided that a heating system with a constant, reproducible heating rate was required for accurate measurements. A slow heating apparatus (section 2.1.3) was designed, for which the heating rate of 1°C/sec. was kept constant by manually varying the power to the heating coil by means of a variac. However at this heating rate it was not possible to measure the natural thermoluminescence of ceramics with sufficient accuracy because of interference from the photomultiplier and d.c. amplifier noise (section 2.2.3). Therefore for the age determination programme described in Chapter 12, the fast heating apparatus was used and a constant heating rate was achieved by means of a servo-system (section 2.1.2).

2.1.2. Servo-system for fast heating apparatus

The servo-system (fig.2/6) was designed to provide a constant and reproducible heating rate for the graphite plate. A linearly increasing voltage was supplied by a ramp generator, consisting essentially of two 750μf. tantalum condensers charged by means of a 12 volt battery. This linear voltage-rise was compared with the voltage from a thermocouple recording the temperature of the graphite plate. When these two voltages were not equal, the difference was amplified and fed to a thyristor control circuit (A.E.I. type FC 11). This unit varied the fraction of the cycle for which a pair of A.E.I. silicon controlled rectifiers (maximum current 40 amps.), connected back to back, would conduct mains current to the graphite plate. When the thermocouple voltage lagged behind the ramp voltage the time, for which the silicon controlled rectifiers were conducting, was increased and when the thermocouple was ahead of the ramp voltage the time was decreased. This system provided an average heating rate of 20°C/sec., throughout the range room temperature to 500°C, to an accuracy of ±2%. However due to the time lag between changing the length of the conduction period and the resulting change in the temperature observed by the thermocouple, the instantaneous heating rate varied by as much as ± 5%.

By this means the temperature lag between the thermocouple and the surface of the sample was kept constant for a given specimen provided the plate was cooled to below 50°C between measurements and provided the same weight of sample was used for each measurement. If the sample was re-heated from above 50°C, the temperature lag decreased by approximately 5°C.

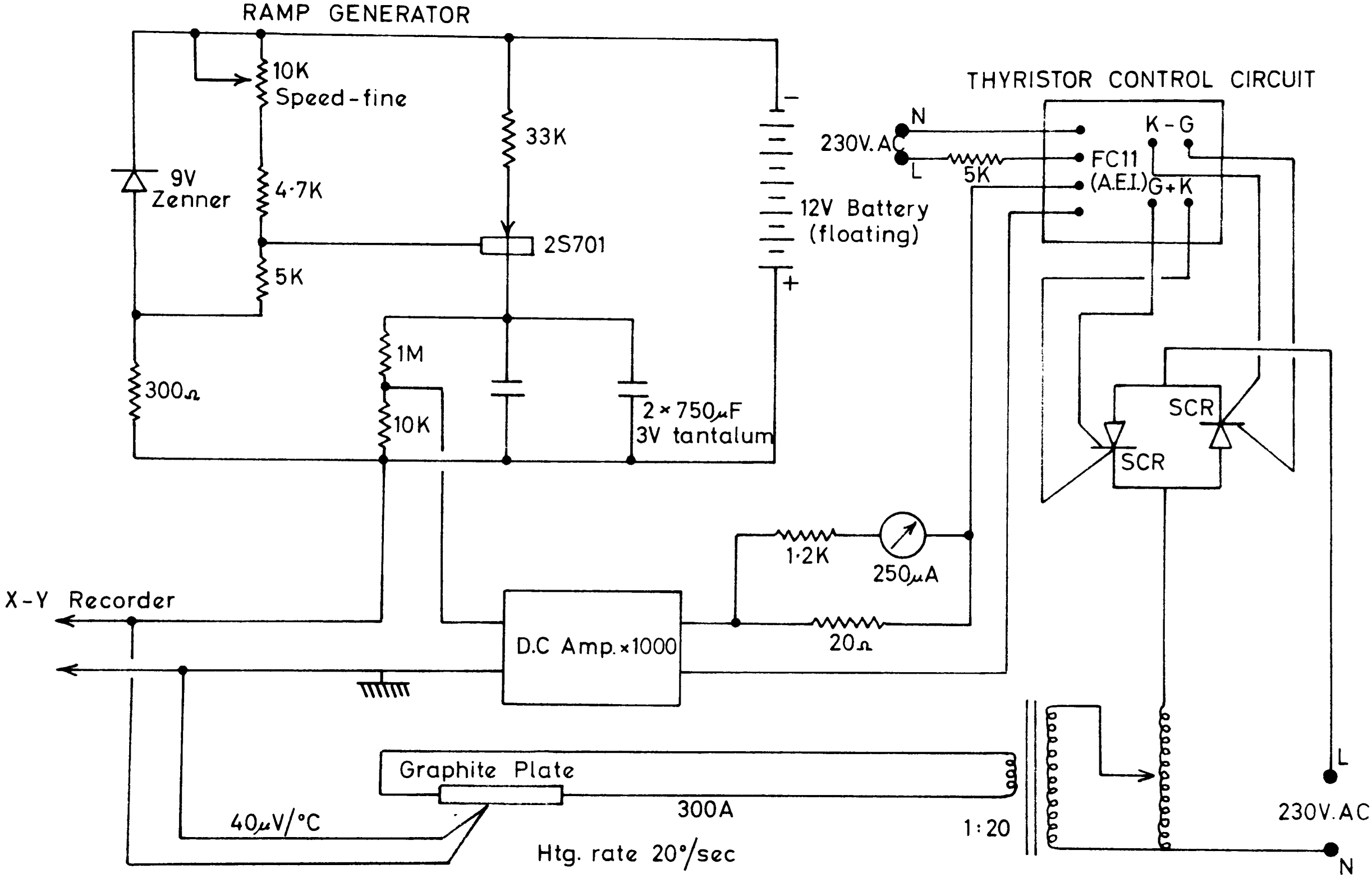

RAMP GENERATOR
10K
Speed-fine
33K
9V
Zenner
4·7K
2S701
5K
12V Battery
(floating)
1M
300Ω
10K
2×750μF
3V tantalum
THYRISTOR CONTROL CIRCUIT
N
230V.AC
L
5K
K-G
FC11
(A.E.I.)
G+K
SCR
SCR
1·2K
250μA
X-Y Recorder
D.C Amp.×1000
20Ω
Graphite Plate
300A
1:20
230V.AC
40μV/°C
Htg. rate 20°/sec
L
N

Fig 2/6

The variation in temperature lag with the weight of sample was determined by measuring the shift in peak position of the natural thermoluminescence from Tarquinia limestone for different weights of sample at the same heating rate of 20°C/sec. (fig. 2/7). The area covered by the sample was reduced to 0.79 cm^2. in order to reduce the temperature gradient across its surface (Reid, 1964) and weights of 7, 15 and 25 mgms. were used. From fig. 2/7 it can be seen that, if a 15 mgm. sample was weighed to an accuracy of ± 0.5 mgms., the variation in temperature lag would be ± 1°C. This variation in temperature lag differed from specimen to specimen depending on their thermal conductivity.

2.1.3. Slow heating apparatus

This heating system consisted of a copper block which was surrounded by a nichrome heating coil, mounted in a cylinder of pyrophillite (fig. 2/8). The thermocouple voltage was fed to the X axis of the X - Y recorder as before and also to a 10 mv. Elliot potentiometric recorder. The latter provided a plot of temperature versus time and the variac, supplying power to the heating coil, was adjusted manually so that the temperature rose linearly with time at a rate of 1°C/sec. At 100°C the variac supplied approximately 5.5 amps. at 65 volts R.M.S. and by 500°C this had been increased to 7.0 amps. at 84 volts R.M.S. The heating rate obtained using this system was constant and reproducible to ±2% in the 75-500°C range.

By observing the thermocouple temperature at which crystals of silver nitrate (m.p.212°C), placed on the copper block, melted it was established that at 212°C the thermocouple temperature lagged behind the temperature of

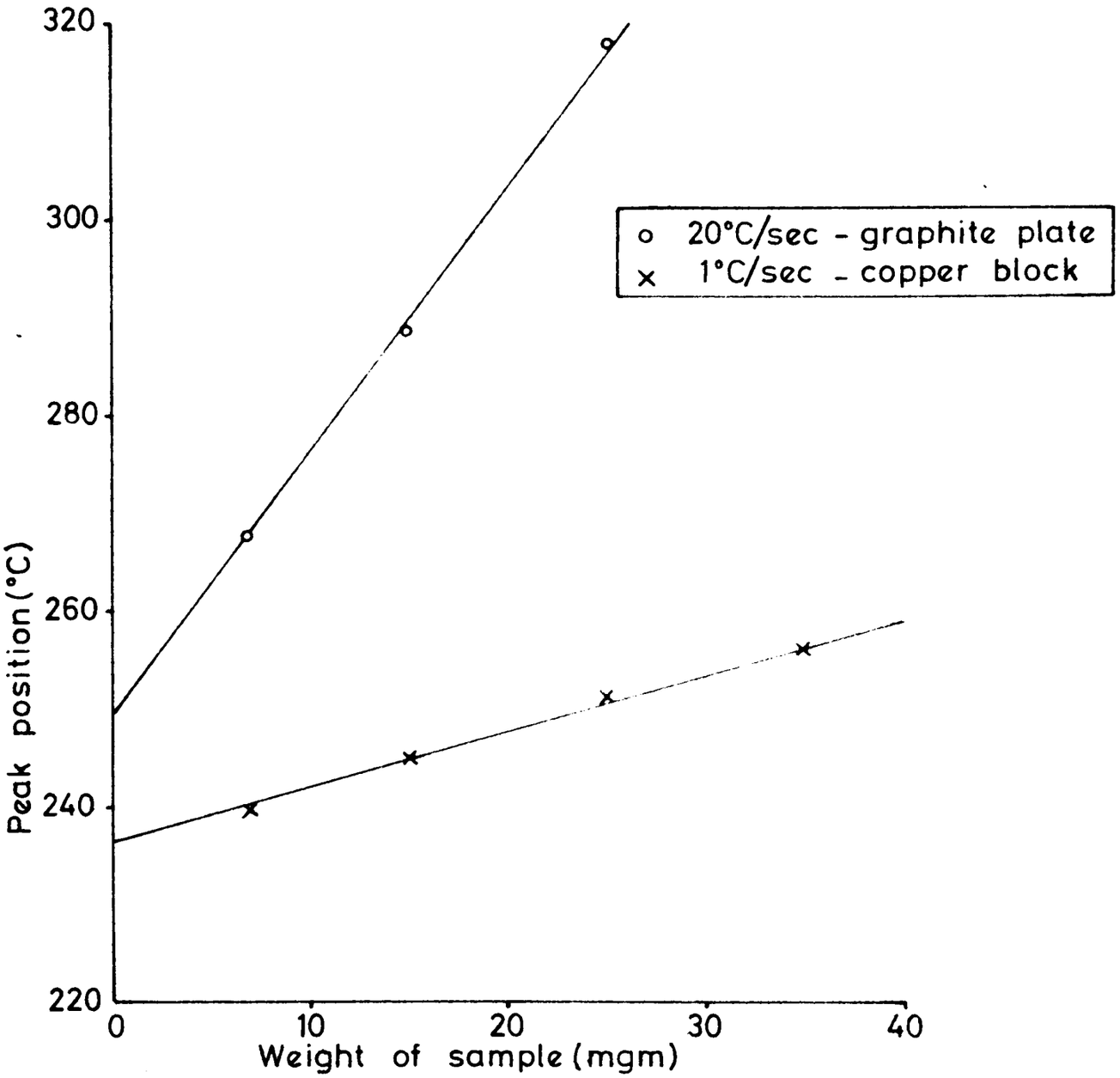

320
300
280
260
240
220
Peak position (°C)
0
10
20
30
40
Weight of sample (mgm)
o 20°C/sec - graphite plate
× 1°C/sec - copper block

Fig 2/7

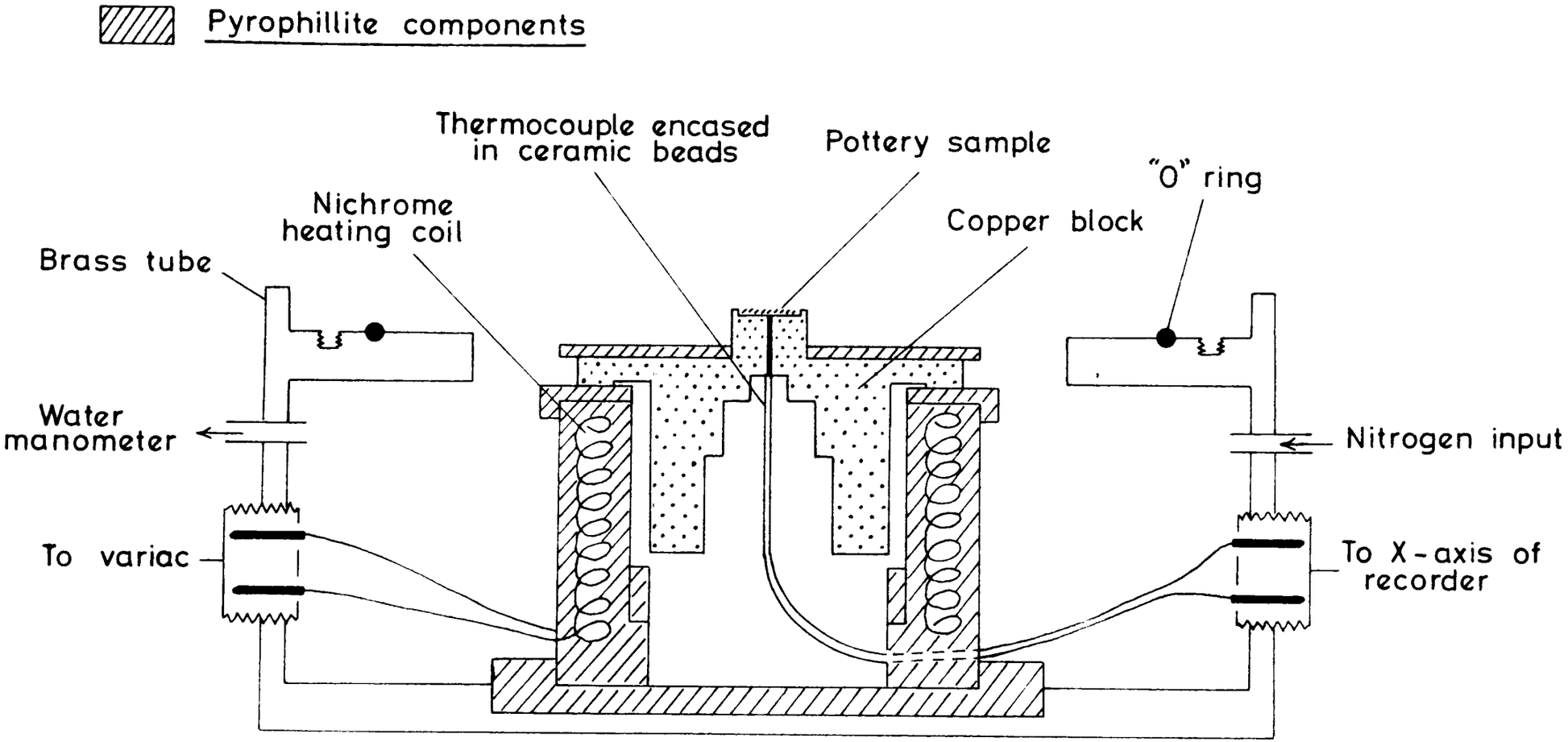

Pyrophillite components
Thermocouple encased in ceramic beads
Pottery sample
"O" ring
Nichrome heating coil
Copper block
Brass tube
Water manometer
Nitrogen input
To variac
To X-axis of recorder

Fig 2/8

the surface of the block by approximately 15°C. The changes in the overall temperature lag with heating rate were required for the determination of the trap depths associated with the glow curve peaks from X-irradiated samples of sherd k (section 3.2.2.). A given intensity of black body radiation from 15 mgm. samples of sherd k occurred at 300°C for a heating rate of 0.5°C/sec. and at 282°C for a heating rate of 2°C/sec. This shift of 18°C was used in the trap depth calculations.

The slow heating apparatus was used for the majority of the measurements of thermoluminescence induced by artificial sources of radiation (Chapters 3 and 5-9) and the results obtained were reproducible to ±5%. A further advantage of the slow heating apparatus, as compared with the fast heating apparatus, was the superior resolution of the peaks observed for some sherds. This was partly due to a theoretical decrease in the peak width for a heating rate of 1°C/sec. (fig. 3/2) and partly due to a reduction in the temperature gradient across the surface of the sample and through its thickness. The decrease in the temperature gradient through the sample was observed by measurement of the shift in peak position for different weights of Tarquinia limestone. From fig. 2/7 it can be seen that for a 15 mgm. sample spread over an area of 0.79cm^2, the temperature difference through the sample was approximately 8°C at a heating rate of 1°C/sec. and 40°C at a heating rate of 20°C/sec.

The slow heating apparatus also included provision for the measurement of glow curves with the sample under vacuum and this was made use of in the study of spurious thermoluminescence (Chapter 10).

2.2. Measurement of the light output

For the age determination measurements described in chapter 1, an E.M.I. photomultiplier, type 6097, was used without any filter to reduce the black body radiation. Consequently by 400°C the natural thermoluminescence was completely masked by the black body radiation (fig.1/4). In order to reduce this black body radiation, and hence push the measurement of the natural thermoluminscence to higher temperatures, a selection of Chance-Pilkington coloured filter glasses of thickness 2 mm., together with a cell containing cupric chloride solution, was tested (section 2.2.1).

For standard thermoluminescence measurements an E.M.I. photomultiplier, type 6255S, was used instead of type 6097 since the ratio of the overall gain to the dark current was larger for type 6255S. The selection of the E.H.T. voltage applied to the photomultiplier, the d.c. amplifier and photomultiplier noise levels and the ultimate accuracy of the measurements are discussed in section 2.2.3.

A further advantage of type 6255S was that it was sensitive down to 2000Å and slightly less sensitive than type 6097 in the red region of the spectrum. For the determination of the optical spectrum of the thermoluminescence (section 3.3), type 6255S was used in conjunction with type 9558 and together they provided a means of detecting light in the range 2000-8000Å (fig. 2/9). The lucite light guide was replaced by a quartz light guide since lucite only transmitted light above 3000Å compared with the lower limit for quartz of 1600Å, furthermore it had a higher optical absorption coefficient than quartz throughout the visible range.

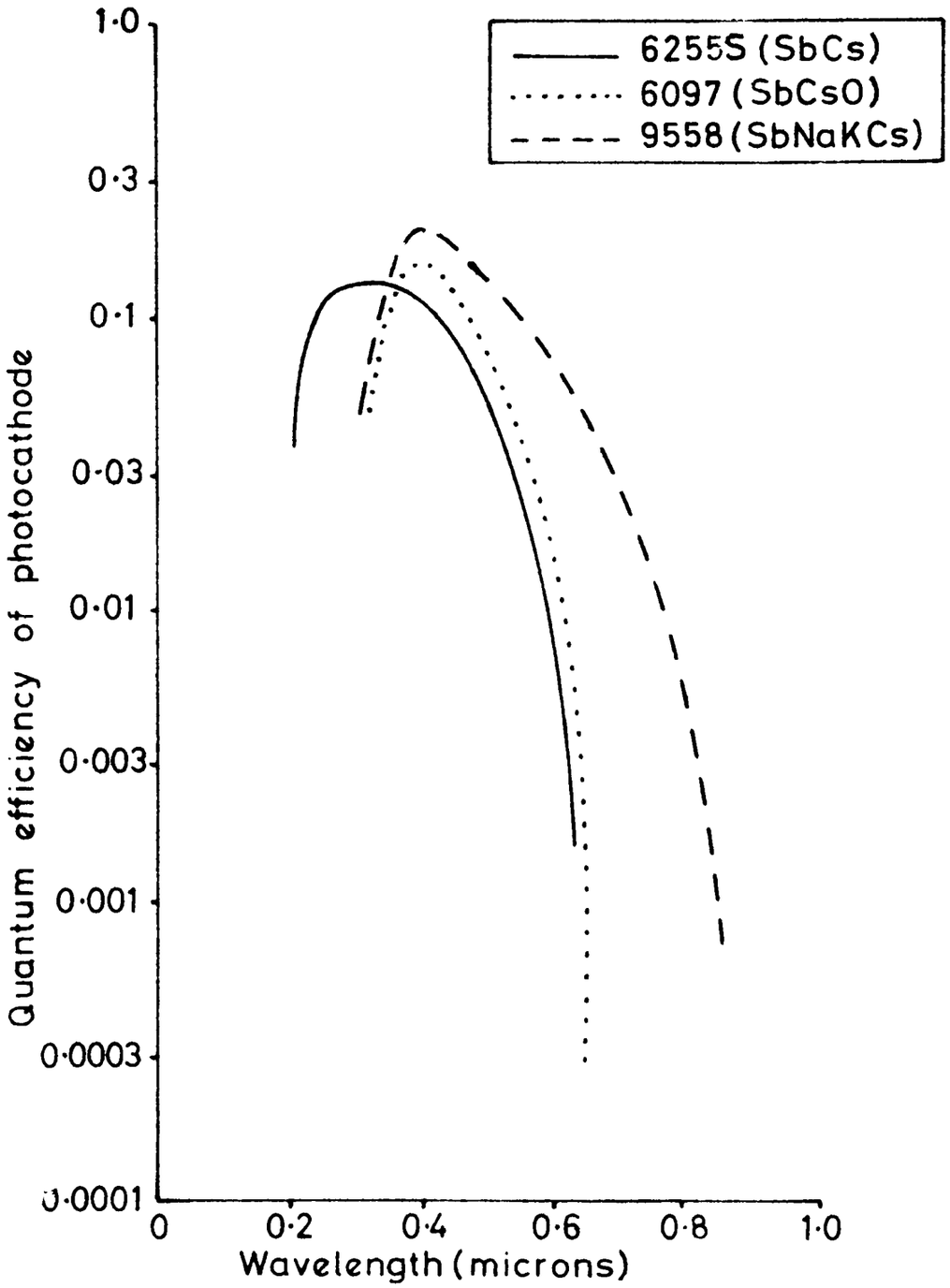

6255S (SbCs)
6097 (SbCsO)
9558 (SbNaKCs)
1·0
0·3
0·1
0·03
0·01
0·003
0·001
0·0003
0·0001
Quantum efficiency of photocathode
0
0·2
0·4
0·6
0·8
1·0
Wavelength (microns)

Fig 2/9

Finally the linearity of response of the photomultiplier type 6255S was checked by means of a standard light source (section 2.2.4).

2.2.1. Reduction of black body radiation

The thermoluminescence (L) and black body radiation (B) from samples of sherd r, which had been subjected to a 10 minute X-irradiation, were measured on the slow heating apparatus. Photomultiplier type 6255S was used in conjunction with the quartz light guide, and three Chance-Pilkington filters (OX7, OB10 and OB2) and a 2 cm. long cell containing a 2½% solution of cupric chloride were tested in turn (fig. 2/10). The reductions in the thermoluminescence and black body radiation observed at 400°C are given in Table 2/1.

Table 2/1

Reduction of black body radiation using filters

	$\frac{B - \text{no filter}}{B - \text{filter}}$	$\frac{L - \text{no filter}}{L - \text{filter}}$	$\frac{L}{B}$
No filter	-	-	0.9
OX7	7.2	2.7	2.5
OB2	20.3	3.1	6.0
OB10	101	2.1	43
Cupric chloride solution	8.2	1.4	5.4

From these figures it can be seen that the blue filter glass (OB10) was the most efficient and therefore the combination of the photomultiplier type 6255S, the quartz light guide and the OB10 filter was used for the majority of the measurements described in the remainder of this thesis. This

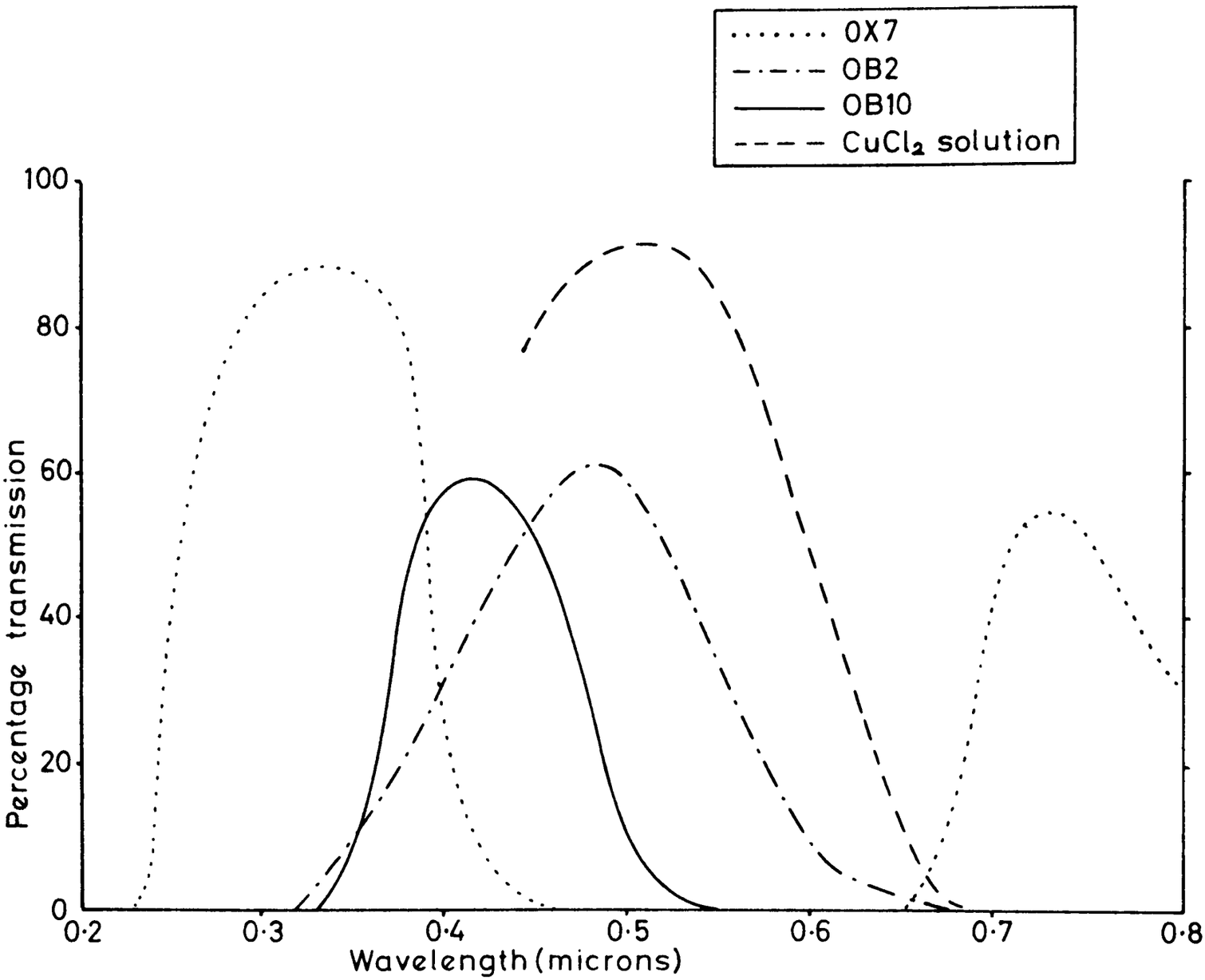

OX7
OB2
OB10
CuCl2 solution
100
80
60
40
20
0
Percentage transmission
0·2
0·3
0·4
0·5
0·6
0·7
0·8
Wavelength (microns)

Fig 2/10

combination made it possible to extend the measurement of the natural thermoluminescence up to between 450-500°C and was therefore employed for the second age determination programme (Aitken, Tite and Reid, 1963).

However for the third age determination programme (Chapter 12) and for the study of radiation effects at high temperatures (section 8.4), two OB10 filters, each of thickness 2 mm., were used. The addition of a second OB10 filter further reduced the black body radiation of a typical sherd (4b2) at 450°C by a factor of 7 while the natural thermoluminescence was only reduced by a factor 1.7. The ratio of the natural thermoluminescence to the black body radiation at 500°C became 0.32 and hence measurement was possible up to 500°C. Similarly it was possible to measure the saturation levels for alpha and beta irradiations up to 650°C.

2.2.2. Theoretical value for black body radiation

The theoretical value for the black body radiation was calculated in terms of the current output from photomultiplier type 6255S, when used in conjunction with OB10 filters, and compared with the output observed in the case of black body radiation from the graphite plate itself.

According to Planck's law, the number of photons emitted in the wavelength range λ to $\lambda + d\lambda$ per second per 2π solid angle by a black body at temperature T°K is given by:

$$N_\lambda \, d\lambda = \frac{2\pi c}{\lambda^4 \left[\exp(C'/\lambda T) - 1 \right]} . \, d\lambda \qquad \text{2/1}$$

where c = velocity of light (cm./sec.)

$C' = hc/k = 1.436$ (h = Planck's constant, k = Boltzmann's constant).

Hence the number of electrons emitted per second from the cathode of the photomultiplier for black body radiation in the range λ to $\lambda + d\lambda$ is given by:

$$N_e \, d\lambda = \frac{N_\lambda \, q_\lambda \, t_\lambda \, A \Omega}{2\pi} . d\lambda$$

where q_λ = quantum efficiency of photomultiplier at wavelength λ

t_λ = % transmission of filters at wavelength λ ,

A = area of black body,

Ω = solid angle subtended at the black body by the photomultiplier.

Therefore the anode current of the photomultiplier due to black body radiation from the graphite plate is given by :

$$i = \frac{A \Omega \, Ge}{2\pi} \sum (N_\lambda \, q_\lambda \, t_\lambda \, d\lambda) \text{ amps.} \qquad \text{2/2}$$

where G = gain of the photomultiplier.

e = electronic charge in coulombs.

Table 2/2 contains the values for N_λ , $N_\lambda \, t_\lambda$ and $N_\lambda \, t_\lambda \, q_\lambda$ for the single OB10 Filter and two OB10 filters in conjunction with photomultiplier type 6255S, calculated at 500°C for wavelengths ranging from 4000 - 5800Å.

A = 0.79 cm^2, $\Omega = 2\pi \times 0.26$, $G = 1.11 \times 10^7$,

$e = 1.6 \times 10^{-19}$ coulombs, and $d\lambda$ = 200Å.

Summation of the results given in Table 2/2 produce a value for $\sum N_\lambda \, q_\lambda \, t_\lambda$ and therefore the anode current can be calculated from equation 2/2. From the results discussed in section 2.1.1, it was anticipated that the thermocouple temperature lagged behind the surface of the graphite plate by approximately 40°C for a heating rate of 30°C/sec. in the 400-500°C range. Therefore Table 2/3 contains the theoretical values for the anode current

Table 2/2

Black Body Radiation

		OB10 filter		2x OB10 filters	
λ (Å)	N_λ	$N_\lambda t_\lambda$	$N_\lambda t_\lambda q_\lambda$	$N_\lambda t_\lambda$	$N_\lambda t_\lambda q_\lambda$
4000	4.97×10^{8}	2.85×10^{8}	3.42×10^{7}	1.62×10^{8}	1.95×10^{7}
4200	3.25×10^{9}	1.95×10^{9}	2.07×10^{8}	1.17×10^{9}	1.24×10^{8}
4400	2.20×10^{10}	1.12×10^{10}	1.05×10^{9}	6.27×10^{9}	5.90×10^{8}
4600	1.28×10^{11}	6.24×10^{10}	4.99×10^{9}	2.99×10^{10}	2.40×10^{9}
4800	5.30×10^{11}	1.70×10^{11}	1.12×10^{10}	5.43×10^{10}	3.58×10^{9}
5000	2.34×10^{12}	2.34×10^{11}	1.22×10^{10}	2.34×10^{10}	1.22×10^{9}
5200	7.80×10^{12}	2.73×10^{11}	1.06×10^{10}	9.55×10^{9}	3.73×10^{8}
5400	2.65×10^{13}	5.30×10^{11}	1.54×10^{10}	1.06×10^{10}	3.07×10^{8}
5600	7.80×10^{13}	7.80×10^{11}	1.56×10^{10}	7.80×10^{9}	1.56×10^{8}
5800	2.05×10^{14}	6.15×10^{11}	7.40×10^{9}	1.84×10^{9}	2.21×10^{7}
$\sum$			7.84×10^{10}		8.79×10^{9}

at 500°C and the experimental values at a thermocouple temperature of 460°C. The thermocouple temperatures (T_c), for which the theoretical and experimental values were equal, are also given.

Table 2/3

Black body radiation from graphite plate

Filter	Anode current (10^{-9} amps.) Theoretical (500°C)	Experimental (460°C)	T_c
OB10	57	111	445°C
2XOB10	6.4	17	440°C

Considering the inaccuracy in the estimate of the temperature lag and the rapid increase of black body radiation with temperature, the agreement obtained between the theoretical and experimental values was thought to be satisfactory.

2.2.3. Accuracy of light measurements

The accuracy with which the light output could be measured was governed by the noise level of the voltage output from the d.c. amplifier and the stability of the overall gain of the system.

The optimum E.H.T. voltage for the photomultiplier was determined by measuring the ratio of the anode current when exposed to the standard light source, without a filter, to the photomultiplier dark current for voltages ranging from 0.8 to 1.5 kilovolts (fig. 2/11). The voltage finally selected was that which provided the maximum value for this ratio or, in the case of type 9558, the maximum voltage of the E.H.T. unit. Table 2/4 contains the values for the anode current, when exposed to the standard light source, and the dark current for these voltages.

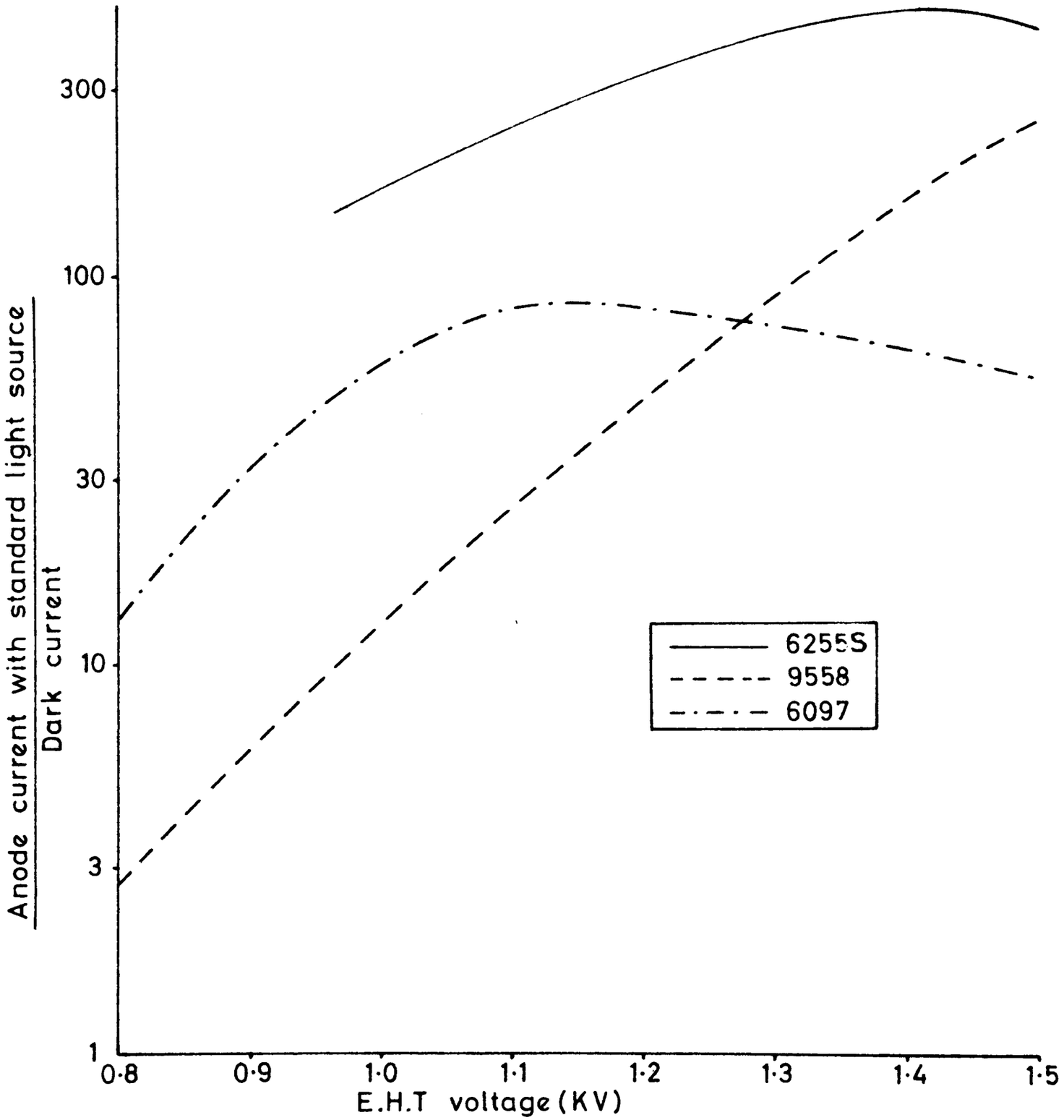

300
100
30
10
3
1
Anode current with standard light source / Dark current
0·8
0·9
1·0
1·1
1·2
1·3
1·4
1·5
E.H.T voltage (KV)
6255S
9558
6097

Fig 2/11

Table 2/4

Comparison of photomultipliers

	6097	6255S	9558
Operating voltage	1.14 kv.	1.4 kv.	1.5 kv.
Anode current for standard light source.	0.58 μa.	0.44 μa.	0.48 μa.
Dark current	7 mμa.	1 mμa.	2 mμa.
D.C. amplifier noise (N_d)	2 mv.	2 mv.	2 mv.
Photomultiplier noise (N_p)	6 mv.	1.5 mv.	1.5 mv.
$\sqrt{N_d^2 + N_p^2}$	6 mv.	2.5 mv	2.5 mv.
Total noise in operation (N).	10 mv.	6.5 mv.	4.5 mv.

The peak-to-peak values for the d.c. amplifier noise (N_d) and the total noise $(N_d^2 + N_p^2)^{1/2}$, when no light reached the photomultiplier, were measured for an anode load of 10^4 ohms and a.d.c. amplifier gain of 1000 (Table 2/4). Increasing the anode load resulted in an increase in both the d.c. amplifier and photomultiplier noise. The total peak-to-peak noise (N) when the photomultiplier was used to measure a typical glow curve on either the fast heating (6097) or the slow heating (6255S and 9558) is also given in Table 2/4.

The total noise (N) was essentially the same for high and low light intensities and was not a constant percentage of the voltage output. It was therefore thought to be due either to the statistical nature of the process by which light emission occurred (section 3.1) or to magnetic fields produced by the heating current, rather than to small changes in the heating rate. These results indicated that, although type 6255S was vastly superior

to type 6097 when compared in terms of the signal to dark current ratio, when the total noise was taken into account it was only marginally superior.

Using photomultiplier type 6255S in conjunction with the slow heating apparatus (heating rate 1°C/sec.), the voltage output from the d.c. amplifier (gain = 10^3, anode load = 10^4 ohms), for a typical natural glow curve, was 20 millivolts and hence the signal to noise ratio was 3:1. The slow heating apparatus was not therefore suitable for the measurement of the natural thermoluminescence from ceramics and hence the third age determination programme was carried out, at a heating rate of 20°C/sec., on the graphite plate using the servo-system. The accuracy of the results obtained with this system is discussed in Chapter 12. However when the slow heating apparatus was used to measure the thermoluminescence from a sample, subjected to alpha or beta irradiations, a typical value for the voltage output, following a radiation dose of 10^4 rads, was 1 volt and hence the signal to noise ratio was 150 : 1. Therefore the error in these measurements due to photomultiplier and d.c. amplifier noise was less than ± 1%.

The overall gain of the photomultiplier, d.c. amplifier and X - Y recorder was measured after each glow curve using the 0.24 microlumen standard light source (section 1.1). The accuracy of this measurement was ± 2%. The gain of the system decreased by approximately 10% during a working day and this was thought to be caused by the decrease in gain of the photomultiplier. Because of heat conducted from the furnace, the temperature of the outer case of the photomultiplier rose by between 10-20°C when used with the slow heating apparatus and figures provided by E.M.I. showed

that, if such temperature increases occurred for the cathode and dynodes, the gain of the photomultiplier would decrease by approximately 20%.

2.2.4. Linearity of response of the photomultiplier

The linearity of response of photomultiplier type 6255S, plus a single OB10 filter, to increasing light intensity was checked using a scintillator activated by beta radiation. The diameter of this light source was 0.1 inches and its intensity was unchanged by exposure to daylight.

The photomultiplier was mounted horizontally on an optical bench in a dark room; the light level was such that, when the shutter protecting the photomultiplier was opened, the increase in anode current was less than 2×10^{-9} amps. The light source was then placed along the axis of the photomultiplier at distances of 0.5 - 27 inches from its window and the voltage output was measured.

The solid angle (Ω) subtended at the source by the photomultiplier is given by:

$$\Omega = 2\pi \left[\frac{(d^2 + a^2)^{1/2} - d}{(d^2 + a^2)^{1/2}}\right]$$

where d = perpendicular distance between the source and the photomultiplier cathode,

2a = diameter of cathode (1.74 inches).

The light source was regarded as a point source and therefore the solid angles calculated for the different values of d were proportional to the light reaching the photomultiplier. Fig. 2/12 shows the solid angle plotted

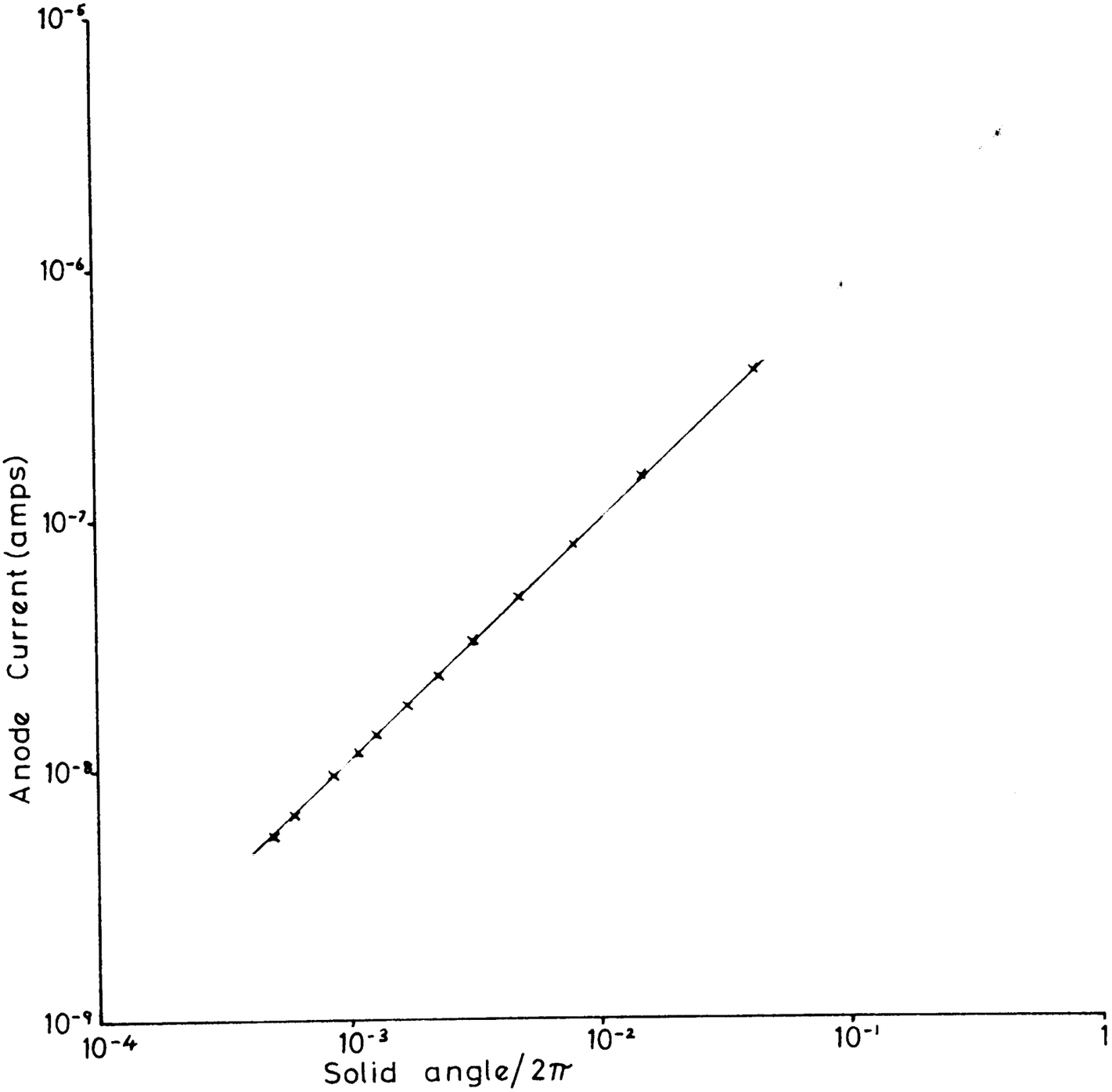

10^{-5}
10^{-6}
10^{-7}
10^{-8}
10^{-9}
Anode Current (amps)
10^{-4}
10^{-3}
10^{-2}
10^{-1}
1
Solid angle/2π

Fig. 2/12

against the anode current. In the range 5.5×10^{-9} - 3×10^{-6} amps., no systematic deviation from a straight line was observed and the deviation for individual points was less than ± 3%.

The anode currents observed when making thermoluminescence measurements, at a heating rate of 1°C/sec . ranged from 2×10^{-9} amps. for a typical natural glow curve to 5.6×10^{-6} amps. for a sample of sherd [illegible] subjected to a 1000 minute beta irradiation. The above results indicated that for the major part of this range, the output from the photomultiplier increased linearly with the amount of light reaching its cathode.

CHAPTER 3 GLOW CURVE THEORY

Fig. 3/1 shows the model, suggested by Halperin and Braner (1960), for the energy levels in a non-conducting material. Situated in the energy gap between the valence and conduction bands are two basic groups of energy levels, the electron traps and the luminescence centres. These energy levels are due to imperfections in the crystal lattice in the form of impurity atoms, vacancies in the lattice structure or interstitial atoms.

For an unirradiated material, the luminescence centres are filled with electrons while the electron traps are empty. The effect of high energy radiation is to excite electrons from the valence to the conduction band. A percentage of these electrons fill electron traps while a percentage of the electrons in the luminescence centres fill the holes created in the valence band, the mechanism of trap filling is discussed in more detail in section 4.3.1. At the completion of the irradiation there are a number of filled electron traps and an equal number of empty luminescence centres. If the material is now heated, the trapped electrons are thermally excited into the conduction band and then recombine with the luminescence centres with the emission of light or are retrapped. The temperature at which they are excited into the conduction band depends on the trap depth (E) and its frequency factor(s) while the wavelength of the light emitted depends on the energy gap between the conduction band and the luminescence centre. It is equally valid to regard the luminescence centres as hole traps and the electron traps as luminescence centres, in which case the trapped holes are thermally excited into the valence band and recombine with the trapped

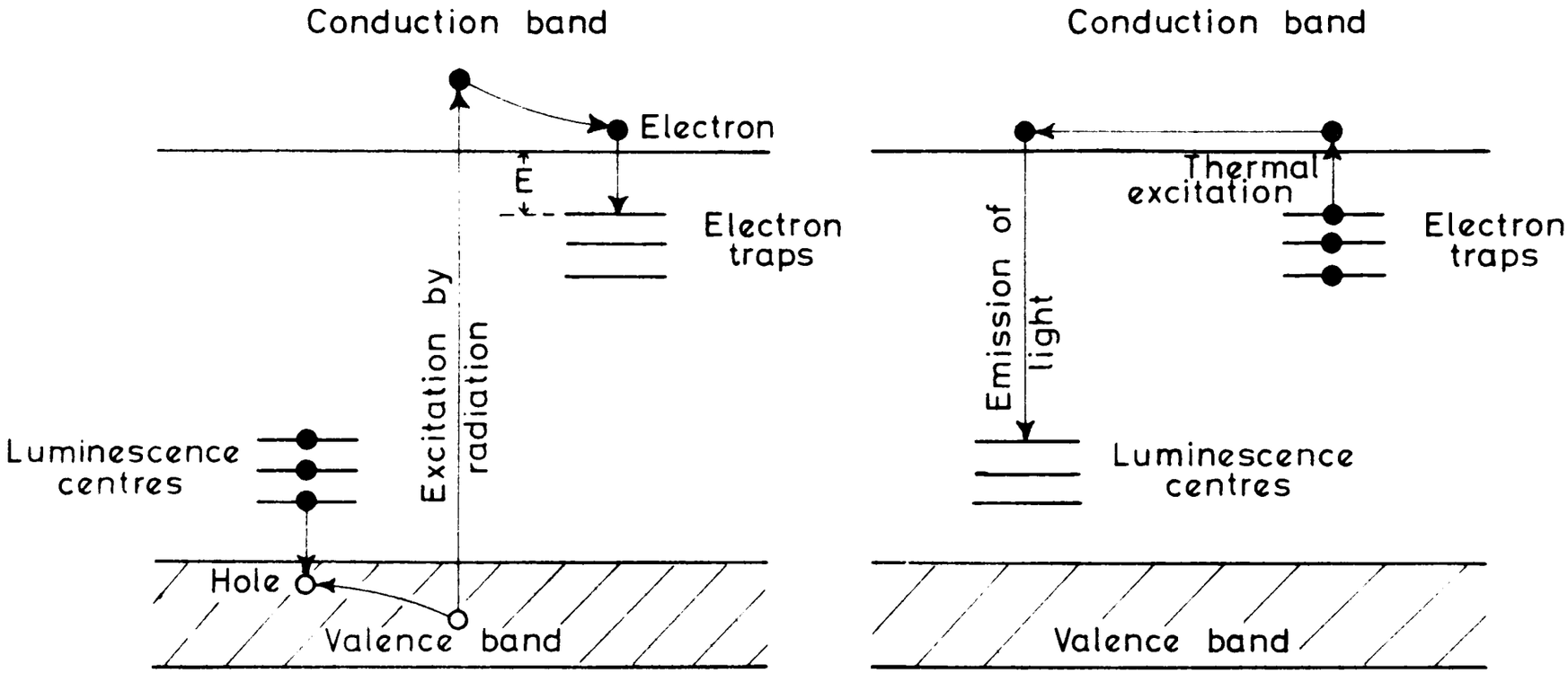

Conduction band
Electron
E
Electron traps
Excitation by radiation
Luminescence centres
Hole
Valence band
(a) IRRADIATION
Conduction band
Thermal excitation
Electron traps
Emission of light
Luminescence centres
Valence band
(b) HEATING

Fig 3/1

electrons with the emission of light. For simplicity however the theory for thermoluminescent emission (section 3.1) is presented in terms of electron traps only.

If the number of electron traps, filled since the pottery was fired, is to be used as a criterion for age determination, then the extent to which the traps have been emptied by thermal excitation at room temperature if of fundamental importance. Consequently an attempt was made to determine the trap depths (E) and their associated half-lives (τ) at room temperature in the case of those ceramics whose glow curves contained reasonably well-defined peaks (section 3.2).

The optical spectrum of the thermoluminescence was measured, using a series of filters, in order to obtain some information about the position of the luminescence centres in the energy gap between the valence and conduction bands (section 3.3.).

X-ray diffraction patterns were obtained for a number of sherds in order to determine the minerals responsible for the thermoluminescence from ceramics and the glow curves for two sherds (k and 6b4), from which pieces of limestone and quartz could readily be extracted, were studied (section 3.4.)

3.1. Glow curve theory

For electrons in traps at an energy, E, below the conduction band, the rate of thermal excitation at a temperature, $T^{o}K$, is given by:

$$\frac{dn}{dt} = -nS \exp\left(\frac{-E}{kT}\right) \qquad \text{---- } 3/1$$

where n = number of trapped electrons at time t,

S = frequency factor,

k = Boltzmann's constant.

If the recombination of the electron, excited into the conduction band, with the luminescence centre predominates over retrapping then the process is monomolecular while if retrapping of the electron occurs the process is bimolecular.

3.1.1. Monomolecular process

In this case the thermoluminescence (I) at time, t, is given by:

$$I(t) = -c'(dn/dt) \qquad \text{——3/2}$$

where c' is a constant. The half-life (τ) for a trapped electron is equal to $\frac{0.69}{S} \exp(E/kT)$.

If the heating rate (dT/dt) is equal to H, then, using equations 3/1 and 3/2, it can be shown (Randall and Wilkins, 1945) that the thermoluminescence, associated with a single trap depth, at temperature, $T^{\circ}K$, is of the form:

$$I(T) = c'n_o S \exp(-E/kT)\exp\left[-\int_{T_o}^{T} \frac{S}{H} \exp(-E/kT)dT\right] \qquad \text{——3/3}$$

where n_o = number of trapped electrons at time, t = 0,

$T_o{}^{\circ}K$ = temperature at time, t = 0.

Initially the thermoluminescence increases with temperature according to the relationship:

$$I(T) = c'n_o S \exp(-E/kT) \qquad \text{——3/4}$$

but as the temperature increases, the number of filled traps decreases and the

second exponential term in equation 3/3 becomes dominant. The thermoluminescence reaches a maximum value at temperature T_g °K and subsequently decreases, reaching zero when all the traps are empty.

The peak temperature (T_g) can be determined by differentiation of equation 3/3 and is given by the relationship:

$$E = k T_g \log_e \left(\frac{Sk T_g^2}{\beta E}\right) \qquad \text{3/5}$$

From these equations it can be seen that the area under the glow curve is proportional to n_0 while the peak temperature, for fixed values of E and S, moves to higher temperatures with increasing heating rate. Similiarly the width of the peak (δ), at half its maximum value, increases with increasing heating rate. Fig. 3/2 shows the theoretical values for T_g and δ plotted against heating rate for an electron trap at depth, E = 1.0 ev., and with a frequency factor, S = 10^{10} sec.$^{-1}$

3.1.2. Bimolecular process

In this case the thermoluminescence depends on the relative number of empty electron traps and luminescence centres available. Assuming that the probability of recombination with a luminescence centre and of retrapping are equal, and that the number of filled traps (n) at energy, E, equals the number of empty luminescence centres (m), then the probability of an electron in the conduction band being captured by an empty luminescence centre is given by (Garlick, 1949):

$$p = \frac{m}{m + (N-n)} = \frac{n}{N}$$

where N = total number of electron traps.

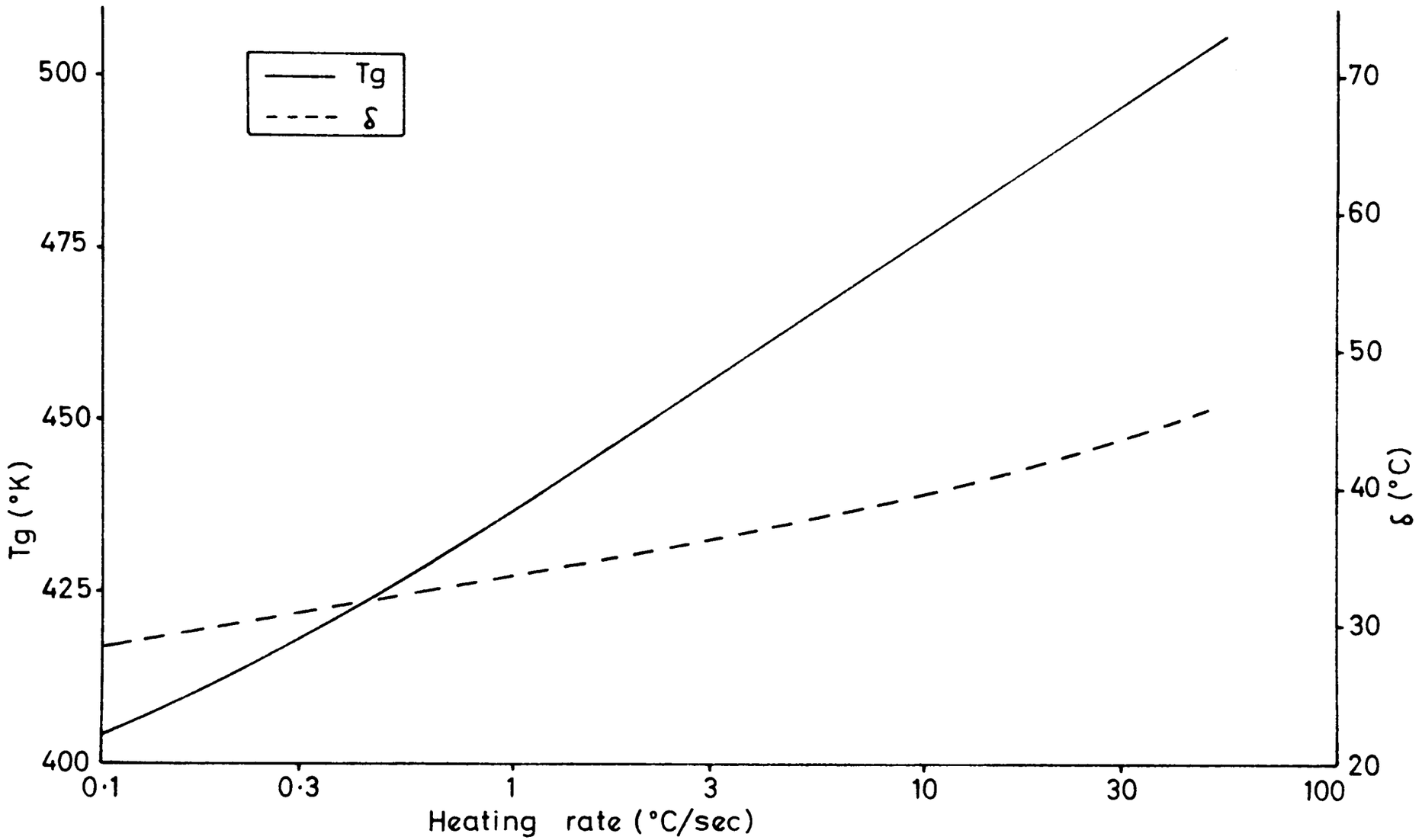

Tg
δ
500
475
450
425
400
Tg (°K)
70
60
50
40
30
20
δ (°C)
0·1
0·3
1
3
10
30
100
Heating rate (°C/sec)

Fig 3/2

Hence from equations 3/1 and 3/2:

$$I(t) = c'\frac{dm}{dt} = -c'\frac{n^2}{N} S \exp\left(\frac{-E}{kT}\right)$$

and therefore the equation for the glow curve in the case of a bimolecular mechanism is given by:

$$I(T) = \frac{c'n_o^2 S \exp(-E/kT)}{N\left[1 + \frac{n_o}{N}\int_{T_o}^{T}\frac{S}{H}\exp(-E/kT)dT\right]^2} \qquad 3/6$$

Initially therefore the thermoluminescence increases with temperature according to the relationship:

$$I(T) = c'n_o^2 S \exp(-E/kT)$$

As for the monomolecular process, the thermoluminescence reaches a maximum value at temperature $T_g{}^oK$ and subsequently decreases to zero. Again the area under the glow curve is proportional to n_o but in this case the peak temperature (T_g) and the shape of the curve are dependent on the total number of traps (N) and the number of filled traps at time t = 0. For fixed values of n_o, N, E and S, the peak temperature increases with increasing heating rate.

3.2. Trap depths and half-lives

From the above calculations it can be seen that, with a single trap depth, the glow curve is a well-defined peak. However the glow curves from ceramics, subjected to high energy radiation, either contained several peaks (fig. 3/3) or the thermoluminescence reached a maximum at approximately 100°C and subsequently decreased throughout the temperature range 100-500°C (fig.3/3)

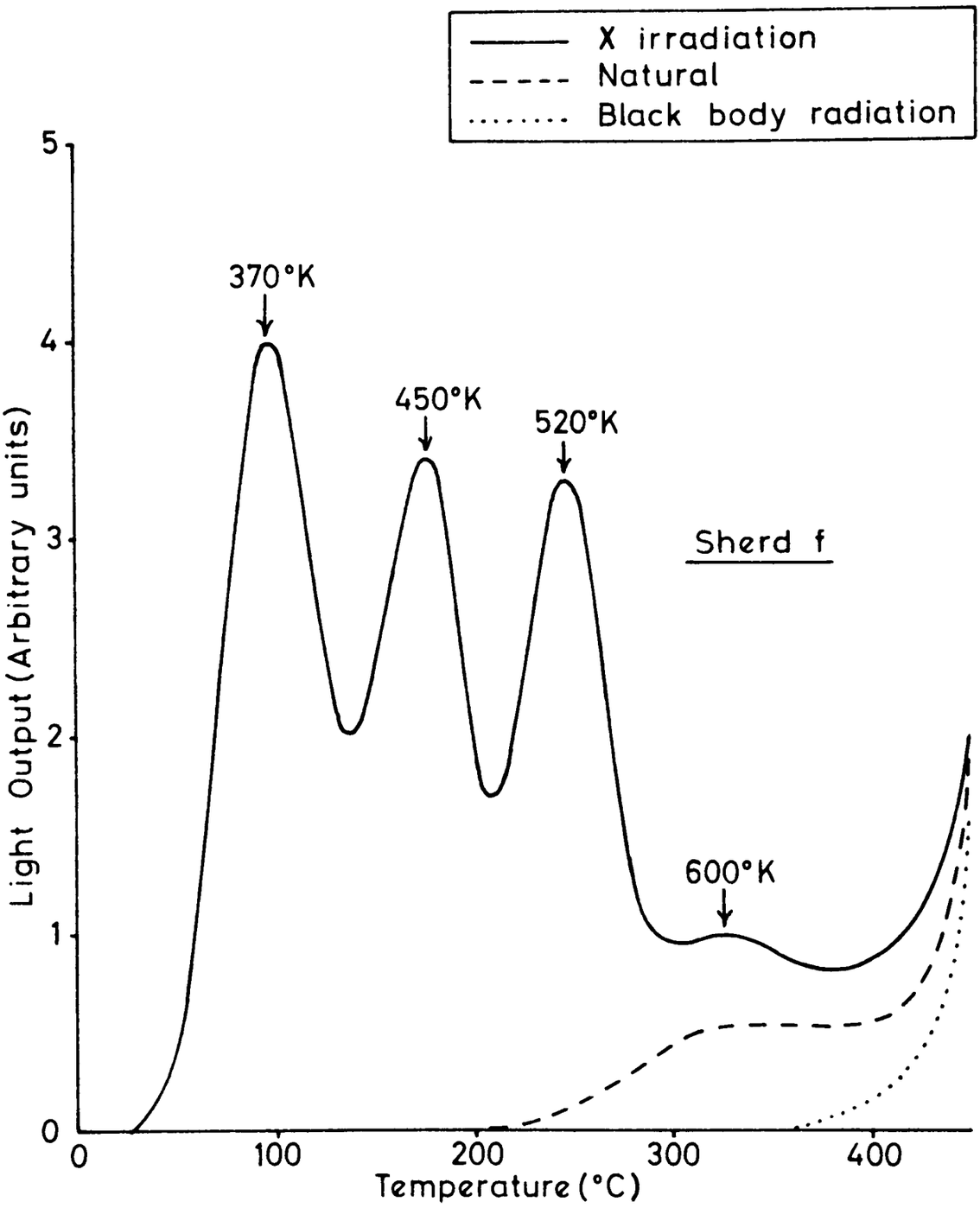

X irradiation
Natural
Black body radiation
370°K
450°K
520°K
600°K
Sherd f
Light Output (Arbitrary units)
Temperature (°C)
0
1
2
3
4
5
0
100
200
300
400

Fig 3/3

In the case of ceramics, therefore, we are dealing either with a series of well defined trap depths or a continuum of trap depths. For the former group, whose glow curves contained several peaks, an attempt was made to determine the associated trap depths and half-lives.

3.2.1. "Initial rise" method

According to equation 3/4, if log I is plotted against 1/T for the rising edge of the glow curve peaks, then the slope is equal to (-E/k) provided each peak corresponds to a single trap depth. The frequency factor, S, can then be determined from equation 3/5 and hence the half-lives for the filled traps can be calculated.

These measurements were carried out with sherds f and k each of which, when subjected to X-irradiation, provided four glow curve peaks (fig. 3/3). The slow heating apparatus ($1^{\circ}C$/sec.) was used and the rising edge of each peak was obtained by first heating the samples to a temperature $40^{\circ}C$ below the peak temperature for 5 minutes. No correction was made for the temperature lag between the surface of the pottery and the thermocouple since the results, presented in section 2.1.2, indicated that this was less than $10^{\circ}C$ in all cases. Fig. 3/4 shows the plots of log I versus 1/T for sherd f, while the values of T_g, E, S and τ for the two sherds are given in Table 3/1.

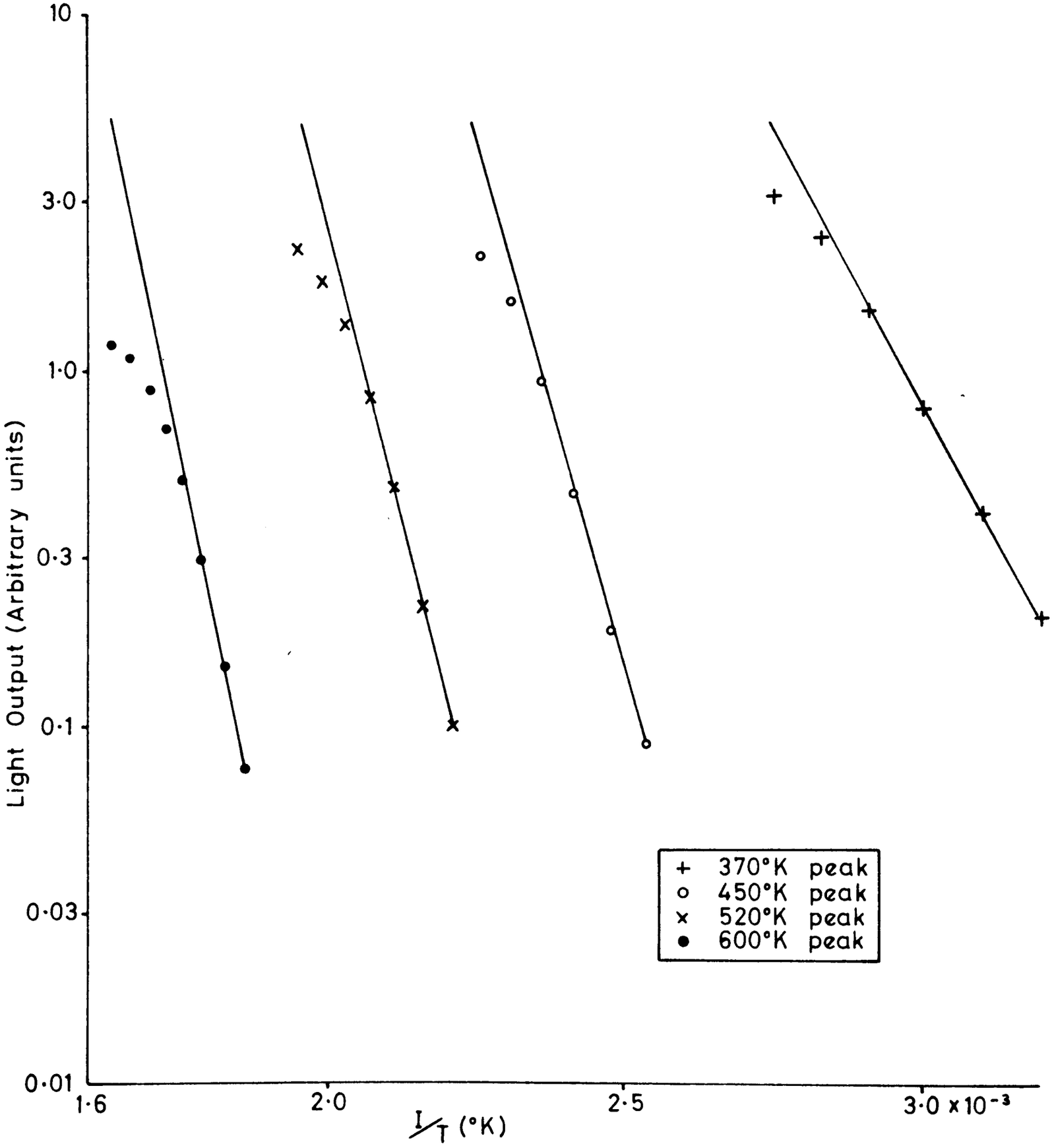

10
3·0
1·0
0·3
0·1
0·03
0·01
Light Output (Arbitrary units)
1·6
2·0
2·5
3·0 x 10⁻³
I/T (°K)
+ 370°K peak
o 450°K peak
× 520°K peak
● 600°K peak

Fig 3/4

Table 3/1

Trap depth and half-life measurements

Sherd	Peak position (T_g K)	Trap depth (Ev.)	Frequency factor (S sec^{-1})	Half-life at 293 K
f	370	0.62	1.4×10^{7}	40 min.
	450	1.12	2.3×10^{11}	685 days
	520	1.31	2.8×10^{11}	2630 years
	600	1.40	2.7×10^{10}	8.9×10^{5} years
k	370	0.61	1.0×10^{7}	32 min.
	450	1.01	1.2×10^{10}	170 days
	520	1.31	2.8×10^{11}	2630 years
	595	1.50	2.0×10^{11}	4.9×10^{6} years

In general terms these results explained the form of the natural thermoluminescence from ceramics. When measured in nitrogen, the natural thermoluminescence was zero at temperatures below 200°C (fig. 3/3) and this agreed with the short half-lives obtained for the 97°C and 177°C peaks. The much longer half-lives observed for the peaks above 200°C explained the presence of natural thermoluminescence in this higher temperature range and indicated that, above 320°C, the filled traps would not be emptied at room temperature during the time that had elapsed (less than 10^{4} years) since the pottery was fired. However the accuracy of the values was extremely doubtful since it was uncertain whether or not the hypothesis, that each peak was associated with a single trap depth, was justified in the case of ceramics and also whether the process involved was monomolecular.

Consequently an attempt was made to determine the trap depth by measuring the peak positions for two different heating rates since, in this case, the existence of other trapping levels adjacent to those producing the peak was less important.

3.2.2. "Peak shift" method

For a monomolecular process it can be shown, from equation 3/5, that E is given by:

$$\frac{E\left(\frac{1}{T_{g1}} - \frac{1}{T_{g2}}\right)}{k} = \text{Log}_e\left[\frac{H_2}{H_1}\left(\frac{T_{g1}}{T_{g2}}\right)^2\right] \qquad \text{3/7}$$

where T_{g1} is the peak position for heating rate, H_1, and T_{g2} is the peak position for heating rate, H_2.

Hence the trap depth can be calculated from the peak position obtained for two different heating rates and the frequency factor can be calculated using equation 3/5.

Measurements were carried out on samples of sherd k which had been subjected to beta irradiations and the slow heating apparatus was used at heating rates of 0.5°C/sec. and 2°C/sec. In section 2.1.2 it was shown that the temperature lag, at 300°C, between the thermocouple and the surface of the sample changed by 18°C when the heating rate was increased from 0.5°C/sec. to 2°C/sec. It was assumed that this change in temperature lag was proportional to the temperature measured by the thermocouple, and it was used to correct the values of T_{g1} and T_{g2} (Table 3/2).

The values for the half-lives obtained by this method agreed, to within an order of magnitude, with those determined using the "initial rise" method.

Table 3/2

Trap depth and half-life measurements for sherd k

Peak temperatures as measured (°K) 0.5°C/sec.	2.0°C/sec.	Temperature correction (°K)	Peak temperatures after correction (°K) 0.5°C/sec.	2.0°C/sec.	E (ev.)	S (sec.$^{-1}$)	Half-lives 293°K	393°K	493°K
357	368	5	357	373	0.92	3.8×10^{11}	220min.		-
434	443	10	434	453	1.16	1.2×10^{12}	670dys.	8min.	-
501	509	14	501	523	1.34	9.2×10^{11}	2150yrs.	31hrs.	37sec.
577	585	19	577	604	1.48	6.8×10^{10}	6.5×10^{5}yrs.	215dys.	56min.

Again they explain, in general terms, the form of the natural glow curves for ceramics and justify the assumption that filled traps associated with glow curve temperatures above 300°C are thermally stable at room temperature. However the half-lives calculated for ambient temperatures of 120°C and 220°C indicated that the temperatures experienced by the pottery since firing would govern the extent to which thermal bleaching occurred above 300°C.

Thermal bleaching experiments carried out on a selection of the sherds used in the third age determination programme are discussed in Chapter 11.

3.3. Wavelength of thermoluminescence

The wavelength (λ) of the thermoluminescence is characteristic of the luminescence centre and is governed by the energy gap for optical transitions between the conduction band and the luminescence centre ($E_c - E_a$) where:-

$$E_c - E_a = \frac{hc}{\lambda}$$

where h = Planck's constant

and c = velocity of light.

Fig. 3/5 shows the potential energies, associated with an electron in a luminescence centre or an electron trap and in the conduction band, plotted against the configuration coordinate, which is a measure of the displacement of the centre or trap from its equilibrium position in the crystal lattice. According to the Franck-Condon principle (Schulmann and Compton, 1962), an electron transition occurs in a time interval so short that the centre is unable to move. Hence to excite an electron from the luminescence centre or electron trap into the conduction band, a photon must have energy, $E_b - E_1$,

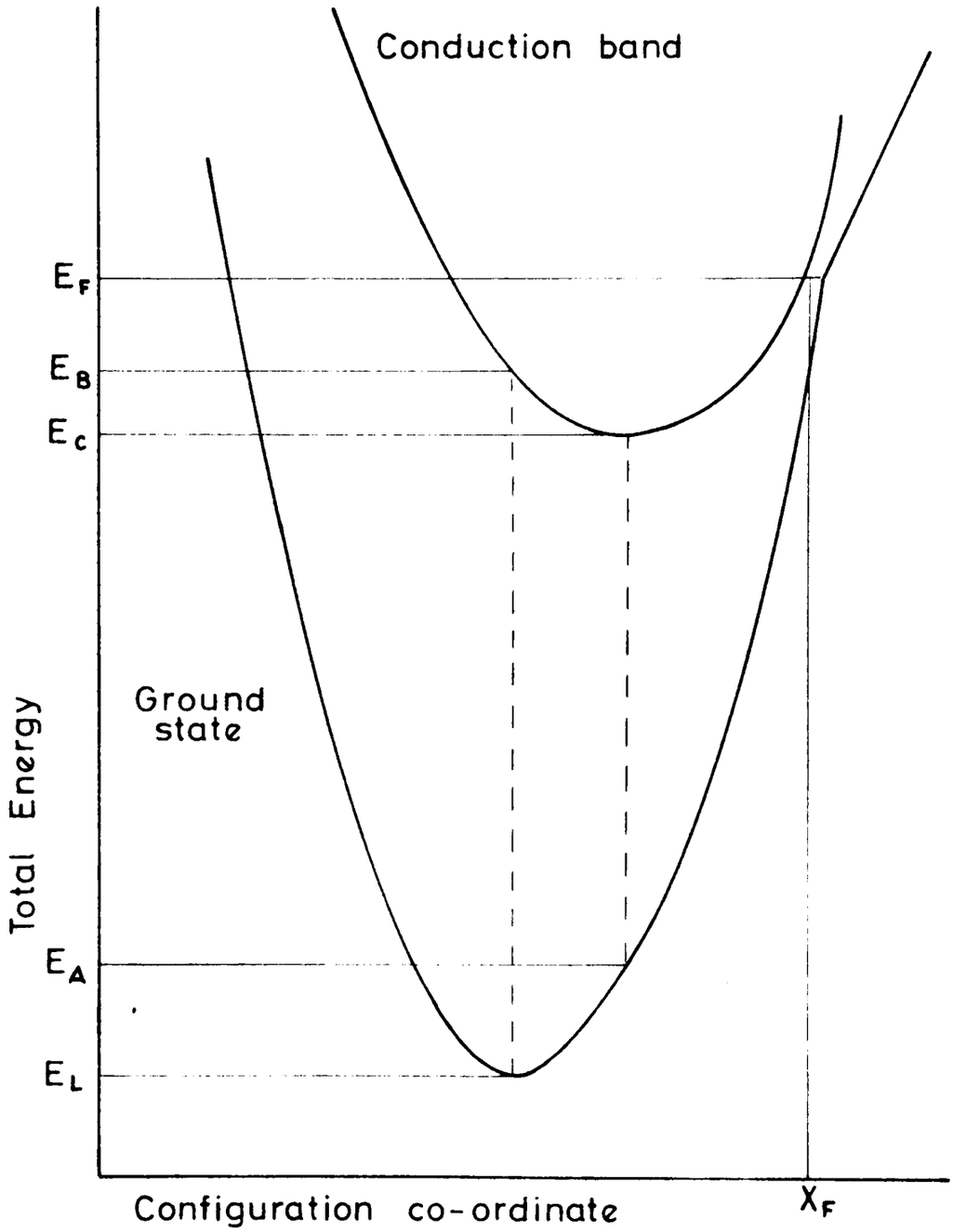

Conduction band
E_F
E_B
E_C
Ground state
Total Energy
E_A
E_L
Configuration co-ordinate
X_F

Fig 3/5

while when the reverse occurs, the emitted photon has energy, $E_c - E_a$, the remainder of the energy being dissipated in the form of heat. For thermal excitation from the ground state to the conduction band, the Franck-Condon principle no longer applies and the energy required is only $E_c - E_1$.

Finally it should be noted that the electron in the conduction band can return to the luminescence centre without the emission of light, if the luminescence centre and conduction band potential curves have the same energy (E_f) at some configurational coordinate (X_f). Increase of temperature can provide the activation energy ($E_f - E_c$) required for a non-radiative transition.

3.3.1. Measurement of optical spectrum

In order to determine whether a specific luminescence centre was associated with each glow curve peak or temperature range, a crude estimate of the spectral composition of the thermoluminescence from sherds k and r was obtained using a series of Chance-Pilkington colour filter glasses.

Samples of the sherds were subjected to 10 minute X-irradiations and their thermoluminescence was measured on the slow heating apparatus (1°C/sec.). The light was detected with photomultiplier type 6255S in conjunction with f filters OW1, OY10 and OY6 and with type 9558 in conjunction with filters OY10, OY6 and OR1. The transmission properties of the filters and the spectral response of the photomultipliers are shown in fig. 3/6 and fig.2/9 respectively.

The light output (L_1) in the spectral range 2300 - 3700 Å is given by the relationship:

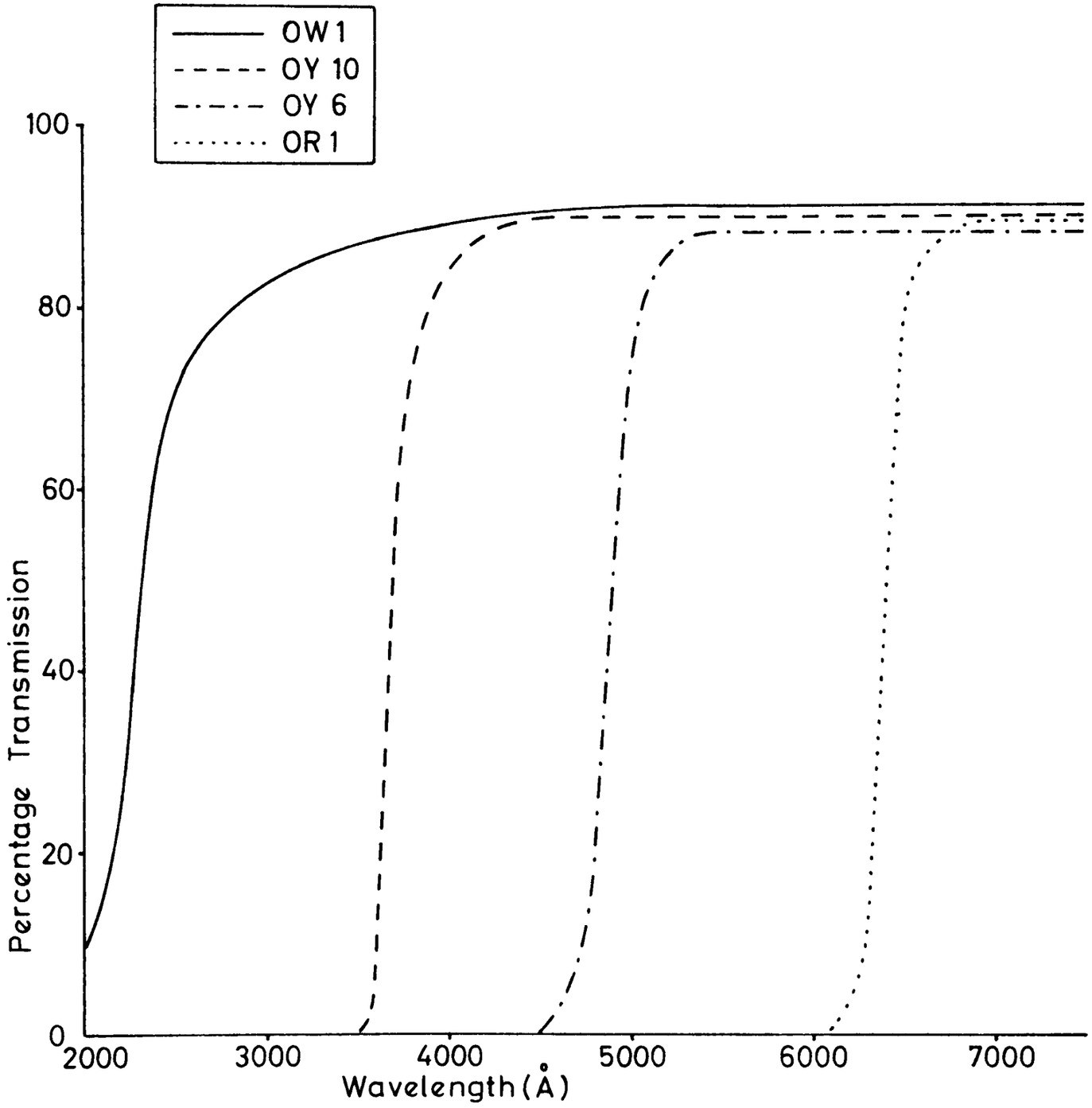

OW 1
OY 10
OY 6
OR 1
100
80
60
40
20
0
Percentage Transmission
2000
3000
4000
5000
6000
7000
Wavelength (Å)

Fig 3/6

$$L_1 = \frac{C'}{q_1 G} \left[A(OW1) - A(OY10) \right]$$

where A (OW1) = glow curve area using OW1 and photomultiplier type 6255S,

A (OY10) = glow curve area using OY10 and photomultiplier type 6255S,

q_1 = average quantum efficiency of photomultiplier type 6255S in the 2300 - 3700 Å range.

G = gain of photomultiplier type 6255S,

C' = constant which includes the transmission properties of the filter and the quartz light guide and which is taken to be the same for all the spectral ranges considered.

Values for the light output in the ranges, 3700 - 4900 Å, 4900 - 6400 Å, and 6400 - 8000 Å, can be similarly calculated for both photomultipliers. A figure for the relative gain of the two photomultipliers was determined by comparing the glow curve areas in the 3700 - 6400Å range and hence comparable figures for all ranges were obtained.

Table 3/4

Optical spectrum of thermoluminescence

(i) Sherd r

Range	Percentage of thermoluminescence in each spectral range			
	75 - 175°C	175 - 250°C	250 - 300°C	300 - 400°C
2300-3700Å	12.6	22.4	28.4	24.6
3700-4900Å	56.1	60.0	54.2	58.8
4900-6400Å	19.5	11.1	7.4	16.6
6400-8000Å	11.8	6.5	10.0	

(ii) Sherd k

Range	Percentage of thermoluminescence in each spectral range			
	75 - 155°C	155 - 220°C	220 - 300°C	300 - 400°C
2300-3700Å	<1	<1	3.7	<1
3700-4900Å	1.8	7.6	15.6	32.5
4900-6400Å	36.8	40.6	46.0	67.5
6400-8000Å	61.0	51.8	34.7	

The percentage contributed by each spectral range in the overall range 2300-8000Å was calculated and the results are presented in Table 3/4. No measurements were possible in the 6400-8000Å range above 300°C since the thermoluminescence was masked by the black body radiation and therefore the percentages given are for the 2300-6400Å range.

The results show that the wavelength of the thermoluminescence emitted by sherd k ranged from 3700-8000Å while for sherd r it was emitted throughout the range 2300-8000Å, thus indicating that there were a wide range of luminescence centres associated with a particular temperature range.

3.4. Nature of traps

In order to determine the minerals responsible for the thermoluminescence from ceramics, X-ray powder diffraction patterns were obtained for a number of the sherds.

The ground-up sample was mixed with gum tragacanth and made into a paste using distilled water. This was then rolled between two microscope slides to form a rod, 1 cm. in length and approximately 0.7 mm. in diameter. The

rod was inserted in a short length of glass capillary tube and held in position by means of Durofix. It was then mounted centrally in a Debye-Scherrer powder camera (Phillips type PW1024/10) and this was loaded, in darkness, with Ilford Industrial X ray film (A764). Four cameras were loaded in the above manner and were set up on a Phillips X-ray diffraction unit (model PW1009). The X ray diffraction pattern was then measured by exposing the samples, which were rotated at 1 revolution per minute, to an X ray tube (Phillips type 25296/52) operated at 50 kilovolts with a 5 ma. filament current. An iron filter was used and the exposure times ranged from 5-20 hours.

Eleven sherds were examined by this method and in all cases the X-ray diffraction pattern for quartz was observed. With seven of these sherds the diffraction pattern for limestone was also present. Freeman (1958), working with clays that contained a high percentage of limestone, showed that dissociation into calcium oxide and carbon dioxide occured in the range 800-900°C depending on the amount of carbon dioxide present in the kiln atmosphere. Therefore the presence of limestone, in the sherds examined, suggested that they had not been fired above 900°C. As anticipated the diffraction patterns associated with kaolin and other clay minerals were not present since these dehydrate at about 600°C and are no longer fully crystalline (Richardson, 1961). The results are presented in Table 3/5a together with a description of the sherd in terms of its colour, its texture and the homogeneity of the body material as seen with the naked eye.

In addition ten of the sherds were analysed for their minor and trace

Table 3/5a

Results of X ray Diffraction measurements

Sherd	Description	Diffraction patterns
c	Red, fine grained homogeneous.	Quartz and Limestone.
d	Red, fine grained, homogeneous.	Quartz and Limestone.
f	Red, fine grained homogeneous.	Quartz and Limestone
g	Red, fine grained homogeneous.	Quartz and Limestone.
h	White, coarse grained homogeneous.	Quartz.
i	Red, fine grained homogeneous.	Quartz and Limestone (weak).
k	Red/grey, coarse grained inhomogeneous.	Quartz and Limestone.
q	Buff, coarse grained homogeneous.	Quartz and Limestone.
r	Grey, coarse grained homogeneous.	Quartz.
t	Red/grey, coarse grained inhomogeneous.	Quartz.
6b4	Grey/brown, coarse grained, inhomogeneous.	Quartz.

The provenance of sherd 6b4 was Lezoux, France and the provenance for the remainder is given in Table 1/1.

Table 3/5b

Spectrographic analysis (% of oxide)

Sherd	Al	Mg.	Fe	Mn	Ti.	Cr.	Ca.	Na.	Ni.
c	7.2	4.3	4.4	0.077	0.57	0.081	>30	1.4	0.018
d	15.5	5.1	8.6	0.18	0.76	0.11	24.0	0.82	0.019
f	10.8	1.7	4.2	0.028	0.48	0.023	19.4	1.2	0.0014
g	10.7	2.8	5.0	0.056	0.68	0.024	>30	1.1	0.0022
h	<0.1	0.043	0.17	0.011	<0.1	nd	0.74	0.51	0.0022
i	9.2	4.1	4.9	0.079	0.69	0.096	7.2	0.93	0.021
k	31.5	0.34	4.3	0.0067	0.74	0.088	>30	0.17	0.0057
q	9.5	7.0	6.5	0.093	0.95	0.096	18.9	2.1	0.026
r	14.1	2.0	7.5	0.017	0.82	0.035	0.84	0.59	0.0029
t	12.9	1.1	4.7	0.0094	0.57	0.028	0.75	0.20	0.0014

constituents using optical emission spectrometry (Richards, 1959). These results are also given in Table 3/5b, the amount of each element being expressed as the percentage of its oxide. The correlation between the presence of the diffraction pattern for limestone and the percentage of calcium was excellent and the latter provided an estimate of the amount of limestone in the pottery. It was not possible to obtain a figure for the amount of quartz present, by this method, since silicon was also present in the clay minerals.

The results suggested that a part of the thermoluminescence from ceramics would be due to the quartz and limestone present in, or added to, the clay used to manufacture the pottery and this was confirmed by work on sherds k and 6b4 (sections 3.4.1 and 3.4.2).

3.4.1. Limestone

Samples of the sherds which contained limestone were subjected to X-irradiation and their glow curves were measured on the slow heating apparatus (1°c/sec.). In the glow curves from sherds d, f, i, k and q, a number of well defined peaks were recorded (fig. 3/3 and 3/7). The temperatures at which these peaks occurred are given in Table 3/6 together with the peak temperatures for a sample of Tarquinia limestone and those reported by Medlin (1959), Zeller (1954) and Debenedetti (1958) for a selection of limestone samples. The agreement between the peak temperatures observed for ceramics and those reported for limestone suggested that the peaks in the former case were in fact due to the limestone in the pottery.

Table 3/6

Glow curve peaks

Sample	Peak position (°C)				
Sherd d	80		175	235	
Sherd f	97		177	247	327
Sherd i	78	124	184	242	
Sherd k	97		177	247	322
Sherd q	85	120	185	260	325
Limestone					
Tarquinia	85			270	330
Medlin	80	140		230	330
Zeller	110			235	312
Debenedetti	135		175	230	360

This hypothesis was confirmed in the case of sherd k. This sherd contained relatively large pieces of limestone and these were easily extracted. The glow curves for the limestone extraction, after being subjected to a 10 minute X-irradiation, was measured and compared with the glow curves from the untreated sherd and from a sample, from which the limestone had been completely removed by leaching with dilute hydrochloric acid. As can be seen from fig. 3/7, the effect of leaching was to remove the peaks at 247°C and 322°C and to reduce the 97°C peak, all of which were prominent in the glow curve for the limestone extraction. The very much larger glow observed for the limestone extraction was due to the fact that its optical absorption was less than for the sherd itself.

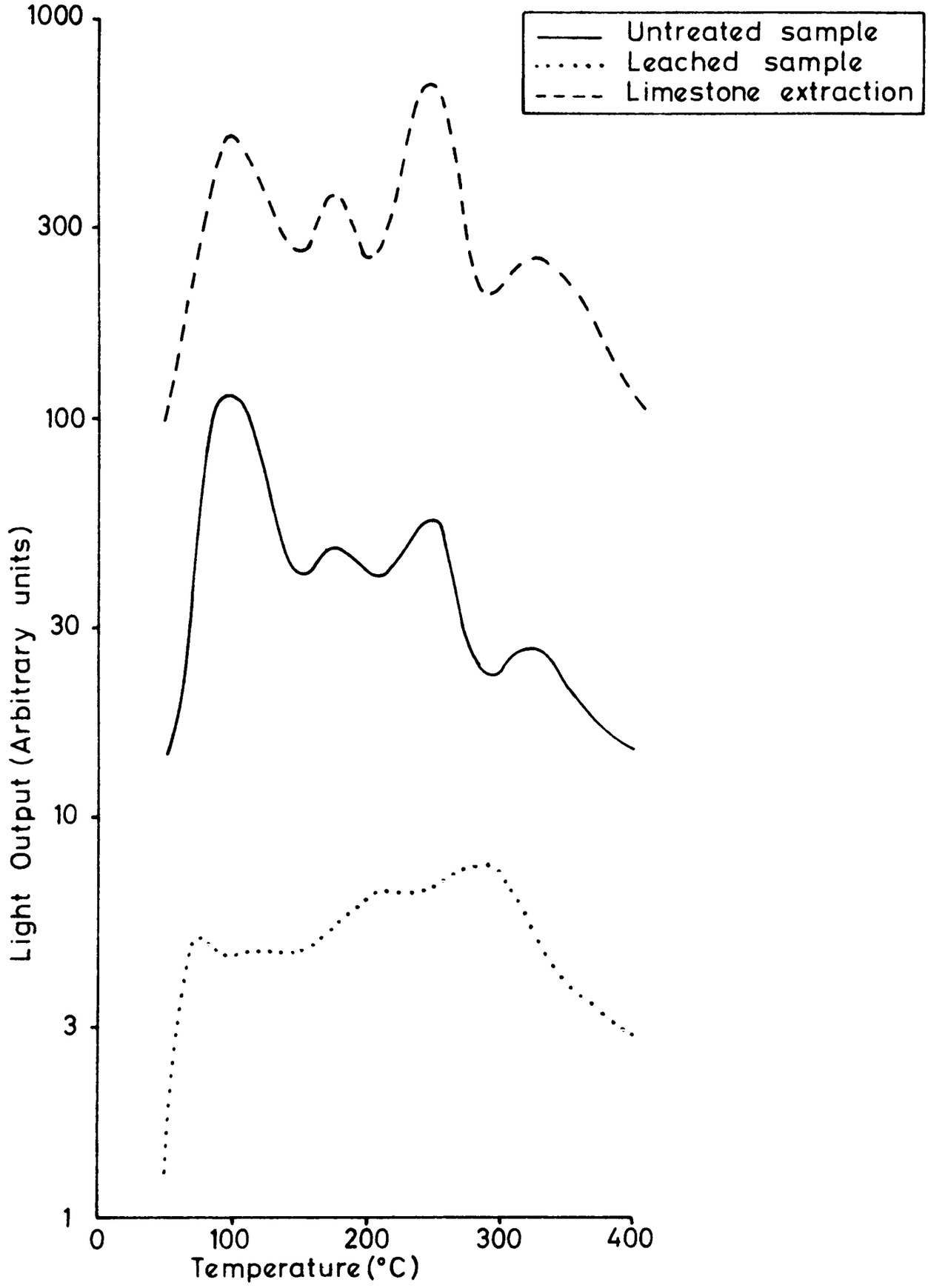

Untreated sample
Leached sample
Limestone extraction
1000
300
100
30
10
3
1
Light Output (Arbitrary units)
0
100
200
300
400
Temperature (°C)

Fig 3/7

The spectral analysis of the thermoluminescence from sherd k (section 3.3.1) showed that the majority of the light was emitted in the 4900-8000Å range. Medlin (1963) using samples of calcium carbonate, to which specific impurities had been added, showed that for the 80°C and 230°C peaks, the thermoluminescence was emitted in the 5000-8000Å range with maximum emission occurring at 6500Å. He was also able to establish that the 80°C and 230°C peaks for limestone were caused by the presence of Mn^{++} ions and that the 330°C peak was due to Mn^{++} ions in combination with Ni^{++} ions. Electron spin resonance measurements carried out at Hull University on two of the sherds, listed in Table 3/6 (Garlick, 1964), established the presence of manganese centres.

3.4.2 Quartz

Sherd 6b4 contained relatively large pieces of quartz and, as with the limestone, these were removed. The glow curve for the quartz extraction, after subjection to X-irradiation, was compared with those obtained using the untreated sherd and the part remaining after the pieces of quartz had been removed. This latter sample still contained some quartz since it was only possible to remove the larger pieces. Because of this and the fact that the only peak was at 100°C, the results were not so conclusive. However it can be seen from fig. 3/8 that a significant proportion of the thermoluminescence from the sherd was due to the quartz. Again the larger glow observed for the quartz extraction was due to its lower optical absorption.

Medlin (1963), working with X-irradiated samples of natural quartz, observed a thermoluminescence peak at 80°C and continuous, decreasing light

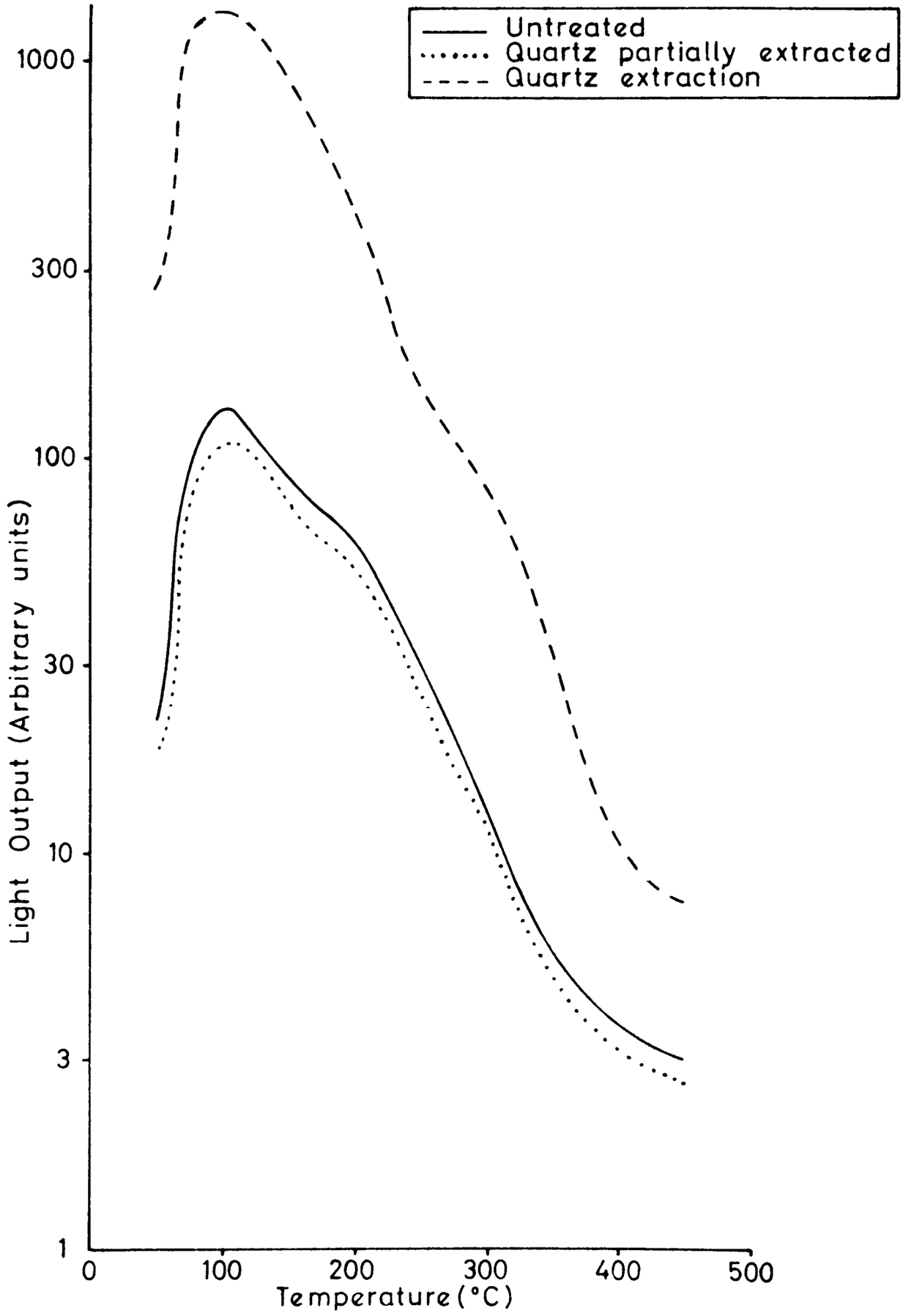

Untreated
Quartz partially extracted
Quartz extraction
1000
300
100
30
10
3
1
Light Output (Arbitrary units)
0
100
200
300
400
500
Temperature (°C)

Fig 3/8

emission from 80°C to 330°C. He was unable to associate this thermoluminescence with any impurities present in the quartz and suggested that it was due to non-impurity lattice imperfections. He showed that, for the 80°C peak, the maximum emission occured at 3800Å and that there was a long wavelength tail extending to 7000Å. This spectral distribution was similar to that obtained from sherd r (section 3.3.1) which was also known to contain quartz (Table 3/5).

3.5. Conclusions

The results described above indicate that quartz and limestone make a significant contribution to the thermoluminescence from ceramics. The contribution from the clay minerals is more difficult to ascertain but since they will retain some degree of crystalline order, although not producing an X ray diffraction pattern, their contribution cannot be disregarded.

The complex nature of the glow curves prevent an accurate determination of the trap depths and half-lives but the results suggest that, above 350°C, the trapped electrons are stable at room temperature and this was confirmed for a number of sherds by the thermal bleaching results described in Chapter 11.

PART II

CHAPTER 4. RADIATION EFFECTS - REVIEW

The natural radiation to which a pottery sherd is subjected consists principally of alpha particles (4.01 - 8.78 Mev.), beta particles (17 kev. - 3.26 Mev.) and gamma rays (15 kev. - 2.62 Mev.) from the uranium 238 and thorium 232 series, together with 1.4 Mev. beta particles and 1.5 Mev. gamma rays from potassium 40. As indicated in the Introduction, the interaction of this radiation with the target material can be divided into two classes; elastic collisions which result in the displacement of atoms from their equilibrium position in the crystal lattice and thus the creation of electron and hole traps, and inelastic collisions in which energy is lost through electronic excitation. The latter interaction can result in ionization of electrons into the conduction band and thus the filling of these newly created traps, as well as the filling of existing traps.

In section 4.1 a rough estimate is made of the number of atomic displacements achieved by an alpha particle and its associated recoil nucleus. On the basis of these calculations, the total number of displacements due to the natural radiation dose received by a typical sherd, since firing, and the number due to a 1000 minute irradiation with a polonium 210 alpha source are calculated (sections 4.1.4 and 4.1.5).

The effect of high energy radiation on the physical properties of non-metals is described briefly in section 4.2. The difficulties involved when thermoluminescence measurements are used for the study of radiation effects are discussed in section 4.3, while section 4.4 contains a summary of the

work carried out on archaeological ceramics, in order to establish a technique for age determination.

4.1. Theory for production of atomic displacements

The alpha and beta particles can produce atomic displacements directly but with gamma rays, the primary effect is the formation of high energy electrons and the atomic displacements result from the interaction of those electrons with the atoms of the target material. In considering the effects of the alpha and beta particles emitted from the radioactive impurities in the sherd, the interaction of the recoil nuclei must also be taken into account. The recoil energy of a nucleus (A.W. = 222), following the ejection of a 6.3 Mev. alpha particle, is 113 kev. while that of a potassium 40 nucleus, following the ejection of a 1.4 Mev. beta particle, is only 19 ev.

While the particles have a high energy, inelastic collisions predominate and elastic collisions only become important as the particles slow down. The criterion for defining the limiting energy for ionisation (E_i) is that the velocity of the particle must be equal to, or greater than, the velocity of the electrons in the target material. Seitz (1949) has suggested that, for non-metals:

$$E_i = \tfrac{1}{8} (M_1/m)I$$

where M_1 = mass of the moving particle,

m = mass of the electron,

I = lowest electron excitation energy, given by the low-energy limit of the optical absorption band.

If the value of I is taken as 8.6 ev., the energy of the main optical absorption band of quartz, then E_i equals 7.9 kev. for an alpha particle, approximately 1 ev. for a beta particle and 440 kev. for the recoil nucleus. Consequently the beta particles lose the majority of their energy through inelastic collisions throughout their range while the recoil nuclei lose their energy through elastic collisions. Seitz has also shown that, for particle energies greater than E_i, the ratio (R) of the energy expended on ionisation to that expended on elastic collisions is approximately 1000 : 1. Therefore, as far as the creation of traps by the natural radioactive impurities in the ceramic is concerned, the beta particles are unimportant and the main agents, for trap creation, are the recoil nuclei and the alpha particles.

The calculation of the total number of atomic displacements falls essentially into two parts. First the average energy imparted by the incident particle to the target atom, when the latter is displaced, must be determined (section 4.1.1) and then the number of secondary displacements due to this recoil atom is calculated (section 4.1.2). From these figures, the total number of displacements due to a single alpha particle and recoil nucleus are calculated (section 4.1.3) and the values are used to determine the number of displacements due to the natural radioactive impurities in the ceramic (section 4.1.4) and to an irradiation with a polonium 210 alpha source (section 4.1.5).

4.1.1. Interaction of incident particles

According to Seitz (1949) the energy expended, by an alpha particle or recoil nucleus, in elastic collisions (E_c) in being brought to rest in the target material is:

$$E_c = E_i + \frac{(E - E_i)}{R} \qquad \text{---- } 4/1$$

where E = initial energy of the incident particle.

The approximate values for E_c and E_i are given in Table 4/1 for 1.8 Mev. and 6.3 Mev. alpha particles and for a 113 kev. recoil nucleus of atomic weight, 222. The target material is assumed to be monatomic with an atomic weight (M_2) of 28, the value of I is taken as 8.6 ev. and R is assumed to be equal to 1000.

The energy transferred to the lattice atom, in an elastic collision, ranges from zero in glancing collisions to a maximum, E_m, which is transferred in a head-on collision. From energy and momentum conservation it can be shown that:

$$E_m = 4\frac{M_1 M_2}{(M_1 + M_2)^2}E \qquad \text{---- } 4/2$$

The average energy ($\bar{E}$) imparted to the target atom when a displacement occurs, will depend on the nature of the interaction between the two particles and this is determined by their distance of closest approach, b. When b is very much less than a, the screening radius, there is virtually no screening of the nuclei by the electron clouds. Nuclear Coulomb repulsion produces the deflection and the Rutherford scattering laws can be applied. When b is very much greater than a, the screening is almost

complete and scattering is of the hard sphere type. The critical energy (E_a), for which b = a, is given by (Dienes and Vineyard, 1957):

$$E_a = E_R \left[2(M_1 + M_2)/M_2\right] Z_1 Z_2 (Z_1 + Z_2)$$

where E_R = 13.54 ev., the Rydberg energy,

Z_1 and Z_2 = the atomic numbers of the incident particle and the target atom respectively.

For an alpha particle in a target material of atomic number, 14, E_a equals approximately 2 kev. and therefore, for the majority of its range, the interaction takes the form of Rutherford collisions. In this case, small energy transfers are more probable than large and the average energy imparted to the target atom, when a displacement occurs, is:

$$\bar{E} = \left(\frac{E_d\, E_m}{E_m - E_d}\right) \log_e \left(\frac{E_m}{E_d}\right)$$

where E_d is the minimum energy that must be transferred to the target atom in order to displace it from its normal lattice position to the closest interstitial position where it will be stable. The value of E_d has been determined for a number of materials (Billington and Crawford, 1961) and is of the order of 25 ev.

For the recoil nucleus, E_a is approximately 8 Mev. and therefore the 113 kev. recoil nucleus will interact through hard sphere collisions and in this case:

$$\bar{E} = \frac{E_m - E_d}{2}$$

The values for E_m and $\bar{E}$ are given in Table 4/1.

4.1.2. Behaviour of primary recoils

The recoil lattice atom, produced by interaction with the incident high energy particle, will undergo secondary collisions with the lattice atoms resulting in a displacement cascade. The value of E_a for the recoil lattice atom is approximately 36 kev. and, on the basis of the values obtained for $\bar{E}$, it is reasonable to assume that the recoil lattice atoms interact by means of hard sphere collisions. In which case it can be shown (Dienes and Vineyard, 1957) that the average value for the number of displacements resulting from each primary recoil lattice atom (ν) is:

$$\nu = \frac{\bar{E}}{2E_d} \quad \text{for } E_i > \bar{E} > 2E_d \qquad \text{4/3}$$

For the recoil lattice atom, E_i is approximately equal to 55 kev. so that loss of energy through inelastic collisions can be neglected.

4.1.3. Total number of displacements

From equations 4/1 and 4/3, it can be seen that the total number of displacements (N), produced when a single incident particle is brought to rest in the target material, is:

$$N = \left[E_i + \frac{(\bar{E} - E_i)}{R} \right] \frac{R_d}{2E_d} \qquad \text{4/4}$$

where R_d is the fraction of the total energy, dissipated in elastic collisions, which is expended in producing atomic displacements rather than in exciting lattice vibrations. For the alpha particles which interact through Rutherford collisions for the majority of their range, R_d equals approximately 0.5 and for the recoil nuclei (A.W. = 222) which interact through hard sphere collisions, it is approximately unity. Using the value of 25 ev. for E_d,

the corresponding values for N have been calculated and are given in Table 4/1.

Table 4/1

Total number of atomic displacements

Particle	Alpha	Alpha	Recoil nucleus
M_1	4	4	222
E	1.8 Mev.	6.3 Mev.	113 kev.
Ei	7.9 kev.	7.9 kev.	440 kev.
Ec	9.7 kev.	14.2 kev.	113 kev.
E_m	780 kev.	2.75 Mev.	45 kev.
$\bar{E}$	260 ev.	290 ev.	22.5 kev.
N	97	142	2260

Using the analysis presented above, the number of displacements produced by a 1.4 Mev. beta particle would be approximately 10. However the 1.4 Mev. beta particle travels at relativistic velocities and although the scattering, involved in collisions that produce displacements, is primarily due to the Coulomb interaction between the electron and the target nucleus, the non-relativistic Rutherford scattering law is inadequate. Hence the above analysis is not strictly applicable to beta particles.

In addition to producing displacements by direct collision with the lattice atoms, ionising radiation, such as beta particles and gamma rays, can displace atoms by a number of indirect processes. These will be discussed in Chapter 6.

4.1.4. Displacements due to natural radioactivity

The figures presented in Table 4/1 indicate that the alpha particles emitted by the uranium 238 and the thorium 232 impurities, together with their associated recoil nuclei, are expected to be the principal cause of the atomic displacements occurring in ceramics since firing. The number of disintegrations per gram per thousand years (N) can be calculated from the number of alpha counts per second (α) recorded by the scintillation counter described in section 1.3. Reid (1964) has shown that:

$$N = 1.58 \times 10^{12} \times \alpha \qquad 4/5$$

Assuming, for simplicity, that all the alpha particles are emitted through the decay of the uranium series and that the U^{238} is in equilibrium with its decay products, then the average energy of the alpha particles is 6.3 Mev. and the average atomic weight of the recoil nuclei is 222. Hence the average number of displacements associated with a disintegration is approximately 2400 (Table 4/1) and from equation 4/5, the number of displacements per gram per thousand years (D) is given by:

$$D = 3.8 \times 10^{15} \times \alpha \qquad 4/6$$

For a typical sherd, α equals 10^{-2} counts per second and therefore, assuming an atomic weight of 28 approximately 2 in 10^9 of the atoms are displaced from their equilibrium positions in the crystal lattice in one thousand years.

4.1.5. Displacements due to Po^{210} alpha sources

In order to calculate the number of atomic displacements produced in the pottery samples due to irradiation with the polonium 210 alpha sources

(Radiochemical Centre, Source nos. PDD/10M and PDD/50M), it was first necessary to determine the number and energy of the alpha particles reaching the sample. The initial strength of 50 millicuries stated by the manufacturers and the 5.3 Mev. energy of the alpha particles could not be used in these calculations because of the unknown absorption of energy in the source itself, the mica window (thickness = 1 mgm./cm.^{2}) and the air-gap between the source and the sample.

The energy and number of alpha particles reaching the pottery samples was determined for a source of nominal strength, 4 millicuries (Appendix 1). The values are given in Table 4/2, together with the values after a mylar window (thickness = 1.5 mgm./cm.^{2}) had been added. In practice a mylar window was added to the alpha sources in order to keep them sealed since, after a few months, the mica window began to crack as a result of the intense irradiation to which it was subjected.

Table 4/2

Energy and number of alpha particles reaching sample

	No mylar window	Mylar window
No. of particles per sec.	$(3.1 \pm 0.3) \times 10^7$	$(2.7 \pm 0.5) \times 10^7$
Average energy (Mev.)	1.8 ± 0.4	0.7 ± 0.2

From the figures presented in Tables 4/1 and 4/2, it is seen that the number of atomic displacements (D), produced in a 15 mgm. sample of pottery when irradiated for t seconds with a polonium 210 source of nominal strength, R millicuries and without a mylar window is given by:

$$D = \frac{97 \times 3.1 \times 10^7 \times t \times R}{4}$$

$$= 7.5\ t\ R \times 10^8 \qquad 4/7$$

In practice the range of the 1.8 Mev. alpha particles is approximately 1.4mgm./cm.^{2} and therefore, in the surface layer of the sample, approximately 1 in 10^4 of the atoms are displaced from their equilibrium positions in the crystal lattice by a 1000 minute irradiation with a 50 mc. polonium 210 source.

4.2. Changes in physical properties

The atomic displacements introduced by the radiation results in important changes in the physical properties of the target material and measurement of these provides a means of determining the number and nature of the defects produced. The physical properties affected by the introduction of defects into the crystal lattice can be crudely divided into two groups - structural and electronic. The former depend on the actual position of the atoms in the crystal lattice and the latter on the localised electron energy levels associated with the defects.

The changes occurring in the structural properties of non-metals are briefly discussed in section 4.2.1. while the changes in the electronic properties are described in section 4.2.2. Annealing experiments also provide information about the nature of the defects and make correlation between the structural and electronic changes possible (4.2.3).

4.2.1. Structural changes

The lattice imperfections, resulting from irradiation with heavy charged particles and neutrons, influence the X-ray diffraction pattern of

the material. The characteristic Bragg reflections are displaced, weakened and broadened, and in addition a diffuse background scattering appears. Associated with these effects is the reduction of the density of the material when irradiated.

A further fundamental change associated with the production of defects is that the energy content of the lattice is increased. This stored energy can be released by heating, and measured. Consequently, if the energy of formation of the defects is known theoretically, the number of defects can be calculated.

In addition to a large amount of work on these structural changes produced in graphite (Hennig and Hove, 1956), diamond (Primak et al., 1956), quartz (Primak, 1958, Wittels, 1957) and the alkali halides (Kobayashi, 1957), the results obtained for the metamict mineral, zircon, are of particular relevance to the age determination of ceramics (Holland, 1954, Holland and Gottfried, 1955). In this case the structural changes arise from the decay of the radioactive impurities over a period of approximately 10^9 years. Working with a series of gem zircons from Ceylon, whose age was approximately 6×10^8 years, Holland and Gottfried (1955) observed that the density decreased and the c dimension of the unit cell, measured by means of X-ray diffraction techniques, increased with increasing natural alpha activity. Approximately 10^{16} alpha disintegrations per mgm. were sufficient to disorder the structure completely. Assuming that the atomic displacements were entirely due to the alpha particles and their associated recoil nuclei, they calculated that each disintegration must cause approximately 2000 displacements in order to displace all the atoms present in the zircon. This

figure was in reasonable agreement with the theoretical value (Table 4/1) and they therefore suggested that measurement of the density or the c dimension of unit cell would provide a method of age determination for zircons.

4.2.2. Electronic changes

Associated with the vacancies and interstitial atoms, introduced by the radiation, are localised electron energy levels situated between the conduction and valence bands (Mott and Gurney, 1953). These localised energy levels act as electron and hole traps and thus radically change the optical absorption spectra, the magnetic behaviour, the electrical conductivity and the thermoluminescence of non-metals. The major difficulty encountered, when these properties are used to determine the number of atomic displacements, is that both the radiation damage traps and impurity traps, already present in the crystal, will be filled with electrons and holes due to the ionising effect of the radiation. Optical absorption spectra provide a very sensitive method of studying the total number of traps filled by irradiation. If the absorption spectra due to the radiation damage traps and the impurity traps can be separated then, by the independent measurement of the oscillator strength associated with a particular absorption band, the number of new traps created by the irradiation can be calculated. Levy (1961), working with synthetic single-crystal alumina (sapphire), found that only slight coloration resulted from gamma irradiation and this rapidly reached a saturation level. In contrast, when irradiated in a reactor, prominent absorption bands were formed at 2050, 2310, 2550 and

4770Å. When the growth of these absorption bands as a function of the radiation dose was studied, it was found that the growth could be resolved into an initial part, which saturated exponentially, and a linear part. The linear part was interpretated as due to the steady rate of production of traps by the fast neutrons. However the rate of production of traps calculated from the optical spectra was less, by a factor of approximately ten, than the theoretical rate of production.

Mitchell and Paige (1956), working with crystalline quartz, have shown that the C absorption band (2150Å) reached a saturation value under X-irradiation, corresponding to the filling of existing traps. However when irradiated in a reactor, the C band continued to increase due to the creation and filling of radiation damage traps and a new absorption band, the E band (1630Å), appeared. Again the rate of trap production estimated theoretically was greater, by an order of magnitude, than that calculated from the absorption spectra.

A second immensely valuable tool for the study of radiation defects is the electron spin resonance spectrum. This enables one to distinguish between defects of different magnetic structure through the measurement of the g-value and the hyperfine splitting of the resonance lines. Griffiths et al. (1954) found that, when samples of quartz were subjected to X-irradiation, there was one set of paramagnetic resonance lines which was present in all specimens and they suggested, on the basis of the hyperfine structure, that this set was due to an unpaired electron moving in an orbit near to the ^{27}Al nucleus. O'Brien (1955) put forward a model which satisfactorily

accounted for the paramagnetic resonance spectrum. Initially ($Al + e^-$) replaced a silicon atom and when subjected to X-irradiation, an electron was removed from the oxygen adjacent to the aluminium atom. By a combination of the optical absorption and paramagnetic resonance results, Mitchell and Paige (1956) were able to show that the A absorption band (4600Å) in quartz was associated with the hole trapped at this substitutional aluminium atom. Similarly Weeks (1956) observed that, when quartz was irradiated in a reactor, there were two groups of paramagnetic resonance lines and he suggested that the C absorption band (2150Å) was due to a trapped electron.

Irradiating n-type germanium with alpha particles, using a polonium 210 source, Braittain and Pearson (1950) found that the electrical conductivity decreased initially and then began to increase with the conversion of the germanium to p-type. This was associated with the creation of electron traps which removed electrons from the conduction band and reasonable agreement between the experimental and theoretical values for the rate of production of traps was obtained. Furthermore it was shown, by progressively removing layers of the crystal, that the alpha particles created 2.5 times as many traps at the end of their path than initially when a larger proportion of their energy was lost through ionisation.

In addition to the optical absorption spectra produced by means of artificial sources of radiation, geologists have studied the colour centres produced in minerals as a result of the decay of the radioactive impurities. Joly (1923) first suggested that the series of concentric dark rings (pleichroic haloes) observed in mica were due to the decay of small radioactive inclusions, the alpha particles creating and filling traps. Titley

and Damon (1962) have shown that the 3050Å absorption band in natural fluorites was due to the radiation damage traps and that, by measurement of the optical absorption coefficient at this wavelength, the alpha activity and the efficiency of the alpha particles at creating traps, the relative ages of the fluorites could be determined.

4.2.3. Annealing experiments

When the temperature of the material is raised, the defects produced by irradiation are capable of moving through the crystal and thus being annealed out. The basic mechanism is the annihilation of vacancies and interstitials by recombination or by absorption at the surface and on grain boundaries.

Levy (1964) has carried out a number of experiments on the annealing of reactor-induced colour centres in single-crystal alumina and in fused silica. Annealing was carried out for periods of 20 minutes at 30°C intervals throughout the range 70 to 790°C and in the former case annealing of the defects, producing the optical absorption bands at 2025, 2310 and 2550Å, commenced at approximately 130°C and was complete by 700°C. Similarly with fused quartz, annealing of the defects producing the optical absorption bands at 2130, 2280, 2480 and 2750Å, commenced at 150°C and was complete by 700°C.

The situation is further complicated by the presence of impurity atoms, if substitutional, they can trap vacancies and interstitials while, if they themselves are interstitial, they can be trapped at vacancies. Mitchell

and Paige (1956) have shown that if, after reactor irradiation, crystalline quartz was annealed at 950°C, subsequent reactor irradiation resulted in a large increase in the A absorption band. The A band was known to be associated with substitutional aluminium atoms and the increase in absorption, following annealing and re-irradiation, was thought to be due to interstitial aluminium atoms moving into silicon vacancies created by the reactor irradiation.

Kobayashi (1957), working with sodium chloride crystals, bombarded with 350 Mev. protons, has carried out annealing experiments in which the removal of F centres has been correlated with the return to the original density and the release of stored energy.

4.3. Thermoluminescence measurements

The application of thermoluminescence measurements to radiation damage studies is analogous to the measurement of the optical absorption spectrum since in both cases electron and hole traps, created and filled by radiation, are being used. However the latter method only involves the optical excitation of the electrons or holes associated with a single trap while thermoluminescence involves two traps. The electron or hole is thermally excited, from a trap, into the conduction band or valence band respectively and is then captured by a luminescence centre with the emission of light.

It has been shown in section 3.1 that the area under the thermoluminescent glow curve is proportional to the number of filled traps. However in order to obtain an absolute figure for the number of filled traps, the proportion of the transitions to the luminescence centre that result in the

emission of light, and the wavelength of this light must be known (section 3.3).

As in the case of optical absorption measurements, it is necessary to distinguish the thermoluminescence due to the filling of impurity traps from that due to the filling of traps created by the radiation. The basic technique employed, when thermoluminescence is used to study radiation damage, is the measurement of the rate curves, i.e. the growth of the thermoluminescence as a function of the radiation dose (section 4.3.1).

The optical absorption and the thermoluminescence results are compared in section 4.3.2 and this comparison emphasizes the difficulties associated with the interpretation of thermoluminescence measurements.

4.3.1. Rate curve theory

The increase in thermoluminescence with radiation dose (rate curves) depends on both the concentration of traps and the rate at which they are filled with the requisite charge carriers.

The radiation excites electrons into the conduction band leaving an equal number of holes in the valence band (fig. 3/1). If a "single centre" model, in which only electrons are trapped and the holes are immobile, is assumed then the equations governing the free electron, trapped electron and hole concentrations are:

$$dn/dt = X - C_1 n (N_1 - n_1) - knp$$

$$dn_1/dt = C_1 n (N_1 - n_1)$$

$$dp/dt = X - knp$$

and in order to maintain charge neutrality:

$$n + n_1 = p$$

where n, p, n_1 and N_1 are the concentrations of free electrons, holes, trapped electrons and electron traps respectively. C_1 and k are the rate constants for the capture of an electron at a trap and for the recombination of an electron and hole. X equals the rate of generation of electron and hole pairs.

Assuming that the free electron concentration reaches an equilibrium value (n'), determined by the occupancy of traps, in a very short time compared with the time constant for the filling of traps, then it can be shown (Paige, 1957) that:

$$n' = \frac{X}{C_1 N_1 + n_1 (k - C_1)}$$

Hence the number of filled electrons traps at time, t, is given by:

$$n_1 = N_1 \left[1 - \exp\left(\frac{n_1 (C_1 - k)}{N_1 k} \right) \exp(-X C_1 t / N_1 k) \right] \qquad 4/8$$

If $k = C_1$, then the equilibrium concentration of free electrons is independent of the number of filled traps and therefore:

$$n_1 = N_1 \left[1 - \exp(- Xt / N_1) \right] \qquad 4/9$$

Under these conditions $\log \left(\frac{N_1 - n_1}{N_1} \right)$ varies linearly with the radiation time (fig. 4/1) but when C_1 is not equal to k, the relationship is no longer linear. The plots obtained for $C_1 = 2k$ and $C_1 = k/2$ are also shown in fig. 4/1.

When both charge carriers are mobile and when two groups of traps are present, one trapping electrons and the other trapping holes, the free

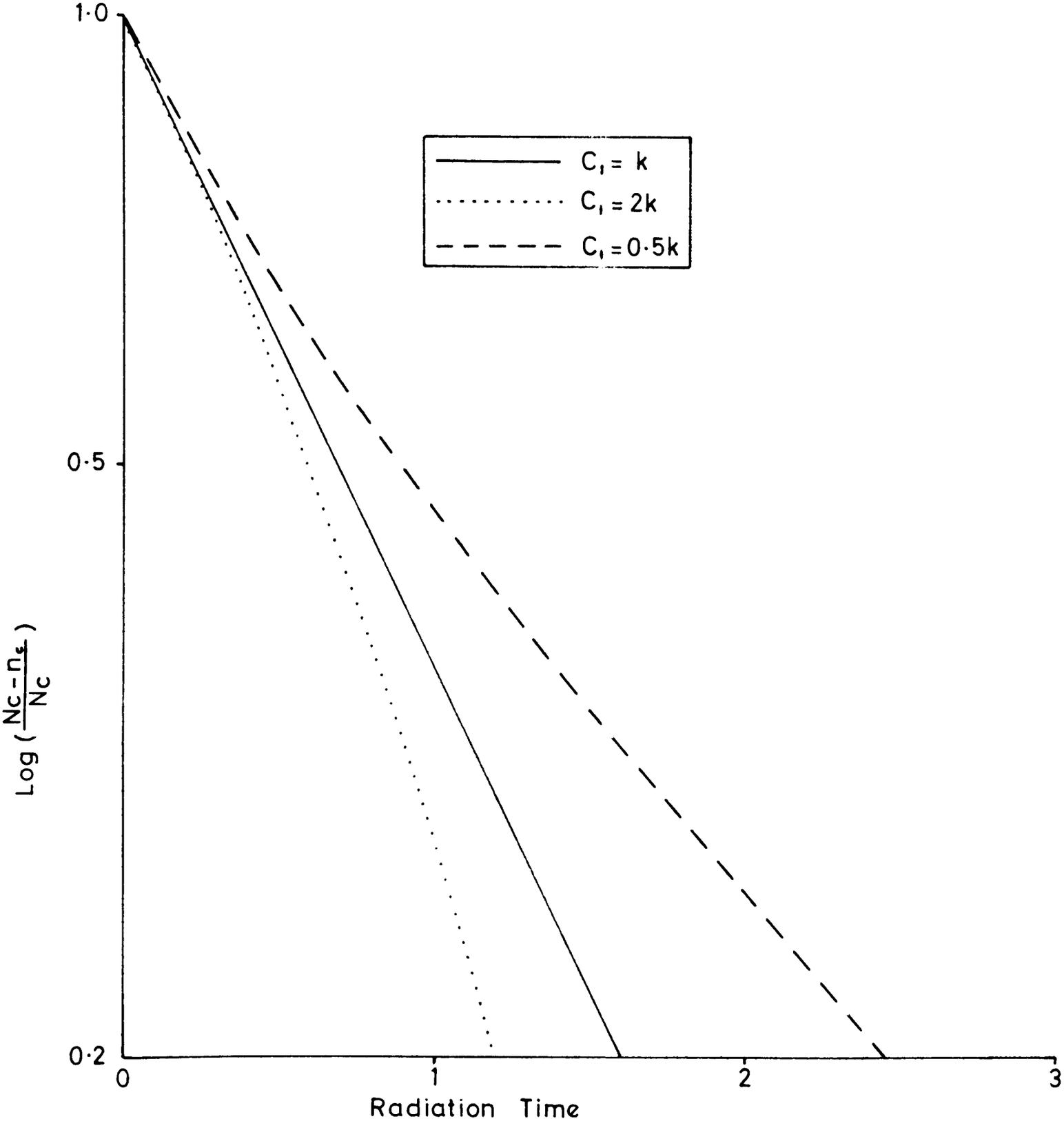


Fig 4/1

conduction band electrons can recombine with free valence band holes (k) and with trapped holes (C) or can fill electron traps (C_1). Similarly the free valence band holes can recombine with trapped electrons (A_1) or can fill hole traps (A). The equations governing the concentration of free and trapped carriers are:

$$dn/dt = X - C_1 n (N_1 - n_1) - Cnp_1 - knp$$

$$dp/dt = X - Ap (P_1 - p_1) - A_1 pn_1 - knp$$

$$dn_1/dt = C_1 n (N_1 - n_1) - A_1 pn_1 \qquad 4/10$$

$$dp_1/dt = Ap (P_1 - p_1) - C np_1 \qquad 4/11$$

and in order to maintain charge neutrality

$$n + n_1 = p + p_1$$
$$N_1 = P_1$$

where p_1 and P_1 are the concentration of trapped holes and hole traps respectively.

Again the form of the rate curve is critically dependent on the relative values of the various rate constants since these govern the equilibrium concentration of free electrons and holes. Only when $C_1 = A_1 = C = A$, are these equilibrium concentrations independent of the fraction of filled traps. Under these circumstances the number of filled traps at time, t, is given by:

$$n_1 = p_1 = \frac{N_1}{2} \left[1 - \exp(-2Xt/N_1) \right] \qquad 4/12$$

and $\log \left(\frac{N_1 - 2n_1}{N_1} \right)$ varies linearly with radiation time. When the rate constants are not all equal the equilibrium concentrations of free electrons

and holes are a function of the concentration of filled traps and a linear relationship between log $\left(\frac{N_1 - 2n_1}{N_1}\right)$ and time is no longer obtained. However the saturation concentration of filled traps, and hence the saturation value for the thermoluminescence, remains proportional to the concentration of traps.

When more than two groups of traps are present, the kinetics of trap filling becomes very complicated (Paige, 1957) and will depend radically on the relative values for the rate constants, the extent to which other traps in the material are already filled when irradiation commences and the rate at which new traps are created. This situation is further discussed with respect to the Forman effect observed for X-rays and beta particles (sections 6.1 and 7.1) and with respect to radiation bleaching (section 8.1).

4.3.2. Comparison of thermoluminescence and optical absorption

Working with potassium chloride and subjecting the samples to X-irradiation, Braner and Halperin (1957) have established that the F centre absorption band was responsible for a whole series of thermoluminescent glow curve peaks (100 - 600°K); excellent correlation being obtained between the temperature at which the F absorption band was bleached and the temperature of the thermoluminescent peaks. Halperin et al. (1960) also found that each peak was associated with a particular trap depth and that the wavelength of the light associated with each peak was often the same. The F centre absorption is due to an electron trapped at a negative ion vacancy while V centre absorption bands, also found in the alkali halides, are associated with trapped holes. Braner and Halperin (1957) therefore suggested that the

thermoluminescence and the bleaching of the F centre absorption band was due to the excitation of the holes, trapped at the V centres, into the valence band and their subsequent recombination with the electrons trapped at the F centres; each peak being associated with a particular group of V centres.

The correlation between the optical absorption bands and the thermoluminescent peaks has not been conclusively established for quartz. Arnold (1960) suggested, on the basis of thermal bleaching and annealing experiments, that the C absorption band (2150Å) and the 340°C peak were due to the same centres. However the results obtained by Levy (1964) suggested that, as in the case of the alkali halides, the traps responsible for a particular absorption band could give rise to thermoluminescence throughout the range 150 to 600°C.

Thomas and Houston (1964), working with a magnesium oxide, were able to prove, by means of thermal and optical bleaching experiments, that the 2.3 ev. and 3.0 ev. optical absorption bands were due to the same centres as the 400°K and 500°K peaks respectively.

These results, together with rate curve theory discussed in section 4.3.1, emphasise the difficulties involved in determining the total number of traps and the number of radiation dame traps present in a non-metal using thermoluminescence measurements.

4.4. Thermoluminescence from ceramics

As indicated in the Introduction to this thesis, there are two approaches to the age determination of ceramics using thermoluminescence. The first involves the measurement of the number of new traps created, since the pottery

was fired, as a result of the natural radioactive impurities present in the clay and the second involves the measurement of the number of traps filled with electrons or holes, since firing.

The basic aim of the experiments using artificial sources of radiation, described in Chapters 5 - 9, was to decide whether age determination was possible and if so, to establish the technique to be employed. An attempt was first made to determine the number of additional traps created since firing (Chapter 5) but this was found to be impractical because it was impossible to distinguish the radiation damage traps from those already existing at the termination of the firing. However this work involved the measurement of the X-ray rate curves and the form of these curves suggested that the X-rays were creating new traps. This hypothesis was further investigated and the results obtained are presented in Chapter 6.

For age determination, based on the number of traps filled since firing, it was necessary to know the form of the rate curve for doses up to approximately 5×10^4 rads. This was investigated using a beta source and it was found that the number of filled traps did not increase linearly with dose (Chapter 7).

Alpha particle rate curves were also measured using a polonium 210 source, and thermal and optical bleaching experiments were carried out to determine the approximate rate of creation of new traps by alpha particles (Chapter 8). On the basis of these results it was decided that the number of new traps created, since the pottery was fired, as a result of its radioactive impurities was small compared with the number of traps existing

at the termination of firing.

Finally the relative efficiency with which alpha particles, beta particles, X-rays and gamma rays filled existing traps was investigated and the shape of the glow curves*, obtained using these different types of radiation, was compared (Chapter 9).

On the basis of this work, it was decided that age determination, by the measurement of the number of traps, was feasible and the results obtained from a third age determination programme are given in Chapter 12.

---

* The term glow curve refers to the graph of thermoluminescence plotted against temperature, obtained for each sample while the term rate curve refers to the growth of the total thermoluminescence plotted as a function of radiation dose and obtained from measurements on a series of samples.

CHAPTER 5. MEASUREMENT OF RADIATION DAMAGE TRAPS

If the number of new traps created, since the pottery was fired, as a result of the decay of the radioactive impurities present in the clay is to be used as the basis for the age determination of pottery, then it is essential to measure the total number of traps present (section 5.1) and also to distinguish between the traps already present at the termination of firing and those created subsequently (section 5.2).

5.1. Determination of trap concentration

This involves the measurement of the rate curves for a purely ionising radiation and the determination of the saturation value for the thermoluminescence (L_s). From the theory presented in section 4.3.1., it can be seen that, in the case of the single centre and two centre models, the saturation value for a particular thermoluminescent peak will be proportional to the concentration of traps at the appropriate energy level.

Initially X-irradiation was used to determine the saturation value (section 5.1.1) since it was hoped that its effect would be purely ionising. However the form of the rate curves suggested that trap creation was also occurring and consequently rate curves for ultra-violet light (section 5.1.2) and beta particles (section 5.1.3) were also measured.

5.1.1. X-irradiation

The source of X-rays employed was a Machlett tube (type AEG 50T) with a tungsten target and this was operated at 40 kv. with a filament current of 5 ma. The ground-up samples were irradiated in an aluminium tray, transferred to the slow heating furnace under conditions of semi-darkness and

their thermoluminescence was measured six minutes after the completion of the irradiation. The X-ray doses ranged from 2×10^5 to 1.3×10^8 rads.

Rate curves were obtained by this method for a number of sherds and the results for sherd r (fig. 5/1) were typical. In this case the glow curves (fig. 5/2) contained no well-defined peaks but their shape suggested that a number of unresolved peaks were present and the temperature ranges for the rate curves were chosen accordingly.

In the 60-100°C range, a saturation value for the thermoluminescence was attained but for the higher temperature ranges, the rate curves could be resolved into two components, the first increasing to a saturation value, the second increasing linearly with X-ray dose (fig. 5/3). The saturating component was interpretated as the filling of existing traps while the linear increase was thought to be due to the creation of new traps. Further experiments carried out to investigate this hypothesis are described in Chapter 6.

The values for L_s are given in Table 5/1 and fig. 5/4 shows a plot of $\log (L_s - L_t)$ versus the irradiation time (t), for the saturating component of the rate curves. Except for the 100-175°C range, comparison of these curves with the theoretical curves shown in fig. 4/1 indicated that, within the limits of accuracy of the measurements (± 5%), an essentially simple rate law, of the form:

$$L_t = L_s \left[1 - \exp(-ft) \right]$$

where f is a constant, was obeyed. It seemed reasonable, therefore, to assume that the saturation values (L_s) provided a measure of the total

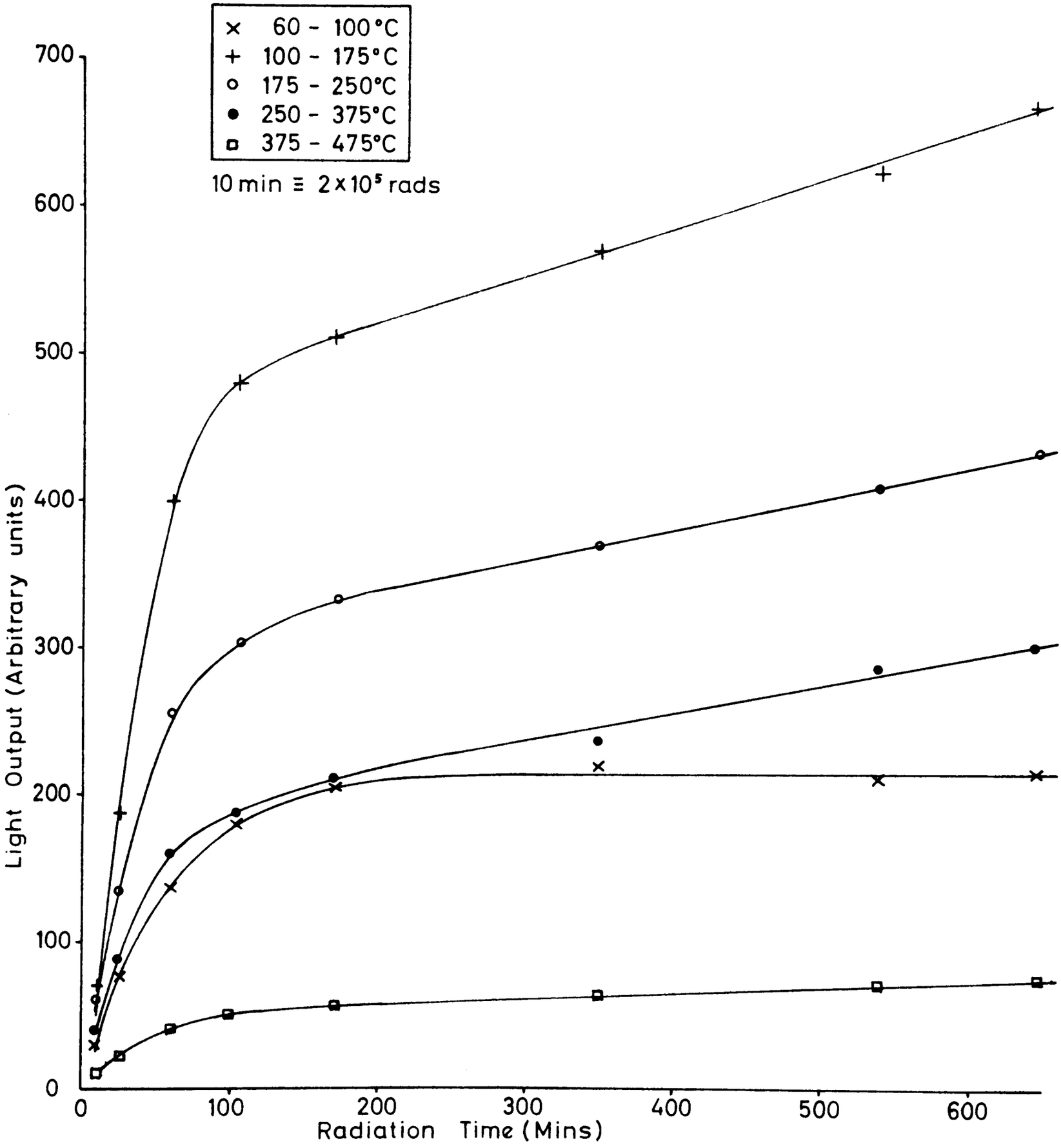

× 60 - 100°C
+ 100 - 175°C
○ 175 - 250°C
● 250 - 375°C
□ 375 - 475°C
10 min ≡ 2×10⁵ rads
Light Output (Arbitrary units)
0
100
200
300
400
500
600
700
Radiation Time (Mins)

Fig 5/1

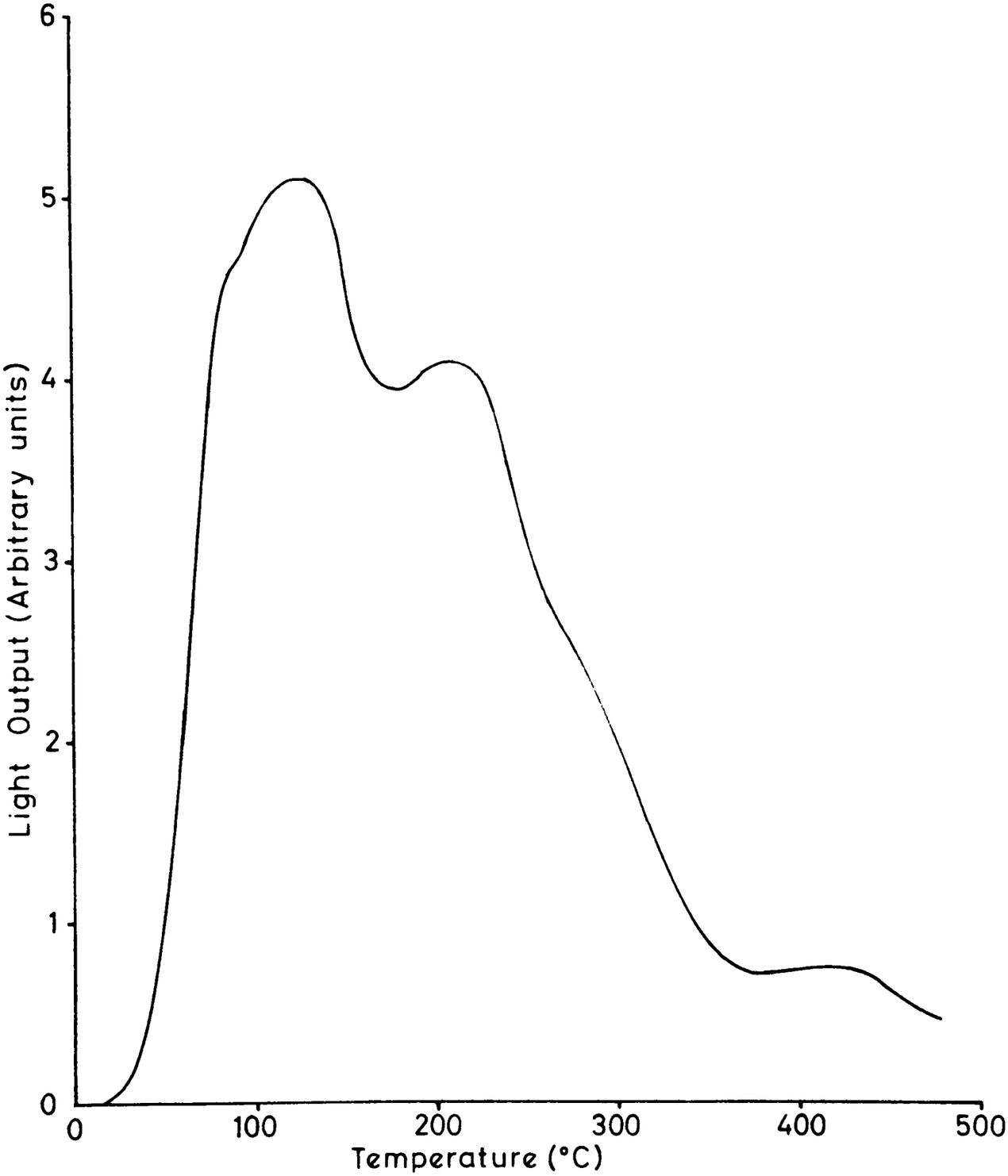

6
5
4
3
2
1
0
Light Output (Arbitrary units)
0
100
200
300
400
500
Temperature (°C)

Fig 5/2

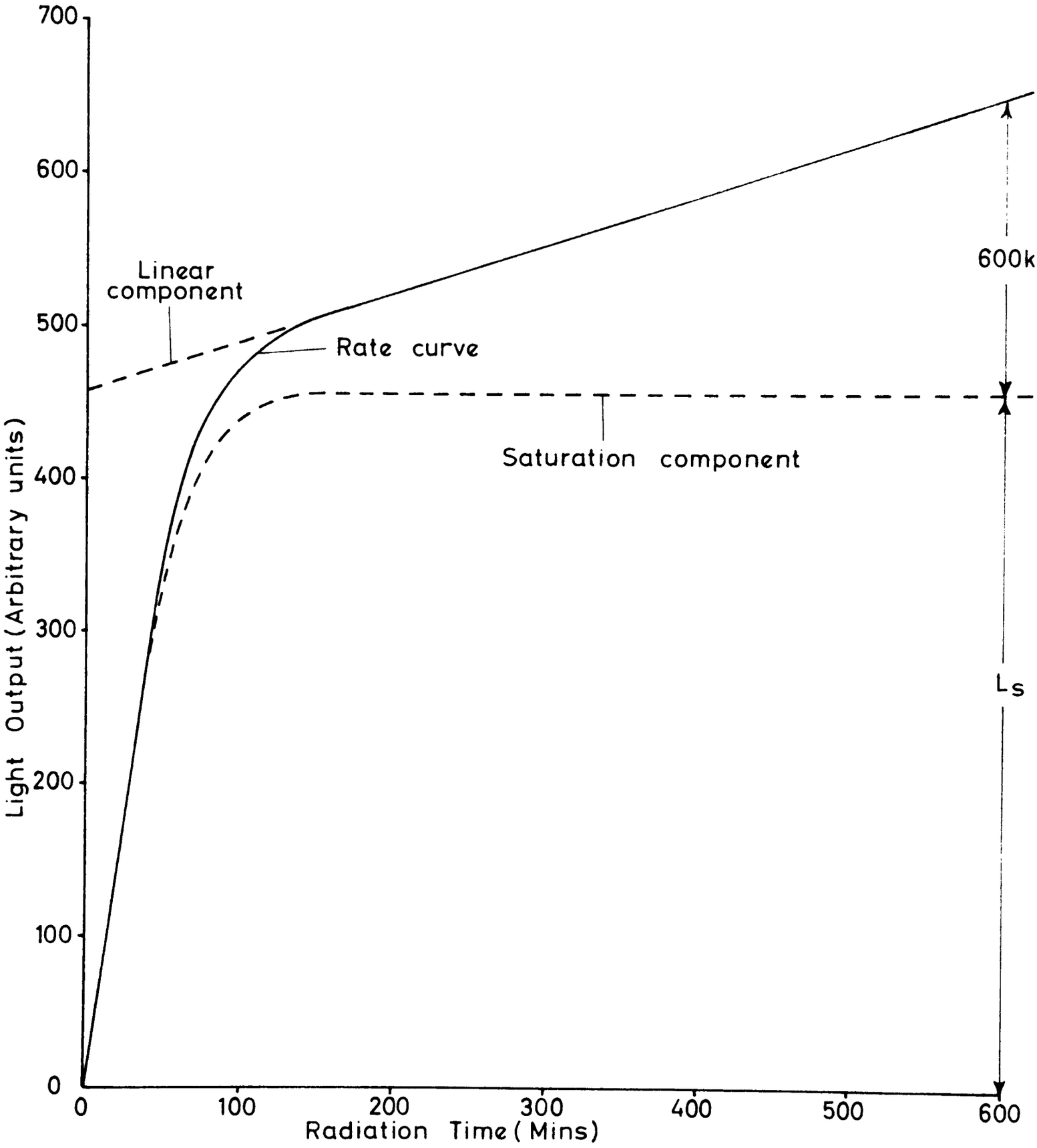

700
600
500
400
300
200
100
0
Light Output (Arbitrary units)
Linear component
Rate curve
600k
Saturation component
Ls
0
100
200
300
400
500
600
Radiation Time (Mins)

Fig 5/3

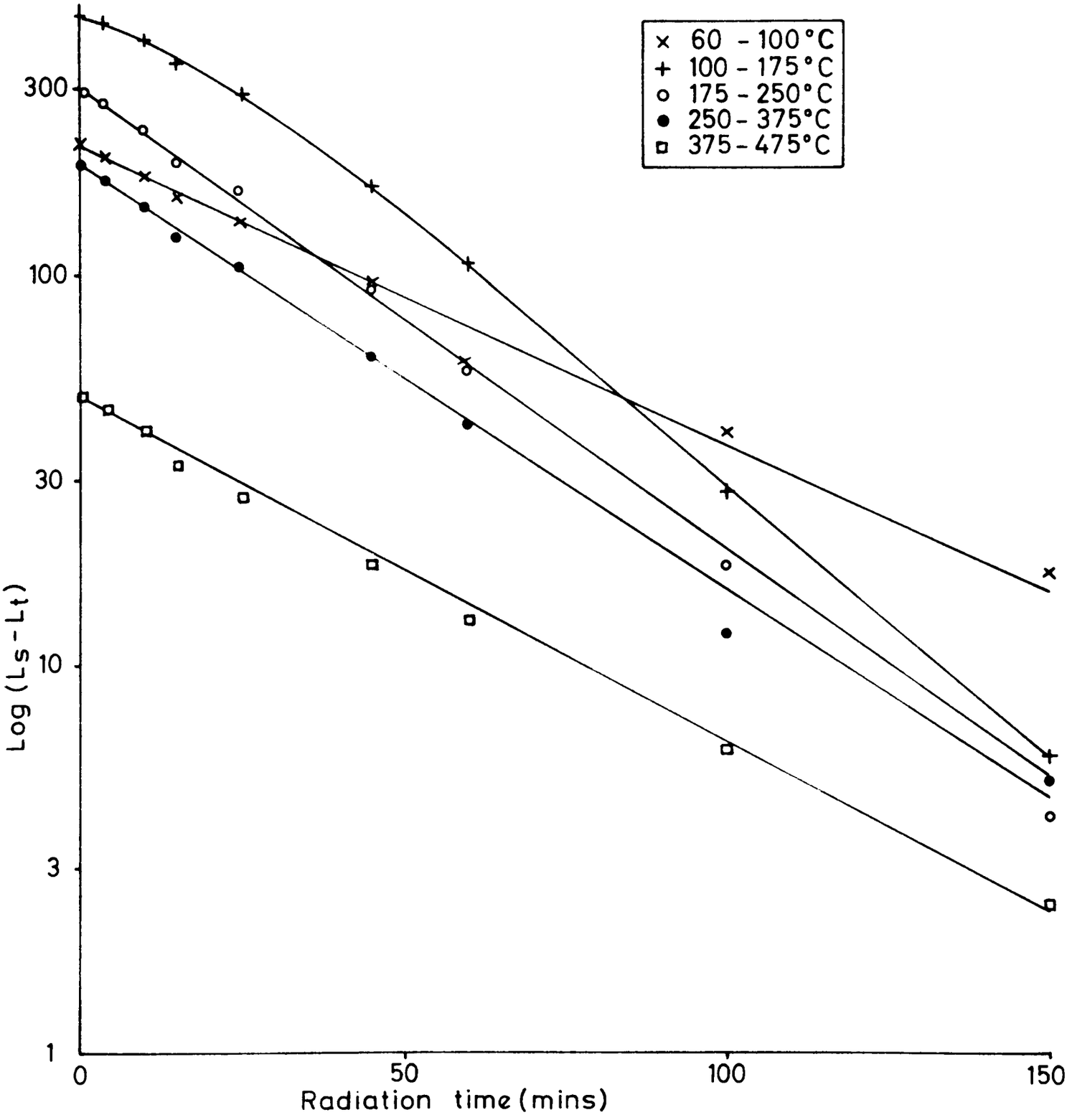

× 60 - 100°C
+ 100 - 175°C
○ 175 - 250°C
● 250 - 375°C
□ 375 - 475°C
300
100
30
10
3
1
Log (Ls - Lt)
0
50
100
150
Radiation time (mins)

Fig 5/4

number of traps associated with a particular temperature range. However because of the correction which had to be made for the linearly increasing component of the X-ray rate curves, rate curves were also measured using ultra-violet light (section 5.1.2) and beta particles (section 5.1.3).

Table 5/1

Saturation values (L_s) for sherd r

	60-100°C	100-175°C	175-250°C	250-375°C	375-475°C
X-rays	215	460	296	192	49
UV light	-	1.25	2.76	2.73	0.84
Beta particles	340	495	280	195	41.3

5.1.2. Ultra-violet light

A Hanovia medium pressure mercury lamp (Model 16), with its principal spectral lines at 2550Å (4.8 ev.), 3090Å (4.0 ev.) and 3600Å (3.4 ev.) and with an intensity of approximately 10^4 ergs per cm.^{2} per second, was used and the sample was irradiated in situ on the slow heating apparatus. The heat generated by the lamp raised the temperature of the sample to an equilibrium value of approximately 60°C.

The rate curves obtained for sherd r, for two typical temperature ranges, are shown in fig. 5/5 (lower curves). After 15 hours of irradiation, the thermoluminescence appeared to be approaching a saturation value but this was very much lower than the values observed for the saturating component of the X-ray rate curves (Table 5/1).

The energy of the ultra-violet light (3.4 - 4.8 ev) is of the same order of magnitude, in the case of insulators, as the energy gap between the

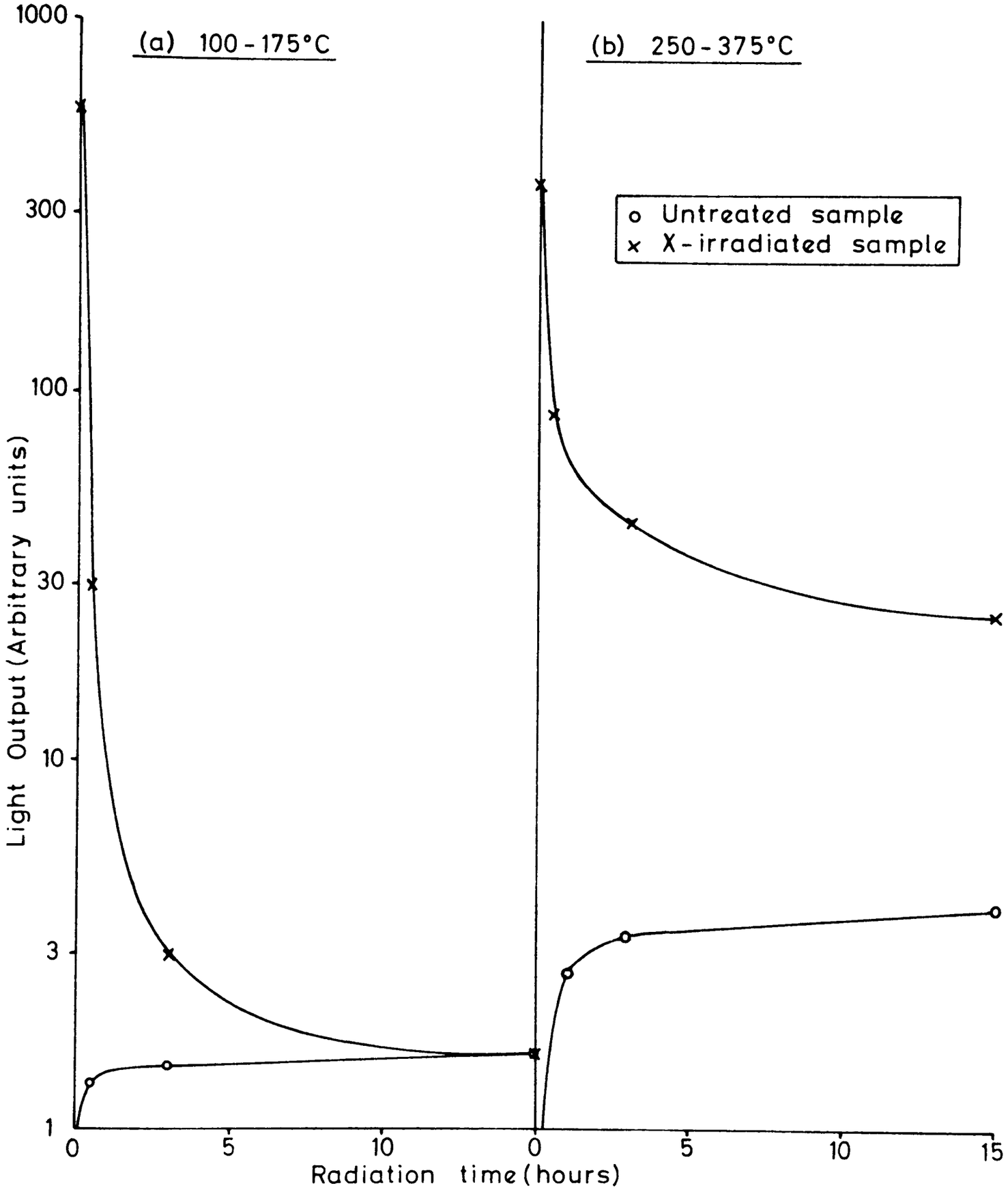

(a) 100 - 175°C
(b) 250 - 375°C
o Untreated sample
× X-irradiated sample
Light Output (Arbitrary units)
1000
300
100
30
10
3
1
0
5
10
0
5
10
15
Radiation time (hours)

Fig 5/5

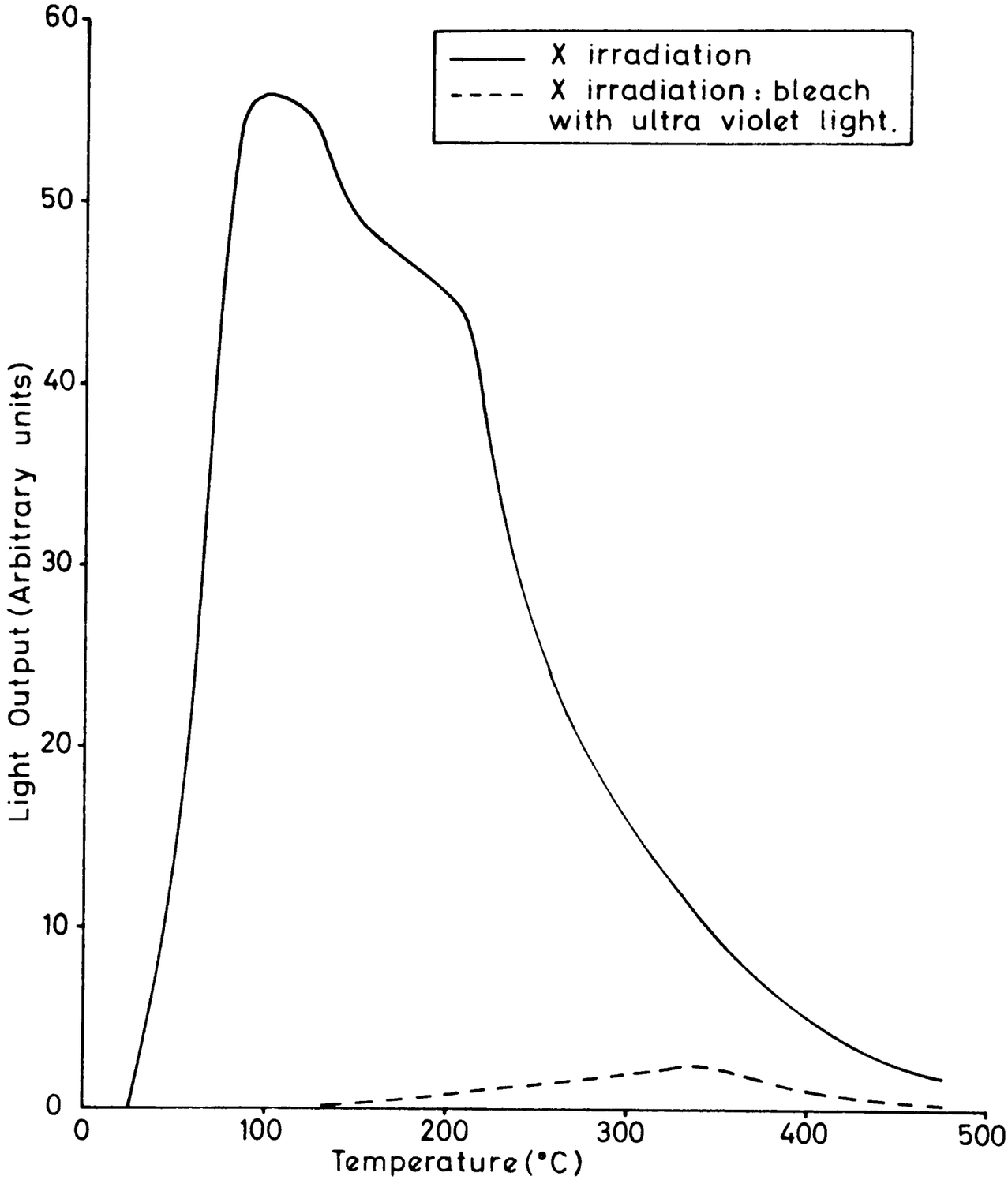

X irradiation
X irradiation : bleach with ultra violet light.
Light Output (Arbitrary units)
60
50
40
30
20
10
0
0
100
200
300
400
500
Temperature (°C)

Fig 5/6

valence and conduction bands and therefore its efficiency at filling and emptying traps is comparable. Samples of sherd r, which had been subjected to a 960 minute X-irradiation (1.9×10^8 rads), were exposed to ultra-violet light for periods of up to 15 hours. It can be seen from fig. 5/5 (upper curves) and fig. 5/6 that exposure to ultra-violet light, in this case, reduced the thermoluminescence and that, in the 100-175°C range, the thermoluminescence from the untreated and X-irradiated samples reached a common value after a 15 hour exposure to ultra-violet light. In the 175-500°C range, no common value had been reached although the form of the curves suggested that this would occur after a sufficiently long exposure to ultra-violet light (greater than 60 hours). These results indicate that the saturation levels, obtained by irradiating untreated samples of sherd r with ultra-violet light cannot be used as a measure of the total number of traps present.

5.1.3. Beta-irradiation

The beta particles rate curves for sherd r were measure using a 40 mc. (Sr^{90} + Yr^{90}) source and again the sample were irradiated in situ on the slow heating apparatus. The radiation doses ranged from 10^4 to 1.4×10^7 rads.

The thermoluminescence reached a saturation value (L_s) and there was no evidence for the existence of a linear component (fig. 5/7). Since the X-rays appeared to be creating new traps, it had been anticipated that the rate of trap creation by the beta particles would be even greater. The apparent absence of trap creation by the beta particles is further discussed

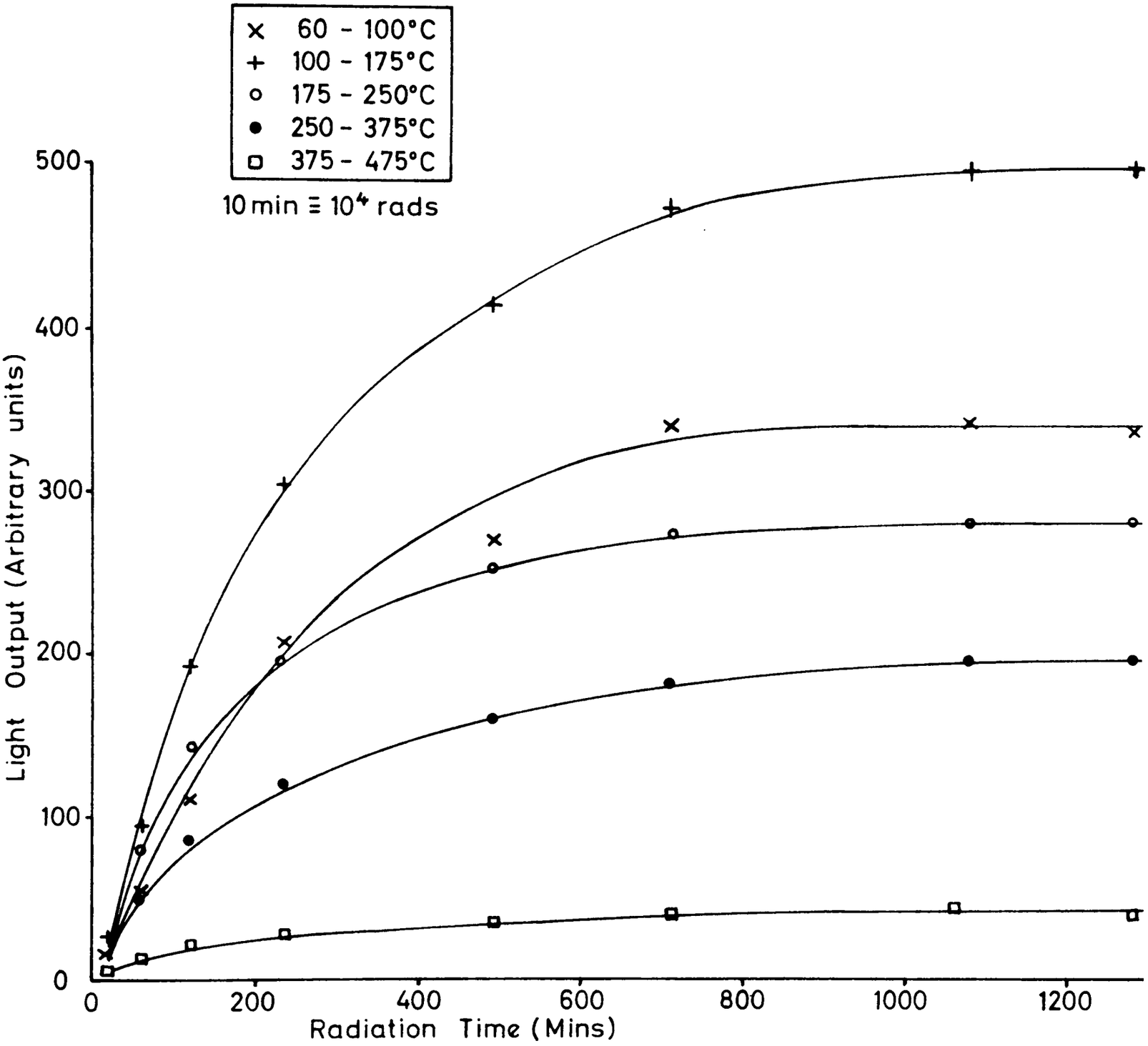

× 60 - 100°C
+ 100 - 175°C
○ 175 - 250°C
● 250 - 375°C
□ 375 - 475°C
10 min ≡ 10⁴ rads
Light Output (Arbitrary units)
0
100
200
300
400
500
0
200
400
600
800
1000
1200
Radiation Time (Mins)

Fig 5/7

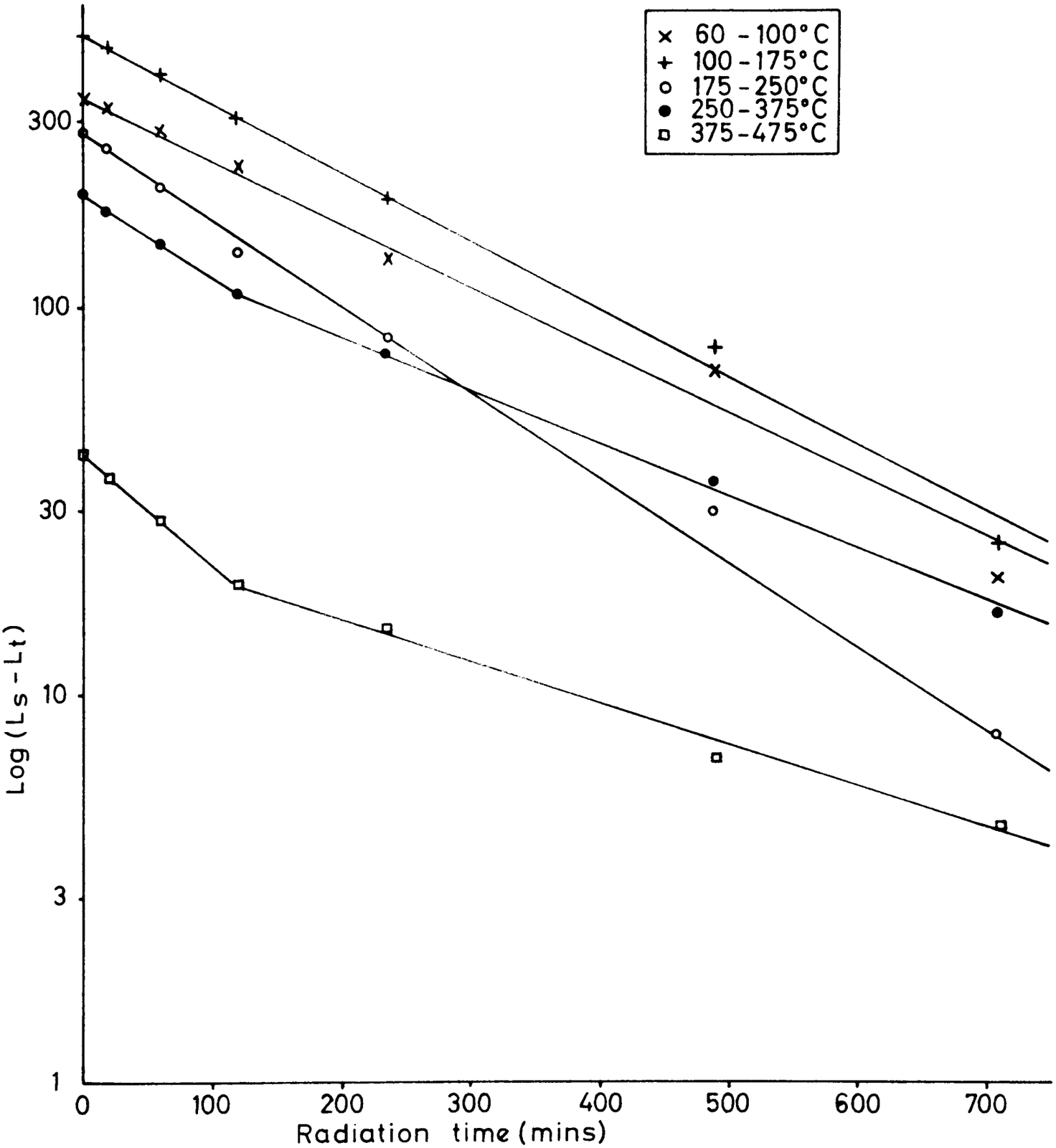

× 60 - 100° C
+ 100 - 175° C
○ 175 - 250° C
● 250 - 375° C
□ 375 - 475° C
300
100
30
10
3
1
Log (Ls - Lt)
0
100
200
300
400
500
600
700
Radiation time (mins)

Fig 5/8

in Chapter 7.

The values of L_s for the beta particle rate curves were close to those obtained from the saturating component of the X-ray rate curves, differing by less than 5% in the 100-375°C range (Table 5/1). Fig.5/8 shows the plot of log $(L_s - L_t)$ versus the irradiation time (t) and it can be seen that, as in the case of X-irradiation, an essentially simple rate law was obeyed in the 60-250°C range. However in the 250-475°C range, the situation was more complicated and the plot of log $(L_s - L_t)$ versus irradiation time could be resolved into two linear components. The deviation of the beta particle rate curves from the simple exponential form is further discussed in Chapter 7.

The excellent agreement between the saturation values obtained using X-rays and beta particles suggested that they would provide a satisfactory figure for the total number of traps associated with a particular temperature range. The problem remaining, if the number of radiation damage traps is to be used as the basis for age determination, is the separation of the radiation damage traps from those already existing at the termination of firing.

5.2. Annealing experiments

It was originally hoped that heating the sample to approximately 500°C for a short period would anneal the traps created since the pottery was fired and that the differing saturation levels produced by the ionising radiation, before and after this annealing, would provide a measure of the number of radiation damage traps.

The effect of heat on the pottery was first tested, using the slow heating apparatus, by subjecting an untreated sample of the sherd to an X-ray dose of 2×10^5 rads (10 minutes) and measuring the resulting thermoluminescence. This thermoluminescence was then compared with the value obtained from a second sample which had been heated in air at 500°C for a few minutes before being given the same X-ray dose. The values for the ratio of the thermoluminescence from the pre-heated sample (L_a) to that from the untreated sample (L) are given in Table 5/2.

Table 5/2

Annealing sherds to 500°C in air

Sherd	L_a/L			
	50-150°C	150-225°C	225-300°C	300-425°C
c	0.96	0.98	0.92	1.06
f	0.62	0.69	0.69	0.80
i	1.08	1.01	1.04	1.28
r	1.30	1.20	1.11	1.06

The anticipated decrease in the susceptibility of the sherd to X-irradiation, corresponding to the annealing of radiation damage traps, was only observed in the case of sherd f. For the other sherds an increase in the susceptibility was observed, indicating that the effect of heat on the pottery could not be satisfactorily explained in terms of the annealing of radiation damage traps.

The changes in the susceptibility of the pottery were further investigated at higher annealing temperatures and in different atmospheres (sections

5.2.1 and 5.2.2.) and finally a technique for obtaining thermally stable samples of sherd r was established (section 5.2.3).

5.2.1. Annealing to 600°C in air and nitrogen

Samples of sherd r and sherd G/Ash. were heated for one hour at 600°C using an electrical resistance tube furnace. These annealing experiments were carried out first in air and then in an atmosphere of nitrogen. The susceptibility of the untreated and annealed samples to an X-ray dose of 2×10^5 rads was then determined (Table 5/3).

Table 5/3

Annealing sherds to 600 C in air and nitrogen

	L_a/L				
	60-100°C	100-175°C	175-250°C	250-375°C	375-475°C
Sherd r					
Air	1.40	1.21	1.27	1.20	1.15
Nitrogen	0.85	0.91	0.98	1.19	1.76
Sherd G/Ash.					
Air	1.11	1.23	1.32	1.16	1.11
Nitrogen	1.29	1.58	2.65	4.40	3.72

From the figures presented in Table 5/3, it can be seen that the susceptibility of the pottery to X-irradiation depended on the atmosphere in which the specimen was annealed. In addition radical changes in the physical appearance of the samples occurred as a result of heating. When annealed in air, the colour of sherd r changed from grey to red while in nitrogen its colour darkened. The colour of sherd G/Ash. changed from red

to grey when annealed in nitrogen and was unchanged when annealed in air.

These colour changes indicated that one effect of the annealing was the conversion of the iron oxides, present in the pottery, to their oxidised form (haemitite, Fe_2O_3) when heated in air and their reduced form (magnetite, Fe_3O_4) when heated in nitrogen. The mechanism by which these mineralogical changes could effect the susceptibility of the sample to X-irradiation is not fully understood. However Medlin (1959), using samples of calcium carbonate to which specific impurities had been added, found that the addition of Fe^{++} and Fe^{+++} ions "quenched" the thermoluminescence observed and that the two ions differed in their "quenching" efficiency.

5.2.2. Annealing to 900°C in air

Samples from a selection of sherds were subjected to more intensive annealing by heating them at 900°C for 12 hours in an electrical resistance furnace. As before, the susceptibility of the untreated and annealed samples to an X-ray dose of 2×10^5 rads was determined. In all cases the effect of annealing was to produce an increased susceptibility (Table 5/4) and for sherd k and the quartz extraction from sherd 6b4, the shape of the resulting glow curves was radically changed (fig. 5/9 and 5/10).

Table 5/4

Annealing sherds to 900°C in air

Sherd	L_a/L				
	60-100°C	100-175°C	175-250°C	250-375°C	375-475°C
r	1.5	1.1	1.4	1.3	1.1
i	1.2	2.0	1.1	1.1	1.0
6b4	1.1	1.8	6.3	23	106
	50-150°C	150-200°C	200-275°C	275-375°C	375-475°C
k	56	23	3.4	5.2	11

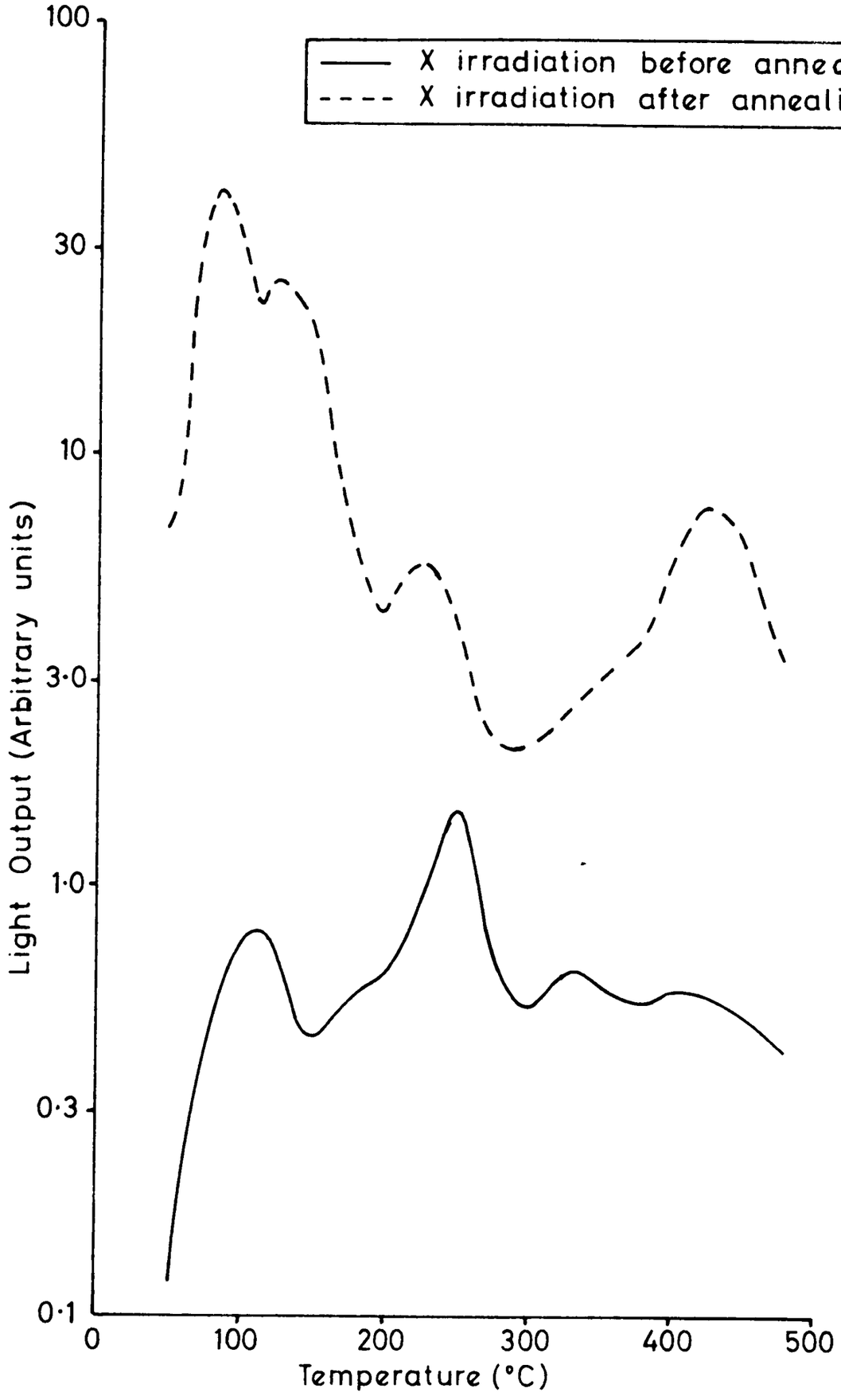


Fig 5/9 Sherd k

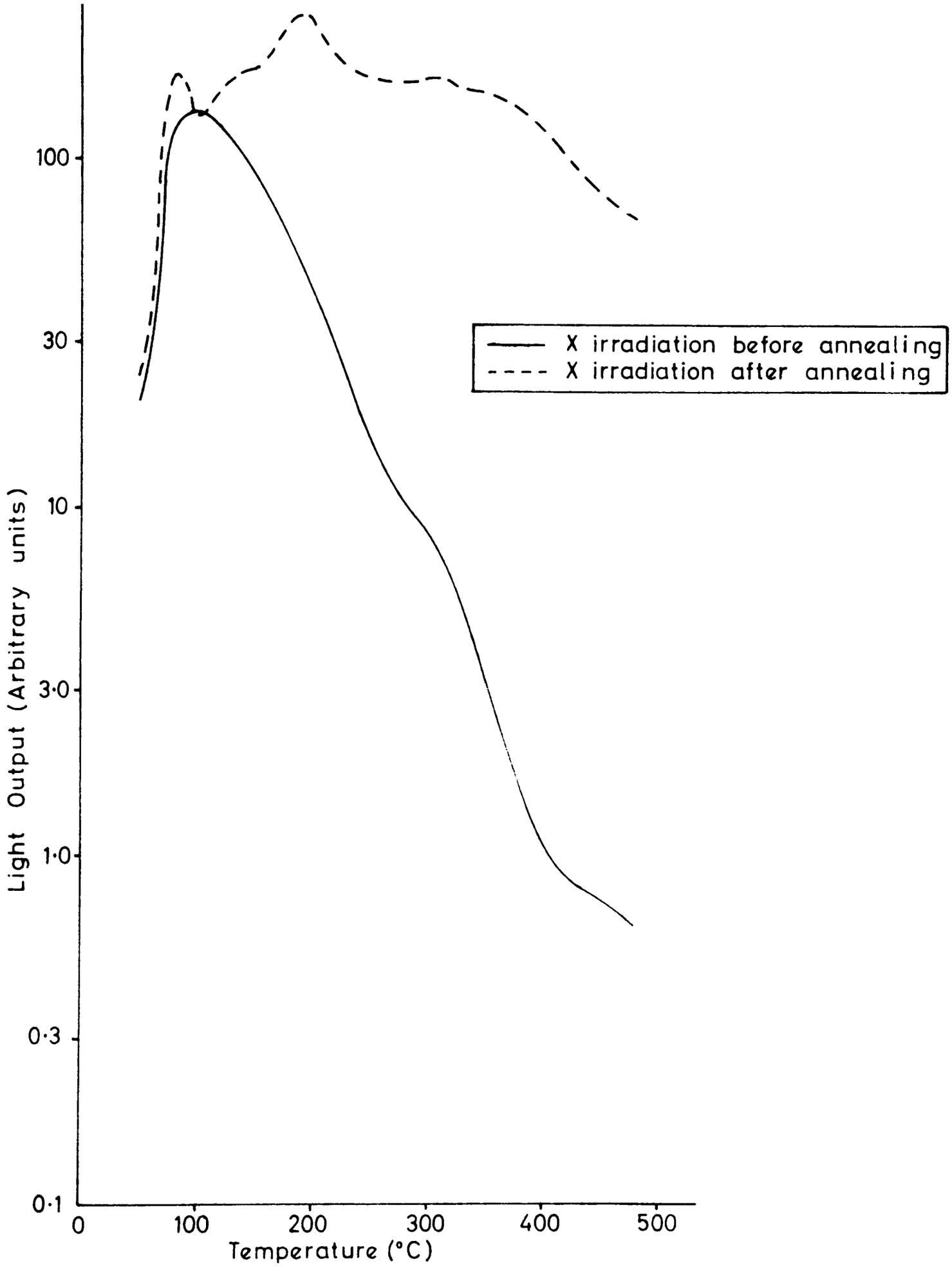


Fig 5/10. Sherd 6b4 - quartz extraction

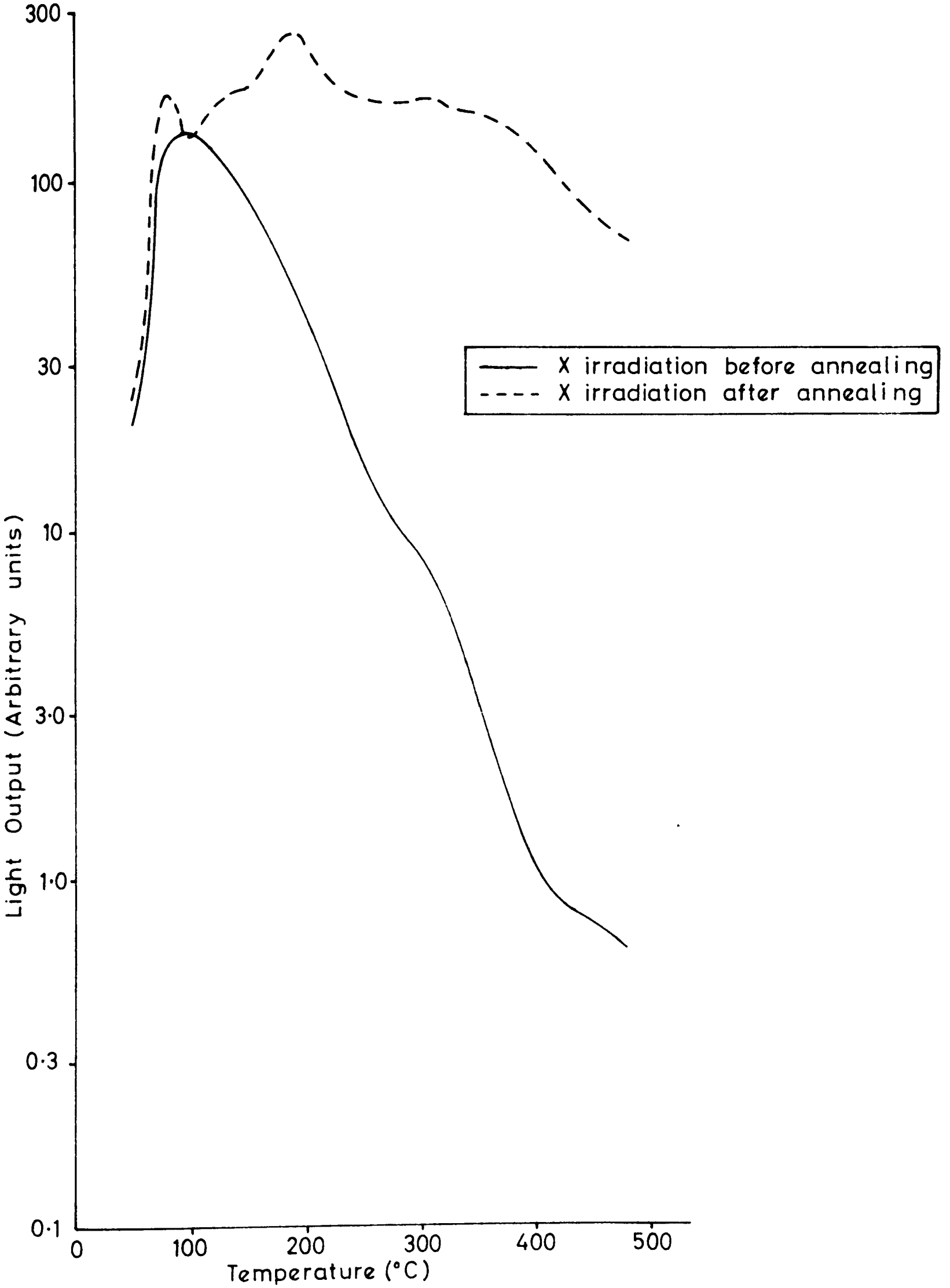


Fig 5/10. Sherd 6b4 - quartz extraction

A similar increase in the susceptibility to radiation has been observed by other workers using calcite (Medlin, 1959), quartz (Medlin, 1963; Cohen and Friqueler, 1963) and potassium chloride (Halperin and Schlesinger, 1959).

With potassium chloride, Halperin and Schlesinger (1959) observed that, annealing to 500°C for 6 hours before irradiation, caused the thermoluminescent peaks in the 200-300°K range to increase by a factor of 4000 while the F and V centre optical absorption bands only increased by a factor of 3. They therefore suggested that annealing did not radically alter the number of F and V centres present but instead increased the luminescence efficiency, i.e. increased the probability of radiative transitions from the valence or conduction bands to the luminescence centres. They further suggested that this increase in luminescence efficiency was due to K^+ ion vacancies diffusing into the crystal and approaching Cl^- ion vacancies.

Similarly Medlin (1963), using quartz, observed that, annealing to 900 C for two hours before irradiation, caused the thermoluminescent peak at 350°K to increase by a factor of approximately 10^4 while a much smaller increase was observed for the electrical conductivity glow curves. He associated the enhanced susceptibility, in the former case, with an increase in the luminescence efficiency rather than with an increase in the number of traps and suggested that it was due to an improvement in the crystallinity of the sample.

The experiments, described above, failed to provide a method for separating the radiation damage traps from those already existing at the termination of firing and indicated that the effect of annealing, on the

thermoluminescence observed after subjecting ceramics to irradiation, was extremely complex. The situation was more complicated than in the case of optical absorption measurements, since thermoluminescence emission was a two-stage process.

5.2.3. Thermally stable samples of sherd r

For the thermal bleaching experiments, described in sections 6.2 and 8.5, thermally stable samples of sherd r were required. These were obtained by heating 500 mgms. of the ground-up sherd at 600°C for one hour in an atmosphere of nitrogen using the electrical resistance tube furnace. If this annealed sample was either reheated to 600°C for one hour in nitrogen using the tube furnace or reheated to 600°C in nitrogen on the slow heating apparatus, then its susceptibility to an X-ray dose of 2×10^5 rads was altered by less than 8% (Table 5/5).

Table 5/5

Thermally stable samples of sherd r

	Thermoluminescence (Arbitrary units)			
Heat treatment	60-175°C	175-250°C	250-375°C	375-475°C
Untreated	3.32	1.60	1.12	0.29
Anneal at 600°C for 1 hr. (x1)	2.96	1.57	1.33	0.50
Anneal at 600°C for 1 hr. (x2)	2.93	1.48	1.20	0.50

5.3 Conclusions

From the results described in section 5.1, it seemed likely that a satisfactory figure, proportional to the concentration of traps associated with a particular temperature range, could be obtained using the saturation values from the X-ray and beta particle rate curves. However the complexity of the changes occurring when the pottery was annealed (section 5.2) meant that there was no obvious way of separating those radiation damage traps, created since firing, from the remainder. Furthermore the results, discussed in Chapter 8, indicated that the number of traps created by the natural radioactivity was less than 1% of the total number of traps present and therefore their detection by the method described above would be extremely difficult.

It is, of course, possible that some of the radiation damage traps emit light of a particular wavelength in a particular temperature range which is different from that emitted by the traps existing at the termination of the firing. Under these circumstances, the saturation values for the X-ray and beta particle rate curves would provide a direct measure of the number of radiation damage traps. However the present work, which has covered the spectral range of 2500-6400Å and the temperature range of room temperature to 600°C has provided no evidence to support this hypothesis and therefore the only practical approach to the age determination of ceramics by thermoluminescence measurements seems to be through the measurement of the number of traps that have been filled with electrons or holes since the pottery was fired.

CHAPTER 6 X-IRRADIATION

It was shown in section 5.1.1. that the X-ray rate curves for sherd r (fig. 5/3) could be resolved into two components. The saturating component was interpreted as the filling of existing traps while the linear increase with X-ray dose was thought to be due to the creation of additional traps by the X-rays.

The normal mechanism by which traps are created is the direct displacement of atoms from the equilibrium positions in the crystal lattice. In the case of X-rays, interaction with electrons, either by Compton scattering or by the photo-electric effect, occurs first and it is these electrons which are involved in elastic collisions with the atoms making up the crystal lattice. Using equation 4/2, it can be shown that the maximum energy (E_m) transferred to an atom (atomic weight = 28) in an elastic collision, by 40 kv. X-rays, is approximately 3 ev. The displacement energies (E_d), determined experimentally for a number of monatomic materials, lie between 10 and 50 ev. (Billington and Crawford, 1961) and it is therefore unlikely that X-rays will produce atomic displacements by direct collisions.

There are however two other possible mechanisms by which low energy electrons might produce atomic displacements, these were put forward to explain the creation of F centres in the alkali halides by means of X-rays. The first, suggested by Seitz (1954), involves the "evaporation" of vacancies from existing lattice dislocations when localised regions of electronic excitation (excitons) discharge their energy at these lattice irregularities. The second, proposed by Varley(1954), involves the

multiple ionisation of atoms; these atoms are left in a highly unstable position from which they are ejected into interstitial sites with the creation of lattice vacancies.

A second possible explanation of the linearly increasing component of the X-ray rate curves was to associate it with the filling of traps with a very low probability of capturing electrons and holes. In order to ascertain which of these hypotheses was correct, samples of four sherds were subjected to a long X-irradiation, thermally bleached by heating to 450°C and then given a standard X-ray dose (section 6.1). The enhanced susceptibility, observed for the pre-irradiated samples, favoured the hypothesis of trap creation but further consideration of the results (section 6.1.1) suggested that this enhanced susceptibility was due, at least in part, to the "Forman effect".

The experiment was therefore repeated using thermally stable samples of sherd r and on this occasion the samples, after pre-irradiation and thermal bleaching, were subjected to X-ray doses ranging from 3×10^5 to 1.4×10^7 rads in order to avoid the "Forman effect" (section 6.2). This work established fairly conclusively that the X-rays were creating new traps.

It was hoped that the optical bleaching experiments, described in section 6.3, would provide further evidence for trap creation but the results were inconclusive and indicated that the effect of X-irradiation was more complicated than originally anticipated.

6.1. Thermal bleaching of X-irradiated sherds

Samples of sherds c, f, i and r were subjected to an X-ray dose of 1.4×10^7 rads (720 minutes), were thermally bleached by heating to 450°C on the slow heating apparatus and then each sample was given a standard X-ray dose of 2×10^5 rads (10 minutes). The thermoluminescence (L_x) resulting from this second irradiation was compared with that (L_o) obtained from a sample which had merely been heated before receiving the standard X-ray dose of 2×10^5 rads. It can be seen in Table 6/1 that the effect of pre-irradiation was to increase the susceptibility to the standard X-ray dose in all cases; this increase being greatest in the high temperature ranges (fig. 6/1).

Table 6/1

Thermal bleaching results

Sherd	L_x/L_o			
	50-150°C	150-250°C	250-325°C	325-425°C
c	1.08	1.02	1.44	4.05
f	1.18	1.09	1.02	1.66
i	1.03	1.09	1.14	2.80
r	1.47	1.46	3.85	5.28

For sherds i and r the experiment was repeated for pre-irradiation doses ranging from 1.2×10^6 to 1.8×10^7 rads and the values of L_x were plotted against the pre-irradiation dose for the high temperature ranges (fig. 6/2).

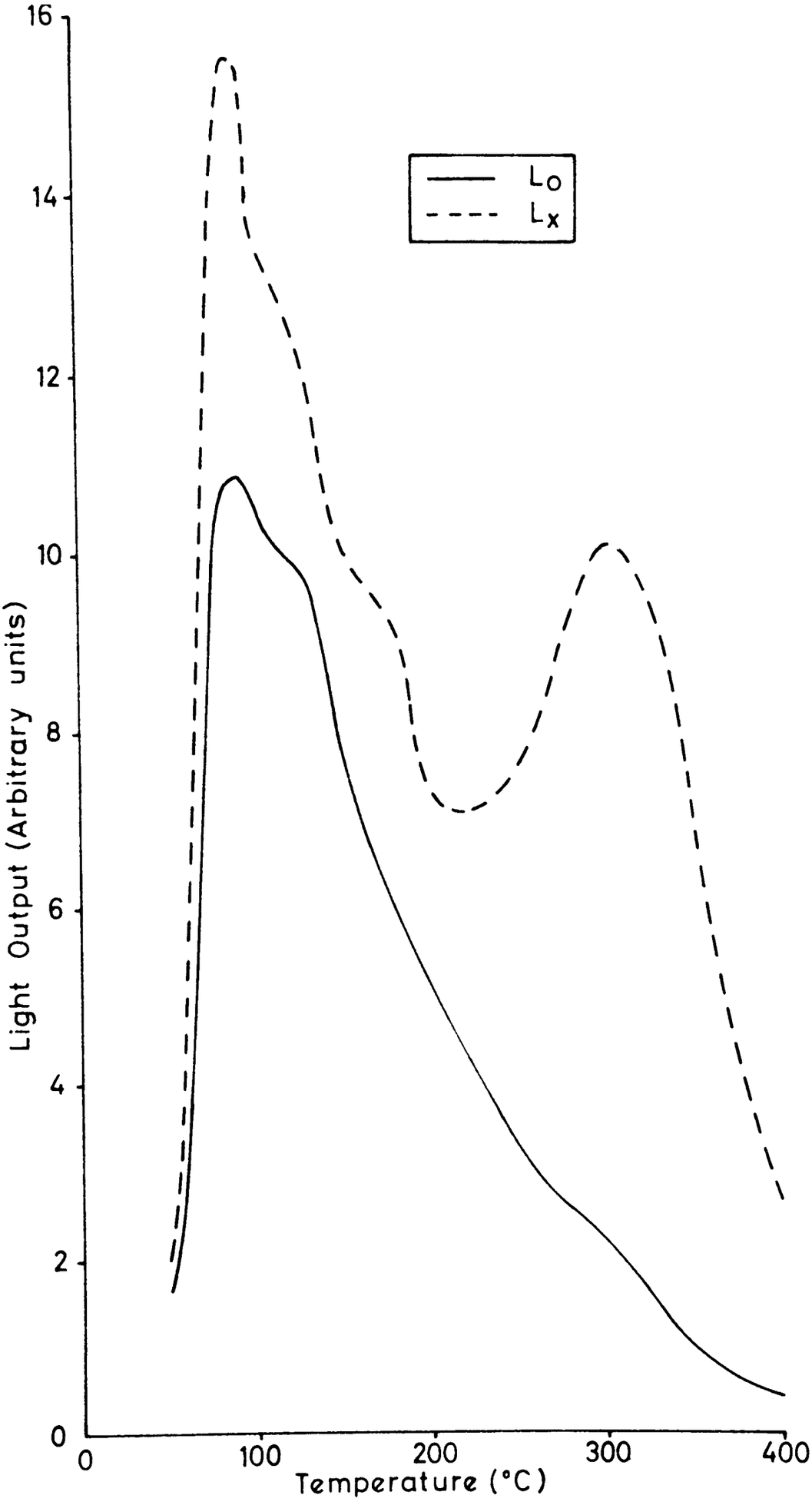

16
14
12
10
8
6
4
2
0
Light Output (Arbitrary units)
0
100
200
300
400
Temperature (°C)
Lo
Lx

Fig 6/1

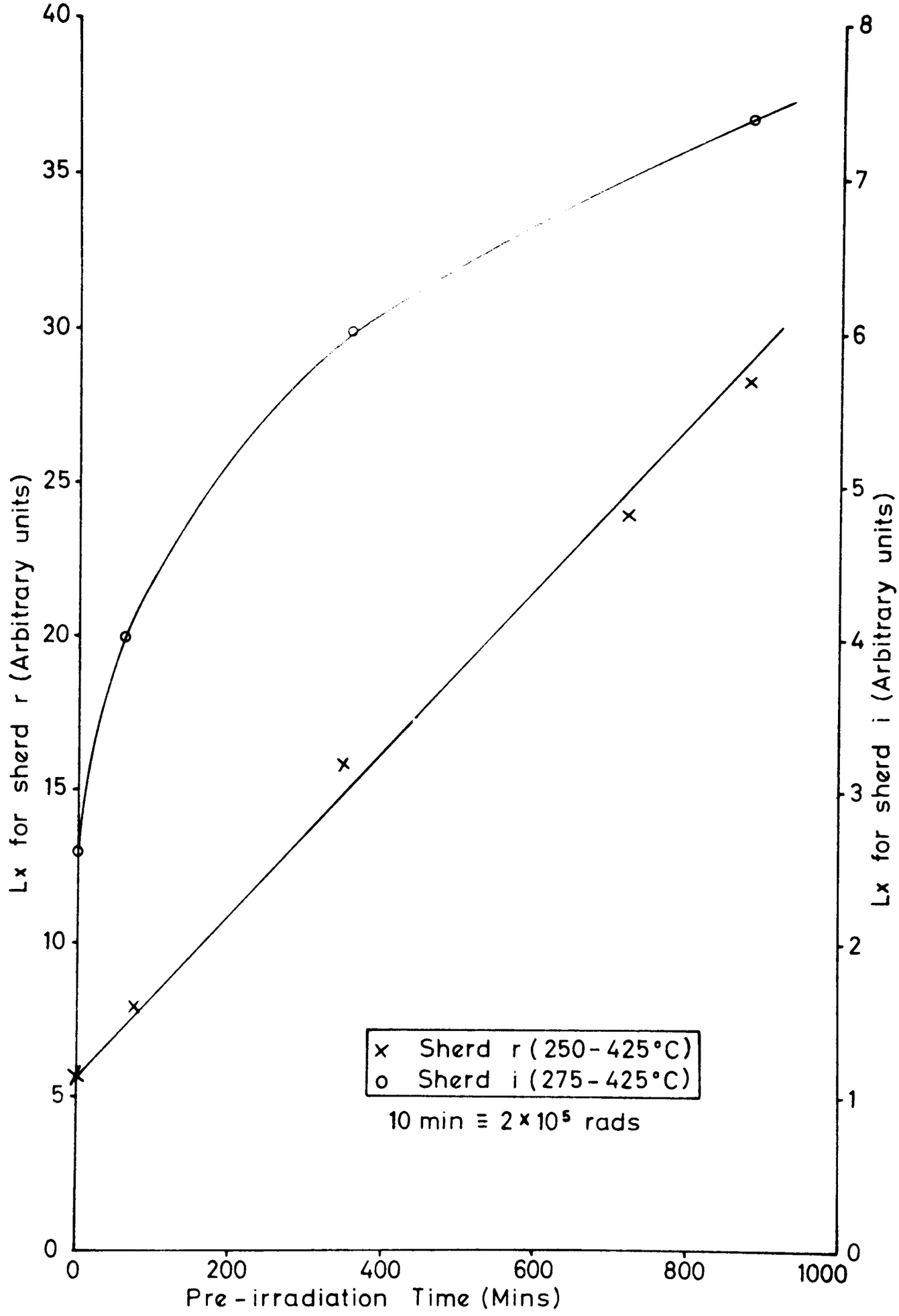

40
35
30
25
20
15
10
5
0
8
7
6
5
4
3
2
1
0
0
200
400
600
800
1000
Pre-irradiation Time (Mins)
Lx for sherd r (Arbitrary units)
Lx for sherd i (Arbitrary units)
x Sherd r (250-425°C)
o Sherd i (275-425°C)
10 min ≡ 2 x 10⁵ rads

Fig 6/2

This increased susceptibility was consistent with the existence of a linearly increasing component in the X-ray rate curves and with the hypothesis that the X-rays were creating additional traps. However when a quantitative correlation was attempted, agreement was poor (section 6.1.1).

6.1.1. Comparison with X-ray rate curves

In section 5.1.1 it was shown that the X-ray rate curves could be represented by an equation of the form:

$$L = L_s \left[1 - \exp(-ft)\right] + kt \qquad 6/1$$

where L = thermoluminescence for an irradiation of time, t,

L_s = saturation thermoluminescence for exponential component of rate curve (fig. 5/3).

k = slope of linearly increasing component of rate curve

f = constant, governing rate at which traps are filled.

The ratio $(L_s f)/k$ was approximately 30 for the X-ray rate curves, indicating that the rate at which traps were filled was very much greater than the rate of trap creation. Hence the ratio of the number of traps created (N_t) by an irradiation of time, t, to the number already existing in the pottery (N_s) is given by:

$$\frac{N_t}{N_s} = \frac{kt}{L_s} \qquad 6/2$$

For a sample which is subjected to a pre-irradiation of time, t_p, and is then thermally bleached the form of the rate curve obtained on re-irradiation is given by:

$$L^1 = (L_s + kt_p)\left[1 - \exp(-ft)\right] + kt \qquad 6/3$$

where L^1 = thermoluminescence for a re-irradiation of time, t. Therefore the values for L_x and L_o, discussed above, are given by:

$$L_x = (L_s + 720k)\left[1 - \exp(-10f)\right] + 10k$$

$$L_o = L_s\left[1 - \exp(-10f)\right] + 10k$$

In the case of the X-ray rate curves for sherd r, $L_s\left[1 - \exp(-10f)\right]$ was approximately ten times as large as 10k and therefore:

$$\frac{L_x - L_o}{L_o} = \frac{720k}{L_s}$$

Table 6/2 contains the values for $(L_x - L_o)/L_o$ obtained from the thermal bleaching experiments on sherd r together with the values for $720k/L_s$, derived from the X-ray rate curves obtained for untreated samples of sherd r.

Table 6/2

Comparison of thermal bleaching results and rate curves

	50-150°C	150-250°C	250-325°C	325-425°C
L_s	11000	6560	1350	1080
k	8.85	4.32	2.67	1.40
$\frac{720k}{L_s}$	0.58	0.48	1.42	0.93
$\frac{L_x - L_o}{L_o}$	0.47	0.46	2.85	4.28

The effect of pre-irradiation was, for the 250-425°C range, greater than anticipated from the calculations made on the X-ray rate curves. A possible reason for this discrepancy was that the ratio $720k/L_s$ was derived

from the rate curves for an untreated sample while the ratio $(L_x - L_o)/L_o$ was measured for a sample which had been pre-heated on the slow heating apparatus to 450°C. Although the effect of heat on the susceptibility of the sample to the standard X-ray dose (2×10^5 rads) was small (Table 5/2), its effect on the saturation level (L_s) may have been very much larger. Furthermore the effect of the thermal bleaching on the radiation damage traps (kt_p) was unknown.

However the most likely reason for the increased susceptibility to the standard X-ray dose, following pre-irradiation and thermal bleaching, was in terms of the "Forman effect". Forman (1951) found that if samples of crystalline quartz were X-irradiated until a saturation value for the optical absorption (A band) was reached and were then thermally bleached by heating to 400°C, on re-irradiation the rate of filling of the A centres was faster but the saturation values for the optical absorption remained unchanged. The explanation proposed (Paige, 1957) was that, although the A band was completely bleached by heating to 400°C, other filled traps associated with the C and D optical absorption bands still existed in the crystal. Hence on re-irradiation there was less competition for the electron-hole pairs than previously and consequently the A centres were filled more rapidly, although the same saturation level was reached. The "Forman effect" was observed when thermoluminescence measurements were made on sherd r using beta radiation and the theory is therefore discussed in more detail in Chapter 7.

In comparing the ratios $(L_x - L_o)/L_o$ and kt/L_s, no correction for the

"Forman effect" was possible and therefore the experiment was repeated using X-ray doses which were sufficient to produce saturation (Section 6.2). Although thermally stable samples of sherd r were used in this case, it was still possible that some of the radiation damage traps were annealed by heating to 500°C. Consequently optical bleaching experiments were also carried out (Section 6.3).

6.2. Rate curves for thermally stable samples of sherd r

150 mgms. of the thermally stable sample (Section 5.2.3) were irradiated with X-rays for 720 minutes (1.4×10^7 rads). They were then, together with a further unirradiated 150 mgms., thermally bleached by heating them for one hour in the tube furnace at 500°C in an atmosphere of nitrogen. X-ray rate curves were then measured for both samples using the slow heating apparatus (fig. 6/3). After an irradiation of 700 minutes, the thermoluminescence appeared to have reached a saturation value but this X-ray dose was not sufficient to establish conclusively whether or not the rate curves contained a linearly increasing component.

The ratios of the thermoluminescence from the pre-irradiated and thermally bleached sample (L_x) to that from the sample which had merely been thermally bleached (L_o) are given in Table 6/3 for re-irradiation times ranging from 15 to 700 minutes.

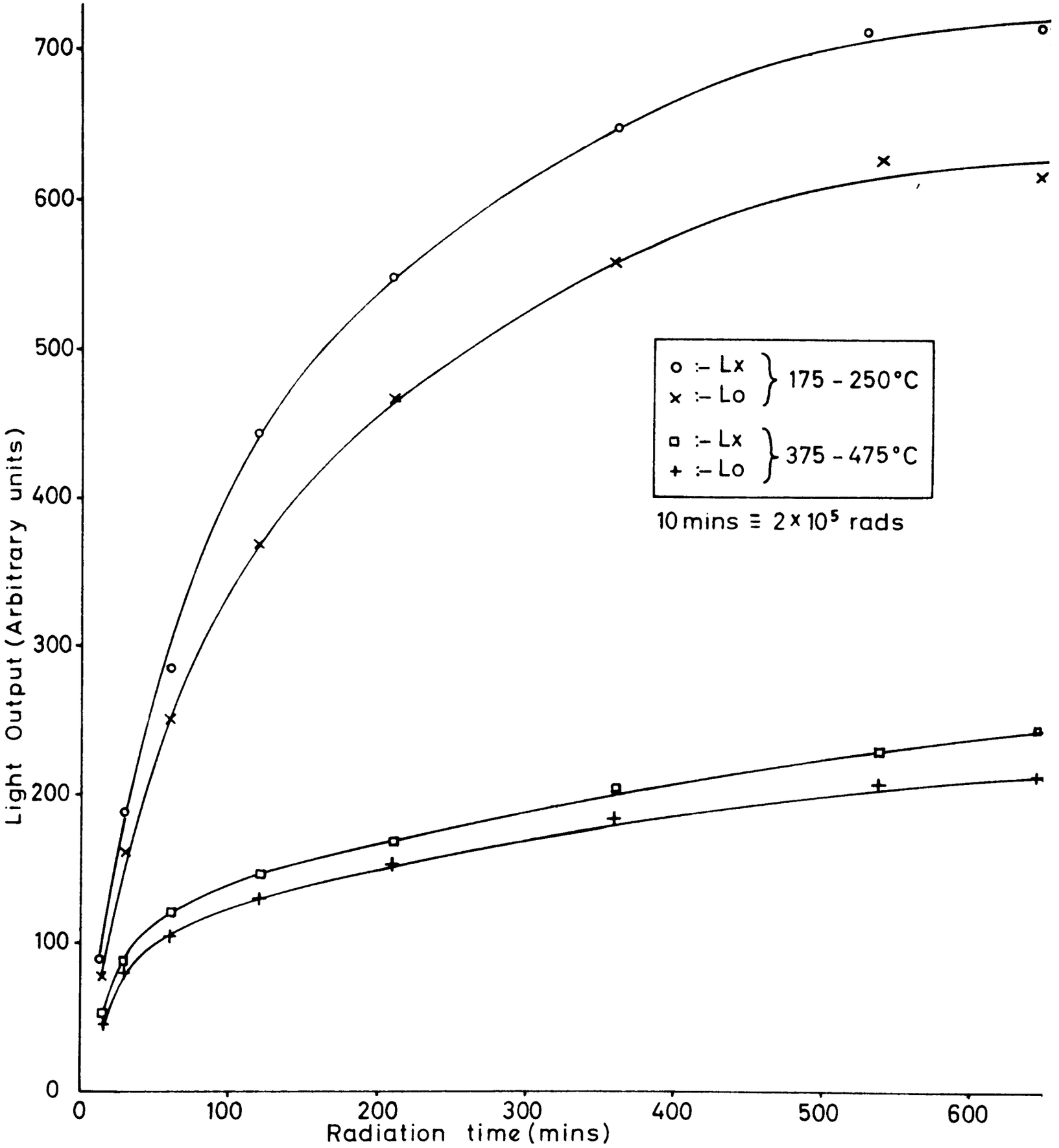

700
600
500
400
300
200
100
0
Light Output (Arbitrary units)
0
100
200
300
400
500
600
Radiation time (mins)
o :- Lx
x :- Lo
} 175 - 250°C
□ :- Lx
+ :- Lo
} 375 - 475°C
10 mins ≡ 2 x 10⁵ rads

Fig 6/3

Table 6/3

Effect of pre-irradiation

Re-irradiation time (mins).	L_x/L_o 60-100°C	100-175°C	175-250°C	250-375°C	375-475°C
15	1.89	1.06	1.15	1.21	1.15
60	1.32	1.11	1.17	1.19	1.18
360	1.12	1.09	1.15	1.19	1.15
700	1.11	1.08	1.18	1.20	1.17

Assuming that trap creation occurred then, from equation 6/3, it can be seen that:

$$\frac{L_x}{L_o} = \frac{(L_s + 720k)\left[1 - \exp(-f_x t)\right] + kt}{L_s \left[1 - \exp(-f_o t)\right] + kt}$$

where f_x and f_o are constants governing the rate at which traps are filled. If the "Forman effect" occurs then f_x will be greater than f_o and initially

$$\frac{L_x}{L_o} \approx \frac{(L_s + 720k)}{L_s} \frac{f_x}{f_o}$$

while for large re-irradiation doses, the ratio decreases to:

$$\frac{L_x}{L_o} \approx \frac{L_s + 720k + kt}{L_s + kt} \qquad \text{6/4}$$

and provides a method for calculating the rate at which new traps are being created.

In the 60-100°C range, the ratio L_x/L_o decreased from approximately 2, for small re-irradiation doses, to an essentially constant value of approximately 1.1 for large doses (Table 6/3). The large initial value obtained for L_x/L_o could be explained in terms of the "Forman effect" ($f_x > f_o$) while

assuming trap creation, the value of 1.1 obtained for large doses indicated that a 720 minute X-irradiation (1.4×10^7 rads) increased the trap concentration by approximately 10% (equation 6/4).

In the 100-475°C range, the ratio L_x/L_0 was constant, within the limits of experimental error, for all re-irradiation doses. Hence f_x equalled f_0 and no "Forman effect" occurred. From equation 6/4, it can be shown that a 720 minute X-irradiation increased the trap concentration by between 10 and 25% depending on the temperature range considered.

These results provided strong evidence for the hypothesis that X-rays created additional traps in ceramics and indicated that the linearly increasing component of the X-ray rate curves for sherd r (fig. 5/1) was more probably due to the creation of traps rather than to the filling of traps with a very low capture cross-section.

6.3. Optical bleaching experiment

A 60 mgm. sample of sherd r was irradiated with X-rays for 740 minutes (1.5×10^7 rads) and was then optically bleached for 90 minutes in sunlight (400 units on Weston Mark III light-meter). The effect of the bleaching was to reduce the thermoluminescence by between 30 and 60% depending on the temperature range considered. After thorough mixing, 10 mgm. portions of the bleached sample were subjected to X-irradiations of 30, 60 and 270 minutes respectively and their thermoluminescence was measured using the slow heating apparatus. Fig. 6/4 shows the X-ray rate curves obtained for untreated samples of sherd r, the effect of optical bleaching following a 740 minute X-irradiation and the rate curves resulting from the re-irradiation.

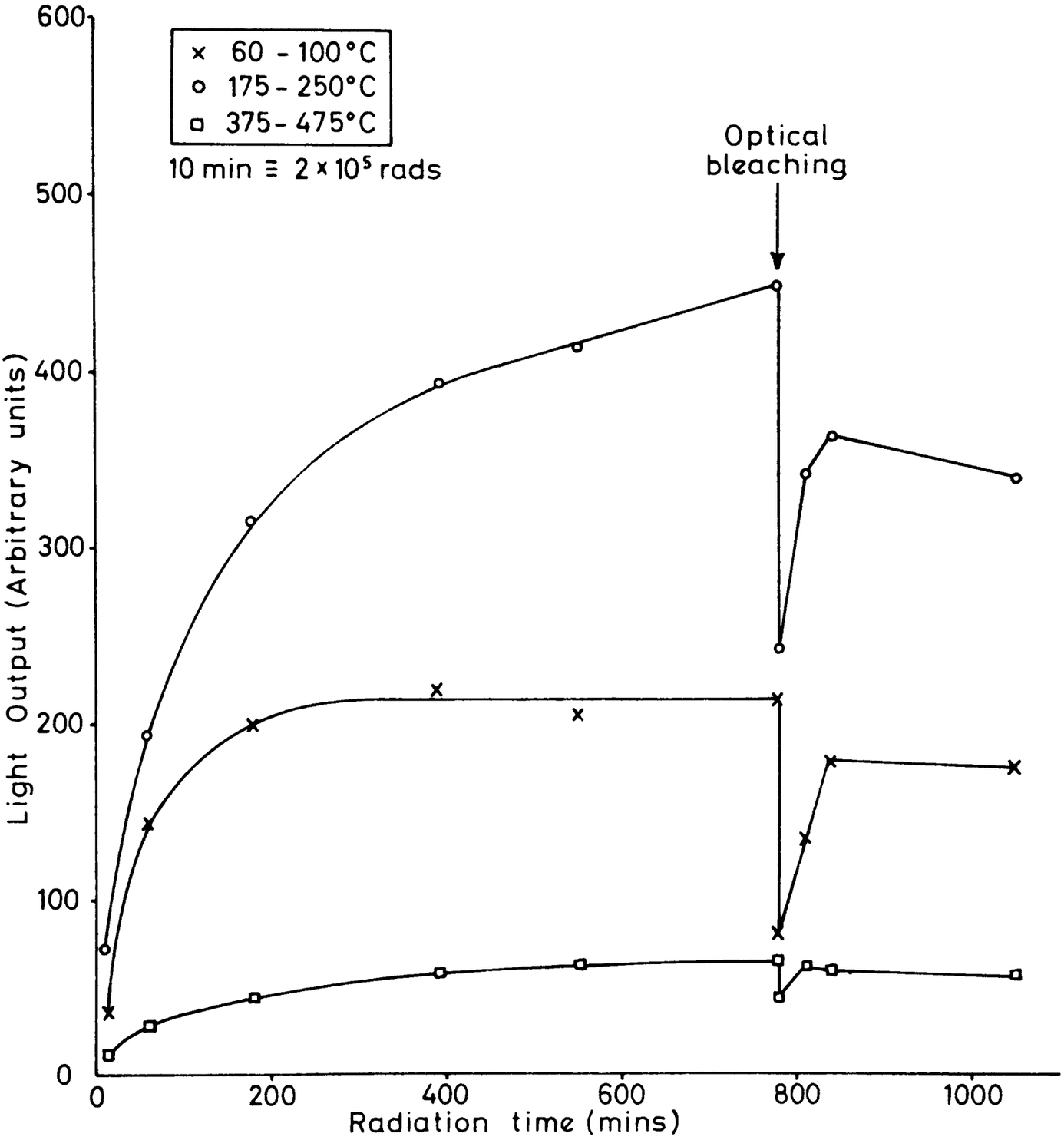

× 60 - 100°C
o 175 - 250°C
□ 375 - 475°C
10 min ≡ 2 × 10⁵ rads
Optical bleaching
Light Output (Arbitrary units)
0
100
200
300
400
500
600
0
200
400
600
800
1000
Radiation time (mins)

Fig 6/4

It was thought that, if on re-irradiation the shape of the original rate curve was followed, the linearly increasing component could be interpreted as the filling of traps with a low capture cross-section. However if the thermoluminescence rose rapidly to the value obtained from the 740 minute X-irradiation and then continued to increase linearly with the same slope as for the initial rate curve, the linearly increasing component could be associated with trap creation; the bleaching having emptied the newly created traps which, on re-irradiation, were rapidly refilled before further trap creation occurred (Amelincky, 1962).

In the case of sherd r (fig. 6/4), the initial effect of re-irradiation was to produce an increase in thermoluminescence, greater than that anticipated from the basic rate curves, and this result was consistent with trap creation. However further re-irradiation produced a slight decrease in thermoluminescence and the value associated with the initial X-irradiation of 740 minutes was not reached. An explanation of these results was not immediately apparent but since the optical bleaching can only have altered the distribution of electrons and holes in the various traps, they emphasize the strong dependence between this initial distribution and the subsequent effects of X-irradiation.

6.4. Conclusions

The fact that the X-ray rate curves contained a linearly increasing component provided the initial evidence for the creation of new traps by means of X-irradiation. The increased thermoluminescence observed when

thermally stable samples of sherd r were subjected to large re-irradiation doses, after pre-irradiation and thermal bleaching (section 6.2), confirmed this hypothesis.

The optical bleaching experiment (section 6.3) did not provide the additional confirmation anticipated. Instead, together with the "Forman effect" observed during the thermal bleaching experiments, it indicated that the effects of X-irradiation depended on the initial distribution of filled traps.

CHAPTER 7 BETA IRRADIATION

As indicated in section 5.1.3, the beta particle rate curves for sherd r, measured using a (Sr^{90} + Yr^{90}) source, reached a saturation level and there was no evidence for the existence of a linearly increasing component (fig. 5/7). These results indicated that the beta particles, unlike the X-rays (Chapter 6) and the alpha particles (Chapter 8), were not creating a significant number of new traps.

This difference between the alpha and beta particles is in agreement with the calculations presented in section 4.1. A 1.4 Mev. beta particle, when stopped in the target material, will produce less than one tenth of the displacements produced by a 1.8 Mev. alpha particle. Furthermore the alpha particles are stopped in the surface layer of a 15 mgm. sample while the 1.4 Mev. beta particles lose less than 10% of their energy in the sample.

The apparent absence of trap creation by the Varley and Seitz mechanisms (Chapter 6) for the beta particles can be explained in terms of the relative dose rates used for beta and X-irradiations. The radiation dose per unit time using beta and X-irradiation was in the ratio 1 to 20 and hence an irradiation time of several days would be necessary to produce an observable effect. Furthermore if the multiple ionisation of the atoms (Varley mechanism) was responsible for trap creation by the X-rays, then the probability of this occurring would decrease with the beta irradiations because of the decrease in dose rate.

A second distinctive feature of the beta particle rate curves was their non-linearity for small doses (Section 7.1). A simple model is proposed

to explain this non-linearity and the same model provides an explanation for the "Forman effect" observed after a large pre-irradiation followed by thermal bleaching (Section 7.2).

The revelance of these results to the age determination of ceramics is discussed in section 7.3.

7.1. Non-linearity of beta particle rate curves

In fig. 7/1 it can be seen that, for small doses, the beta particle rate curves for sherd r were not linear. A beta dose of 2×10^4 rads (20 minutes) produced more than twice the thermoluminescence resulting from a dose of 10^4 rads (10 minutes), while for larger doses there was a point of inflexion in the rate curves.

These results can be qualitatively explained by means of a "single centre" model in which only electrons are trapped and holes are immobile (Section 4.3.1). Two groups of electron traps (E_1 and E_2) are assumed. The rate constant for the recombination of an electron and a hole (C) equals that for the capture of an electron by an E_1 trap, while the rate constant for the capture of an electron by a E_2 trap is δC, where δ is greater than unity. From the theory presented in section 4.3.1, it can be shown that the equilibrium concentration of electrons in the conduction band (n') is given by:

$$n' = \frac{X}{C\left[N_1 + \delta N_2 - (\delta - 1)\, n_2\right]} \qquad 7/1$$

where N_1 and N_2 are the concentrations of E_1 and E_2 traps and n_2 is the

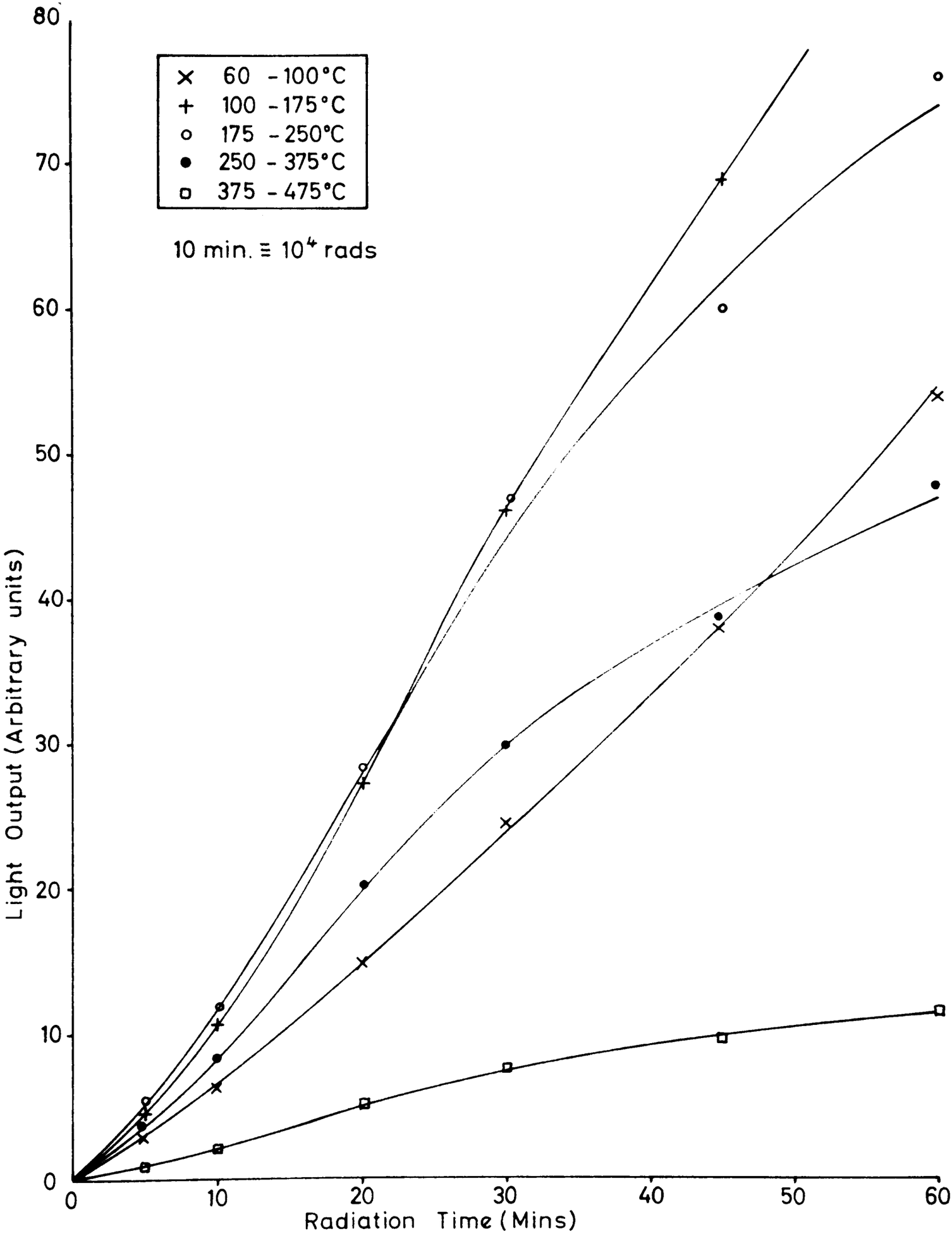

60 - 100°C
100 - 175°C
175 - 250°C
250 - 375°C
375 - 475°C
10 min. ≡ 10⁴ rads
Light Output (Arbitrary units)
Radiation Time (Mins)
0
10
20
30
40
50
60
70
80

Fig 7/1

concentration of filled E_2 traps at time, t. X equals the rate of generation of electron-hole pairs.

Hence as the E_2 traps are filled, the concentration of free electrons (n') increases (equation 7/1) and therefore the rate at which E_1 traps are filled increases. Assuming $N_1 = N_2 = N$, then it can be shown that the number of filled E1 traps (n1) and E2 traps (n_2) at time, t, is given by:

$$n_1 = N\left\{1 - \left[\frac{N - n_2}{N}\right]^{1/\delta}\right\}$$

$$n_2 = N\left[1 - \exp\left(\frac{\delta - 1}{2N}\right)n_2 \exp(-\delta X t/2N)\right]$$

Fig. 7/2 (Curve I) shows the rate curve that would be obtained for the E_1 traps if $N = 10^{18}$ cm^{-3}, $X = 5 \times 10^{14}$ cm.$^{-3}$ sec.$^{-1}$ and $\delta = 10$. This rate curve shows the non-linearity and inflexion exhibited by the beta particle rate curves in the 60-475°C range. Further evidence for the existence of the E_2 traps was provided by the thermal bleaching experiments described in section 7.2.

7.2. Thermal bleaching - "Forman effect"

Samples of sherd r were irradiated in situ on the slow heating apparatus for 900 minutes (9×10^6 rads) using the 40 mc. (Sr^{90} + Yr^{90}) beta source. They were then thermally bleached by heating to 500°C in nitrogen at a heating rate of 1°C/sec. Beta particle rate curves were measured for these samples and were compared with the rate curves obtained for samples which had merely been heated to 500°C in nitrogen (fig. 7/3). Table 7/1 contains the values for the ratio of the thermoluminescence from the irradiated and

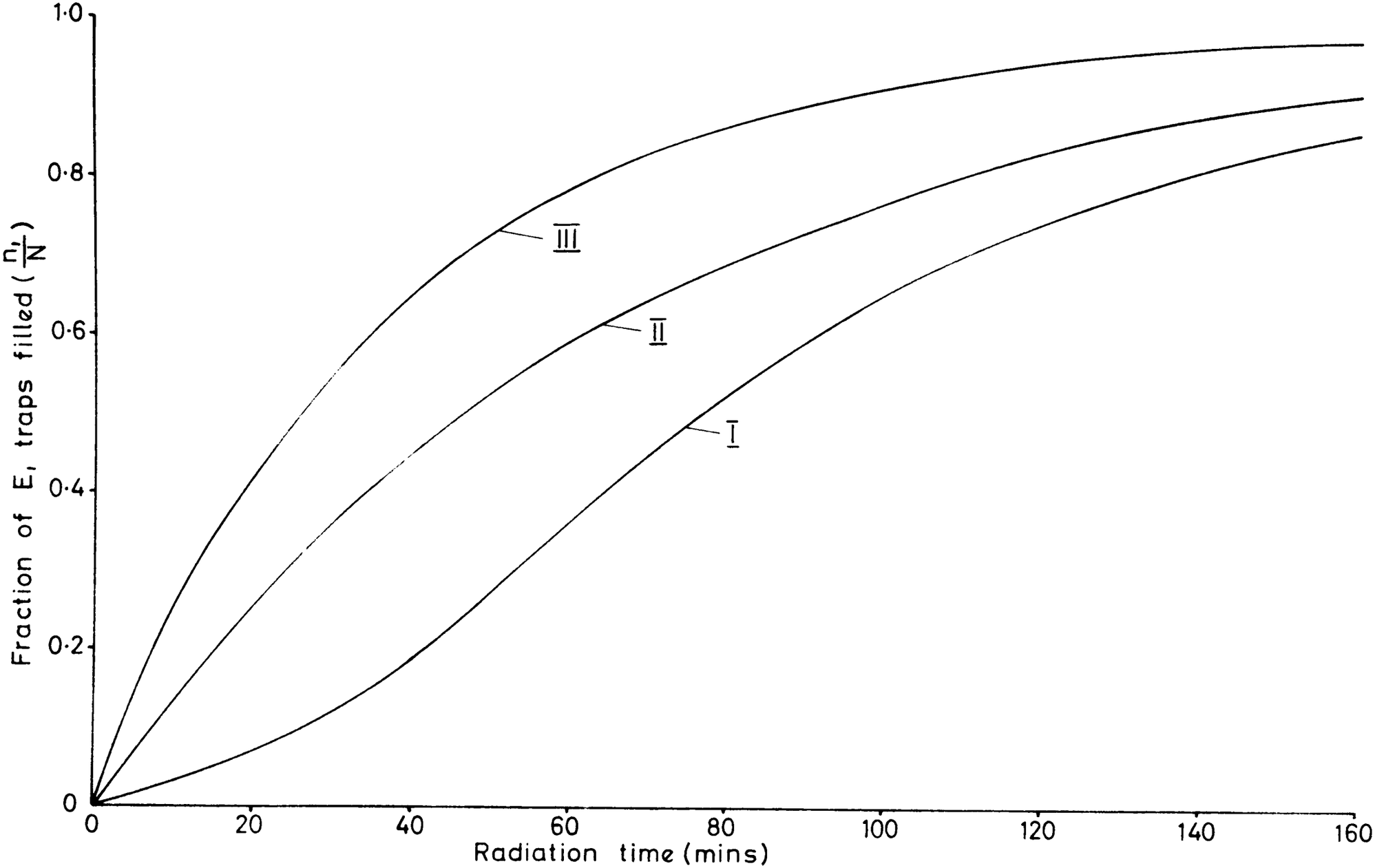

1·0
0·8
0·6
0·4
0·2
0
Fraction of E, traps filled ($\frac{n_1}{N}$)
III
II
I
0
20
40
60
80
100
120
140
160
Radiation time (mins)

Fig 7/2

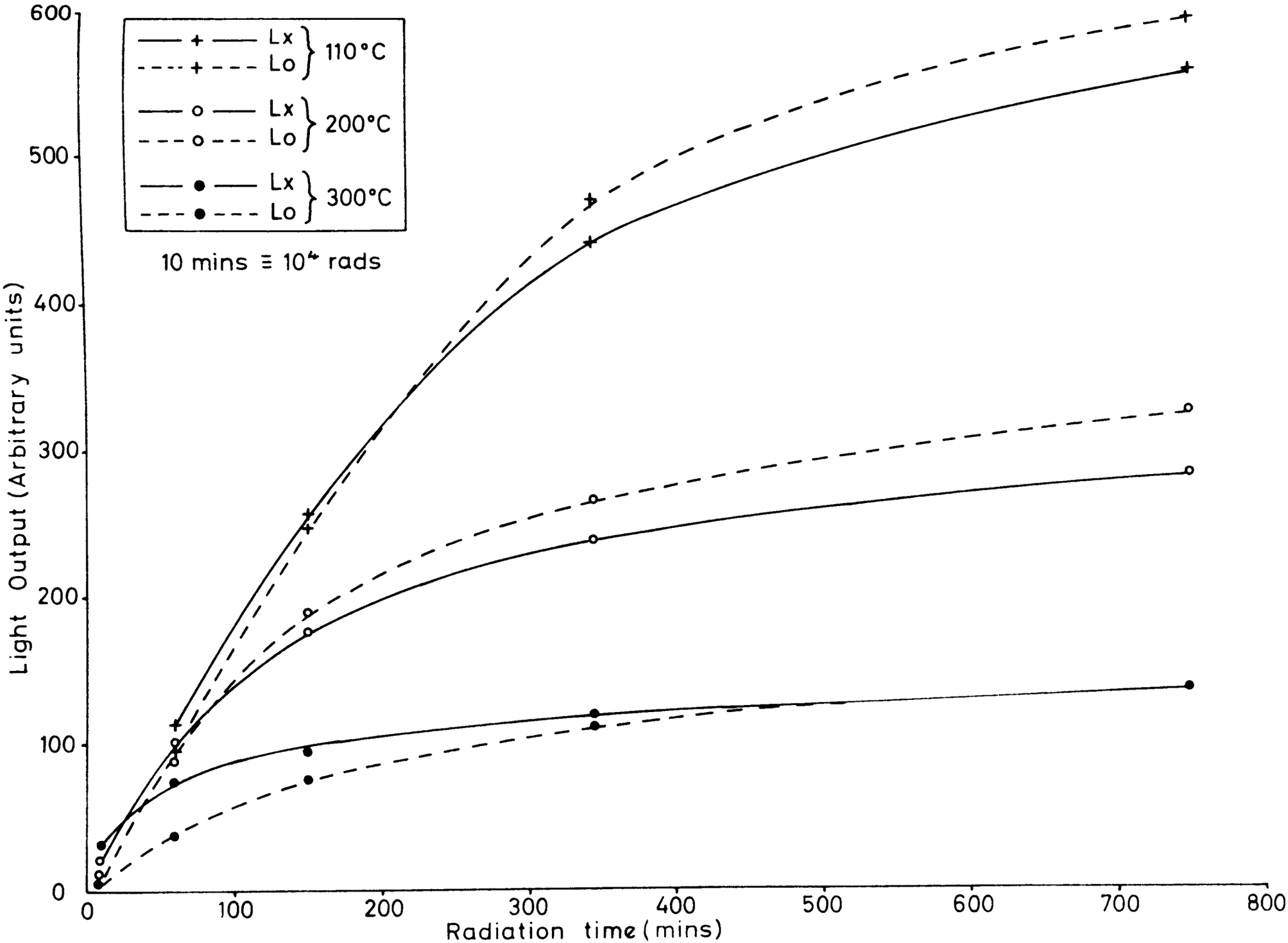

Lx
Lo
110°C
Lx
Lo
200°C
Lx
Lo
300°C
10 mins ≡ 10⁴ rads
Light Output (Arbitrary units)
Radiation time (mins)
0
100
200
300
400
500
600
700
800

Fig 7/3

preheated sample (L_x) to that from the preheated sample (L) for various re-irradiation times and fig. 7/4 shows the glow curves obtained from these two types of sample for a 10 minute beta re-irradiation.

Table 7/1

Effect of pre-irradiation on sherd r

Re-irradiation time (mins.)	L_x/L 65°C	110°C	200°C	300°C	400°C
10	3.7	1.3	1.7	4.8	5.3
60	1.8	1.1	1.1	2.0	1.8
150	1.3	1.0	0.9	1.3	1.3
340	1.0	0.9	0.9	1.1	1.0
750	0.9	0.9	0.9	1.0	1.0

Although attaining the same or slightly lower saturation values, the irradiated and preheated samples showed a considerable increase in susceptibility for small re-irradiation doses compared with the preheated samples. These results are comparable with those obtained for X-irradiation (section 6.1) and are also explicable in terms of the "Forman effect".

The model, proposed in section 7.1 to account for the non-linearity of the beta particle rate curves, also predicts the appearance of the "Forman effect" if it is assumed that the E_2 traps are not emptied by bleaching to 500°C. After a large beta irradiation, followed by thermal bleaching to 500°C, the E_1 traps associated with the 60-475°C range will be empty while the E_2 traps are still filled ($n_2 = N_2$). Hence on re-irradiation the equilibrium concentration of free electrons is given by (equation 7/1):

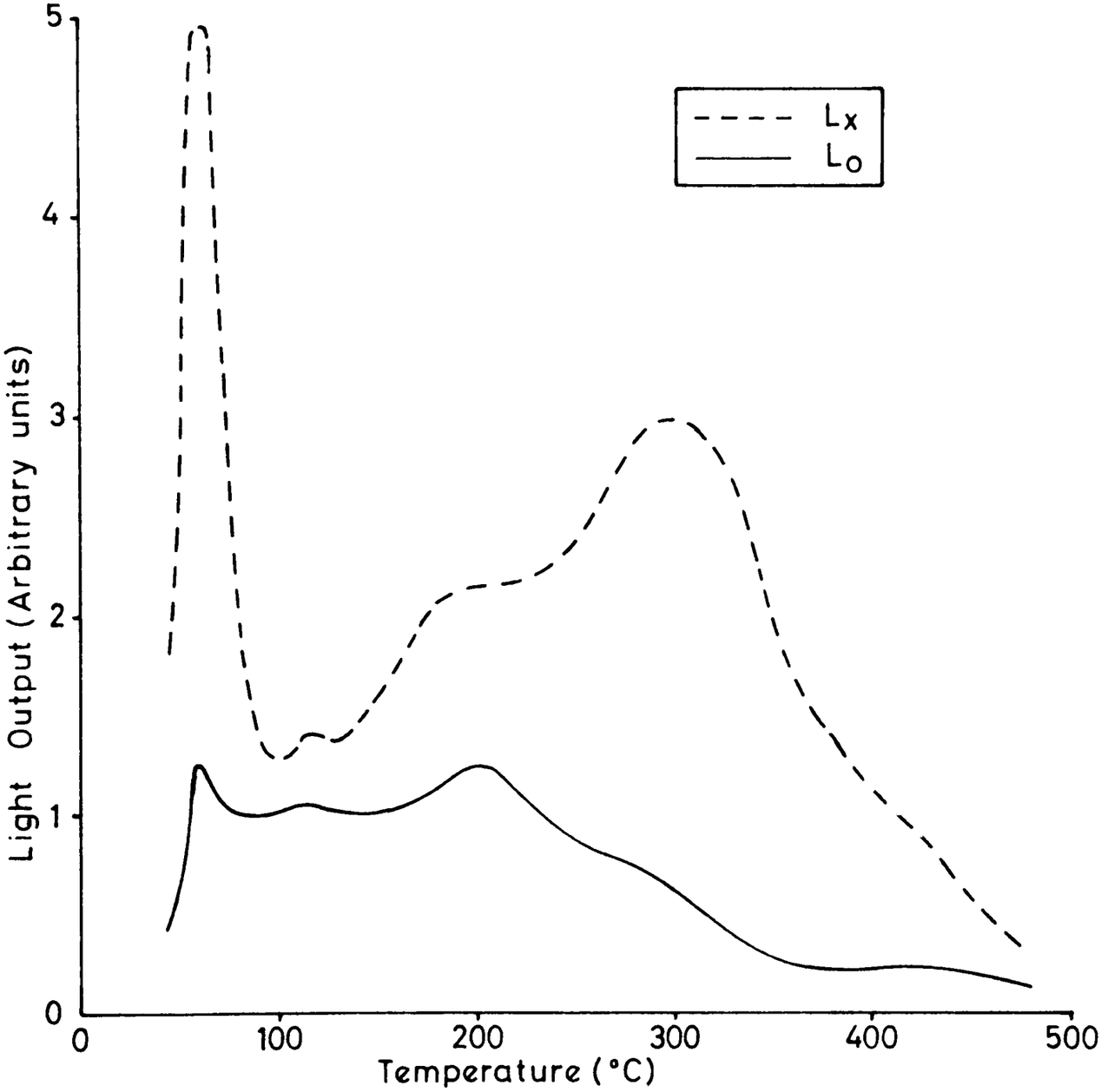

5
4
3
2
1
0
Light Output (Arbitrary units)
0
100
200
300
400
500
Temperature (°C)
Lx
Lo

Fig 7/4

$$n' = \frac{X}{C(N_1 + N_2)} \qquad 7/2$$

This concentration is greater than the initial value for an untreated sample (equation 7/1) since the E_2 traps are no longer competing for electrons. Hence the E_1 traps will be filled more rapidly, although reaching the same saturation value. Assuming $N_1 = N_2 = N$, the number of filled E_1 traps at time, t, when re-irradiated is given by:

$$n_1 = N\left[1 - \exp(Xt/2N)\right]$$

and fig. 7/2 (Curve II) shows the rate curve for the E_1 traps, using the same values for N and X as previously (section 7.1).

Although this model explains both the non-linearity of the beta particle rate curves and the "Forman effect", it cannot be used to explain the "radiation bleaching" observed for alpha irradiation (section 8.2). In this case the model must be extended to include the assumption that both conduction band electrons and valence band holes are mobile. Under these circumstances, trapped electrons can escape by direct recombination with valence band holes.

Finally it should be noted that there would be no point of inflexion in the rate curves and no "Forman effect" if the rate constant for the capture of electrons by the E_2 traps was less than that for the E_1 traps and for the recombination of free electrons and holes (i.e. $\delta < 1$). In this case the concentration of free electrons (n') would decrease as the E_2 traps were filled and the concentration after irradiation and thermal bleaching would also be reduced compared to the untreated sample (equations

7/1 and 7/2). Fig. 7/2 shows the theoretical rate curves for E_1 traps for:

Curve III - untreated sample

Curve II - irradiated and thermally bleached sample

The values for N and X are those used previously and $\delta = 0.1$.

7.3. Age determination

The second age determination programme (Aitken, Tite and Reid, 1963) was based on the measurement of the number of traps filled since firing. To measure the susceptibility the samples were irradiated without prior heat treatment and the age of the pottery was assumed to be proportional to:

$$\frac{L_N\, t}{L_\beta\, R} \qquad 7/3$$

where L_N equals the natural thermoluminescence; L_β equals the beta particle thermoluminescence, after correction for the natural thermoluminescence, for a t minute irradiation and R is the natural radiation dose to which the sherd is subjected. In practice all the sherds were given a 10 minute beta irradiation and the values obtained for the ratio L_β/L_N varied from 3 to 20.

Equation 7/3 will only provide the correct value for the age if the rate of acquisition of thermoluminescence is constant up to the value $(L_\beta + L_N)$. However the results presented in section 7.1 showed that the rate curves are not necessarily linear even for small doses well below the saturation level. In these circumstances the value obtained for the age will depend on the duration of the beta irradiation. For sherd r, the values for the susceptibility, L_β/t, initially increased with increasing irradiation time. When the point of inflexion in the rate curve was passed

and saturation commenced, the susceptibility decreased (Table 7/2).

Table 7/2

Variation in susceptibility of sherd r (375-475°C)

Irradiation time (t mins)	$\frac{L_\beta}{t}$
5	0.19
10	0.22
20	0.25
30	0.25
60	0.19
120	0.18

Hence to obtain a completely satisfactory figure for the age, it would be necessary to first empty all the traps; both in the 375-475°C range (E_1 traps) where the thermoluminescence is measured and at higher temperatures (E_2 traps) since these traps will also affect the rate at which E_1 traps are filled. The beta irradiation time (t'), necessary to reproduce the natural thermoluminescence, could then be measured. Unfortunately no satisfactory method for emptying all the traps has been found. Heating the sherd to 600 or 700°C produced large changes in the susceptibility, possibly due to the alteration of the luminescence efficiency of the sherd (section 5.2). Exposure to ultra-violet light filled, rather than emptied, traps for the low level of natural thermoluminescence observed in pottery (section 6.1.3). Bleaching with visible light only partially emptied the traps associated with the 300-500°C range while no measurements were possible above 500°C and hence the extent to which the E_2 traps were emptied was

unknown.

Therefore for the third age determination programme (Chapter 12), samples were irradiated in the untreated state. The beta irradiation time (t_1) was varied from sample to sample so that

$$L_\beta \approx L_N$$

since, from the rate curves obtained for sherd r, it can be seen that this irradiation time (t_1) was closest to that necessary to reproduce the natural thermoluminescence if all the traps had been emptied (t'). In addition each sherd was subjected to a beta irradiation of 3 x t_1 minutes in order to obtain some estimate of the extent to which the rate curve was non-linear. However no attempt was made to calculate the value of t' by extrapolation since, when an apparently linear rate curve was observed for the beta irradiation, this was not conclusive evidence that the rate curve had been linear during the acquisition of the natural thermoluminescence.

7.3.1. Thermal bleaching to 170°C

A second difficulty associated with the age determination measurements was that, since no natural thermoluminescence is observed below 200°C, the low temperature traps (20-200°C) will have been comparatively empty during the natural irradiation of the sherd. However during the beta irradiation they will have been progressively filled. The possible effect of the extent to which the low temperature traps (20-200°C) are filled, on the rate at which the high temperature traps (200-500°C) are filled, was investigated for sherd r.

A sample of sherd r was subjected to a 10 minute beta irradiation,

was thermally bleached to 170°C and was then subjected to a second 10 minute beta irradiation. The resulting thermoluminescence (L_1) was then compared with that from a sample which had received an uninterrupted 20 minute irradiation (L_2). It was established that heating to 170°C removed all the thermoluminescence below 150°C and that no bleaching occurred above 250°C.

Table 7/3

Effect of thermal bleaching to 170°C

	Thermoluminescence			
	60-150°C	150-250°C	250-375°C	375-475°C
L_1	18.7	31.3	20.3	5.02
L_2	32.6	34.2	20.1	5.22

The results (Table 7/3) showed that, in the 250-475°C range, the susceptibility to a 20 minute irradiation was, within the limits of experimental accuracy (± 5%), unchanged by emptying the low temperature traps (20-150°C) half-way through the irradiation. Hence, for sherd r, the comparison of the natural and beta thermoluminescence provides a valid figure for the age of the sherd as far as the influence of the low temperature traps is concerned.

CHAPTER 8 ALPHA IRRADIATION

As indicated in Chapter 4, it was expected that irradiation with alpha particles would produce additional electron and hole traps in the ceramic and that these would be detected through thermoluminescence measurements.

Preliminary results (section 8.1) showed that, in the 100-500°C range, the thermoluminescence reached a maximum value after a 100 minute alpha irradiation with a 60 mc. polonium 210 source and subsequently decreased. Further work on a second sherd (section 8.2) showed a similar decrease in the 60-250°C range while, in the 375-475°C range, the rate curve could be resolved into a saturating component and a linearly increasing component. The explanation proposed for the decrease in thermoluminescence for large alpha doses is that of "radiation bleaching" due to the creation of traps associated with the linearly increasing component in the 375-475°C range.

The radical differences between the alpha particle, beta particle and X-ray rate curves and their relevance to the hypothesis of trap creation are discussed in section 8.3. Further and more conclusive proof of this hypothesis is inferred from the thermal and optical bleaching experiments (section 8.4). Samples were subjected to a large alpha irradiation, bleached either by heating to 500°C or by exposing to ultra violet light for 4 hours and were then irradiated to saturation using a beta source.

In an attempt to establish the temperature range of the traps responsible for "radiation bleaching", thermally stabilised samples were given a large alpha irradiation, were thermally bleached to successively higher temperatures and were then subjected to a small alpha irradiation (section 8.5).

In order to simulate the natural radiation dose received by the sherds, ground-up samples were soaked in Ra^{224} solution and their rate curves were measured (section 8.6). In this case both the alpha particles and their associated recoil nuclei were present to produce traps. However the results obtained were not conclusive since it was difficult to provide a sufficiently strong dose using Ra^{224} solution.

In section 8.7, the rate curves obtained using polonium sources of different strengths are described. Finally in section 8.8 the evidence for the creation of traps is summarised and its relevance to the age determination of ceramics is discussed.

8.1. Preliminary results

The effects of alpha irradiation were first studied using a 60 mc. polonium 210 source, sealed with a 1 mg./cm.^{2} thick mica window (Radiochemical Centre, source no. PDD/50M). Samples of sherd i were irradiated in situ on the graphite plate for periods ranging from 1 minute to 30 hours and their glow curves were measured. Fig. 8/1 shows the thermoluminescence plotted against irradiation time. It can be seen that a maximum value was reached after approximately 100 minutes and subsequently the thermoluminescence decreased by approximately 50% throughout the 100-500°C range.

Samples of the same sherd were then subjected to alpha irradiations of 10, 60 and 1000 minutes in situ on the graphite plate. After thermal bleaching at 500°C for a few minutes, each sample was given a standard 10 minute X-irradiation (2×10^5 rads). The thermoluminescence (L_A) resulting

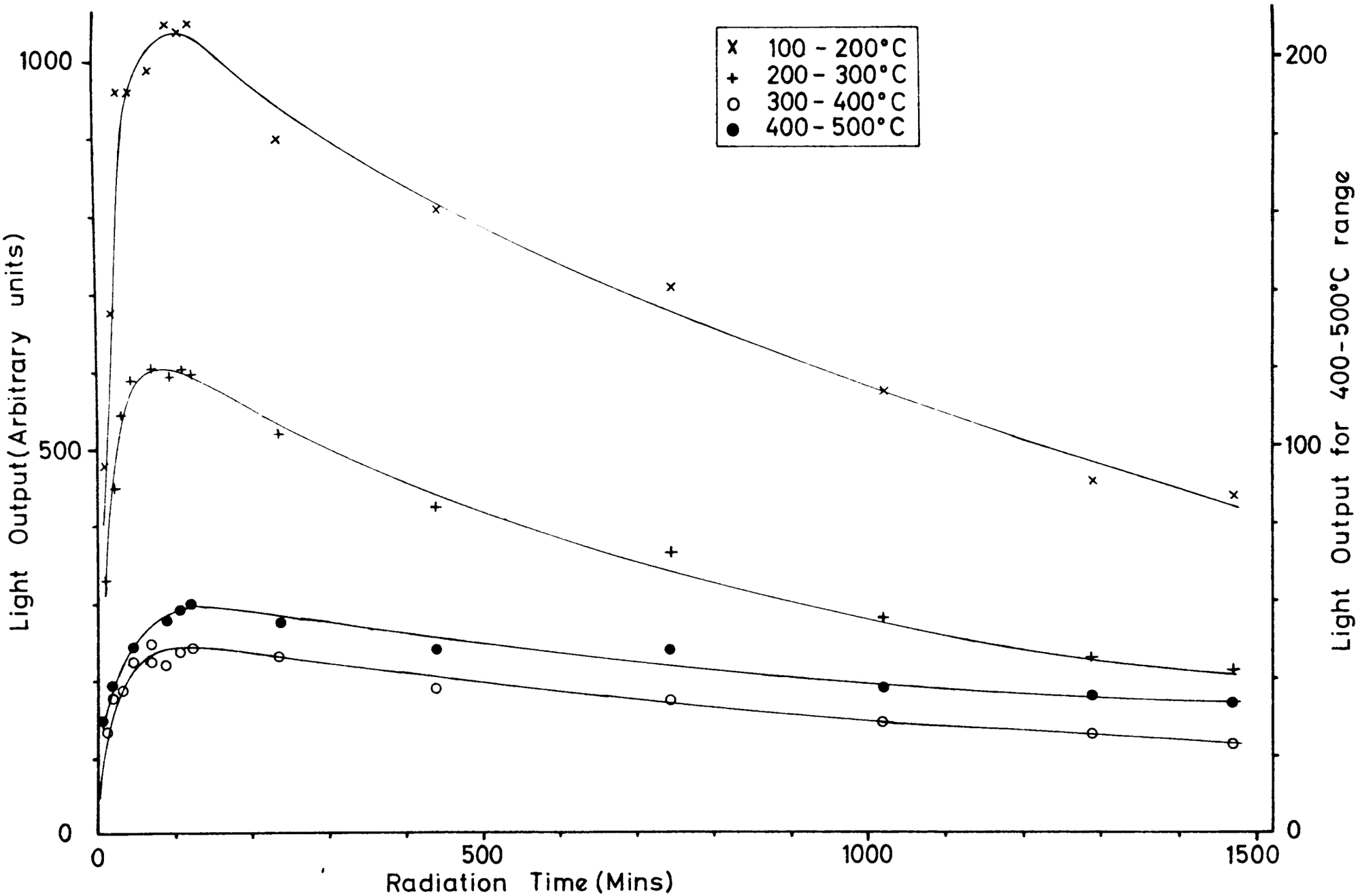

100 - 200°C
200 - 300°C
300 - 400°C
400 - 500°C
Light Output (Arbitrary units)
Light Output for 400-500°C range
Radiation Time (Mins)
0
500
1000
1500
0
500
1000
0
100
200

Fig 8/1

from this second irradiation was compared with that obtained from a sample which had only been thermally bleached before receiving the standard X-ray dose (L).

Table 8/1

Effect of pre-irradiation with alpha particles

Pre-irradiation time (mins.)	L_A/L 100-200°C	200-300°C	300-400°C	400-500°C
10	1.30	1.04	1.11	1.13
60	1.06	0.94	0.93	1.00
1000	0.77	0.73	0.75	0.83

The results are shown in Table 8/1 and it can be seen that a pronounced decrease in the susceptibility to the standard X-ray dose occurred after a 1000 minute alpha pre-irradiation, compared to the increase in susceptibility following a 720 minute pre-irradiation with X-rays (Table 6/1). This result was therefore consistent with the form of the alpha particle rate curves (fig. 8/1) but a precise interpretation was not possible because of the effect of the high temperature traps, which were still full after thermal bleaching at 500°C, on the initial rate of trap filling when the sample was re-irradiated. It has been shown in section 7.2 that filled high temperature traps can cause either an increase or a decrease in the initial rate of trap filling on re-irradiation, depending on the relative values of their rate constants.

A possible explanation of the decrease in thermoluminescence observed for long alpha irradiations was that the luminescence efficiency (i.e. the probability of an electron in the conduction band recombining with the

luminescence centre with the emission of light) was decreased because of the disordering of the crystal lattice by the alpha particles. However it can be seen from equation 4/7 that a 1000 minute irradiation with a 60 mc. polonium 210 source will displace only 1 in 10^4 of the atoms, in the surface layer of 15 mgm. sample, from their equilibrium positions in the crystal lattice. Since these displaced atoms will only affect the luminescence efficiency if they are produced in the vicinity of the luminescence centre, it seemed unlikely that this degree of disorder could produce a 50% decrease in the luminescence efficiency. Instead "radiation bleaching" was thought to be the more likely explanation since, in this case, the radiation damage traps associated with the displaced atoms all interact directly with the existing traps through the kinetics of trap filling.

The phenomena of "radiation bleaching", together with the results obtained for sherd r, is discussed in the next section 8.2).

8.2. "Radiation bleaching"

The alpha particle rate curves were measured for sherd r on the slow heating apparatus. The samples were irradiated in situ on the copper block using a 47 mc. polonium 210 source. The results (fig. 8/2) were similar to those previously obtained for sherd i except that the rate curve for the 375-475°C range could be resolved into a saturating component plus a linearly increasing component.

The results have to some extent been paralleled in the work on the effects of radiation on the optical absorption coefficient of fused and

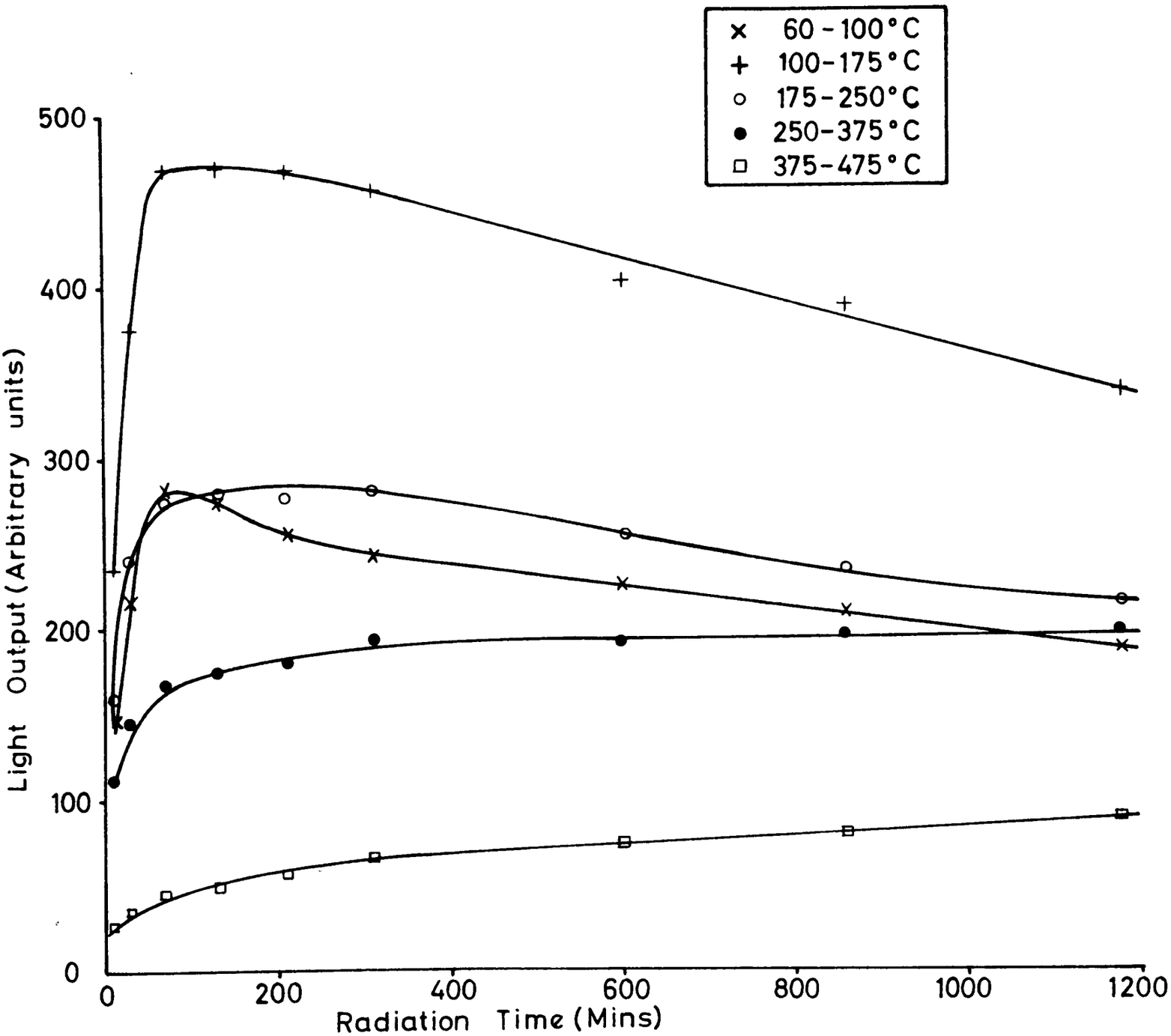

60 - 100° C
100-175° C
175-250° C
250-375° C
375-475° C
Light Output (Arbitrary units)
500
400
300
200
100
0
0
200
400
600
800
1000
1200
Radiation Time (Mins)

Fig 8/2

crystalline quartz. Ditchburn et al. (1954) have shown that X-irradiation caused the A band absorption coefficient of crystalline quartz to pass through a maximum before decreasing to a constant value, while fast neutron bombardment (Mitchell and Paige, 1956) in a reactor resulted in the continuous reduction of the A band, after reaching a maximum value. In addition the C band absorption coefficient increased linearly with neutron dose and a new absorption band, the E band, appeared. These phenomena have been satisfactorily explained by Paige (1957) in terms of trap creation and radiation bleaching.

On the basis of theory outlined by Paige, the following model is proposed to explain the thermoluminescence results. It is assumed that the thermoluminescence in the 60-250°C range is associated with one group of electron traps (E_1) and that in the 250-475°C range, it is associated with a second group of electron traps (E_2). In addition there is a group of hole traps or luminescence centres (L). It is further assumed that the rate constants (C) for recombination of electrons and holes (section 4.3.1) are all equal except for the rate constant for the recombination of the electrons in the E_2 traps with holes in the valence band, which is zero. Hence electrons in the E_2 traps are not released during the irradiation. The differential equations governing the concentration of electrons and holes in the traps and in the conduction and valence bands are, neglecting trap creation for the moment:

$$dn_1/dt = Cn(N_1 - n_1) - Cpn_1 \qquad \text{8/1}$$

$$dn_2/dt = Cn(N_2 - n_2) \qquad \text{8/2}$$

$$dn/dt = X - Cn(N_1 - n_1) - Cn(N_2 - n_2) - Cnp_1 - Cnp$$

$$dp/dt = X - Cp(P_1 - p_1) - Cpn_1 - Cpn$$

where N_1, N_2 and P_1 are the concentrations of E_1, E_2 and L traps respectively; n_1, n_2 and p_1 are the concentrations of these traps that are filled and n and p are the concentrations of free electrons and holes. X equals the rate of generation of electron - hole pairs.

Assuming that the equilibrium concentrations of free electrons (n') and holes (p') are small compared with the concentration of traps, it can be shown that:

$$n' = \frac{X}{CP_1} \qquad p' = \frac{X}{C(P_1 - n_2)} \qquad \text{8/3}$$

where, in order to conserve charge neutrality,

$$N_1 + N_2 = P_1$$

Therefore the concentration of filled E_2 traps at time, t, is given by (equations 8/2 and 8/3).

$$n_2 = N_2\left[1 - \exp(-Xt/P_1)\right] \qquad \text{8/4}$$

The concentration of filled E_1 traps, when all the E_2 traps, are filled is given by (equations 8/1 and 8/3)

$$n_1' = N_1^2/(P_1 + N_1) \qquad \text{8/5}$$

Under these equilibrium conditions, the number of electrons entering the E_1 traps from the conduction band equals the number escaping from the E_1 traps to recombine with holes in the valence band.

If the linearly increasing component of the alpha particle rate curves in the 375-475°C range is interpreted as the creation of E_2 traps, then the form of the rate curves indicate that the rate at which traps are filled is very much greater than the rate of trap creation (fig. 8/2). Hence the E_2 traps will be completely filled and the E_1 traps will have reached an equilibrium concentration given by equation 8/5 before a significant number of new traps are created. The effect of the continued increase in the number of E_2traps and also an equal increase in the number of L traps, introduced to maintain charge neutrality, is to reduce the number of free electrons in the conduction band (equation 8/3). Consequently the number of electrons entering the E_1 traps is reduced and this depresses the equilibrium concentration of filled E_1 traps - the phenomenon of "radiation bleaching". If the rate of creation of E_2 and L traps is ct where c is a constant, then the equilibrium concentration of filled E_1 traps is given by (equation 8/5):

$$n_1' = \frac{N_1^2}{(N_1 + P_1 + ct)} \qquad \text{8/6}$$

and the equilibrium concentration of filled E_2 traps is given by:

$$n_2' = N_2 + ct \qquad \text{8/7}$$

Hence on the basis of this model, the thermoluminescence in the 60-250°C range, associated with the E_1 traps, should increase to a maximum value given by equation 8/5 and then decrease continuously according to equation 8/6 because of the creation of E_2 traps. This is in qualitative agreement with the alpha particle rate curves measured for sherd r (fig.8/2).

Similarly the observed rate curve for the 375-475°C range which can be resolved into saturating and linearly increasing components is in agreement with the rate at which E_2 traps are filled (equations 8/4 and 8/7). Quantitative correlation is not possible since not all the E_2 traps are observable and anyway the luminescence efficiency for E_1 and E_2 traps may be different.

Unfortunately the occurrence of "radiation bleaching" does not provide conclusive proof that new traps are being created (Paige, 1957). "Radiation bleaching" will also occur if the linearly increasing component in the 375-475°C range is due to the filling of traps with a very low capture cross-section (rate constant = δ C where $\delta \ll 1$) and if the rate constant for recombination of electrons in these traps with valence band holes is zero. In this case the differential equations governing the number of free electrons and holes are;

$$dn/dt = X - Cn(N_1 - n_1) - \delta Cn(N_2 - n_2) - Cnp_1 - Cnp$$

$$dp/dt = X - Cp(P_1 - p_1) - Cpn_1 - Cpn$$

and the equilibrium concentrations are;

$$n' = \frac{X}{C\,[N_1 + \delta N_2 + (1 - \delta)n_2]} \qquad p' = \frac{X}{C\,(P_1 - n_2)} \qquad \text{8/8}$$

Again the concentration of filled E_1 traps will reach its equilibrium value before a significant number of the traps with low capture cross-section are filled. The continued increase in the number of these traps filled (n_2) will reduce the number of free electrons in the conduction band and increase the number of free holes in the valence band (equation 8/8). Hence

"radiation bleaching" will occur in the 60-250°C range, associated with E1 traps.

The possibility of associating the linearly increasing component with trap creation or the filling of traps with a low capture cross-section is further discussed in section 8.3 while conclusive evidence for trap creation by the alpha particles is presented in section 8.4. Measurements were made on sherd r and the limestone extraction from sherd k and were extended up to 625°C and also into the spectral range, 2300 - 3900Å.

8.3. Comparison of rate curves

Table 8/2 contains a summary of the data provided by the various rate curves which have been obtained for sherd r and the limestone extraction from sherd k. For the beta irradiations, the saturation values (L_s) for the rate curves have been listed. The X-ray rate curves and some of the alpha particle rate curves could be resolved into a saturating component (L_s) and a linearly increasing component whose slope (k) has also been listed (fig. 5/3). For those alpha particle rate curves which exhibited "radiation bleaching", the values of the maximum thermoluminescence (L_m) and the average rate of the subsequent decrease (k^1) during a 1000 minute irradiation have been given.

All the rate curves for sherd r and the X-ray rate curves for the limestone extraction were measured using the slow heating apparatus (1°C/sec) with a single CB10 filter to reduce the black body radiation while the alpha and beta particle rate curves for the limestone extraction were measured using the fast heating apparatus (20°C/sec.) with two CB10 filters, thus

Table 8/2

Summary of data provided by rate curves

Sherd r		Alpha particles (fig. 8/2)	Beta particles (fig. 5/7)	X-rays (fig. 5/1)
60-100°C	L_s	280	340	215
	k	-0.09	-	-
100-175°C	L_s	475	492	472
	k	-0.13	-	+0.29
175-250°C	L_s	280	280	296
	k	-0.05	-	+0.20
250-375°C	L_s	203	195	196
	k	-	-	+0.16
375-475°C	L_s	60.0	41.3	49
	k	+0.021	-	+0.036

Limestone extraction from sherd k

		Alpha particles (fig. 8/3)	Beta particles		X-rays
95°C peak	Ls	13	23.5	75-100°C	L_s 379
	k	+0.18	-		k +0.10
150°C peak	L_s	210	223	150-200°C	L_s 162
	k	+0.44	-		k +0.09
280°C peak	L_s	150	304	200-290°C	L_s 585
	k	-0.009	-		k -
360°C peak	L_s	29	72	290-400°C	L_s 78
	k	-0.002	-		k -
440°C	L_s	15.6	20	400-475°C	L_s 15.8
	k	+0.008	-		k +0.017
560°C	L_s	5.1	6.5		
	k	+0.002	-		

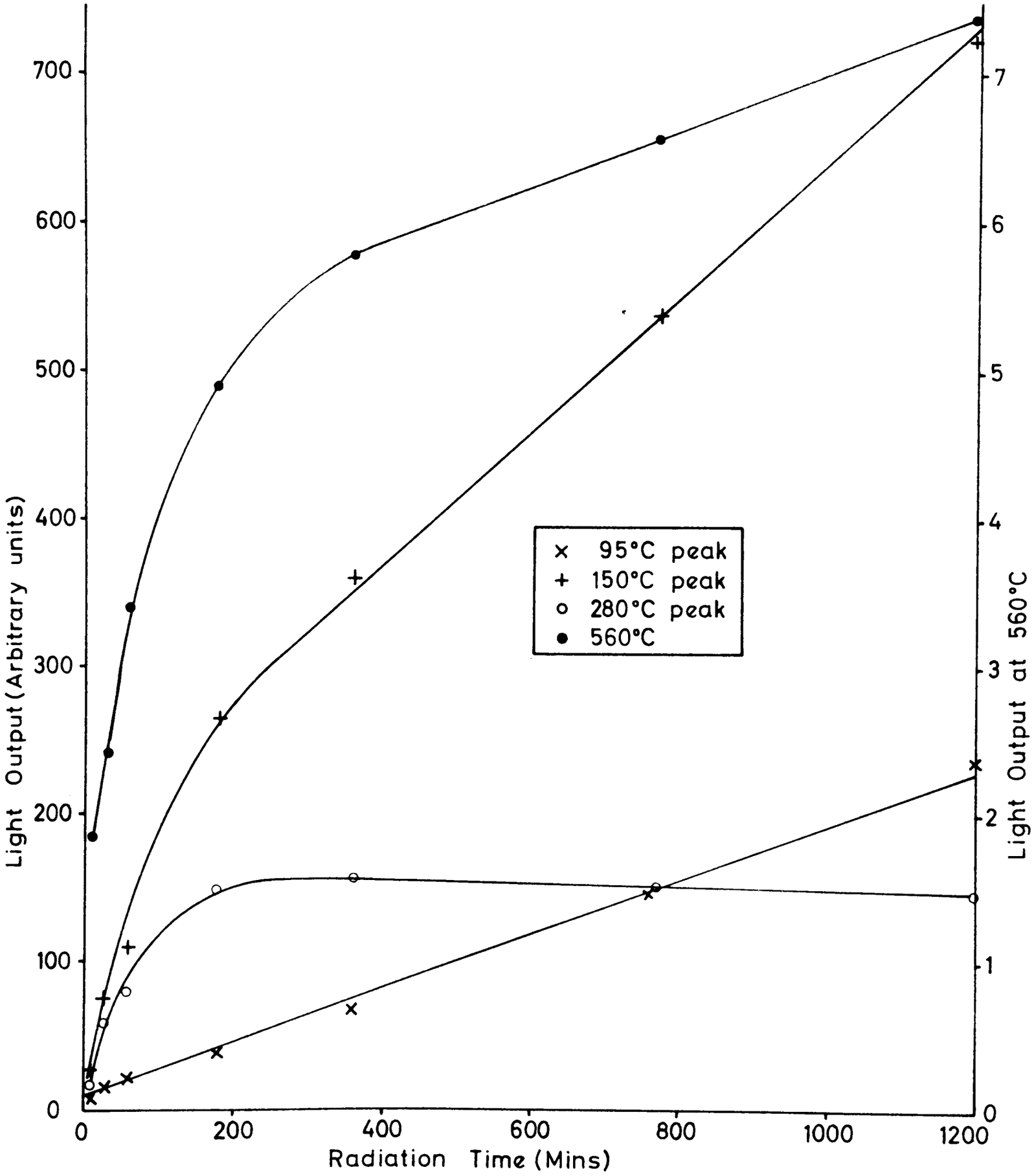

700
600
500
400
300
200
100
0
Light Output (Arbitrary units)
7
6
5
4
3
2
1
0
Light Output at 560°C
0
200
400
600
800
1000
1200
Radiation Time (Mins)
× 95°C peak
+ 150°C peak
o 280°C peak
● 560°C

Fig 8/3

enabling results to be obtained up to 600°C.

For sherd r, the values of L_s obtained using beta particles and X-rays were approximately equal in the 100-475°C range suggesting that in this case both types of radiation were filling the same groups of traps. The values of L_s for beta particles and X-rays could not be compared in the case of the limestone extraction since the measurements were made under different experimental conditions. The fact that the alpha particles only irradiate the surface layer of the sample, while the beta particles provide essentially uniform irradiation throughout the sample, prevented comparison of the values of L_s obtained from the alpha and beta particle rate curves.

The widely differing form of the rate curves obtained for a specific sherd using alpha, beta and X-irradiation indicated either that new traps were being created by the alpha particles and X-rays, the mechanism for trap creation being different for the two types of radiation (section 4.1 and Chapter 6), or that each type of radiation preferentially filled different groups of traps. Alternatively both processes contributed to the difference in the form of the rate curves.

The results presented in Chapter 6 suggested that the X-rays were creating new traps while evidence for trap creation by the alpha particles is given in section 8.4. However the differing shapes of the glow curves obtained for small alpha, beta and X-ray doses suggested that, in addition to trap creation, different groups of traps were preferentially filled (Chapter 9).

8.4. Thermal and optical bleaching

8.4.1. Sherd r

A sample of sherd r was irradiated in situ on the graphite plate for 900 minutes using the 10 mc. polonium 210 alpha source and was thermally bleached by heating it to 700°C in nitrogen at a rate of 20°C/sec. and cooling immediately. It was then given a 720 minute beta irradiation (7×10^5 rads) with the 40 mc. ($Sr^{90} + Yr^{90}$) source and its thermoluminescence (L_1) was compared with that obtained from a sample which had merely been heated to 700°C before the beta irradiation (L_2). The 720 minute beta irradiation was sufficient to produce saturation, thus avoiding the effect of the filled high temperature traps (greater than 700°C) on the initial rate of trap filling when the sample was re-irradiated, (Chapter 7).

On the basis of the model proposed in section 8.2, it can be seen that, assuming trap creation, the ratio L_1/L_2 will be less than unity (equations 8/4 and 8/7) for those temperature regions in which trap creation occurs. However if the linearly increasing component of the rate curve is due to filling traps with a low capture cross-section then the ratio L_1/L_2 will be unity throughout the temperature range observed.

The results obtained (Table 8/3) provided no conclusive evidence for trap creation but their reliability was doubtful because of the large changes in the saturation values brought about by heating alone. The ratio of the thermoluminescence from a sample subjected to a 720 minute beta irradiation after preheating to 700°C (L_2) to that from an untreated sample (L_5) ranged from 0.9 at 125°C to 2.4 at 625°C. Furthermore it was possible that the heating

to 700°C annealed a percentage of the radiation damage traps since Levy (1964), working with fused quartz and single-crystal alumina, observed that all the defects produced by irradiation in a reactor and detected by optical absorption measurements, were annealed by heating at 730°C for 20 minutes.

Consequently a further sample of the sherd was, after 900 minute alpha irradiation, optically bleached for 4 hours with ultra-violet light from an Hanovia lamp while still in situ on the graphite plate. It was then given the standard 720 minute beta irradiation and its thermoluminescence was measured (L_3). Direct comparison of L_3 with the thermoluminescence from an untreated sample (L_5) was not however permissible since, in the high temperature region, only 75-80% of the traps were emptied by optical bleaching. It was possible that the remaining traps were those with low capture cross-section which were not filled by beta irradiation, and would not therefore be included in L_5, but which might have been the cause of the linear portion of the alpha particle rate curve. Therefore the thermoluminescence from a sample which had merely been alpha irradiated and optically bleached (L_4) was also measured and the ratio $(L_3 - L_4)/L_5$ was calculated (Table 8/3 and fig. 8/4).

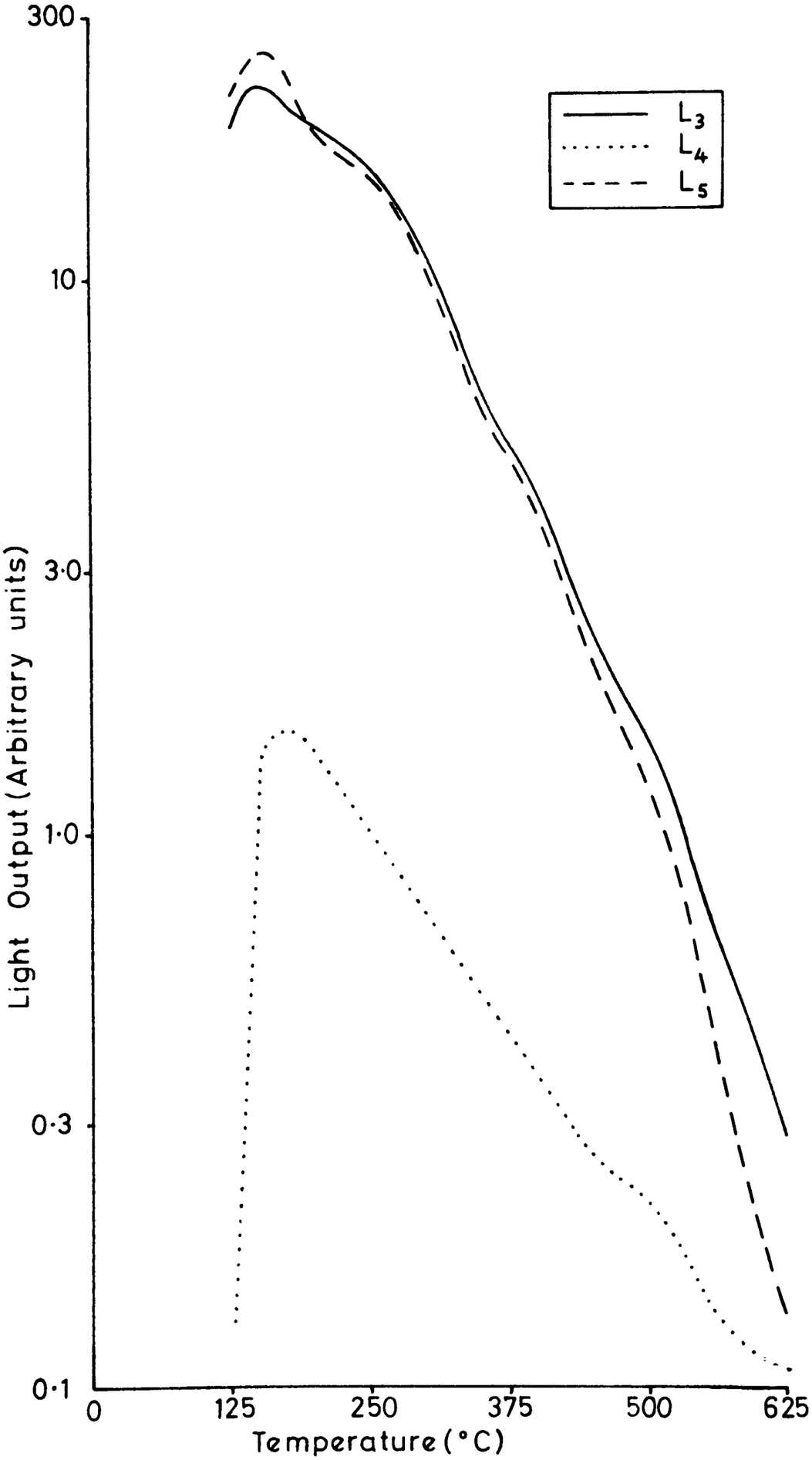

300
10
3·0
1·0
0·3
0·1
Light Output (Arbitrary units)
0
125
250
375
500
625
Temperature (°C)
L3
L4
L5

Fig 8/4

Table 8/3

Thermal and optical bleaching results for sherd r

		60-175°C	175-250°C	250-375°C	375-475°C	475-625°C
Thermal	$\frac{L_1}{L_2}$	1.04	0.85	0.80	0.84	1.01
Optical	$\frac{L_3 - L_4}{L_5}$	0.80	0.94	0.99	1.01	1.26

These results support the theory that the alpha particles create new traps in the range 475-625°C, while the fact that the ratio $(L_3 - L_4)/L_5$ was less than unity in the 60-250°C range was consistent with the "radiation bleaching" observed in this range for the alpha particle rate curves.

The lack of correlation between the linearly increasing component of the alpha particle rate curves in the 375-475°C range and the optical bleaching results could be because the subtraction of L_4 was not a valid correction. Therefore the above experiments were also carried out on the limestone extraction from sherd k (section 8.4.2) since its alpha particle rate curves contained a linearly increasing component in the 75-150°C range where the optical bleaching was 95% complete (fig. 8/5).

8.4.2. Limestone extraction from sherd k

As for sherd r, the thermal bleaching results did not correlate satisfactorily with the alpha particle rate curves (Table 8/4). However the heating alone again caused large changes in the saturation values, the ratio L_2/L_5 varying from 1.2 at 95°C to 0.6 at 560°C. Furthermore it was again possible that a percentage of the radiation damage traps were annealed by heating to 700°C.

The optical bleaching results, obtained by measuring the thermoluminescence in the ranges 2500-3900Å (0X7 filter) and 3700-4800Å (two 0B10 filters) showed much more conclusively that the alpha particles were creating additional traps (Table 8/4 and fig. 8/5). The increased saturation value for the beta irradiation for the 95 and 150°C peaks can be associated with the linearly increasing portions of the corresponding alpha particle rate curves (Table 8/2 and fig. 8/3) while the decrease in the saturation value for the 280 and 360°C peaks was consistent with the "radiation bleaching" previously observed for these peaks. In the 360-560°C range, bleaching with ultra-violet light only emptied between 10 and 30% of the associated traps so that there was no way of comparing the saturation values for the beta irradiation before and after the sample had been subjected to a large alpha dose.

Table 8/4

Thermal and optical bleaching results for limestone extraction

		95°C peak	150°C peak	280°C peak	360°C peak	440°C	500°C	560°C
Thermal								
3700-4800Å	L_1/L_2	0.97	1.36	1.24	0.72	0.79	0.94	1.14
Optical								
3700-4800Å	L_3	97	245	214	34.5	24.9	15.4	7.6
	L_5	23.5	220	304	72	20	11.2	6.4
	$(L_3 - L_4)/L_5$	3.9	1.1	0.6	-	-	-	-
2500-3900Å	L_3	436	700	320	21.0	6.9		
	L_5	48	440	404	32.0	7.3		
	$(L_3 - L_4)/L_5$	9.1	1.6	0.8	-	-		

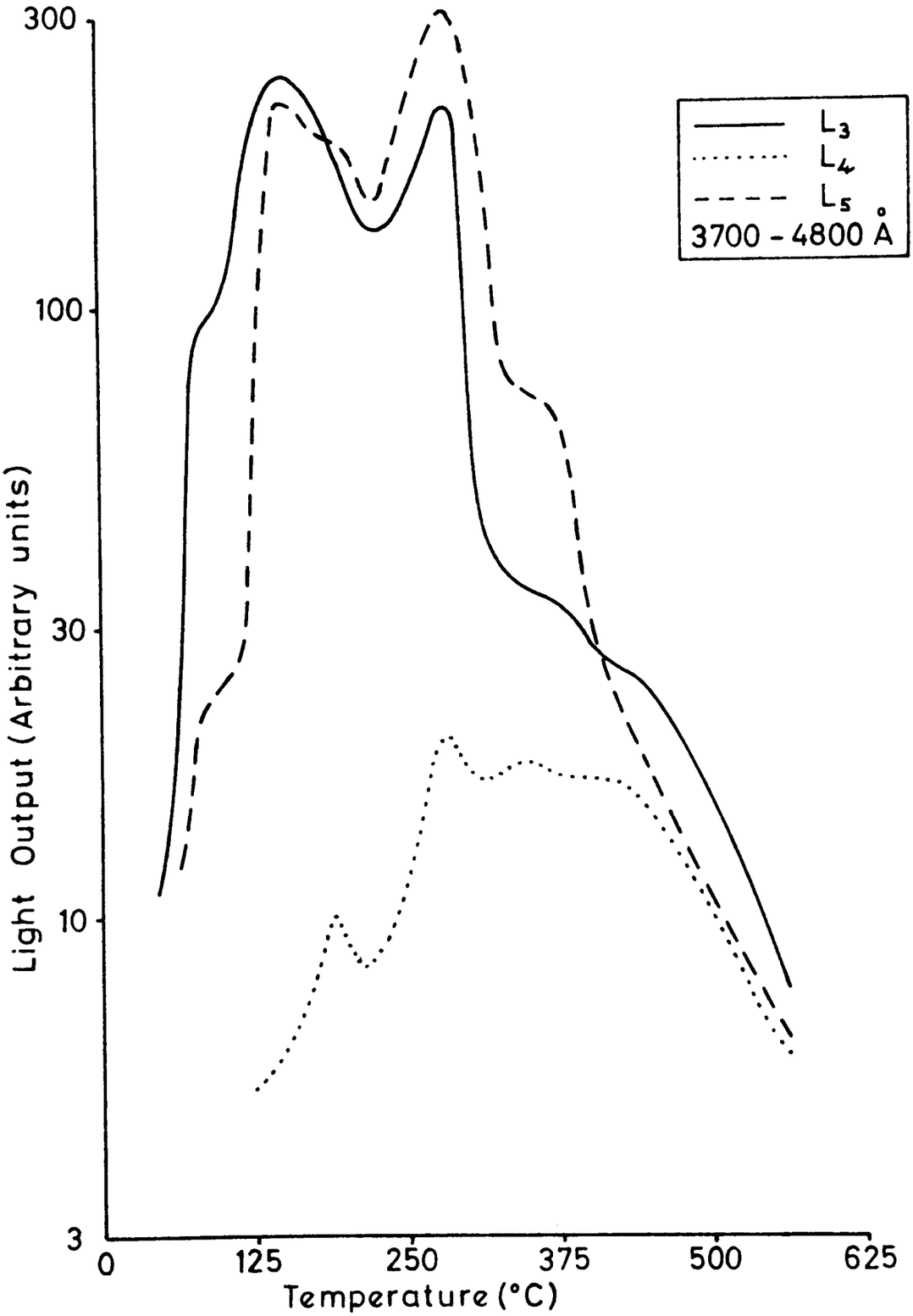

300
100
30
10
3
Light Output (Arbitrary units)
0
125
250
375
500
625
Temperature (°C)
L3
L4
L5
3700 - 4800 Å

Fig 8/5

Quantitative correlation between the alpha particle rate curves and the optical bleaching results obtained using beta particle saturation levels was not possible since the alpha particles only affect a surface layer of the sample (thickness $\approx$ 1.4 mgm./cm.^{2}) while the beta particles produced essentially uniform irradiation throughout the sample. The optical bleaching experiment was therefore repeated using 900 minute alpha irradiations for the measurement of L_3 and L_5 in the spectral range 3700-4800Å (Table 8/5).

Table 8/5

Optical bleaching results for the limestone extraction (re-irradiation with alpha particles)

	95°C peak	150°C peak	280°C peak
L_3	360	820	136
L_5	173	600	142
L_3/L_5	2.1	1.4	0.95
L_3/L_5 calculated from rate curves	1.9	1.6	0.88

For this sherd, in the model proposed in section 8.2, the E_1 traps are associated with the 280°C and 360°C peaks, for which "radiation bleaching" occurred, while the E_2 traps are associated with the 95°C and 150°C peaks and the 440-560°C range, for which the rate curves contained a linearly increasing component. Hence, assuming that the linearly increasing component is due to trap creation, it is seen that for the E_2 traps (equation 8/7):

$$\frac{L_3}{L_5} = \frac{(L_s + 900k) + 900k}{L_s + 900k} \qquad 8/9$$

where L_s = saturation value for alpha rate curves

k = slope of linearly increasing component

For the E_1 traps it is seen that (equation 8/6):

$$L_3 \propto \frac{N_1^2}{N_1 + P_1 + 1800c} \qquad L_5 \propto \frac{N_1^2}{N_1 + P_1 + 900c} \qquad L_m \propto \frac{N_1^2}{N_1 + P_1}$$

where L_m equals the maximum value for the alpha rate curve and therefore

$$\frac{L_3}{L_5} = \frac{L_m - L_3}{2(L_m - L_5)} \qquad 8/10$$

If the linearly increasing component is due to filling traps with low capture cross-section, then the ratio L_3/L_5 is unity provided all the traps with low capture cross-section are emptied by the optical bleaching.

In Table 8/5 it can be seen that, for those peaks which were reduced to less than 5% of their original strength by optical bleaching, the agreement between the values of L_3/L_5 measured directly and those calculated from the alpha particle rate curves was reasonable. These results therefore provided further proof that the alpha particles were creating new traps and that these radiation damage traps were the cause of the linearly increasing component of the alpha particle rate curves, observed in some temperature ranges, and the "radiation bleaching", observed in other ranges.

8.5. Thermal bleaching of stabilised samples of sherd r

Since the initial rate at which at a given type of trap is filled depends radically on the distribution of electrons and holes already present

in other traps, it was hoped that measurement of the alpha susceptibility of samples which had been thermally bleached to progressively higher temperatures, after being subjected to large alpha doses, would provide further evidence for the temperature range of the traps responsible for "radiation bleaching". On the basis of the model proposed in section 8.2, it was anticipated that pre-irradiation followed by low temperature bleaching would reduce the susceptibility to a small alpha dose in the 60-250°C range since the high temperature traps, responsible for "radiation bleaching", would remain filled and the initial equilibrium concentration of free holes in the valence band would be increased from $X/C(P_1 - n_2)$ to $X/C(P_1 - N_2)$ while the equilibrium concentration of free electrons would be decreased from X/CP_1 to $X/C(P_1 + ct_p)$ where tp is the pre-irradiation time (equation 8/3). As the bleaching temperature was increased and the traps responsible for "radiation bleaching" were emptied, the susceptibility in the 60-250°C should increase; the final value depending on the number of new traps that had been created.

The experiment was performed on thermally stabilised samples of sherd r (section 5.2.3) which were irradiated, in situ, on the copper block with a 30 mc. polonium 210 source for 840 minutes and were heated in nitrogen to temperatures of 120°C, 220°C, 320°C, 410°C, 500°C and 600°C respectively at a heating rate of 1°C/sec. When the maximum temperature was reached, the furnace was switched off and the samples were cooled in nitrogen to room temperature. They were then given a 5 minute alpha irradiation using the 10 mc. source and the resulting thermoluminescence was measured. The effect of heating to 600°C without pre-irradiation changed the susceptibility of the

sample to a 5 minute alpha irradiation by less than 10%.

Fig. 8/6 shows the thermoluminescence observed at various temperatures plotted against the bleaching temperature; the data for the low temperature region of the glow curve was the most complete since, above the bleaching temperature, the effect of the 5 minute irradiation was masked by the thermoluminescence resulting from the 840 minute irradiation.

The susceptibility showed the anticipated reduction in the 60-250°C range until the sample was thermally bleached to 410°C, and then the susceptibility rose rapidly with increasing bleaching temperature so that at 75°C the ratio of the thermoluminescence from a pre-irradiated sample, bleached to 600°C, to that from an untreated sample equalled approximately three, whereas on the basis of the model proposed in section 8.2 it should have been unity. This very large increase in susceptibility cannot be explained in terms of the model proposed in section 8.2. However the fact that it was predominant in the low temperature region (60 - 100°C) suggested that the effect was analogous to that observed for thermally stabilised samples of sherd r when pre-irradiated with X-rays (section 6.2) and that it was due to high temperature filled traps with a large capture cross-section (i.e. the "Forman effect"). The failure of these filled high temperature traps to produce an increased susceptibility, before the sample was thermally bleached to 500°C, was possibly due to rearrangement of the trap populations as a result of the heating.

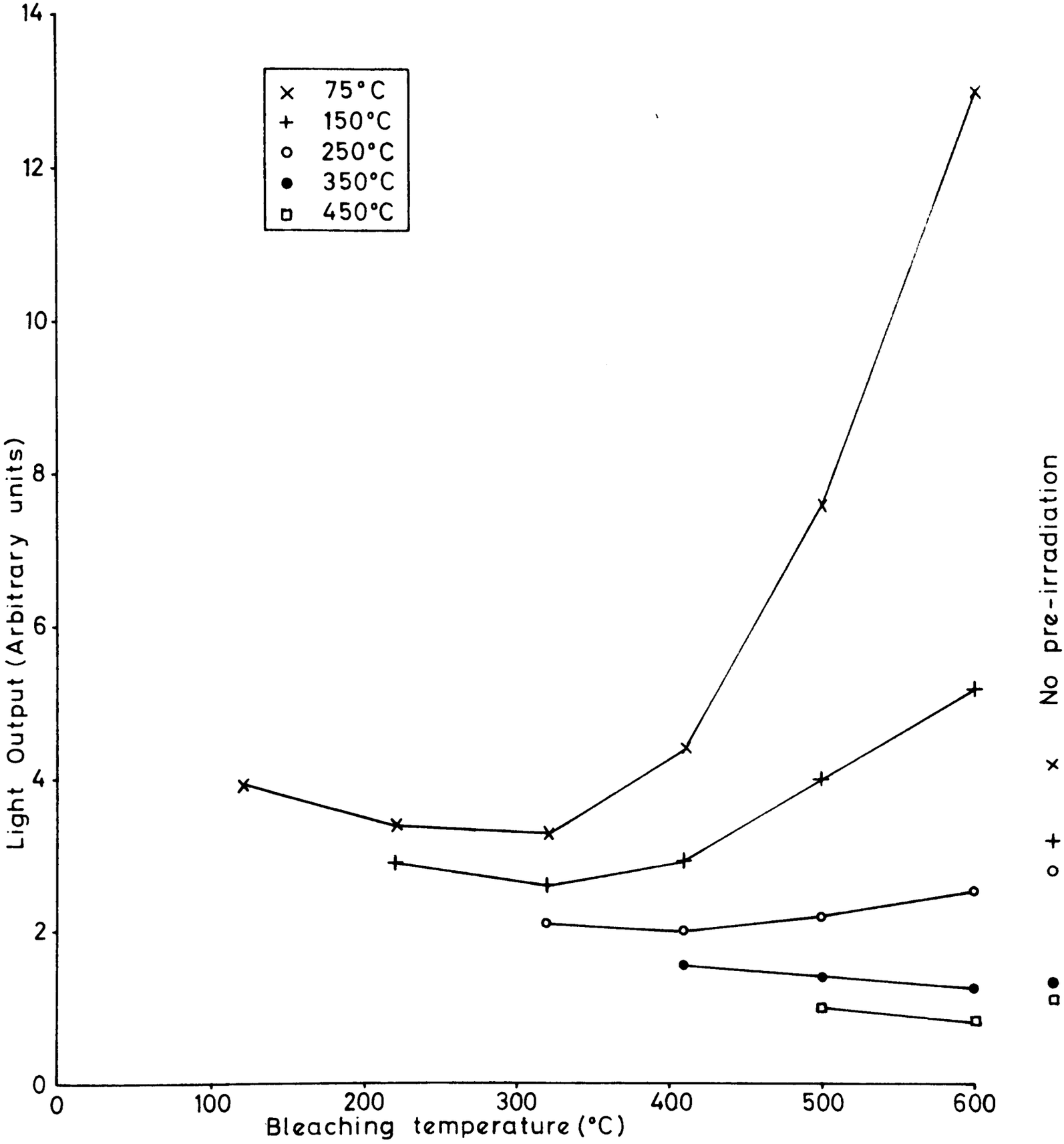

14
12
10
8
6
4
2
0
0
100
200
300
400
500
600
Light Output (Arbitrary units)
Bleaching temperature (°C)
× 75°C
+ 150°C
o 250°C
● 350°C
□ 450°C
No pre-irradiation
×
+
o
●
□

Fig 8/6.

8.6. Use of radium 224 solution

The radiation dose received by the pottery from the naturally occurring radioactive impurities consists of high energy alpha, beta and gamma particles together with their recoil nuclei. The energy of the recoil nucleus from a 6.3 Mev. alpha particle is 113 kev. and as shown in section 4.1, this is capable of displacing approximately 2000 atoms from their equilibrium positions in the crystal lattice compared with approximately 150, displaced by the alpha particle itself. Consequently as far as trap creation is concerned the polonium 210 sources do not satisfactorily reproduce the natural radiation dose received by the pottery. Therefore thermoluminescence measurements were made after adding a solution of radium 224 (ThX) in alcohol to ground-up samples of sherd r. The energy of the alpha particles emitted in this case were 5.8 Mev.

The strength of the solution used was 70 μc./ccs. and amounts ranging from 0.06 to 0.74 ccs. were added to 100 mgm. samples of sherd r using a micro-pipette. Only 0.06 ccs. were added at any one time and the alcohol was allowed to evaporate off in a fume cupboard before adding the next 0.06 ccs., thus ensuring that there was never any solution lying above the powder and failing to act on it. These samples were sealed and left in darkness for 44 days before measuring the thermoluminescence. The activity at that time was negligible since the half-life of radium 224 was 3.64 days.

In order to ascertain the effect, if any, of the alcohol itself on the susceptibility of the sherd, a further 100 mgms. were dosed with 0.06 ccs. of alcohol. After being left for 44 days, a sample was subjected to a

5 minute irradiation with a 24 mc. polonium 210 source and its thermoluminescence was found to be equal to that from an untreated sample. However it was observed that the physical appearance of the samples dosed with more than 0.2 ccs. of radium 224 solution had changed markedly. Even after passing hot air from a hair-dryer over them for an hour, in order to evaporate the alcohol, the particles tended to coagulate and after heating to 500°C on the slow heating apparatus they formed into a hard compact layer.

The validity of the rate curves obtained (fig. 8/7) was therefore in doubt. Furthermore the thermoluminescence emitted by a sample, to which 0.74 ccs. of solution had been added, was equal only to that from a sample which had been subjected to a 10 minute irradiation with a 50 mc. polonium 210 source. Because of the difficulties involved in handling stronger solutions, the rate curves could not be extended to sufficiently high doses to establish the presence of "radiation bleaching" or of a linearly increasing component. Consequently work with the radium 224 solution was discontinued.

8.7. Dependence on the strength of the alpha sources

On the basis of the theory presented in section 8.2, the saturation values for those rate curves which could be resolved into saturating and linearly increasing components should be independent of the strength of the alpha source. Similarly provided the rate at which traps are filled is considerably greater than the rate of trap creation, the maximum value for those rate curves which showed "radiation bleaching" should also be independent of the source strength.

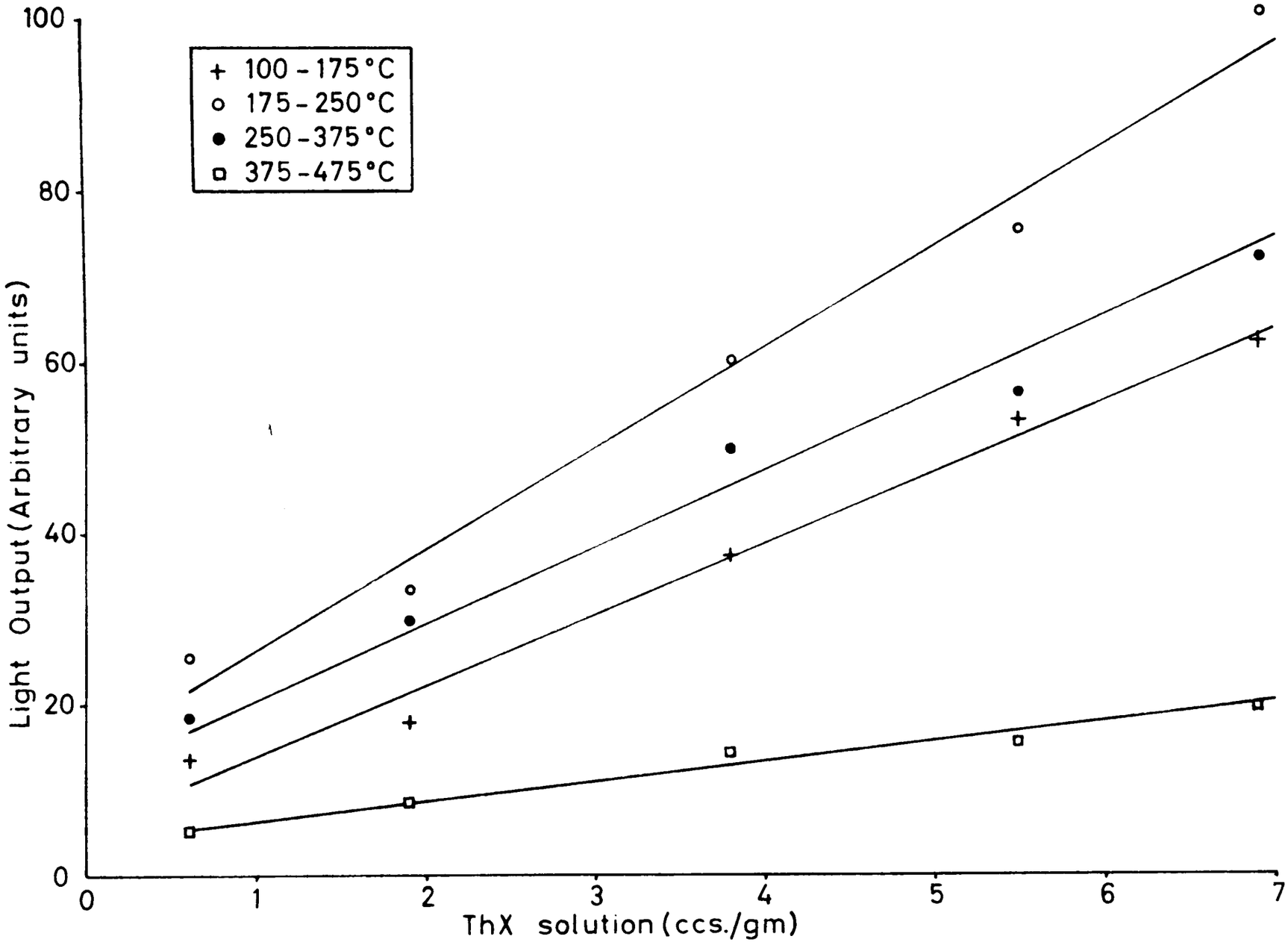

100 - 175 °C
175 - 250 °C
250 - 375 °C
375 - 475 °C
Light Output (Arbitrary units)
0
20
40
60
80
100
0
1
2
3
4
5
6
7
ThX solution (ccs./gm)

Fig 8/7.

Alpha particle rate curves were measured for sherd r using polonium 210 sources of different strengths; the relative source strengths having been determined using a scintillation counter (Appendix 1). The maximum or saturation values (L_s), the irradiation time necessary for the thermoluminescence to reach half its maximum or saturation value (τ), the slope of the linearly increasing component (k) and the percentage decrease in L_s, observed after a 1200 minute irradiation (R), are given in Table 8/6.

The maximum or saturation values (L_S) for sources without a mylar window decreased by less than 25% when the strength of the alpha source decreased by a factor of six. Considering the possible variation in the thickness of the mica windows and the area of the sources, these results suggested that the values for L_S were essentially independent of the source strength. However the effect of adding a mylar window (thickness = 1.5 mgm. /cm^2) was to reduce the values for L_S by a factor of approximately two. It was known (Appendix 1) that the addition of the mylar window reduced the energy of the alpha particles from 1.8 $\pm$ 0.4 Mev. to 0.7 $\pm$ 0.2 Mev. Consequently the range of the alpha particles were reduced by a factor of between two and three and hence the proportion of the sample subjected to alpha irradiation was reduced by the same factor. The agreement between the reduction in the values of L_s and the reduction in the volume irradiated suggested that the depth in the sample, from which light reached the photomultiplier, was greater than the range of the alpha particles. If the depth, from which light was collected, was less than the range of the alpha particles then there should be no reduction in L_s when a mylar window was

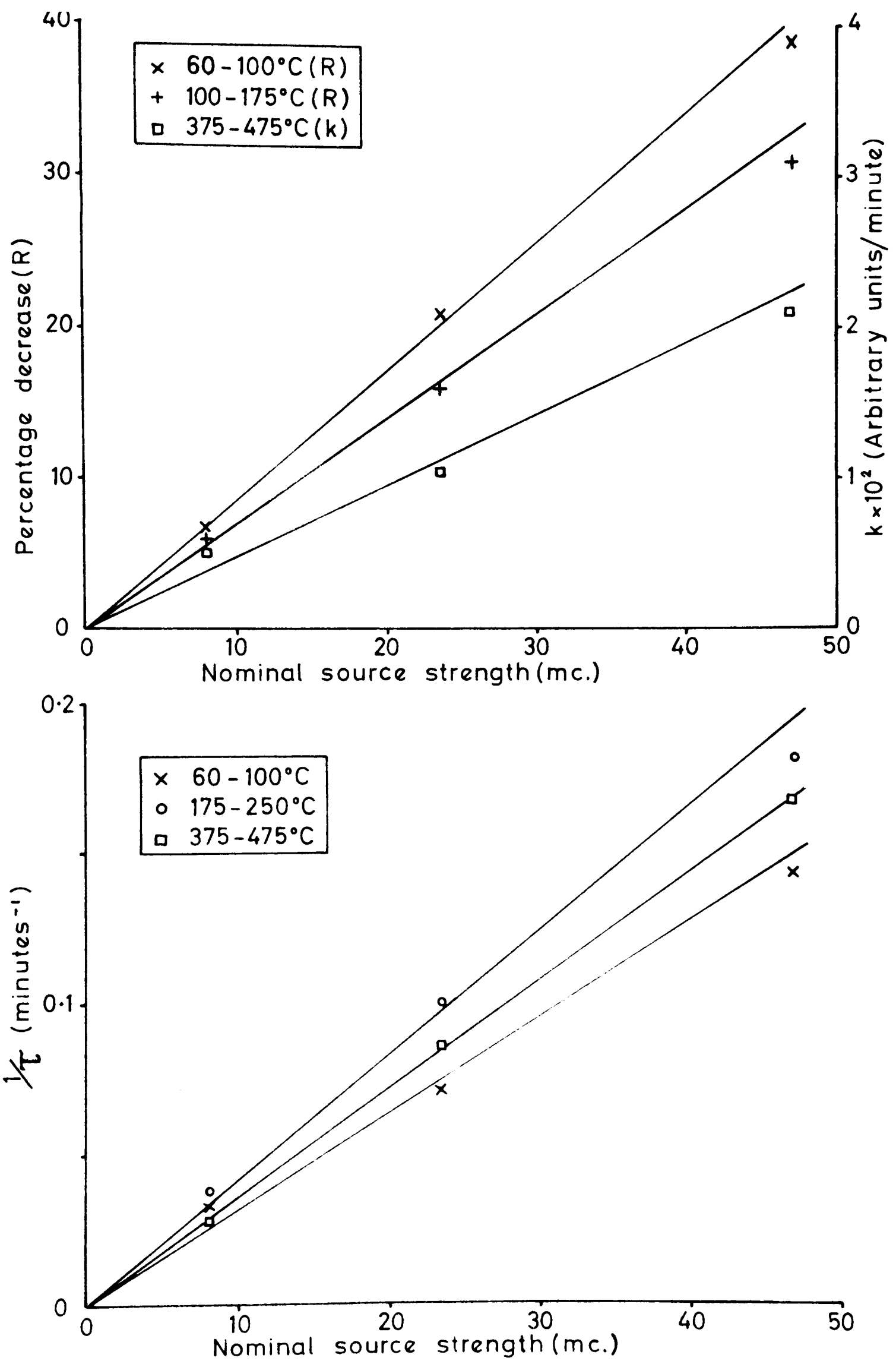

60 - 100°C (R)
100 - 175°C (R)
375 - 475°C (k)
Percentage decrease (R)
$k \times 10^2$ (Arbitrary units/minute)
Nominal source strength (mc.)
60 - 100°C
175 - 250°C
375 - 475°C
$\frac{1}{\tau}$ (minutes^{-1})
Nominal source strength (mc.)

Fig 8/8

Table 8/6

Variations in alpha particle rate curves with source strength

		No mylar			Mylar	
		8 mc.	23 mc.	47 mc.	19 mc.	44 mc.
60-100°C	L_s	250	281	280	118	102
	τ	30	14	7	49	17
	R	7	21	39	6	21
100-175°C	L_s	422	430	475	255	220
	τ	36	18	8	47	20
	R	6	16	31	-	13
175-250°C	L_s	230	234	280	166	146
	τ	26	10	5.5	39	15
	R	5	11	21	-	7
250-375°C	L_s	150	155	203	120	111
	τ	24	10	5.5	35	16
	R	-	-	4	-	-
375-475°C	L_s	44	46	60	28	27
	τ	35	12	6	25	13
	k	0.005	0.610	0.021	0.006	0.011

τ is given in minutes

added. The significance of this result to the measurement of the susceptibility of pottery to small radiation doses is discussed in Chapter 9.

In fig. 8/8 R, k and the reciprocal of τ are plotted against the source strength for those sources without mylar windows. Within the limits of accuracy of the relative source strength measurements ($\pm$ 10%), the values observed were proportional to the source strength.

8.8. Conclusions

The form of the alpha particle rate curves compared with those obtained for the beta irradiation provided the initial evidence that alpha particles might be creating new traps. The linearly increasing component in some ranges could correspond to the creation of traps while the decrease in thermoluminescence in other ranges ("radiation bleaching") could also be due to these newly created traps. However these results were not conclusive since "radiation bleaching" would also occur if the linearly increasing component was due to the filling of traps with low capture cross-section. Optical bleaching experiments (section 8.4) were therefore carried out and, especially in the case of the limestone extraction from sherd k, these provided strong evidence for trap creation. Furthermore approximate quantitative agreement was obtained between these results and the slope of the linearly increasing component and the "radiation bleaching" observed for the alpha particle rate curves.

Assuming that the wavelength of the thermoluminescence and the probability of a radiative transition are the same for electrons excited

from damage traps as for those from existing traps, then the ratio of the number of newly-created traps for a 1000 minute irradiation with a polonium 210 source (N_α) to the number of existing traps (N_s) is given by:

$$\frac{N_\alpha}{N_s} = \frac{1000k}{L_s}$$

where k = slope of the linearly increasing component

L_s = saturation value

8.8.1. Comparison with X-rays

Using a 50 mc. polonium 210 source the ratio, N_α/N_s, for sherd r in the 375-475°C range, was 0.35 for a 1000 minute alpha irradiation (Table 8/2). The range of 1.8 Mev. alpha particles in the pottery is approximately 1.4 mgm./cm.^{2} (section 9.2.1) and hence the energy dissipated in the surface layer of 15 mgm. sample during the 1000 minute irradiation (E_α) is given by (section 4.1.5):

$$E_\alpha = 3.1 \times 10^7 \times 60 \times 1000 \times 1.8 \times 10^6 \times 1.6 \times 10^{-12} \times \frac{50}{4} \text{ ergs.}$$

$$= 6.7 \times 10^7 \text{ ergs.}$$

Similarly for a 1000 minute X-irradiation the ratio N_x/N_s, for sherd r in the 375-475°C range, was 0.73 (Table 8/2) and the energy dissipated in the surface layer (1.4 mgm./cm.^{2} in thickness) of a 15 mgm. sample was approximately 2×10^6 ergs.

On the basis of these calculations the X-rays were more efficient, by a factor of approximately 60, than the alpha particles at creating traps in the 375-475°C range for sherd r. This difference could in part be due to the fact that the comparison was made for limited temperature and spectral

ranges(3700-4800Å) and it is possible that the relative efficiency of the alpha particles would be improved if it were possible to compare the total number of traps created. Furthermore it is possible that, although appearing less efficient in the above comparison, the alpha particles are in fact producing a greater number of atomic displacements than the X-rays. For alpha particles the displacements will be confined to a very small area at the end of their paths while for the X-rays they will be distributed along the entire path length. It is probable that the luminescence efficiency, and hence the thermoluminescence, associated with a cluster of displaced atoms will be less than for individual atomic displacements.

8.8.2. Age determination

The age determination of ceramics by measurement of the number of traps filled since the pottery was fired is based on the assumption that the total number of traps present has remained constant during this period. The results presented in this Chapter provide an approximate estimate of the ratio of the number of new traps, created by the decay of the radioactive impurities since the pottery was fired (N_R), to the number of existing traps (N_S).

The number of atoms displaced (D_R) since firing in the surface layer (1.4 mgm./cm.^{2} in thickness) of a 15 mgm. sample, as a result of the radioactive impurities, can be calculated from equation 4/6 and similarly the number displaced by a 1000 minute irradiation with a polonium 210 source (D_α) can be calculated from equation 4/7. Hence the ratio N_R/N_S is given by:

$$\frac{N_R}{N_S} = \frac{1000k}{L_S} \frac{D_R}{D_\alpha}$$

The values obtained for sherd r and the limestone extraction from sherd k are given in Table 8/7. For these two sherds, the increase in the total number of traps, associated with the high temperature ranges, during the time that has elapsed since firing was less than 1 in 10^3. It is therefore reasonable to assume that, in the range 300-500°C in which the number of filled traps are measured for the age determination of ceramics, the creation of traps by the radioactive impurities is not important and the results further emphasise the difficulties associated with age determination by the measurement of the number of new traps created since firing (Chapter 5). However it must be remembered that these statements are only applicable for temperatures below 600°C and for the spectral range 3700-4800Å although optical bleaching experiments carried out in the 2500-3900Å range (Table 8/4) suggested that no radical changes would occur if measurements were extended into the ultra-violet region.

The results obtained by Zeller and Ronca (1962) for limestones, whose ages ranged from 10^8 to 6 x 10^8 years, suggested that the radiation damage traps, created by the decay of the radioactive impurities, formed a significant proportion of the total number of traps present. However this hypothesis was inferred from the values obtained for the natural radioactivity and the artificial dose required to reproduce the natural thermoluminescence and no direct evidence for trap creation was obtained. In fact a fairly detailed survey of the current literature has shown that no direct evidence for trap creation by alpha particles has previously been obtained by means of thermoluminescence measurements.

Table 8/7

Number of traps created by radioactive impurities

		sherd r	Limestone extraction (sherd k)	
Age		1000 B.P.		2000 B.P.
Alpha counts per sec. (α)		1.04×10^{-2}		4.48×10^{-2}
Strength of Po^{210} source		47 mc.		7 mc.
D_R		4.3×10^{10}		3.7×10^{11}
D_α		2.1×10^{15}		3.1×10^{14}
$1000k/L_s$	375-475°C	0.35	95°C peak	13.7
			150°C peak	2.1
			440°C	0.5
			560°C	0.4
N_R/N_s	375-475°C	7.1×10^{-6}	95°C peak	1.5×10^{-2}
			150°C peak	2.5×10^{-3}
			440°C	6.0×10^{-4}
			560°C	4.8×10^{-4}

CHAPTER 9 COMPARISON OF TRAP FILLING BY DIFFERENT TYPES OF RADIATION

The results presented in Chapter 8 indicated that the primary effect of the radioactive impurities present in the pottery will have been to fill existing traps and that there will have been no significant increase in the number of traps present, since the pottery was fired. If the number of traps filled since firing is to be used as the basis for age determination measurements then the relative susceptibility to small alpha, beta and gamma doses is of fundamental importance. Glow curves were measured for samples of the same sherd which had been subjected to small alpha, beta and gamma doses. The difference in the shape of these glow curves was investigated (section 9.1) and an attempt was made to determine the relative susceptibility for these different types of radiation (section 9.2). The situation is complicated by the fact that for the alpha particles, the ionisation and hence the filled traps are confined to the surface layer while the beta and gamma radiation produce an essentially uniform distribution of filled traps throughout a 15 mgm. sample.

9.1. Comparison of alpha and beta particle glow curves

Samples of sherds a4 and r and the limestone extraction from sherd k were subjected to small alpha and beta doses using 10 mc. Po^{210} and 40 mc. (Sr^{90} + Yr^{90}) sources respectively. The irradiation times were selected so that the thermoluminescence at 400°C was equal for the alpha and beta particles. The glow curves were measured in the 3700-4800Å range on the slow heating apparatus. The results are presented in fig. 9/1, 9/2 and 9/3

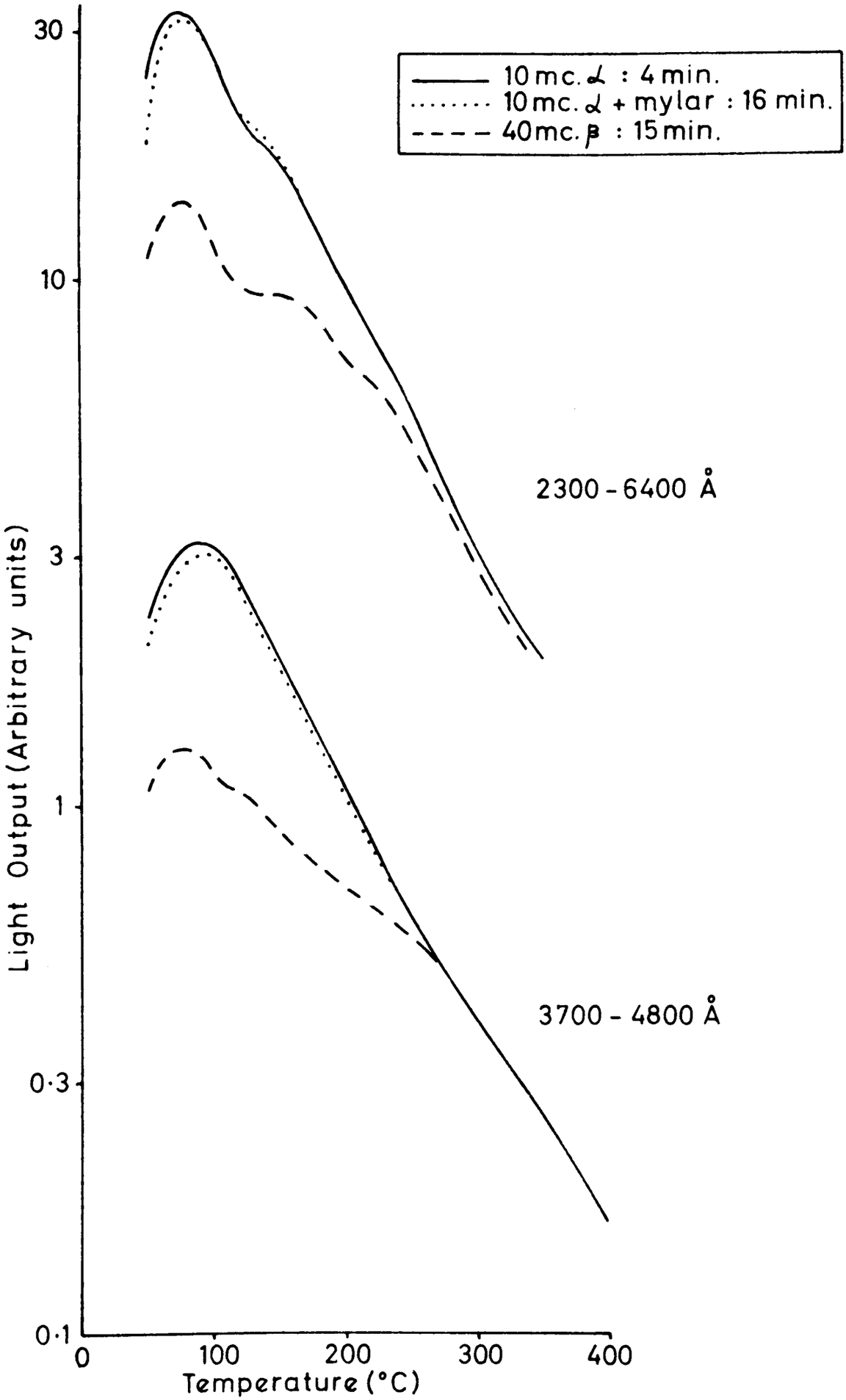

30
10
3
1
0·3
0·1
Light Output (Arbitrary units)
0
100
200
300
400
Temperature (°C)
10 mc. α : 4 min.
10 mc. α + mylar : 16 min.
40 mc. β : 15 min.
2300 - 6400 Å
3700 - 4800 Å

Fig 9/1

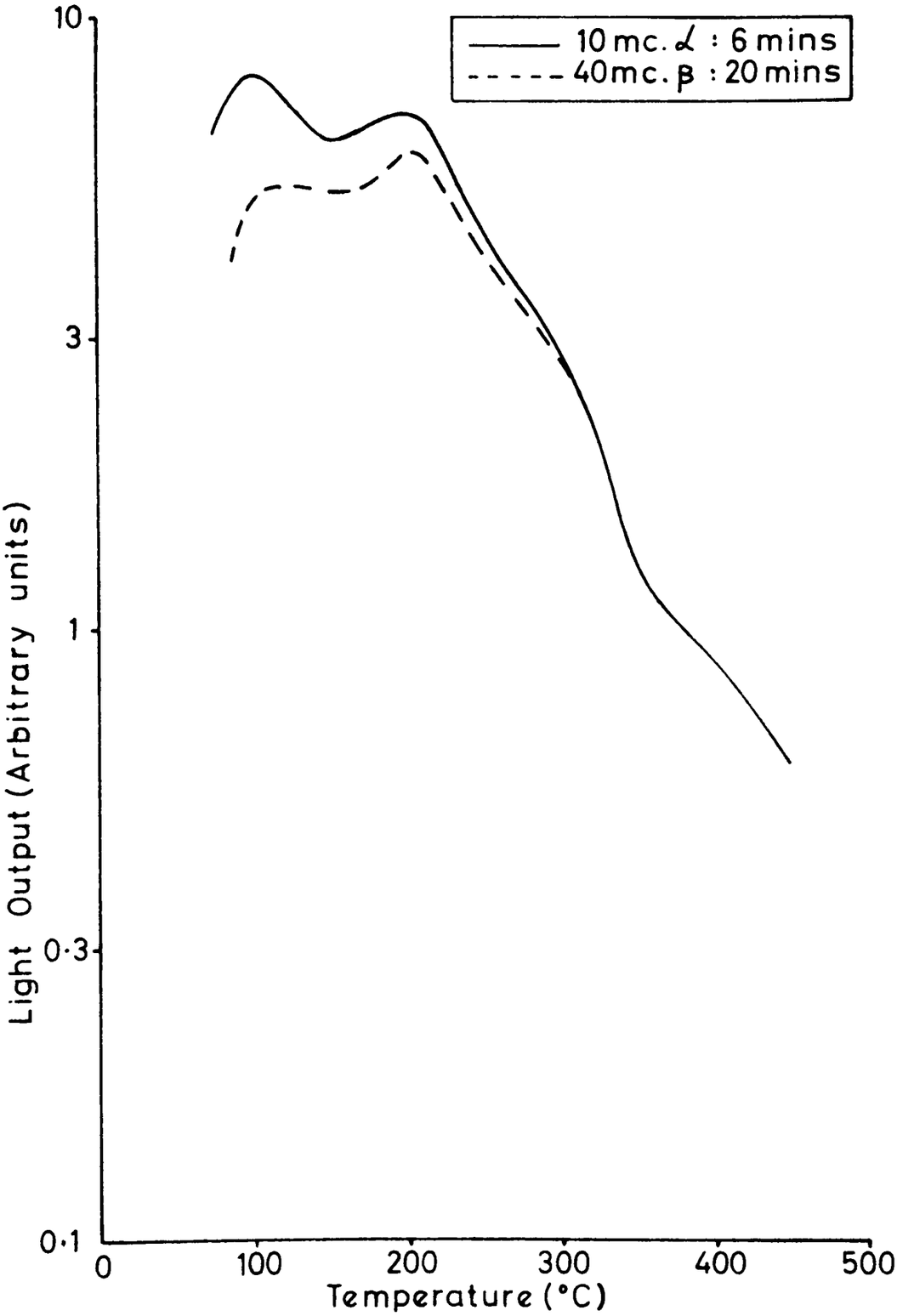

10 mc. α : 6 mins
40 mc. β : 20 mins
10
3
1
0·3
0·1
Light Output (Arbitrary units)
0
100
200
300
400
500
Temperature (°C)

Fig 9/2

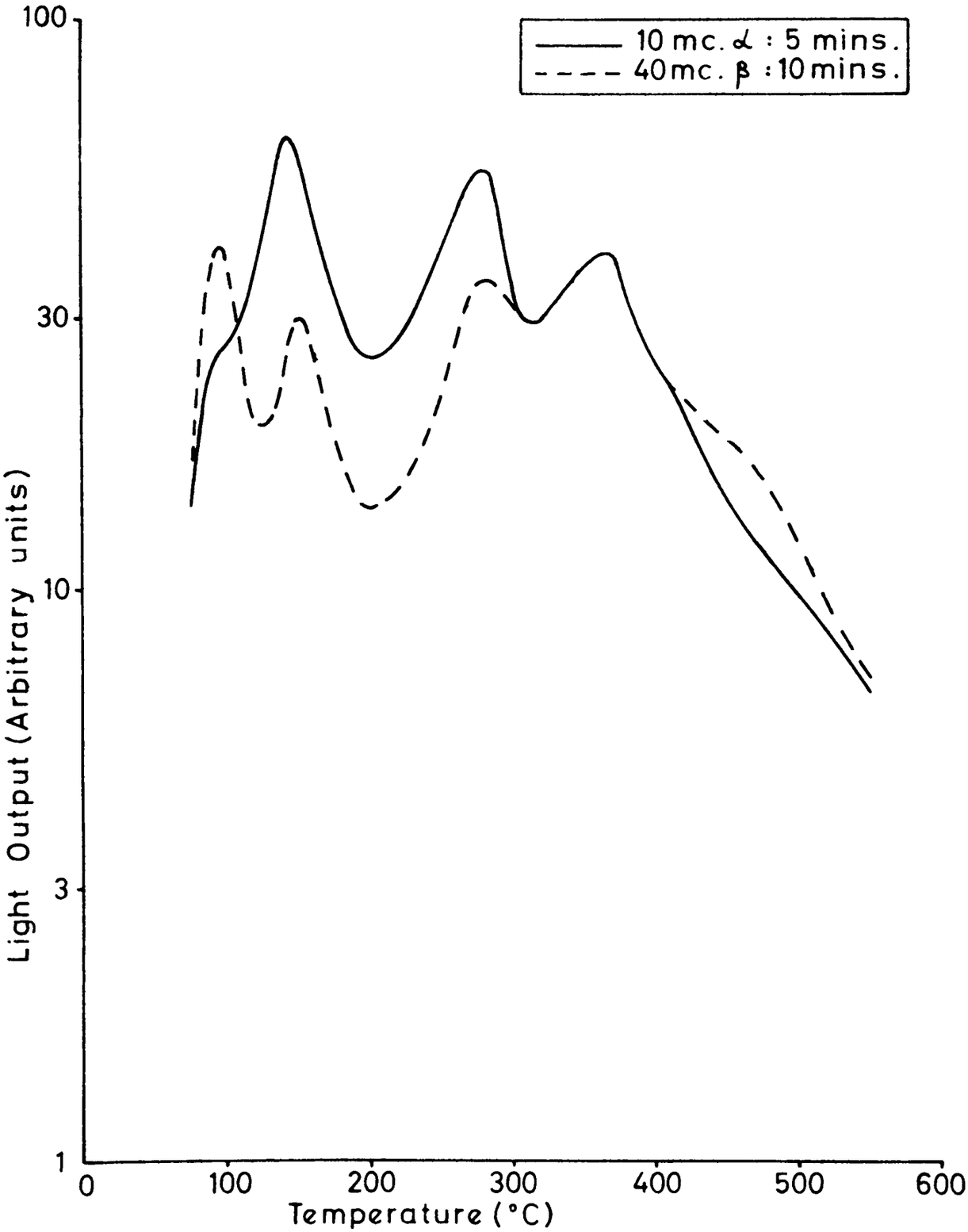

10 mc. α : 5 mins.
40 mc. β : 10 mins.
100
30
10
3
1
Light Output (Arbitrary units)
0
100
200
300
400
500
600
Temperature (°C)

Fig 9/3

respectively, the natural thermoluminescence and black body radiation having been subtracted. The fact that the ratio of the thermoluminescence at 100°C (L_1) to that at 400°C (L_4) was greater in all cases for the alpha irradiation suggested that the alpha particles were filling a greater proportion of low temperature traps. The shape of the gamma ray glow curves, which were also measured for sherds a4 and r, was essentially the same as the beta particle glow curves except in the range, room temperature to 200°C, where thermal bleaching occurred in the former case (section 11.1).

For sherd a4, the alpha and beta particle glow curves were also measured in the range 2300-6400Å. Again the ratio (L_1/L_4) was greater for the alpha particles (fig. 9/1) suggesting that the discrepancy was not due to the thermoluminescence being emitted in different spectral ranges.

Three mechanisms were therefore investigated in order to explain the difference between the alpha and beta particle glow curves. They were as follows:

1) surface traps producing low temperature thermoluminescence (section 9.1.1).

2) optical absorption decreasing with temperature (section 9.1.2).

3) variation in the ratio L_1/L_4 with radiation dose (section 9.1.3).

9.1.1. Surface traps

Provided that the depth from which the thermoluminescence is collected is greater than the range of the alpha particles (section 8.7), then a greater proportion of the alpha particle thermoluminescence will be due to

filled traps at the grain surfaces. If these are emptied at low temperatures, then the ratio L_1/L_4 would be greater for alpha particles than for beta particles.

The average energy of the alpha particles from the Po^{210} source when they reach the sample is 1.8 Mev. and hence their range in the sample is approximately 1.4 mgm/cm^2 (section 9.2.1). The addition of a mylar window (thickness 1.5 mgm./cm.^{2}) to the source reduces their energy to 0.7 Mev. (Table 4/2) and their range to approximately 0.6 mgm./cm.^{2} Hence the filled traps at the grain surfaces will make a greater contribution to the alpha particle thermoluminescence and the ratio L_1/L_4 should increase. However the ratios obtained for sherd a4 using a Po^{210} source with and without a mylar window agreed to within 10% (fig. 9/1). Hence the difference in the shape of the alpha and beta particle glow curves cannot be explained in terms of surface traps which are emptied at low temperatures.

9.1.2. Optical absorption

Assuming that the depth from which the thermoluminescence is collected is greater than the range of the alpha particles, the beta particle thermoluminescence will be collected from a greater thickness of sample or a greater proportion of a particular grain than the alpha particle thermoluminescence. If the optical absorption of the sample decreased with increasing temperature, then the beta particle thermoluminescence would be collected from a progressively greater depth thus accounting for the lower value obtained for the ratio L_1/L_4.

This hypothesis was tested for sherd a4 by measuring the beta particle

glow curves for 2 mgm. and 10 mgm. samples. In addition the alpha particle glow curves for 10 mgm. samples, irradiated in situ, were measured directly and after thorough mixing. For the beta particles, the ratio L_1/L_4 should increase for the 2 mgm. sample since optical absorption will be less important while for the alpha particles, the ratio L_1/L_4 should decrease for the sample mixed after irradiation since optical absorption will be more important.

Fig. 9/4 shows the results obtained, the ratio of the thermoluminescence (L_T) at temperature, T, to L_4 being plotted against temperature. Although the anticipated increase and decrease in the ratio L_1/L_4 was observed, the shape of the alpha and beta particle glow curves was still different. Hence the proposed decrease in optical absorption with temperature is not sufficient to account for this discrepancy.

9.1.3. Change in shape with radiation dose

The ratio L_1/L_4 was measured for sherd a4 for increasing alpha and beta doses (fig. 9/5). For a 4 minute alpha and a 15 minute beta irradiation, the thermoluminescence observed at 400°C was approximately equal (fig. 9/1). However, again assuming that the depth from which the thermoluminescence is collected is greater than the range of the alpha particles, the concentration of filled traps will be different. This difference could account for the different values obtained, in the case of a 4 minute alpha and a 15 minute beta irradiation, for the ratio L_1/L_4 since it can be seen from fig. 9/5, that the ratio is dependent on the concentration of filled traps.

The ratio L_1/L_4 was equal for a 2 minute alpha irradiation and a

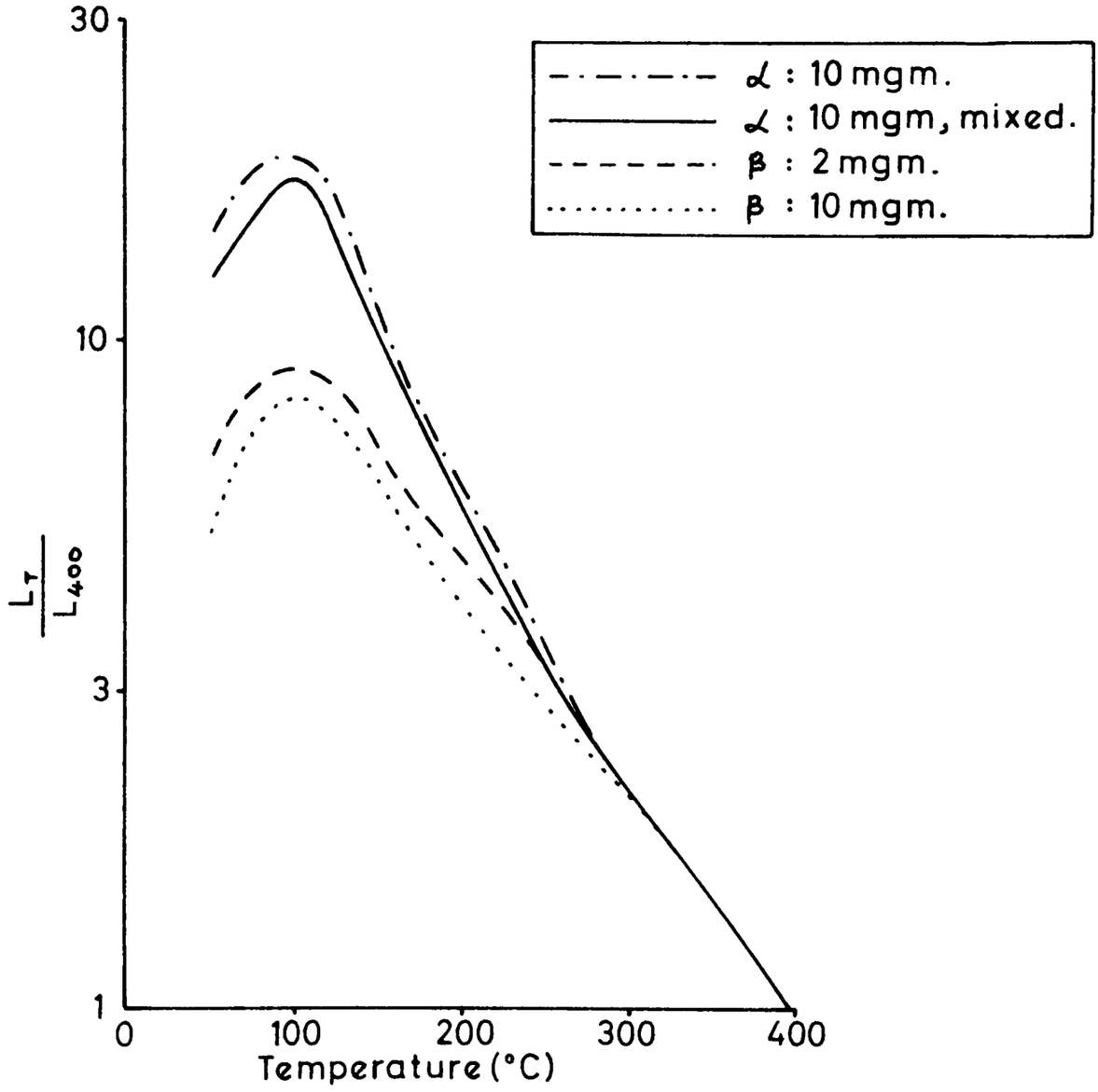

30
10
3
1
0
100
200
300
400
Temperature (°C)
$\frac{L_T}{L_{400}}$
α : 10 mgm.
α : 10 mgm, mixed.
β : 2 mgm.
β : 10 mgm.

Fig 9/4

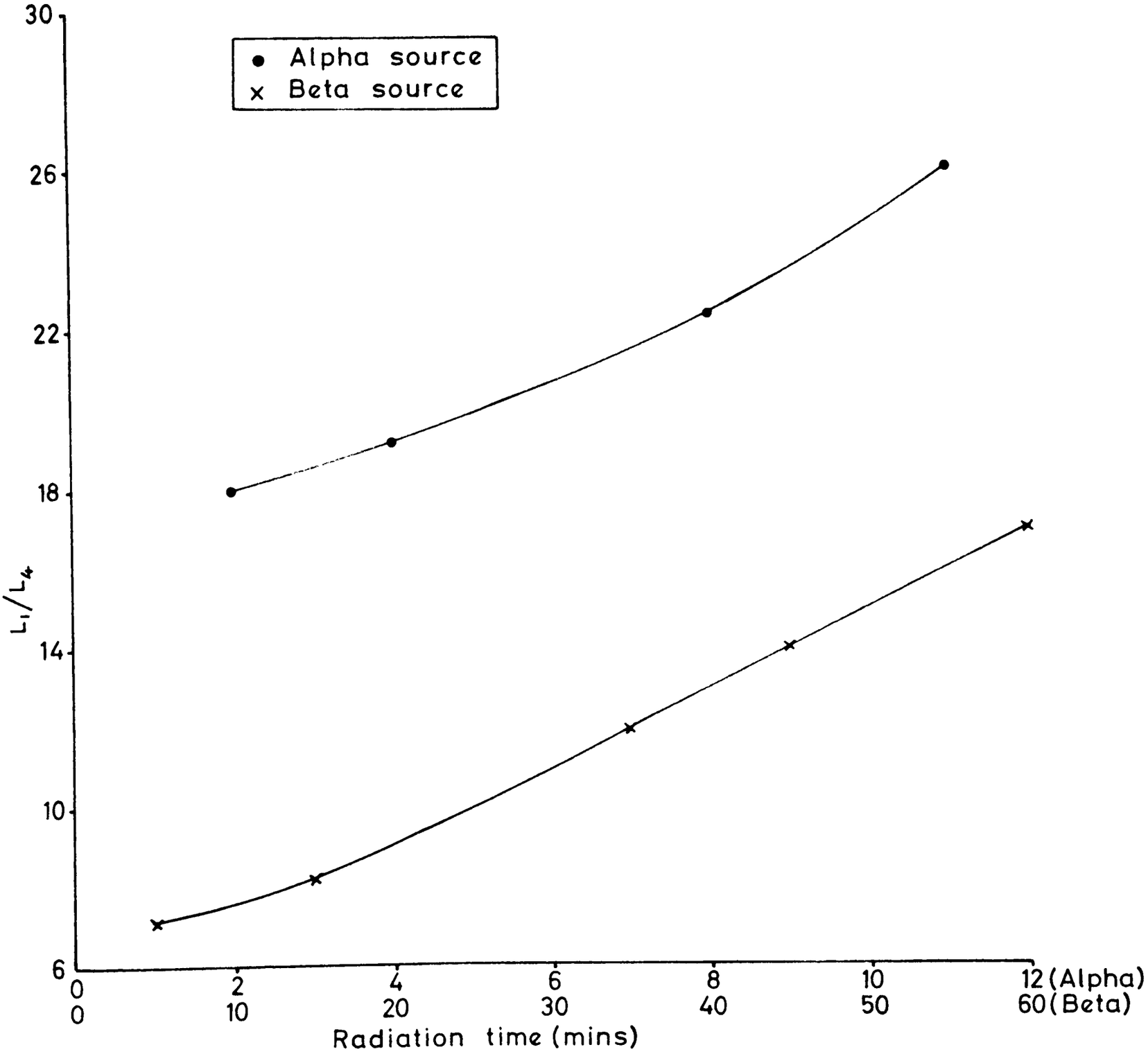

30
26
22
18
14
10
6
L_1/L_4
Alpha source
Beta source
0
0
2
10
4
20
6
30
8
40
10
50
12 (Alpha)
60 (Beta)
Radiation time (mins)

Fig 9/5

65 minute beta irradiation while for these irradiations the ratio of the total beta particle thermoluminescence to the total alpha particle thermoluminescence was approximately 8. Hence if these radiation doses corresponded to equal concentrations of filled traps, the beta particle thermoluminescence must be collected from a depth, approximately 8 times the range of the alpha particles (1.4 mgm./cm.^{2}). Therefore approximately 90% of the beta particle thermoluminescence must be collected from a 10 mgm. sample (thickness = 12.8 mgm./cm.^{2}); considering the opacity of the material this is surprising.

In conclusion therefore, it seems that the difference in the ratio L_1/L_4 for alpha and beta irradiation, when the values for L_4 are equal, arises principally from the different trap concentrations though optical absorption effects make a significant contribution. However the possibility that the alpha particles show a genuine preference for filling low temperature traps still remains, since it is doubtful whether the assumption of 90% collection for the beta particle thermoluminescence is justifiable. To obtain conclusive proof, work must be carried out using either thinner samples or higher energy alpha particles so that uniform ionisation & hence a uniform distribution of filled traps occurs throughout the sample.

9.2. Relative trap filling efficiency

An attempt was made to determine the relative susceptibility for small doses of alpha, beta and gamma radiation in the 350-500°C range used in the age determination measurements. The sources of radiation used were as

follows:

1) 2 mc. Po^{210} alpha source (1.8 Mev.)

2) Solution of Ra^{224} in alcohol (5.8 Mev.)

3) Co^{60} gamma source (1.17 and 1.33 Mev.)

4) 40 mc. (Sr^{90} + Yr^{90}) beta source (0.54 and 2.26 Mev.)

The radiation doses provided by these sources are calculated in section 9.2.1.

The glow curves obtained from a series of sherds when subjected to the above radiation were measured, using the fast heating apparatus, in the spectral range, 3700-4800Å. The sherds were ground so that the powder passed through a 120 mesh sieve (less than 130 microns) and 15 mgm. samples were used throughout. The following comparisons were made:-

1) alpha (Po^{210} source) and beta radiation (section 9.2.2)

2) alpha (Ra^{224} solution) and beta radiation (section 9.2.3)

3) gamma and beta radiation (section 9.2.4)

The revelance of these results to age determination measurements is discussed in section 9.2.5.

9.2.1. Radiation doses

1) Using the figures presented in Table 4/2, it can be shown that the energy (E) reaching the surface of a pottery sample when irradiated with a 2 mc. Po^{210} alpha source is given by:

$$E = 0.5 \times (31 \times 10^{6}) \times (1.8 \times 1.6 \times 10^{-6}) \times 60 \text{ ergs/min.}$$

$$= 2680 \text{ ergs/min.}$$

9/1

The range (r) of alpha particles in a material with density ρ and atomic number Z is given by (Glasson, 1922):

$$r\rho = 3.2 \times 10^{-4} Z^{2/3} r_o \text{ gm./cm.}^2 \qquad \text{9/2}$$

where r_o = range of alpha particles in air. Using the value, $Z^{2/3} = 4.82$, quoted by Turner et al. (1958) for brick dust, it can be shown that the 1.8 Mev. alpha particles which reach the sample from the Po^{210} source will be absorbed in a surface layer of thickness, 1.4 mgm./cm.^{2}

2) The strength of the Ra^{224} solution, supplied by Derby Luminescents Ltd., was 70 μc./ccs. 0.06 ccs. of this solution were added to 100 mgm. samples of the sherds (section 8.6). The thermoluminescence was measured 44 days later and by this time only 0.02% of the Ra^{224} remained. Hence the number of Ra^{224} atoms (N) which decayed with the emission of an alpha particle is given by:

$$N = 0.06 \times (70 \times 3.7 \times 10^4) \times \frac{3.64 \times 24 \times 3600}{0.69}$$

$$= 7.1 \times 10^{10}$$

It is assumed that the thoron atoms (half-life = 54.5 sec.), resulting from the decay of the Ra^{224}, escape from the mixture before they themselves decay with the emission of a second alpha particle. Therefore the energy dissipated in the sample for each Ra^{224} disintegration is approximately 5.8 Mev. and hence the total energy (E) absorbed by a 15 mgm. sample is given by:

$$E = (7.1 \times 10^{10}) \times (5.8 \times 1.6 \times 10^{-6}) \times \frac{15}{100} \text{ ergs}$$

$$= 9.9 \times 10^4 \text{ ergs.} \qquad \text{9/3}$$

The range of the 5.8 Mev. alpha particles in the pottery is approximately 6.8 mgm./cm^2 (equation 9/2) or, assuming that the density of the pottery is 2.3 gm./cm.^{3}, 30 microns. The average diameter of the grains is approximately 100 microns. Therefore assuming no Ra^{224} penetrates into the grains but is uniformly distributed about the surface, ionisation occurs in a mass, m, of a 15 mgm. sample, where m is given by:

$$m = 15 \left[\frac{50^3 - (50 - 30)^3}{50^3} \right] \approx 14 \text{ mgm.}$$

Hence the distribution of filled traps resulting from the Ra^{224} solution is considerably more uniform than that produced by the Po^{210} source.

3) The dose rate for the Co^{60} gamma source (Churchill Hospital, Oxford) is 110 rads/min. in tissue-equivalent material and therefore the total energy (E) absorbed in a 15 mgm. pottery sample is given by:

$$E = 110 \times \frac{15}{103} \times 100 = 165 \text{ ergs/min.} \qquad 9/4$$

since the dose rates for tissue and pottery are approximately equal (Appleton and Krishnoorthy, 1960) and since 1 rad is equivalent to an absorbed dose of 100 ergs/gm.

4) The surface dose-rate for the 40 mc. (Sr^{90} + Yr^{90}) beta source is, according to the manufacturers (Radiochemical Centre, Amershan), 17.0 $\pm$ 5.4 rads/sec. in tissue-equivalent material. By comparison of the thermoluminescence from a small sample placed at the surface of the source with that from a sample irradiated in the standard manner, it was estimated that the dose rate at the surface of the 15 mgm. sample, during the standard

irradiation, was approximately 0.6 of that at the surface of the source. Therefore the total energy (E) absorbed by a 15 mgm. sample is given by:

$$E = (17 \times 0.6) \times \frac{15}{10^3} \times 60 \times 100 = 920 \text{ ergs/min.} \qquad 9/5$$

since, as in the case of gamma rays, the dose rates for tissue and pottery are approximately equal.

9.2.2. Comparison of alpha (Po^{210} source) and beta radiation

Samples of ten of the sherds used in the third age determination programme (Chapter I2) were subjected to a 4 minute irradiation with the 2 mc. Po^{210} source and a 15 minute irradiation with the 40 mc. (Sr^{90} + Yr^{90}) source. The values for the ratio of the resulting thermoluminescence (L_α/L_β) in the 350-500°C range are given in Table 9/1, the natural thermoluminescence having first been subtracted. The colour of the sherds is also listed. The ratio of the total energy absorbed in a 15 mgm. sample (E_α/E_β) for the alpha and beta irradiations equals 0.78 (equations 9/1 and 9/5).

Table 9/1

Comparison of alpha (Po^{210} source) and beta radiation

Sherd	Colour	L_α/L_β	$\frac{L_\alpha/E_\alpha}{L_\beta/E_\beta}$
1a2	Light grey	0.38	0.49
1c1	Grey	0.50	0.64
1c3	Grey	0.48	0.61
1d1	Brown	0.39	0.50
4b1	Dark brown	0.56	0.72
4b2	Dark grey	1.22	1.56
4b3	Dark grey	1.60	2.05
5a3	Red	0.72	0.92
6a4	Dark red	0.74	0.95
6b2	Light grey	0.23	0.29

Since the traps filled by the alpha particles will be confined to the surface layer of sample (1.4 mgm./cm.^{2}) while for the beta particles they will be uniformly distributed throughout the sample, $\frac{L_\alpha/E_\alpha}{L_\beta/E_\beta}$ will only equal the ratio of the alpha and beta susceptibilities (N_α/N_β) for a completely transparent sample; the susceptibility being defined as the number of traps filled per unit of absorbed energy. If the sample is completely opaque (i.e. depth from which light is collected $\ll$ range of alpha particles) then:

$$\frac{N_\alpha}{N_\beta} = \frac{L_\alpha/E_\alpha}{L_\beta/E_\beta} \times \frac{1.4}{19}$$

where 1.4 mgm./cm.^{2} and 19 mgm./cm.^{2} are the range of the alpha particles and the thickness of the sample respectively.

Hence the values for $\frac{L_\alpha/E_\alpha}{L_\beta/E_\beta}$ given in Table 9/1 set an upper limit for N_α/N_β and indicate that for some sherds the alpha particle susceptibility is certainly less than the beta particle susceptibility. However the variation in the values obtained for the L_α/L_β provides no information about the variation in the ratio N_α/N_β because of the differences in the opacity of the sherds. The fact that the darker sherds have higher values for L_α/L_β suggests that this is due to their increased opacity rather than to an increase in their alpha particle susceptibility.

9.2.3. Comparison of alpha (Ra^{224} solution) and beta radiation

Samples of eleven of the sherds used in the second age determination programme (Aitken, Tite and Reid, 1964) were subjected to an alpha irradiation using the Ra^{224} solution, as described in section 9.2.1, and to

a 10 minute beta irradiation with the 40 mc. (Sr^{90} + Yr^{90}) source (Table 9/2). The ratio of the total energy absorbed in a 15 ngm. sample (E_α/E_β) for the two irradiations equals 10.7 (equations 9/3 and 9/5).

Table 9/2

Comparison of alpha (Ra^{224} solution) and beta radiation

Sherd	L_α/L_β	$\frac{L_\alpha/E_\alpha}{L_\beta/E_\beta}$	Sherd	L_α/L_β	$\frac{L_\alpha/E_\alpha}{L_\beta/E_\beta}$
a0	1.30	0.121	b0	1.43	0.134
a1	1.93	0.180	b1	1.54	0.144
a2	1.32	0.123	b2	1.47	0.137
a3	1.64	0.153	b3	1.41	0.132
a4	2.04	0.191	b4	1.19	0.111
a5	2.27	0.212			

As for the Po^{210} source, the values for $\frac{L_\alpha/E_\alpha}{L_\beta/E_\beta}$ set an upper limit for the ratio of the alpha and beta particle susceptibilities (N_α/N_β). However the values are closer to N_α/N_β than in the case of the Po^{210} source since the filled traps resulting from the Ra^{224} solution are more uniformly distributed through the sample. The results indicate that the alpha particle susceptibility is less than the beta particle susceptibility by a factor of at least 9 (sherd b4). This is in agreement with factor of 10 suggested by Moorehead and Daniels (1957) for lithium fluoride.

However, even using Ra^{224} solution, there will be a greater concentration of filled traps at the grain surfaces and the variation observed in the ratio L_α/L_β could again reflect the different opacity of the sherds rather

than differences in the ratio of the alpha to beta susceptibility.

9.2.4. Comparison of gamma and beta radiation

Samples of five of the sherds used in the third age determination programme were subjected to a 100 minute irradiation with the Co^{60} gamma source and a 10 minute irradiation with the 40 mc.(Sr^{90} + Yr^{90}) beta source (Table 9/3). The ratio of the total energy absorbed in a 15 mgm. sample for the two irradiations equals 1.79 (equations 9/4 and 9/5).

Table 9/3

Comparison of gamma and beta radiation

Sherd	L_γ/L_β	$\frac{L_\gamma/E_\gamma}{L_\beta/E_\beta}$
1a1	1.68	0.94
1c1	1.56	0.87
4b2	1.45	0.81
5a1	1.62	0.90
6a1	1.62	0.90

Since the distribution of filled traps will be essentially uniform for the beta and gamma radiation, $\frac{L_\gamma/E_\gamma}{L_\beta/E_\beta}$ will equal the ratio of the gamma and beta susceptibilities(N_γ/N_β). The values given in Table 9/3 indicate that, within the limits of accuracy of the dose rate measurements, the beta and gamma susceptibilities can be assumed equal. Furthermore the variation in the ratio L_γ/L_β for different sherds is less than 10%.

9.2.5. Age determination

For precise age determination measurements the alpha and beta particle thermoluminescence (L_α and L_β) should be measured for samples in which the distribution of filled traps is uniform. Under these circumstances, and assuming that the natural radioactive impurities produce a uniform distribution of filled traps, the age of pottery is given by:

$$\text{Age} = \frac{L_N}{\frac{L_\alpha}{E_\alpha} R_\alpha + \frac{L_\beta}{E_\beta} R_{\beta\gamma}}$$

where L_N = natural thermoluminescence of sample

R_α = energy absorbed/year by a 15 mgm. sample due to alpha particles from the radioactive impurities.

$R_{\beta\gamma}$ = energy absorbed/year by a 15 mgm. sample due beta and gamma particles from radioactive impurities.

To obtain a uniform distribution of filled traps for the alpha radiation, the thickness of the sample must be reduced to 1.4 mgm./cm.^{2} (6 microns) if the Po^{210} source is to be used or the diameter of the grains must be reduced to 30 microns if the Ra^{224} solution is to be used. It would be very difficult to achieve a sample thickness of 6 microns using powdered material but a possible future development is the use of polished thin sections of sherds. Although a grain diameter of 30 microns could be obtained, the danger that the grains would coagulate and prevent the uniform distribution of Ra^{224} about their surface still remains. A further difficulty associated with the use of Ra^{224} solution is that some of the alpha particle energy is probably expended in absorbed alcohol rather than in pottery itself.

Hence for the third age determination programme described in Chapter 12, a powdered sample was used and the susceptibility of the sherd was measured with betaradiation since this, like the natural radiation dose, produced an essentially uniform distribution of filled traps throughout the sample. The age was then calculated using a relationship of the form:

$$\text{Age} = \frac{LN \quad E_\beta}{L_\beta (R_{\beta\gamma} + kR_\alpha)}$$

On the basis of the results presented in section 9.2.3, k was put equal to 0.1 and values obtained for the age of pottery were compared with those obtained using k = 1 and k = 0.02.

PART III

CHAPTER 10 SPURIOUS THERMOLUMINESCENCE

In the context of age determination measurements, spurious thermoluminescence refers to that thermoluminescence which is not induced by high energy radiation.

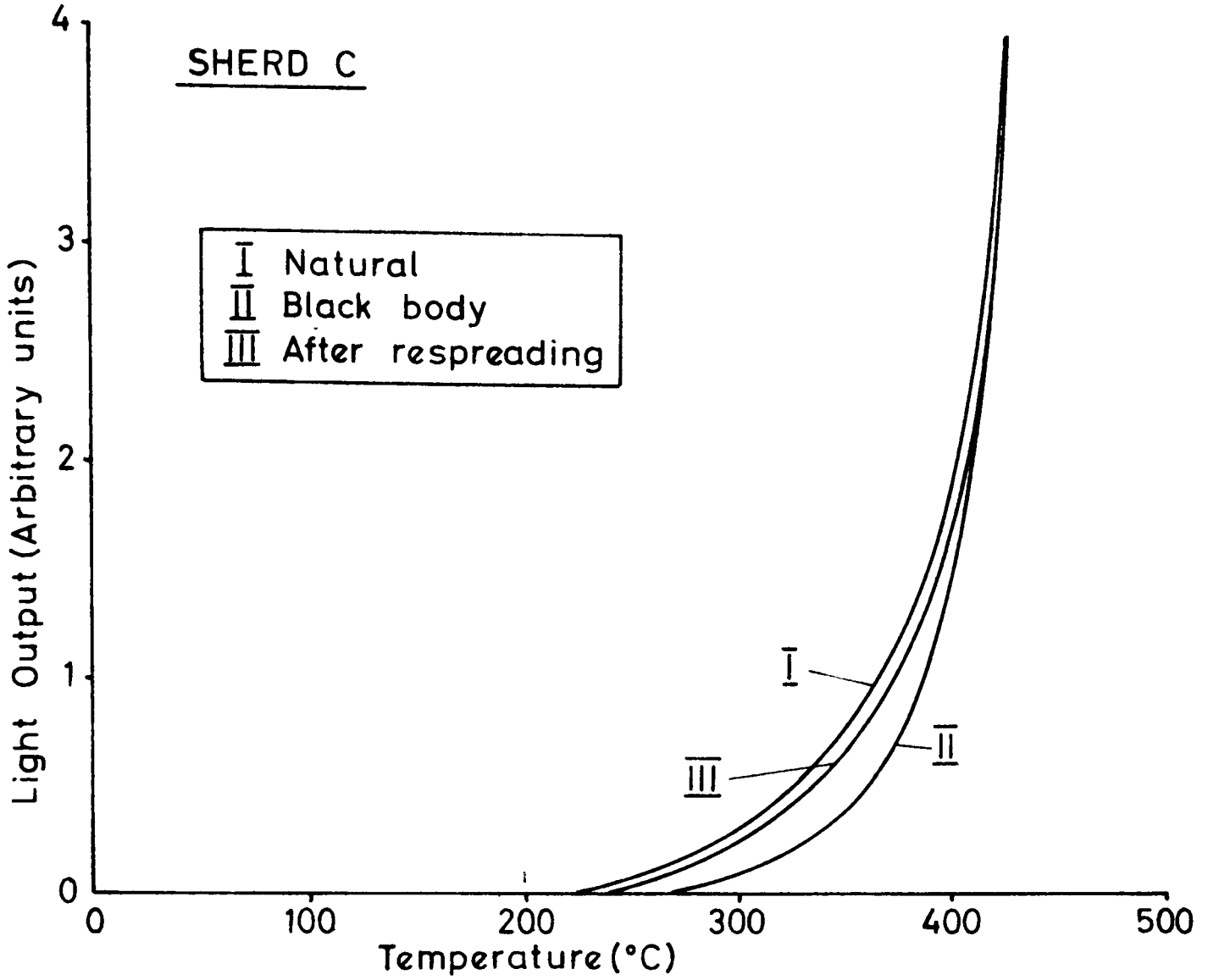
10.1. Glow curve in air - preliminary measurements

In carrying out the first age determination programme (Chapter 1) it was noted that when measurements were made in air, natural thermoluminescence was obtained from modern pottery and from refired ancient pottery which had been ground-up after refiring. A smaller amount of thermoluminescence was also obtained after refiring ground-up samples of ancient pottery (Table 1/2).

An additional experiment carried out on a number of sherds was to measure the natural thermoluminescence and black body radiation in air. The sample was then carefully removed from the graphite plate or copper block using a paintbrush before reppreading and heating in air for a third time. The thermoluminescence obtained from this third heating was in some cases as much as 75% of the natural thermoluminescence. Fig. 10/1 shows the results obtained for sherd c and for Tarquinia limestone using the slow heating apparatus in conjunction with photomultiplier type 9558.

The three mechanisms considered in order to explain this spurious thermoluminescence are as follows:

1) Triboluminescence from grinding (section 10.1.1)
2) Gas adsorption (section 10.1.2)
3) Chemiluminescence (section 10.1.3)


SHERD C
I Natural
II Black body
III After respreading
Light Output (Arbitrary units)
Temperature (°C)
0
1
2
3
4
100
200
300
400
500
I
II
III

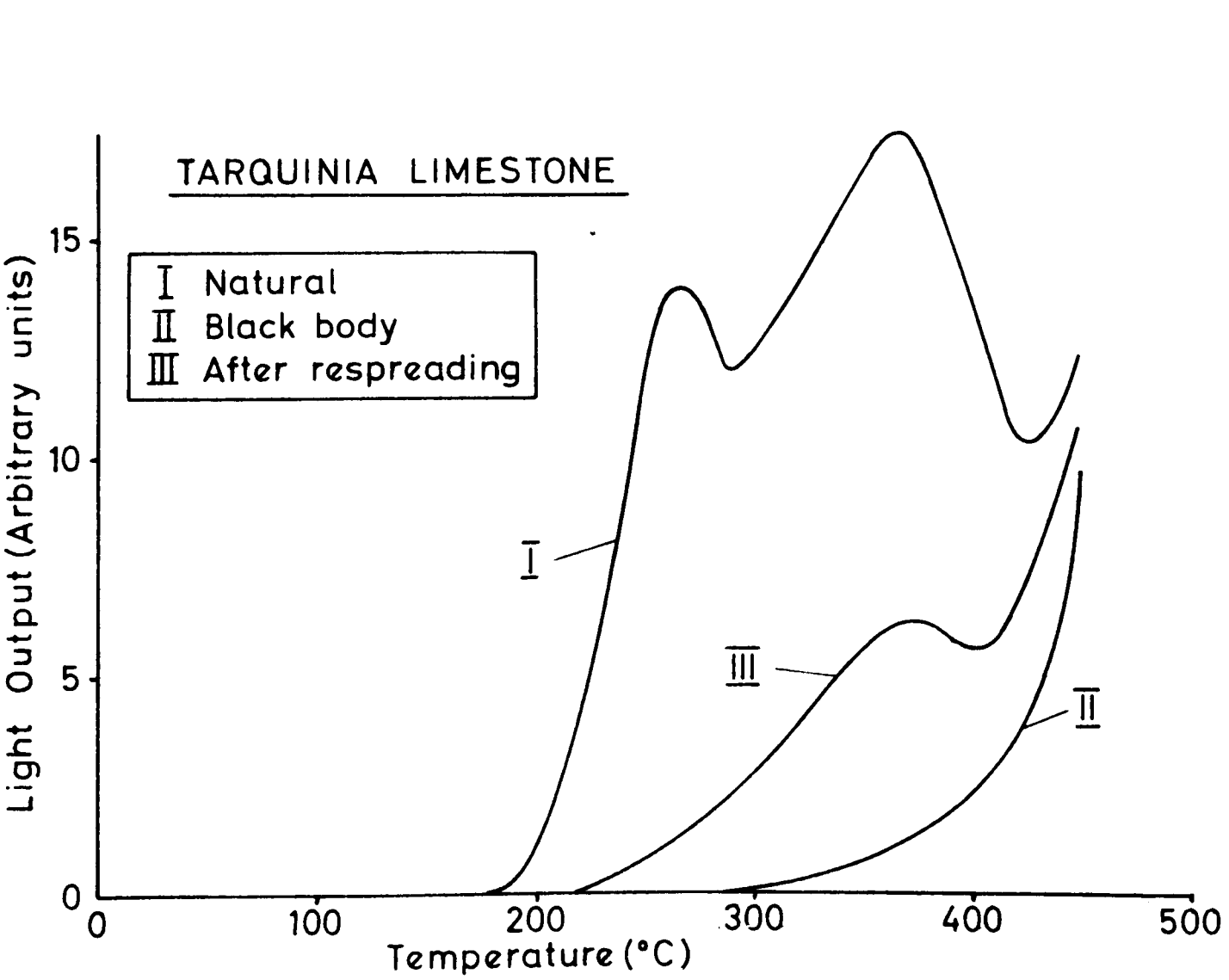

TARQUINIA LIMESTONE
I Natural
II Black body
III After respreading
Light Output (Arbitrary units)
Temperature (°C)
0
5
10
15
100
200
300
400
500
I
III
II

Fig 10/1

10.1.1. Triboluminescence

When crystalline materials are subjected to grinding, luminescence is observed - the phenomena of triboluminescence. This arises because the deforming stresses concentrated on an individual atom are of sufficient magnitude to cause electron excitation either by releasing trapped electrons or by direct excitation of valence electrons. By performing the grinding between the plates of a condenser, Gross et al. (1955) have shown that the amount of triboluminescence is directly proportional to the electric potential induced during the grinding and suggested that the grinding produced positive and negative charges at the surface of the material.

In addition to the luminescence observed during the grinding, the grinding also results in the emission of light when the material is subsequently heated; this light being termed tribo-thermoluminescence. Johnson and Daniels (1961) measured the breadth of the X-ray diffraction lines for ground-up samples of calcite and lithium fluoride, after they had been annealed to progressively higher temperatures. They found that the disappearance of the lattice imperfections, corresponding to a decrease in the breadth of the lines, occurred in the 370-440°C range and this was the same temperature range as that in which thermoluminescence was observed in air. They suggested that the strains introduced into the crystal lattice during grinding led to the creation of lattice imperfections and that the energy released when these imperfections were annealed caused electron excitation and consequently the emission of light.

10.1.2. Gas adsorption

Grogler and Stauffer (1959) working with the clay mineral, dickite, found that when a sample was heated for the first time there was no thermoluminescence but that light was emitted during the cooling period and during the second heating. They noted that this process could be repeated indefinitely and that the intensity of the thermoluminescence depended on the gases present; nitrogen, argon and helium enhanced the effect in contrast with air, oxygen and carbon dioxide. If the apparatus was evacuated to 0.1 mm. of mercury, light emission occurred when the vacuum was released and again the strongest emission was obtained using nitrogen.

They suggested that the phenomena was associated with the adsorption of gas at the surface of the sample. During the first heating the gas is driven out and during the cooling it is re-adsorbed. The energy released by this adsorption is used to excite electrons, some of which recombine with holes to emit light immediately while the remainder are trapped at lattice defects. During the second heating these traps are emptied, again with the emission of light.

10.1.3. Chemiluminescence

The emission of light during chemical reactions falls into three main groups. The first, true chemiluminescence, is associated with vigorous exothermic reactions, and in particular oxidation processes. The energy released by the reaction results in the formation of excited molecules and these lose their energy by the emission of visible light (Bowen, 1946).

The second is the luminescence associated with chemical decomposition

and observed by Johnson and Daniels (1961) for sodium bicarbonate, zinc carbonate and potassium chlorate. They suggested that, in this case, electronic excitation occurred because of the movement and disruption of the crystal parts attending decomposition.

Thirdly there is the possibility of combustion-luminescence due to burning of organic materials. Lloyd (1964), observed this combustion-luminescence while measuring the true chemiluminescence from liquids, and associated it with the burning of dust particles which settled on the samples. He also found that it could be removed if measurements were made in an atmosphere of nitrogen.

10.1.4. Discussion

In the case of modern pottery and ancient pottery, which had been ground after refiring, the most likely explanation for the spurious thermoluminescence appeared to be triboluminescence. However contributions from gas adsorption and combustion-luminescence, arising from organic materials remaining in the pottery, were also possible.

The spurious thermoluminescence observed from samples of ancient pottery, which were refired after grinding, and from samples which had been "respread" could have been due to gas adsorption. However the absence of gas adsorption effects when samples were reheated directly, without removal from the graphite plate and respreading, was not understood. Work carried out by Attix et al. (1964) and discussed in section 10.3.2 suggested that the spurious thermoluminescence observed on respreading was due to surface charges produced by friction.

The phenomena of gas adsorption was further investigated by means of experiments carried out at a reduced pressure (section 10.2). In addition it was shown that, if the pottery samples were heated in nitrogen instead of air, large reductions in the natural thermoluminescence occurred and for a sherd of modern pottery (Boston M/2) no natural thermoluminescence was observed (section 10.3). A detailed investigation of the effect of nitrogen was carried out on sherd 4gl (section 10.3.1) and the relevance of these results to age determination is discussed in section 10.4.

10.2. Measurements at a reduced pressure

For this purpose the slow heating apparatus in conjunction with photomultiplier type 6255S was used and the pressure in the furnace chamber was reduced to approximately 0.1 mm. of mercury using a standard backing pump.

It was not possible to compare the natural thermoluminescence obtained in air with that obtained at the reduced pressure since, in the latter case, the powdered sample moved about on the copper block during its first heating. At 500°C, less than 50% of the sample remained on the copper block. However if the sample was first heated in air to 500°C, it was possible to evacuate the furnace chamber and make subsequent measurements at this reduced pressure without disturbing the sample.

Fig. 10/2 shows the thermoluminescence obtained when samples of Tarquinia limestone were heated to 500°C in air (I) and then reheated in air after cooling under the following conditions:

II - cooled at reduced pressure 500-150°C and in air 150-50°C.

III - cooled at reduced pressure 500-300°C and in air 300-50°C.

IV - cooled in air 500-50°C.

The largest thermoluminescence from the second heating occurred for II. While cooling at a reduced pressure, air was allowed into the furnace chamber at various temperatures and the resulting light output was measured (fig. 10/3). The cooling rate was approximately 0.5°C/sec. in the 150-500°C range.

These results can be qualitatively explained in terms of gas adsorption and agree more or less with Grogler and Stauffer's observations (section 10.1.2). The large burst of light, obtained when air was admitted at 400°C (fig. 10/3), suggested that the electrons excited by the gas adsorption recombined immediately and were not trapped. Hence after cooling from 500-50°C in air, the thermoluminescence on reheating was small (fig. 10/2 : IV). However when the air was admitted at 150°C, the light emitted was reduced by a factor of approximately 200, suggesting that the electrons excited by gas adsorption did not recombine but were trapped. Hence after cooling from 500-150°C at a reduced pressure, the thermoluminescence on reheating was very much larger (fig. 10/2 : II).

Fig. 10/2 also shows the thermoluminescence obtained from the second heating when it was carried out at a reduced pressure, on a sample which had been cooled under the following conditions:

V - cooled in air 500-50°C.

VI - cooled at reduced pressure 500-50°C, no air admitted before reheating.

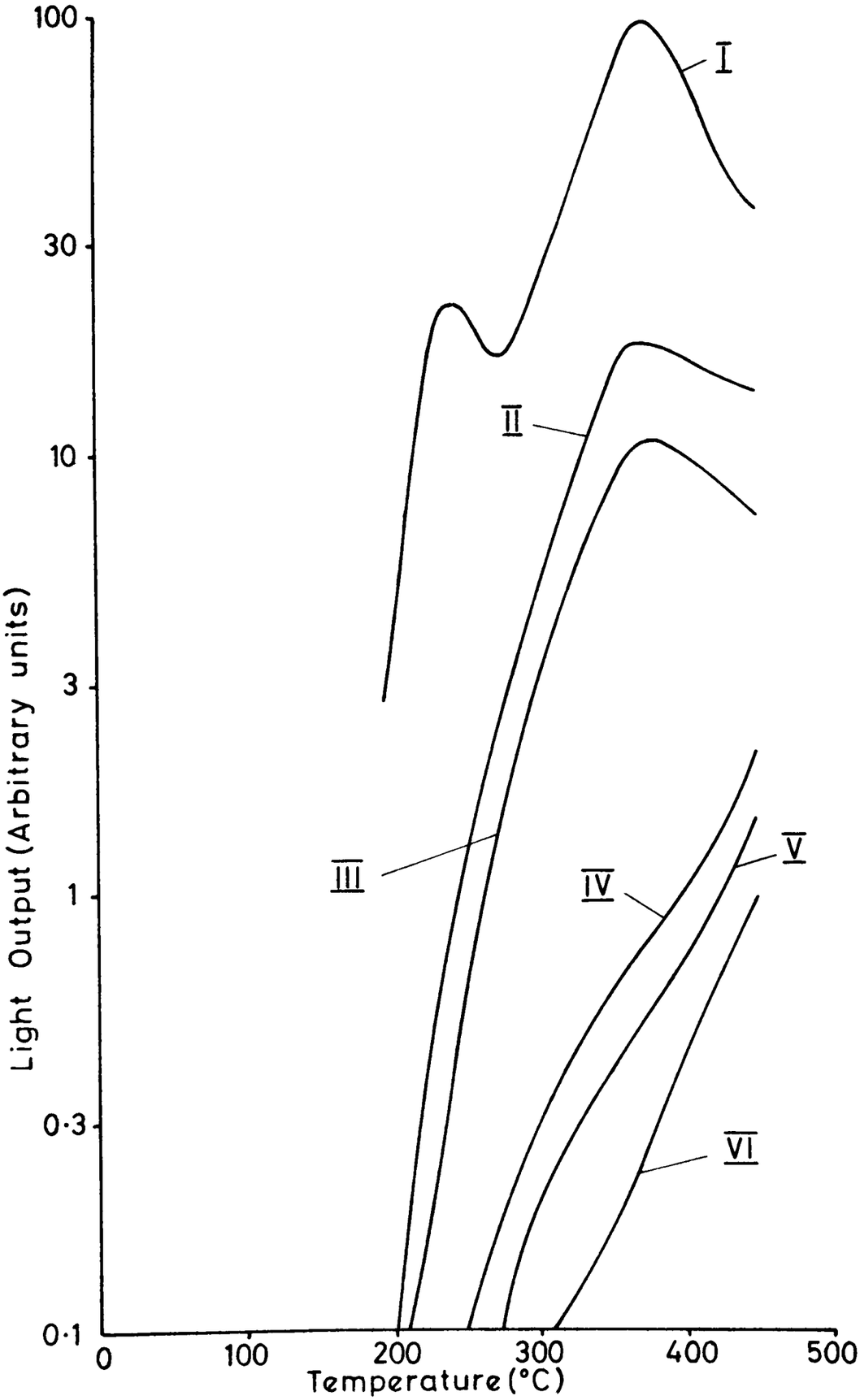

100
30
10
3
1
0·3
0·1
Light Output (Arbitrary units)
0
100
200
300
400
500
Temperature (°C)
I
II
III
IV
V
VI

Fig 10/2

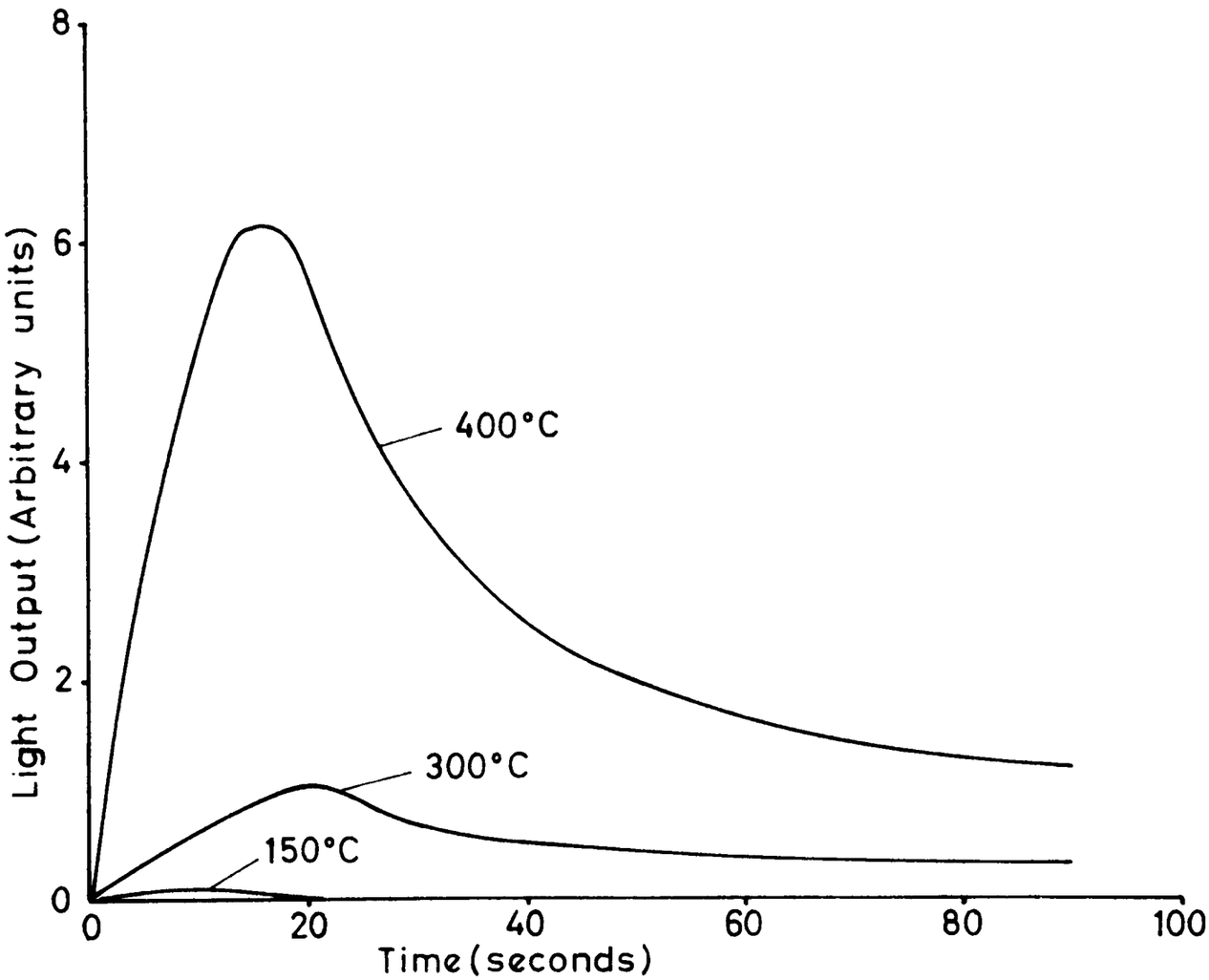

8
6
4
2
0
Light Output (Arbitrary units)
400°C
300°C
150°C
0
20
40
60
80
100
Time (seconds)

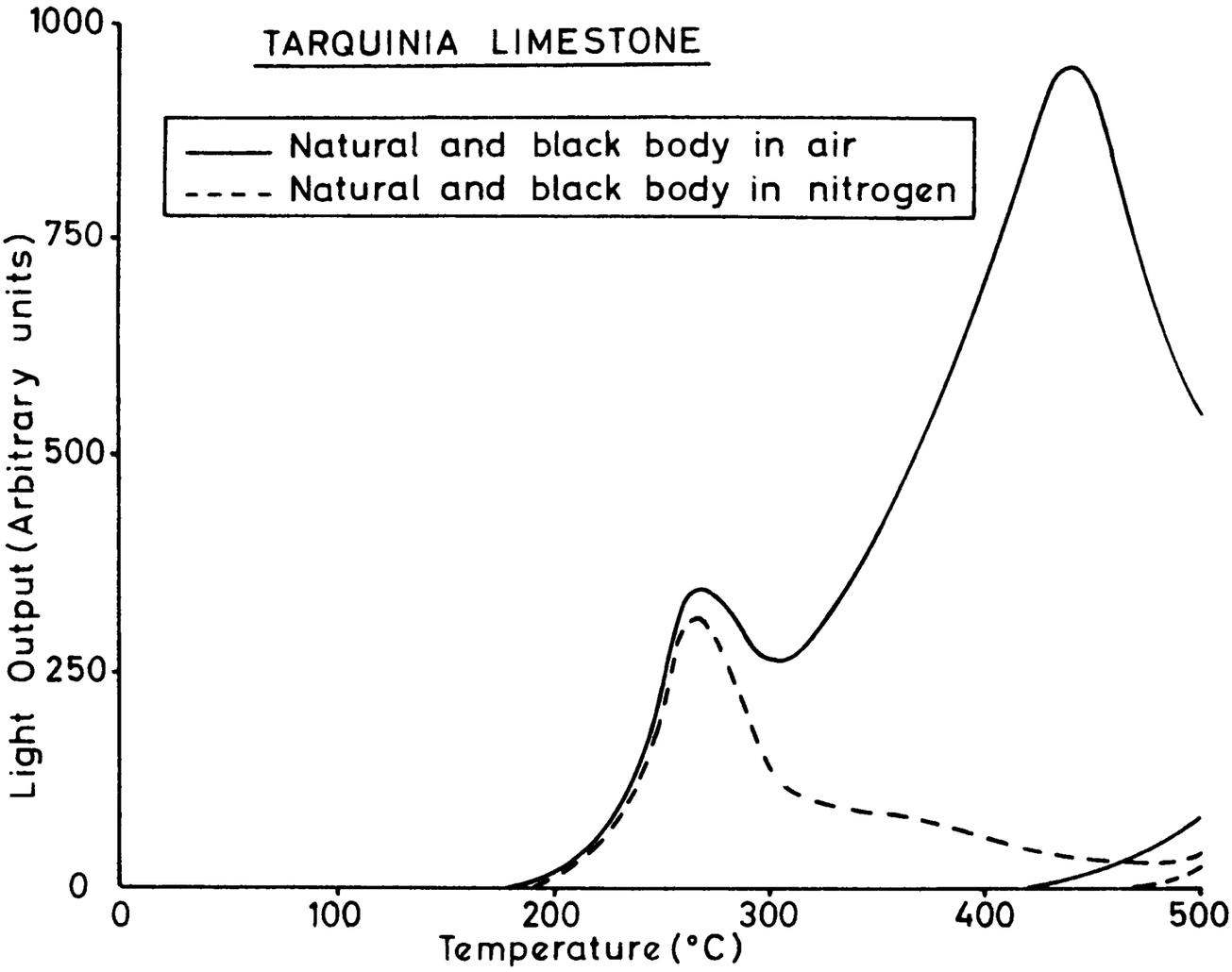
Fig 10/3

The difference between IV and V could be due to differing thermal lags for heating in air and at a reduced pressure. The difference between V and VI suggested that some electrons were trapped during desorption when the pressure was reduced at 50°C.

10.3. Glow curves in nitrogen

Soon after the completion of the work carried out at reduced pressures, the natural thermoluminescence was measured in an atmosphere of nitrogen instead of air (Aitken, Tite and Reid, 1963). This caused a considerable reduction in the amount of natural thermoluminescence from both pottery sherds and Tarquinia limestone. Furthermore zero glow was obtained from a sherd (Boston M/2) fired in 1961 (fig. 10/4). The thermoluminescence after "respreading" and from refired pieces of ancient pottery was also considerably reduced when the measurements were made in an atmosphere of nitrogen and in some cases it disappeared completely. However no change was observed in the thermoluminescence resulting from high energy radiation when the samples were measured under nitrogen.

In these experiments the air was flushed out of the furnace chamber by passing nitrogen through the chamber at a rate of 20 litres/minute and at an overpressure of 2 cm. of water for periods of up to 5 minutes; the nitrogen flow was continued during the measurement of the glow curve. It was found that the reduction in the natural thermoluminescence was critically dependent on the oxygen content of the nitrogen used. The oxy-free nitrogen ("white-spot"), supplied by the British Oxygen Company, was used


TARQUINIA LIMESTONE
Natural and black body in air
Natural and black body in nitrogen
Light Output (Arbitrary units)
1000
750
500
250
0
0
100
200
300
400
500
Temperature (°C)

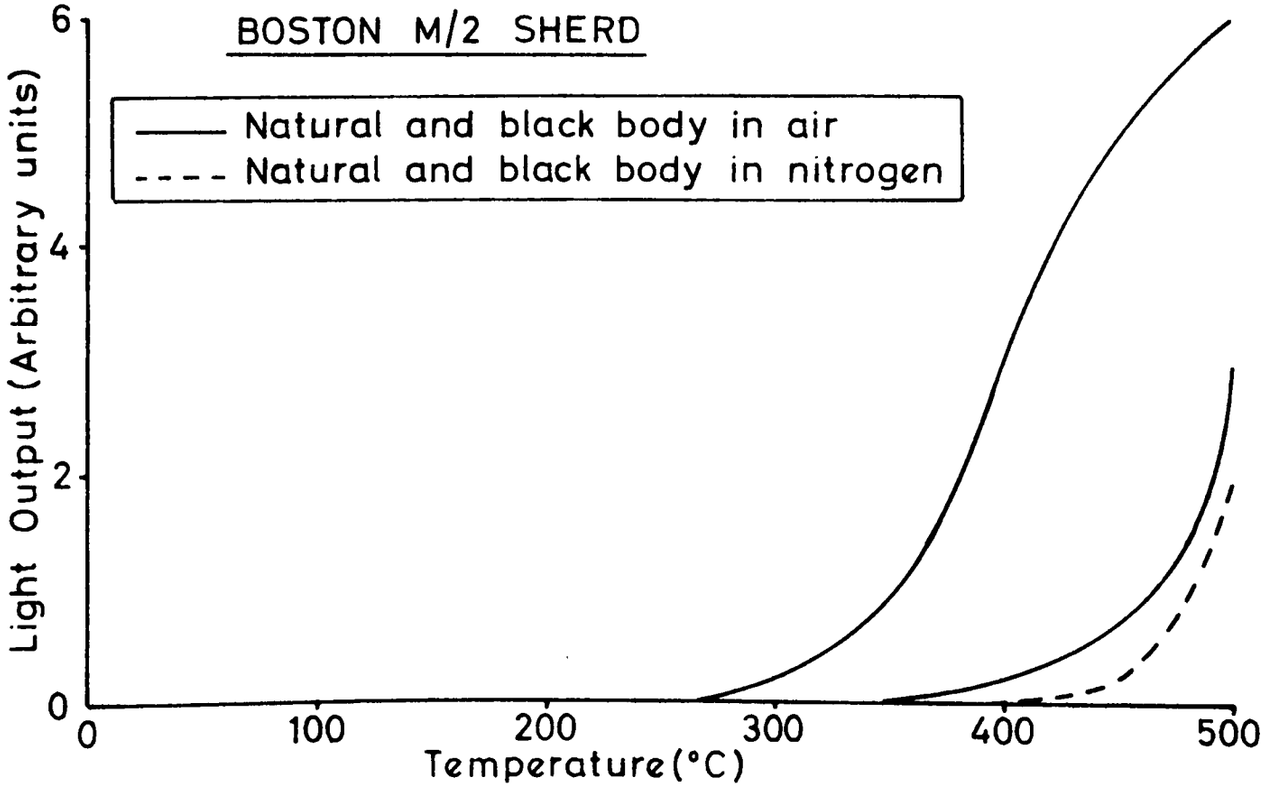

BOSTON M/2 SHERD
Natural and black body in air
Natural and black body in nitrogen
Light Output (Arbitrary units)
6
4
2
0
0
100
200
300
400
500
Temperature (°C)

Fig 10/4

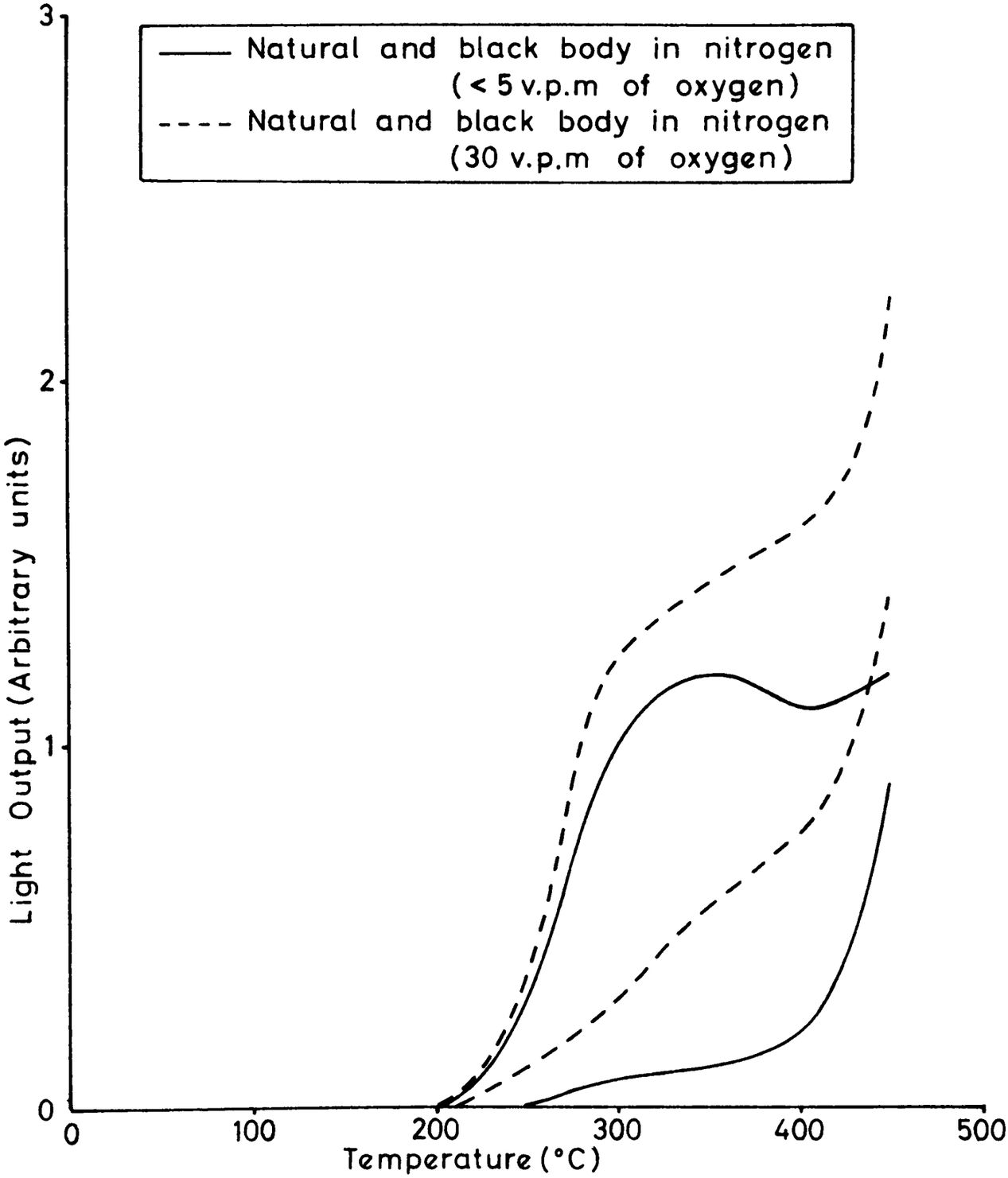

Natural and black body in nitrogen (< 5 v.p.m of oxygen)
Natural and black body in nitrogen (30 v.p.m of oxygen)
Light Output (Arbitrary units)
Temperature (°C)
0
1
2
3
0
100
200
300
400
500

Fig 10/5

throughout this work and its oxygen content was normally less than 5 volumes per million. For sherd 4gl, the natural thermoluminescence in nitrogen was normally about 5% of that observed in air. However using one of the cylinders of oxy-free nitrogen supplied, the natural thermoluminescence was approximately 8% of that measured in air and on analysis, this cylinder was found to contain 30 v.p.m. of oxygen (fig. 10/5). However using a cylinder of oxy-free nitrogen, from which the oxygen had been completely removed by the addition of hydroquinine, produced no further reduction in the natural thermoluminescence compared with that obtained using a standard cylinder of oxy-free nitrogen (less than 5 v.p.m. of oxygen).

The fact that a small amount of spurious thermoluminescence was observed in some cases when measurements were made in nitrogen, was further investigated using sherd 4gl (section 10.3.1).

10.3.1. Glow curves in nitrogen - effect of cooling conditions

Samples of sherd 4gl were heated to 500°C in an atmosphere of nitrogen on the graphite plate (fig. 10/6 : I) and were then cooled under the following conditions, before measuring their glow in nitrogen for a second time (fig. 10/6):-

II - 500-300°C in nitrogen, 300-40°C in air.

III - 500-150°C in nitrogen, 150-40°C in air.

IV - 500-40°C in nitrogen, exposed to air for five minutes.

V - 500-40°C in nitrogen, not exposed to air before reheating.

VI - 500-40°C in nitrogen, exposed to air for 2 hours.

VII - 500-40°C in nitrogen, exposed to air, removed from plate and respread 1 hour later.

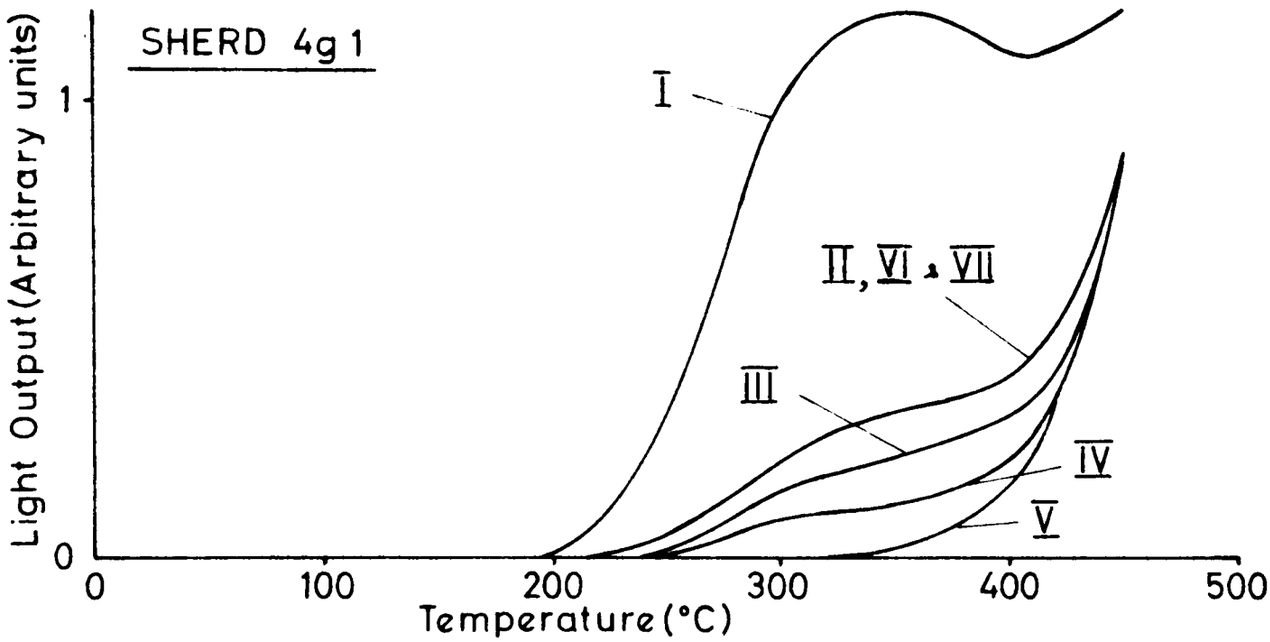

SHERD 4g 1
Light Output (Arbitrary units)
1
0
I
II, VI, VII
III
IV
V
0
100
200
300
400
500
Temperature (°C)

Fig 10/6

The largest thermoluminescence from the second heating occurred for II. These results suggested that the presence of adsorbed oxygen was a pre-condition for spurious thermoluminescence when measurements were made in an atmosphere of nitrogen. If the sample was not exposed to air until 40°C then the presence of adsorbed nitrogen reduced the amount of oxygen adsorbed and hence the second glow was smaller than when the sample was exposed to air at 300°C. The increase in thermoluminescence observed when the oxygen content of the nitrogen rose from less than 5 v.p.m. to 30 v.p.m. (fig.10/5) indicated that the spurious thermoluminescence was affected by very small quantities of oxygen.

The fact that VI was equal to II (fig. 10/6) suggested that oxygen could replace adsorbed nitrogen at room temperature. The converse did not occur since if, after cooling from 300°C in air, nitrogen was flushed through the furnace chamber for 30 minutes before reheating, there was no reduction in the spurious thermoluminescence. The agreement between VI and VII suggested that, when measurements were made in nitrogen, respreading made no contribution to the spurious thermoluminescence.

A series of twelve heatings in nitrogen, followed by cooling from 300°C in air, was performed on the same sample and no significant decrease in the spurious thermoluminescence under nitrogen was observed. This sample was then measured in air and the thermoluminescence observed was more than 50% of that observed when a sample was measured in air directly (fig. 10/7). Subsequent measurements in nitrogen of this same sample still showed spurious thermoluminescence.

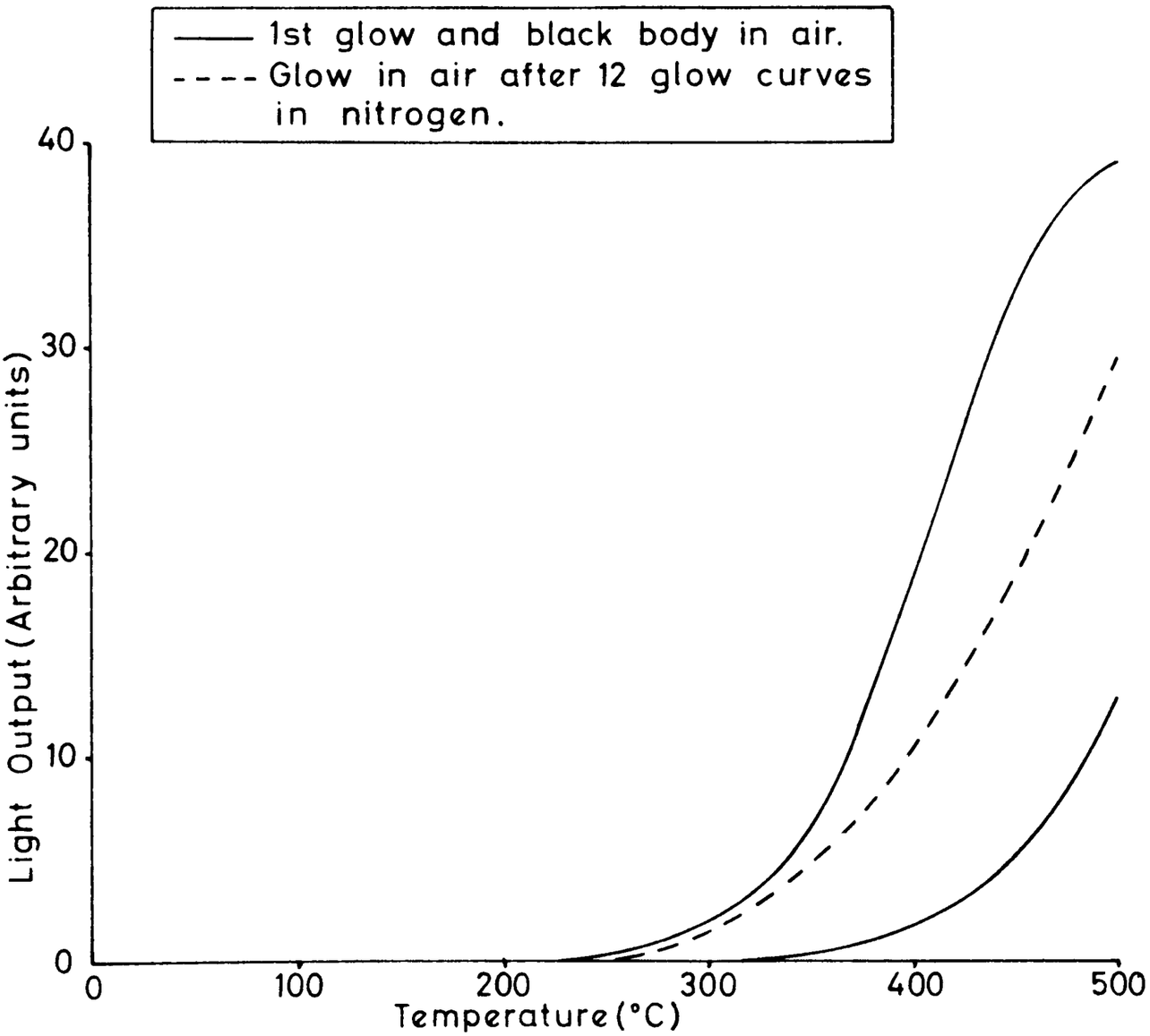

1st glow and black body in air.
Glow in air after 12 glow curves in nitrogen.
Light Output (Arbitrary units)
40
30
20
10
0
0
100
200
300
400
500
Temperature (°C)

Fig 10/7

The optical spectra of the thermoluminescence in both air and nitrogen were measured for sherd 4g1 in the range 2300-8000Å using the set of filters described in section 3.3. The results are presented in Table 10/1. The spurious thermoluminescence, defined as the glow in air minus the glow in nitrogen, occurred mainly in the 4900-6400Å range while the thermoluminescence in nitrogen occurred throughout the range 4900-8000Å.

Table 10/1

Optical spectrum of thermoluminescence in 300-400°C range

	Spurious thermoluminescence	Thermoluminescence in nitrogen
2300-3700Å	2	< 1
3700-4900Å	18	4
4900-6400Å	70	40
6400-8000Å	10	56

10.3.2. Discussion

The reduction of the natural thermoluminescence when measurements were made in nitrogen could, in part, be due to the elimination of the combustion-luminescence, associated with organic materials present in the pottery, or some other unspecified type of chemiluminescence (section 10.1.3). The fact that a large percentage of the spurious thermoluminescence in air still appeared after repeated heatings in nitrogen (fig. 10/7) supports this hypothesis.

However it is unlikely that the reduction in the spurious thermo-luminescence observed from ancient pottery, which has been refired in air after grinding, and from the "respreading" experiments can be explained in

terms of combustion-luminescence. The work carried out on lithium fluoride by Attix et al. (1964) provides a possible explanation although, considering the dissimilarity between lithium fluoride and pottery, this is surprising. Attix et al. observed that the physical agitation of the lithium fluoride granules, either by shaking, stirring or simply pouring them into the heater pan, resulted in a thermoluminescence peak at approximately 350°C and that this peak was suppressed when the samples were heated in an atmosphere of nitrogen. Since, after stirring, the grains were found to carry a nett electrostatic charge, they suggested that this spurious thermoluminescence was equivalent to triboluminescence (section 10.1.1) and that it was associated with positive and negative charges trapped on the surface of the grains. The role played by the nitrogen in "quenching" this spurious thermoluminescence was not however understood. Argon was less effective in the case of lithium fluoride indicating that chemical inertness was not the controlling factor. Furthermore the spurious thermoluminescence observed with CaF_2 : Mn was reduced when measured in argon but not in nitrogen.

Attix et al. also found that if the furnace chamber was evacuated for an hour and then air was admitted, spurious thermoluminescence was observed when the lithium fluoride was heated. This was in agreement with Grogler and Stauffer's observations on dickite and it seems possible that the desorption and re-adsorption of the gases which occurred at the surface of the granules resulted in the formation of a nett electrostatic charge.

In contrast to the results obtained for pottery (fig. 10/7), Attix et al. found that, with lithium fluoride, no spurious thermoluminescence was

observed in air if the sample had first been heated in nitrogen. This difference between pottery and lithium fluoride indicated that, in the former case, there was some interaction, such as the combustion of organic material, between the pottery and the oxygen which, unlike the presence of surface charges discussed above, was not eliminated by prior heating in nitrogen.

In section 10.3.1, it was seen that in the case of sherd 4g1, a small amount of spurious thermoluminescence was present even when measurements were made in an atmosphere of nitrogen. The results showed that the presence of adsorbed oxygen was a pre-condition for the appearance of this spurious thermoluminescence. The most obvious explanation would be that the adsorbed oxygen interacts with organic material to produce combustion-luminescence or reacts to produce some other unspecified type of chemi-luminescence. However the fact that it is still present after heating in air suggests that the light emitted is associated with the gas adsorption phenomena observed in section 10.2.

Consequently it seems that spurious thermoluminescence from pottery may arise from all three mechanisms discussed in section 10.1.

10.4. Age determination

Although the origin of the spurious thermoluminescence and the fact that the majority is "quenched" by heating in an atmosphere of nitrogen, instead of air, is not fully understood, the results described above indicate that all age determination measurements on ceramics must be made in nitrogen.

However although zero thermoluminescence was obtained from a modern sherd when heated in nitrogen (fig. 10/4), the work on sherd 4g1 (section 10.3.1) indicated that nitrogen did not completely quench the spurious thermoluminescence in all cases.

It is therefore necessary to establish criteria for rejecting those samples in which a significant amount of spurious thermoluminescence remains when heated in nitrogen (section 10.4.1) and to determine what effect, if any, the grinding process has on the sample (section 10.4.2).

10.4.1. Spurious thermoluminescence in nitrogen

The main criterion for rejecting samples from the third age determination programme (Chapter 12) was based on the shape of the glow curve obtained from the second heating. Using the relationships presented in section 2.2.2 it can be shown that, if the second glow curve was due to black body radiation only, taking the light output at 500°C as 1 unit the light output at 400°C should be approximately 2×10^{-3} units and is therefore negligible. Consequently any thermoluminescence observed during the second heating at 400°C is due to the interaction between the sample and the adsorbed oxygen. If this was greater than 10% of the natural thermoluminescence in nitrogen, the sample was rejected. On this basis samples such as 4g1 were not included in the age determination programme.

In order to allow for the spurious thermoluminescence in nitrogen when it was small but significant, the values for the natural thermoluminescence from radiation-filled traps (radioluminescence), used in the third age determination programme (Chapter 12), were obtained by cooling the sample in

air from 300-40°C before the second heating. Under these circumstances any contribution from the interaction of adsorbed oxygen with the pottery should be the same for the natural thermoluminescence and the black body radiation (first and second heatings respectively) since the results presented in section 10.3.1 showed that, for sherd 4g1, the same spurious thermoluminescence occurred when the oxygen was adsorbed at 300°C (fig. 10/6 : II) and at room temperature (fig. 10/6 : VI).

Any spurious thermoluminescence due to stirring will, however, only be present during the measurement of the natural thermoluminescence (first heating). To check whether this was quenched in nitrogen, the following procedure was adopted. After its second heating, the sample was cooled in air to 40°C, removed from the plate and then respread. Two further glow-curves were measured, the sample again being cooled from 300-40°C in air before its fourth heating. If the area between this second pair of glow curves was greater than 5% of the natural thermoluminescence, the sample was not used for age determination measurements.

10.4.2. Effect of grinding

Grinding-up the sherd to produce the powdered form used for thermo-luminescence measurements could affect the natural thermoluminescence and the susceptibility to radiation in a number of ways.

First there is the tribo-thermoluminescence observed in air with calcite and lithium fluoride by Johnson and Daniels (section 10.1.1). However the reduction in the thermoluminescence observed from refired pieces of ancient pottery suggests that this source of spurious thermoluminescence is at

least partially quenched when the samples are glowed in nitrogen.

Wick (1939) observed that the triboluminescence emitted when fluorite was ground-up, was increased after irradiation with X-rays. He suggested that this increase was due to the emptying of traps filled by the radiation. Similarly Zeller et al. (1957) reported that when samples of limestone were subjected to pressures of 10-50 tons per sq. in., the natural thermoluminescence in air was reduced in the case of samples older than 10^8 years; again suggesting that the application of pressure can result in the emptying of filled traps.

Zeller (1954) also observed that pressures of 10-50 tons per sq. in. changed the susceptibility of samples to a standard dose of radiation; the susceptibility for the 110°C peak decreased while that for the 350°C peak increased. The application of pressure can therefore alter either the number of traps present or the luminescence efficiency of the sample.

Consequently ground and unground portions of six sherds were subjected to a gamma irradiation of 10^4 rads using a Co^{60} source in order to test whether the grinding:

1) emptied those traps already filled with electrons or holes

2) altered the number of traps present

3) altered the luminescence efficiency

Approximately 18 hours after the completion of the irradiation, the unground samples were ground in semi-darkness (Chapter 11) and the thermoluminescence of both groups was measured in an atmosphere of nitrogen. Table 10/2 contains the values for the thermoluminescence for samples ground

before and after the irradiation (L_1 and L_2 respectively)

Table 10/2

Effect of grinding

Sherd	200-300°C		300-500°C	
	L_1	L_2	L_1	L_2
1a1	22.0	22.5	15.5	15.1
1c1	125	118	206	203
4b2	20.5	20.9	8.0	8.1
5a1	202	192	272	255
6a1	30.5	26.3	54.5	45.8
6b2	14.3	13.4	11.8	12.4

Except for sherd 6a1, the thermoluminescence from the two portions was within 6%. This sherd was however very inhomogeneous as far as its susceptibility to radiation was concerned (section 12.1) and the discrepancy between the two values could have been due to the two portions of the sherd having intrinsically different susceptibility. The experiment therefore establishes the fact that, for these sherds, the grinding does not significantly alter the number of traps present, change the luminescence efficiency or empty traps already filled.

CHAPTER 11 THERMAL AND OPTICAL BLEACHING

Age determination, based on the number of traps filled since the pottery was fired, depends on the fact that the high temperature traps, at least, have not been thermally or optically bleached during the centuries of burial. The experiments carried out to investigate the possibility that thermal bleaching has occurred are described in section 11.1. Optical bleaching is only important after the sherds have been ground-up since the opacity of the material prevents optical bleaching in the unground state. Consequently the degree of illumination permissible during the preparation of the samples was investigated (section 11.2).

11.1. Thermal bleaching

The measurement of the half-lives associated with the glow curve peaks for sherds f and k (section 3.2) suggested that, for these sherds, filled traps associated with temperatures above 300°C would not be thermally bleached at room temperature.

The stability of filled traps when samples are left at room temperature, in darkness, for long periods was further investigated for six sherds included in the third age determination programme (Chapter 12). 100 mgm. samples were subjected to a gamma irradiation of approximately 10^4 rads with a Co^{60} source (Churchill Hospital, Oxford), and their thermoluminescence (L_1) was measured 16 hours after the completion of the irradiation using 15 mgm. portions. The samples were then stored in darkness at room temperature (15-20°C) for 14 days before again measuring their thermoluminescence (L_2).

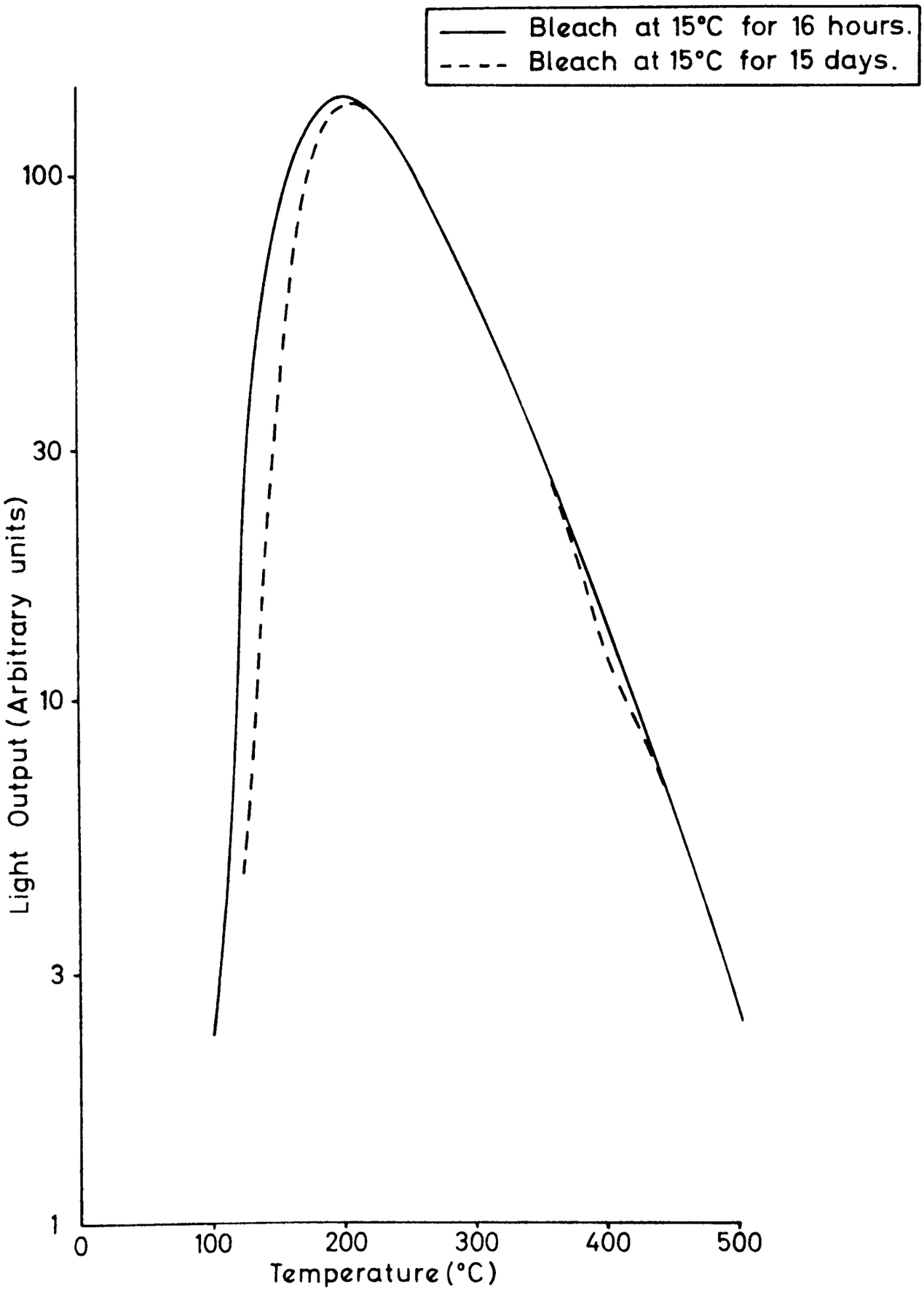

Bleach at 15°C for 16 hours.
Bleach at 15°C for 15 days.
100
30
10
3
1
Light Output (Arbitrary units)
0
100
200
300
400
500
Temperature (°C)

Fig 11/1

Fig. 11/1 shows the two glow curves obtained for sherd 4b2 and Table 11/1 contains the values for L_1 and L_2.

Table 11/1

Thermal bleaching at room temperature

Sherd	200-300°C		300-500°C	
	L_1	L_2	L_1	L_2
1a1	22.0	18.4	15.5	15.3
1c1	125	120	206	203
4b2	20.8	20.6	8.0	7.9
5a1	202	200	272	283
6a1	30.5	26.3	54.5	45.0
6b2	14.3	12.8	11.8	12.2

These results showed that the reduction in the thermoluminescence above 300°C was, except in the case of sherd 6a1, less than 2% and this reduction was within the limits of experimental accuracy (± 4%). Sherd 6a1 was very inhomogeneous as far as its susceptibility to irradiation was concerned (section 12.1) and therefore the discrepancy between the two values for the thermoluminescence may have been due to insufficient mixing of the 100 mgm. sample either before or after the irradiation.

Therefore, on the basis of the above results together with the half-life determinations discussed in section 3.2, the assumption that filled traps, associated with glow curve temperatures greater than 300°C, are not thermally bleached at ambient temperatures of 15-20°C appears to be justified.

11.1.1. Thermal bleaching at 135°C and 195°C

It is possible that, during the time that has elapsed since firing, some

sherds have been subjected to temperatures greater than 20°C. Therefore samples of four sherds were subjected to a 10 minute beta irradiation with the 40 mc. (Sr^{90} + Yr^{90}) source and were then heated, in darkness, to 135°C and 195°C for 5 minutes. The resulting thermoluminescence was compared with that from a sample which had been left at room temperature (15°C) for 5 minutes before measurement. The fast heating apparatus (20°C/sec.) was used and the procedure adopted was identical to that employed for the third age determination programme (sections 12.2.2 and 12.2.3). The results for sherd b3 are shown in fig. 11/2 and the values for the thermoluminescence in the 350-500°C range are given in Table 11/2.

Table 11/2

Thermal bleaching at 135°C and 195°C

Sherd	Thermoluminescence in 350-500°C range		
	15°C	135°C	195°C
b3	2.31	2.40	2.09
4b2	30.4	29.8	29.4
5a1	110	109	113
6a1	25.6	24.9	26.6

Except for sherd b3, the reduction in the thermoluminescence above 350°C was less than 4% and again this was within the limits of the experimental accuracy. Hence for sherds 4b2, 5a1 and 6a1, the filled traps, associated with glow curve temperatures greater than 350°C, are not thermally bleached when the samples are subjected to temperatures of 135°C and 195°C for a few minutes. However the half-life measurements (section 3.2.2)

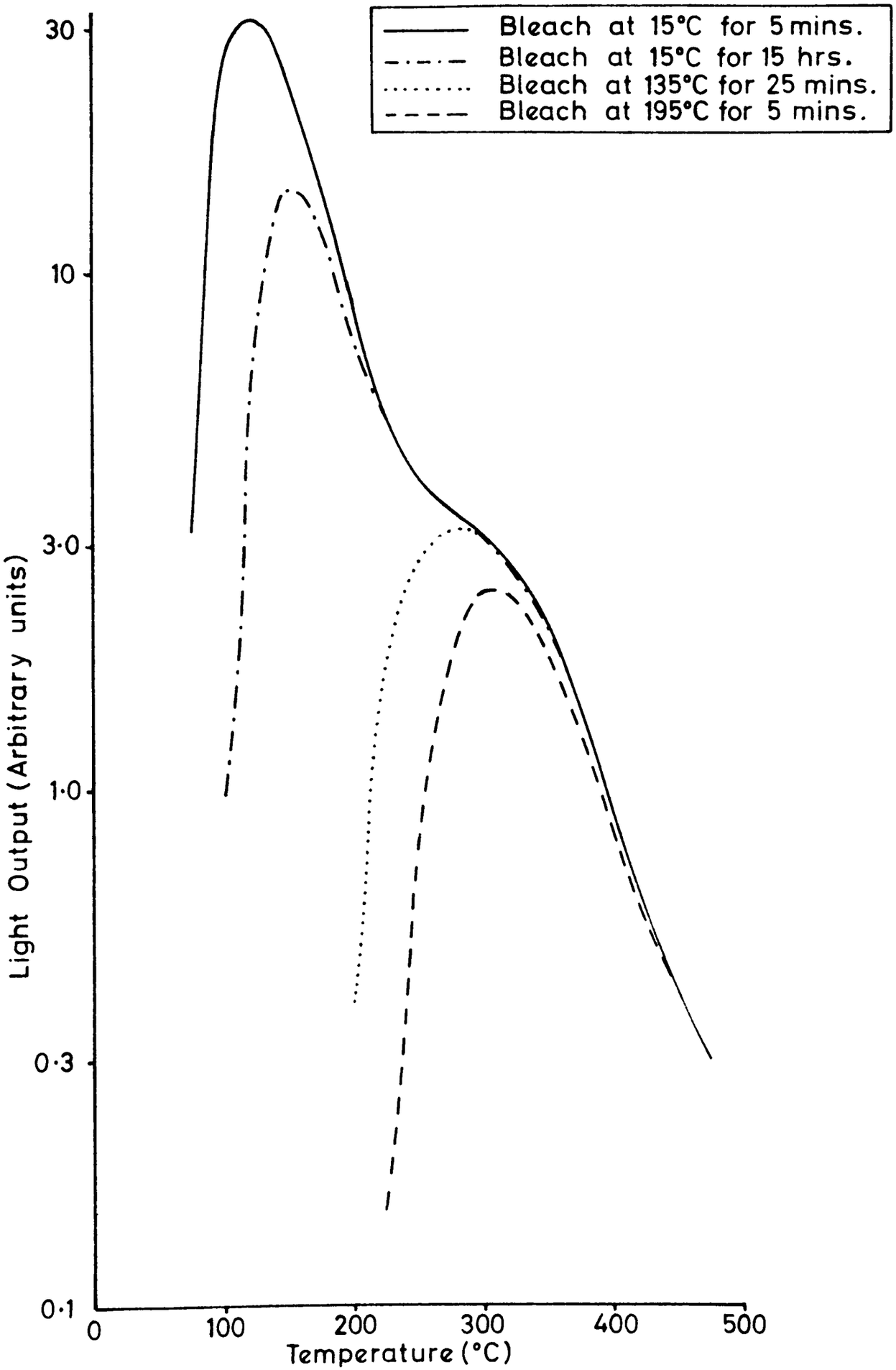

Bleach at 15°C for 5 mins.
Bleach at 15°C for 15 hrs.
Bleach at 135°C for 25 mins.
Bleach at 195°C for 5 mins.
30
10
3·0
1·0
0·3
0·1
Light Output (Arbitrary units)
0
100
200
300
400
500
Temperature (°C)

Fig 11/2

suggest that if, subsequent to firing, the pottery experiences temperatures greater than 100°C for long periods, some bleaching of the high temperature traps will occur.

11.2 Optical bleaching

Since it was well known that ultra-violet light can empty traps (Zeller and Ronca, 1962), the effect of light under the normal working conditions was investigated in order to determine the level of illumination permissible during the grinding, weighing and spreading of the samples. Before grinding only the surface layer of the sherd will be subjected to optical bleaching because of the opacity of the material and therefore, provided this layer is removed, exposure of the sherd to daylight should be unimportant.

It was found that exposure to intense sunlight through glass (400 units on a Weston Master Mk. III exposure meter) for 2 hours reduced the natural thermoluminescence from ground-up samples of sherd A/Ash. by approximately 60% at 250°C and by approximately 15% at 450°C (fig. 11/3).

Experiments were then carried out at a reduced light intensity (25 units). Samples of sherd r were exposed to fluorescent lighting for periods of up to one hour after being subjected to a 10 minute alpha irradiation with a 10 mc. $Po.^{210}$ source. The results are shown in fig. 11/4 for two typical temperature ranges. When stored in darkness, thermal bleaching occurred for the 100-175°C glow curve region but was absent in the 250-375°C range. Exposure to fluorescent light resulted in a sharp initial reduction in the thermo-

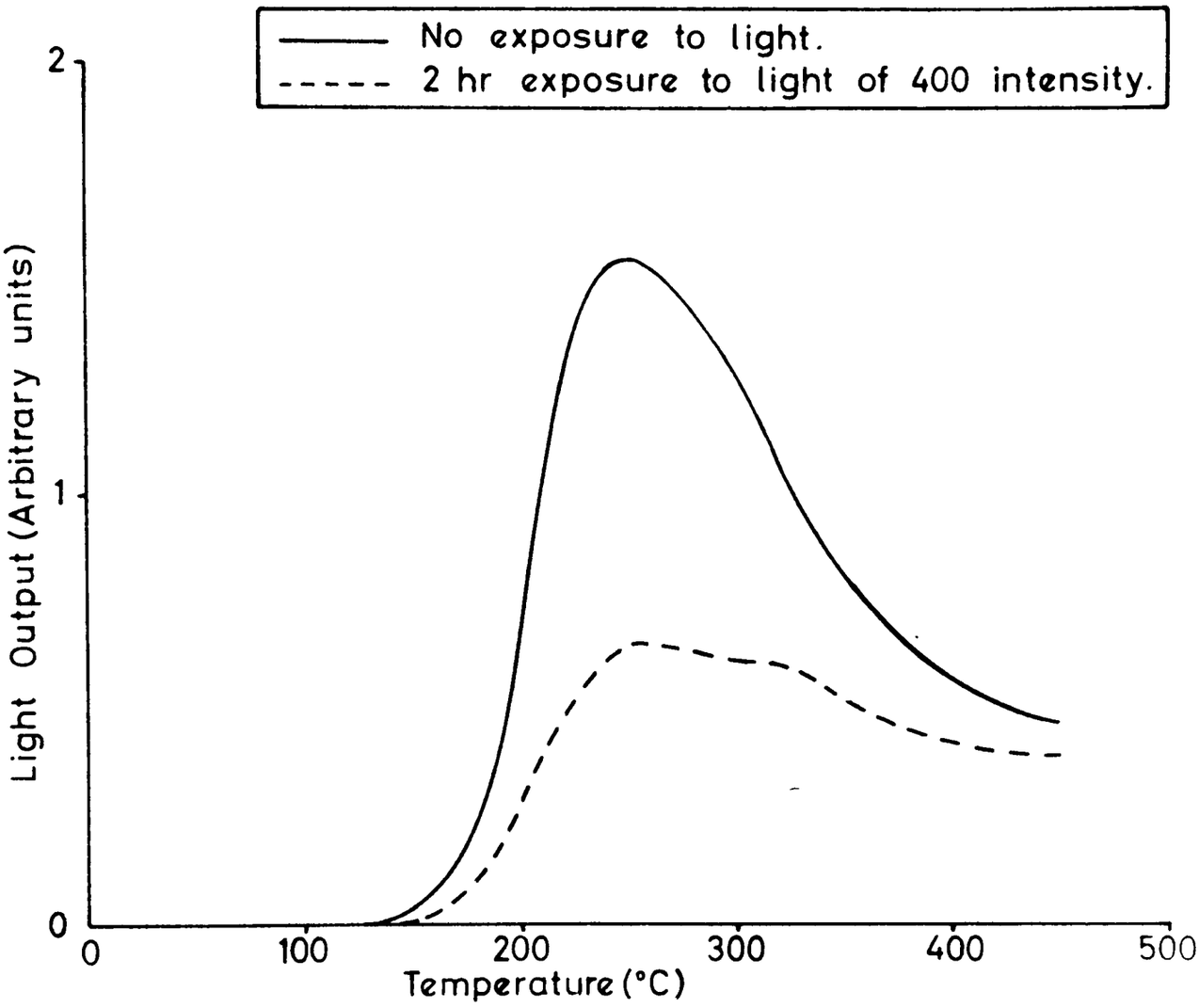

No exposure to light.
2 hr exposure to light of 400 intensity.
Light Output (Arbitrary units)
2
1
0
0
100
200
300
400
500
Temperature (°C)

Fig 11/3

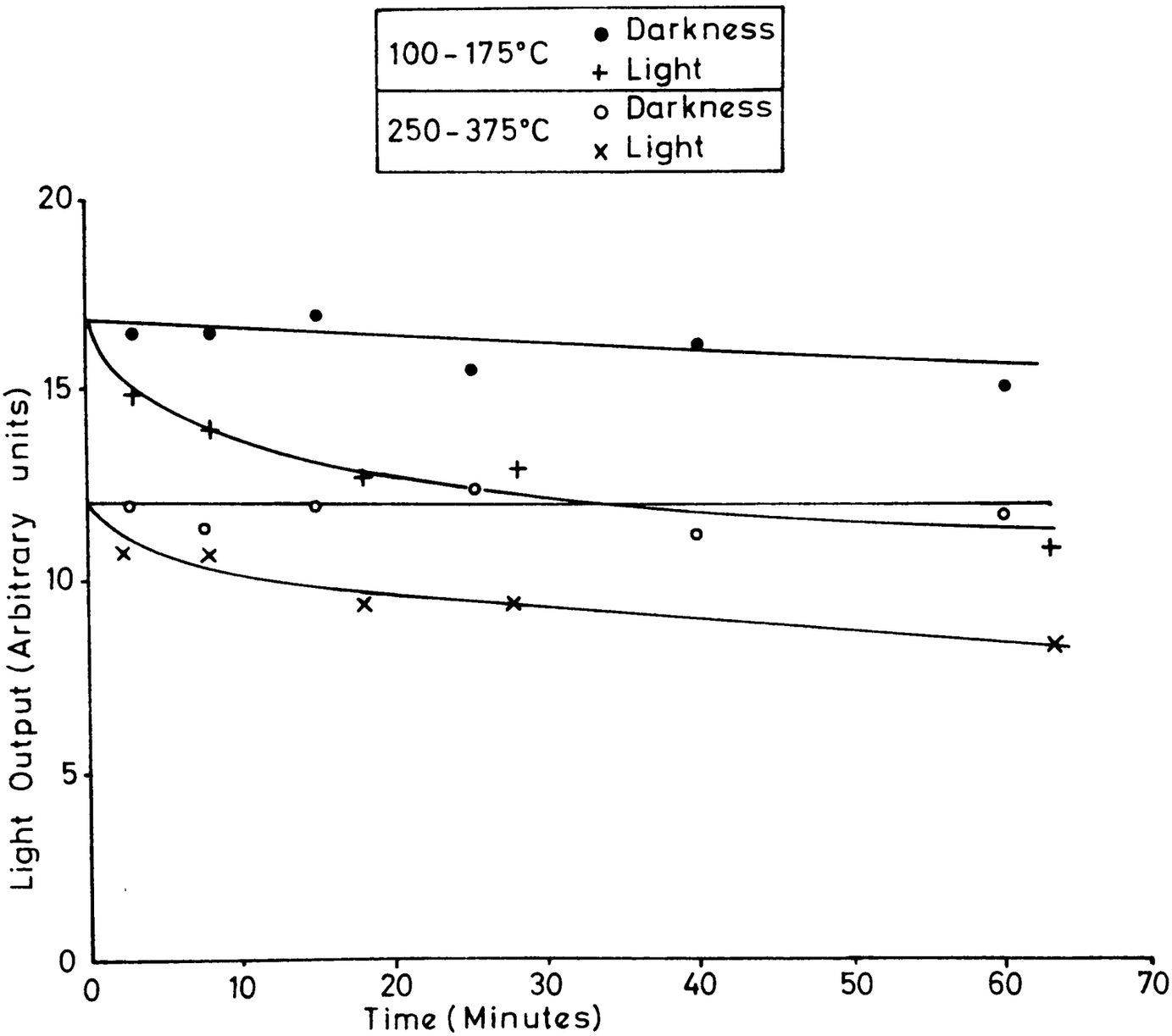

100-175°C
Darkness
Light
250-375°C
Darkness
Light
Light Output (Arbitrary units)
Time (Minutes)
0
5
10
15
20
0
10
20
30
40
50
60
70

Fig 11/4

luminescence, which then levelled off giving an overall decrease of 25% after one hour.

After a 20 minute X-irradiation, samples of sherd r were exposed to sunlight (200 units) for 30 minutes through various filters in order to ascertain whether there was a particular spectral range to which the samples could be safely exposed without optical bleaching occurring. The results (fig. 11/5) showed that light throughout the visible range produced optical bleaching. In the 100-200°C glow curve region, the 4900-6400Å band was most efficient while for higher temperatures the 3200-4900 Å band was most efficient.

Finally the effect of light at the lowest intensity (0.8 units) in which the samples could be satisfactorily spread on the plate, was investigated. After a 10 minute alpha irradiation with a 10 mc. Po^{210} source, samples of sherds r and k were exposed to light of this intensity, compounded of sunlight through glass and fluorescent light, for 15 minutes. The values for the percentage decrease in thermoluminescence, compared with samples kept in darkness after the irradiation, are given in Table 11/3.

Table 11/3

Optical bleaching

Sherd	Percentage decrease in thermoluminescence				
	60-100°C	100-175°C	175-250°C	250-375°C	375-475°C
r	2	7	4	5	5
k	< 1	4	6	2	5

Since the limits of experimental accuracy are approximately ± 4%, these

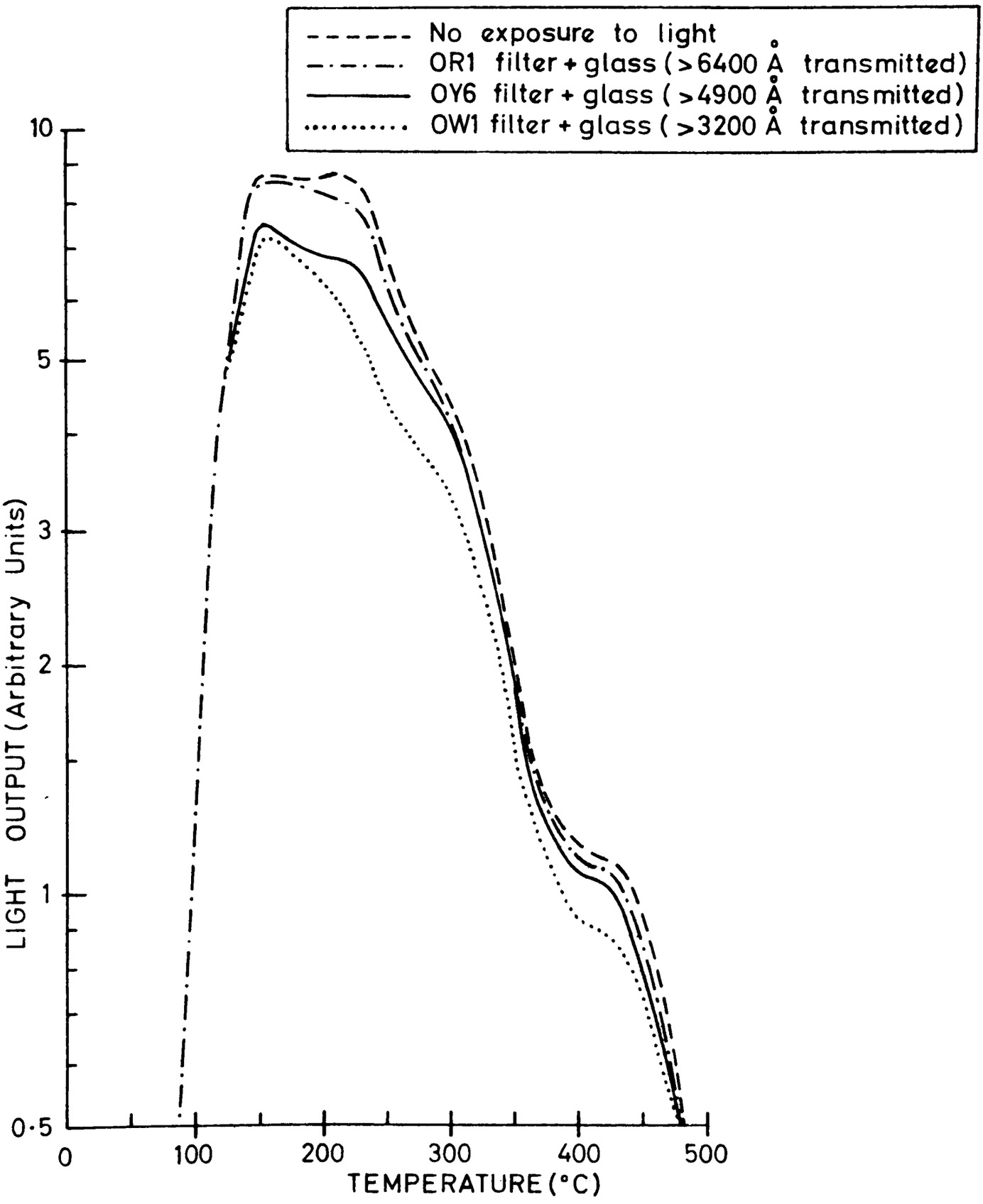

No exposure to light
OR1 filter + glass (>6400 Å transmitted)
OY6 filter + glass (>4900 Å transmitted)
OW1 filter + glass (>3200 Å transmitted)
LIGHT OUTPUT (Arbitrary Units)
10
5
3
2
1
0·5
0
100
200
300
400
500
TEMPERATURE (°C)

Fig 11/5

results suggest that some optical bleaching occurs even at very low light intensities. However since the spreading of the sample only takes 1-2 minutes and since the grinding and weighing can be carried out at a lower light intensity (< 0.2 units), the results indicate that thermoluminescence measurements can be made without a significant amount of optical bleaching occurring, provided that the above levels of illumination are not exceeded during and after the grinding.

CHAPTER 12 AGE DETERMINATION RESULTS

The first age determination programme was carried out on eighteen pottery sherds of known age and the thermoluminescence was measured in air. As indicated in Chapter 1, the results obtained were unsatisfactory.

It was then observed that, if measurements were made in nitrogen instead of air, the natural thermoluminescence was considerably reduced while zero natural thermoluminescence was obtained from a sherd of modern pottery (Boston M/2) and from the majority of the samples of refired ancient pottery (Chapter 10). It was further noted that the exposure of the ground-up sherd to visible light resulted in bleaching of the thermoluminescence (Chapter 11). Because of these results a second age determination programme was carried out on a further group of eighteen sherds of known age (Aitken, Tite and Reid, 1964). In this case all the measurements were made in an atmosphere of nitrogen and care was taken to avoid exposing the ground-up samples to strong visible light. This work indicated that the specific thermoluminescence, defined as:

$$\frac{\text{natural thermoluminescence}}{\left(\begin{array}{c}\text{thermoluminescence from beta}\\ \text{dose of } 6 \times 10^3 \text{ rads}\end{array}\right) \times \left(\begin{array}{c}\text{natural radiation dose}\\ \text{in rads/year}\end{array}\right)}$$

was, within the limits of experimental accuracy, proportional to the age of the pottery. However the absolute age of pottery, calculated from the specific thermoluminescence, was low by a factor of approximately ten.

Since the results obtained when the thermoluminescence was measured in nitrogen, were encouraging, a third and more comprehensive age determination

programme was carried out. Seven groups of sherds whose age varied from c.1350 A.D. to c.5500 B.C. were selected for this purpose (Appendix 2), each group containing several sherds from the same archaeological stratum and hence having the same age. Only sherds whose spurious thermoluminescence in nitrogen was, on the basis of the criteria outlined in section 10.3.1, negligible were selected. In addition the possible effect of grinding on the natural thermoluminescence and the susceptibility, was investigated for six sherds used in the programme and was found to be negligible within the limits of experimental accuracy (section 10.3.2).

The results presented in Chapter 8 indicated that the number of traps created since firing, as a result of the decay of the radioactive impurities, is less than 1% of the total number of traps present. Therefore, as previously, the age determination was based on the number of traps filled since firing and the specific thermoluminescence was measured.

The ratio of the natural thermoluminescence to the thermoluminescence induced by beta radiation was measured for six sherds using samples taken at different depths from the surface (section 12.1). These results indicated that, as far as their thermoluminescent properties were concerned, the sherds were extremely inhomogeneous. Therefore approximately 2 grams of each sherd was ground-up and thoroughly mixed; this sample was then used for the measurement of the natural thermoluminescence, the susceptibility to beta radiation and the uranium, thorium and potassium contents.

The thermoluminescence was measured using the fast heating apparatus. This was modified to produce a constant heating rate (section 2.1.2) and thus

provide more reproducible results than had been obtained in the second programme. In addition the maximum temperature, at which the thermoluminescence could be measured against the back-ground of black body radiation, was increased from 450°C to 500°C by using two OB10 filters instead of a single OB10 filter (section 2.2.1).

Because the beta particle rate curves were not linear even for small doses (less than 10^4 rads), the beta dose for each sherd was chosen to provide a total thermoluminescence equal to approximately twice the natural thermoluminescence. This beta dose provided the closest approximation possible to the natural radiation dose received by the sherd since firing (section 7.3). In addition, on the basis of the results presented in Chapter 9, the effect, on the specific thermoluminescence, of applying a correction for the different susceptibilities for alpha and beta particles was investigated.

It was hoped that these improvements in the technique employed would provide more conclusive evidence for the validity of applying thermoluminescence measurements to the age determination of archaeological ceramics.

A detailed description of the measurement technique is given in section 12.2. The results obtained are analysed in section 12.3 and finally the value of thermoluminescence measurements to age determination and possible future developments are discussed in section 12.4.

12.1. Depth studies

Reid (1964) found that when the natural thermoluminescence was measured for samples taken from different depths in the sherd, its intensity increased

from the surface to the centre of the sherd in some cases. For sherd r, a corresponding increase was observed for the susceptibility to a standard beta dose but for sherds a5 and b4 the beta particle susceptibility remained constant throughout the depth of the sherd, as did the alpha activity.

These results suggested that the natural thermoluminescence had been partially bleached throughout the depth of the sherd and that the bleaching decreased from the surface to the centre of the sherd. Consequently before commencing the third age determination programme, depth studies were performed on a selection of the sherds used.

Samples were obtained from the outer face (O) of the sherd, after first removing surface paint and burnishing, from the centre (C) of the sherd and from a depth intermediate (I) between the outer face and the centre. A tungsten-carbide scraper was used for this purpose and the thickness of the sherd was measured with a micrometer screw-gauge. Approximately 0.05 ins. were removed for each of the three samples.

The values obtained for the natural thermoluminescence (L_N), the thermoluminescence (L_β) induced by a 10 minute beta irradiation with a 40 mc. (Sr^{90} + Yr^{90}) source and the ratio L_N/L_β are given in Table 12/1. It can be seen that although large changes occurred for L_N and L_β, the ratio L_N/L_β remained constant to within ± 10%, for samples from different depths in a particular sherd, except in the case of sherd 4h1. This sherd was not therefore included in the age determination programme.

Table 12/1

Depth studies

Sherd	Depth	L_N	L_β	L_N/L_β
1a1	O	2.29	9.0	0.254
	I	3.75	14.7	0.255
	C	3.38	13.5	0.251
1c1	O	5.06	25.0	0.202
	I	6.21	32.4	0.191
	C	7.01	35.4	0.198
4b2	O	5.36	45.2	0.118
	I	3.95	32.9	0.120
	C	4.65	36.5	0.127
4h1	O	3.30	27.3	0.121
	I	1.44	13.1	0.110
	C	1.46	18.2	0.080
5a1	O	5.54	149	0.0372
	I	6.54	166	0.0394
	C	8.41	211	0.0398
6a1	O	2.80	27.0	0.103
	I	3.93	36.0	0.109
	C	3.55	30.7	0.116

Although the ratio, L_N/L_β, did not vary with depth for five sherds, the results indicate that, as far as their thermoluminescence properties are concerned, the sherds are extremely inhomogeneous even in the case of sherd 6a1 whose fabric appears homogeneous to the naked eye.

12.2 Technique

12.2.1. Preparation of sample

Any paint, glaze or burnishing was first removed from the surface of the sherd using a tungsten-carbide scraper. Approximately two grams of the

sherd were ground-up, in subdued light (< 0.2 units on Weston Master Mark III exposure meter), using an agate pestle and mortar so that it passed through a 120 mesh sieve (< 130 microns). The powder was placed in a polythene container and thoroughly mixed using a Microid Flask Shaker (Griffin and Tatlock Ltd.).

12.2.2. Measurement of thermoluminescence

The same technique was employed for the measurement of both natural and beta induced thermoluminescence. The fast heating apparatus, modified to provide a constant heating rate of 20°C/sec., was used in conjunction with photomultiplier type 6255S, the quartz light guide and two OB10 filters.

15 ± 0.5 mgm. samples were weighed out and spread on the graphite plate in subdued light (0.8 units) using a paint brush. After spreading, the radiation shield covering the remainder of the graphite plate was removed and replaced by a clean shield. This was necessary because, during the spreading, some sample grains fell on the shield. Since the temperature of the shield lagged behind that of the graphite plate by approximately 200°C, the low temperature thermoluminescence from these grains would have appeared at high thermocouple temperatures.

Nitrogen, at an overpressure of 2 cm. of water, was passed through the system at a flow-rate of 20 litres/minute for three minutes before the thermoluminescence was measured. The sample was then heated to 550°C, cooled under nitrogen to 300°C and then exposed to the air. Before heating a second time to measure the black body radiation, the sample was cooled to 50°C so that the temperature lag between the thermocouple and the surface

of the sample was the same for both heatings (section 2.1.2). Heating to 550°C on the first occasion was necessary, since, if the sample was only heated to 500°C, thermoluminescence was emitted in the 450-500°C range during the second heating.

After each measurement the gain of the photomultiplier and the amplifying system was checked using the standard light source (section 1.1).

12.2.3. Susceptibility

The susceptibility of the sherd to radiation was measured using the 5 mc. (Sr^{90} + Yr^{90}) beta source. Accurate measurement of the susceptibility to alpha particles was not possible because of their short range (Chapter 9).

The beta irradiations were performed off the graphite plate since it had been shown (Reid, 1964) that, if the irradiations were carried out with the sample on the plate, the plate itself emitted thermoluminescence.

The samples were irradiated without prior heat treatment to remove the natural thermoluminescence and the beta irradiation time (t_1) was varied from sherd to sherd so that $L_{1\beta} \approx L_N$ in the 350-500°C range. L_N equals the natural thermoluminescence and $L_{1\beta}$ equals the beta particle thermoluminescence, after correction for the natural thermoluminescence, for a t_1 minute irradiation.

In order to obtain some indication of the non-linearity of the beta particle rate curves, the thermoluminescence ($L_{2\beta}$) was also measured for a beta irradiation of t_2 minutes where $t_2 \approx 3 \times t_1$.

In addition, for six sherds, the initial portion of the beta particle rate curve was measured in more detail. Table 12/2 contains the values for

the ratio, L_β/t, in the 350-500°C range for various beta irradiation times.

Table 12/2

Non-linearity of beta particle rate curves

Sherd	t (min.)	$\frac{L_\beta}{t}$	Sherd	t (min.)	$\frac{L_\beta}{t}$
1a2	30	0.484	5a3	7	8.50
	63	0.521		15	8.78
	120	0.560		30	8.50
	240	0.563		60	8.35
1c3	30	0.339	6a4	20	0.136
	60	0.323		40	0.158
	120	0.317		80	0.152
	176	0.313		120	0.170
4b3	20	0.381	6c2	9	1.76
	40	0.402		15	1.79
	75	0.445		30	2.03
	155	0.545		60	2.26

The results for sherds 1a2, 4b3, 6a4 and 6c2 show that, as in the case of sherd r (section 7.1), their beta particle rate curves are definitely non-linear. As discussed in section 7.3, correction for this non-linearity is not possible since an essentially linear rate curve (sherds 1c3 and 5a3) does not necessarily mean that the natural thermoluminescence has been acquired linearly with radiation dose. Therefore in the present programme the ratio, $L_{1\beta}/t_1$, was used for the susceptibility since this gave the closest approximation to the true value for rate at which the natural thermoluminescence had been acquired.

The ratio $L_N/L_{i\beta}$ was plotted against temperature for each of the sherds used in the age determination programme. Some typical "ordinate ratio" graphs are shown in fig. 12/1. For the majority of the sherds this ratio

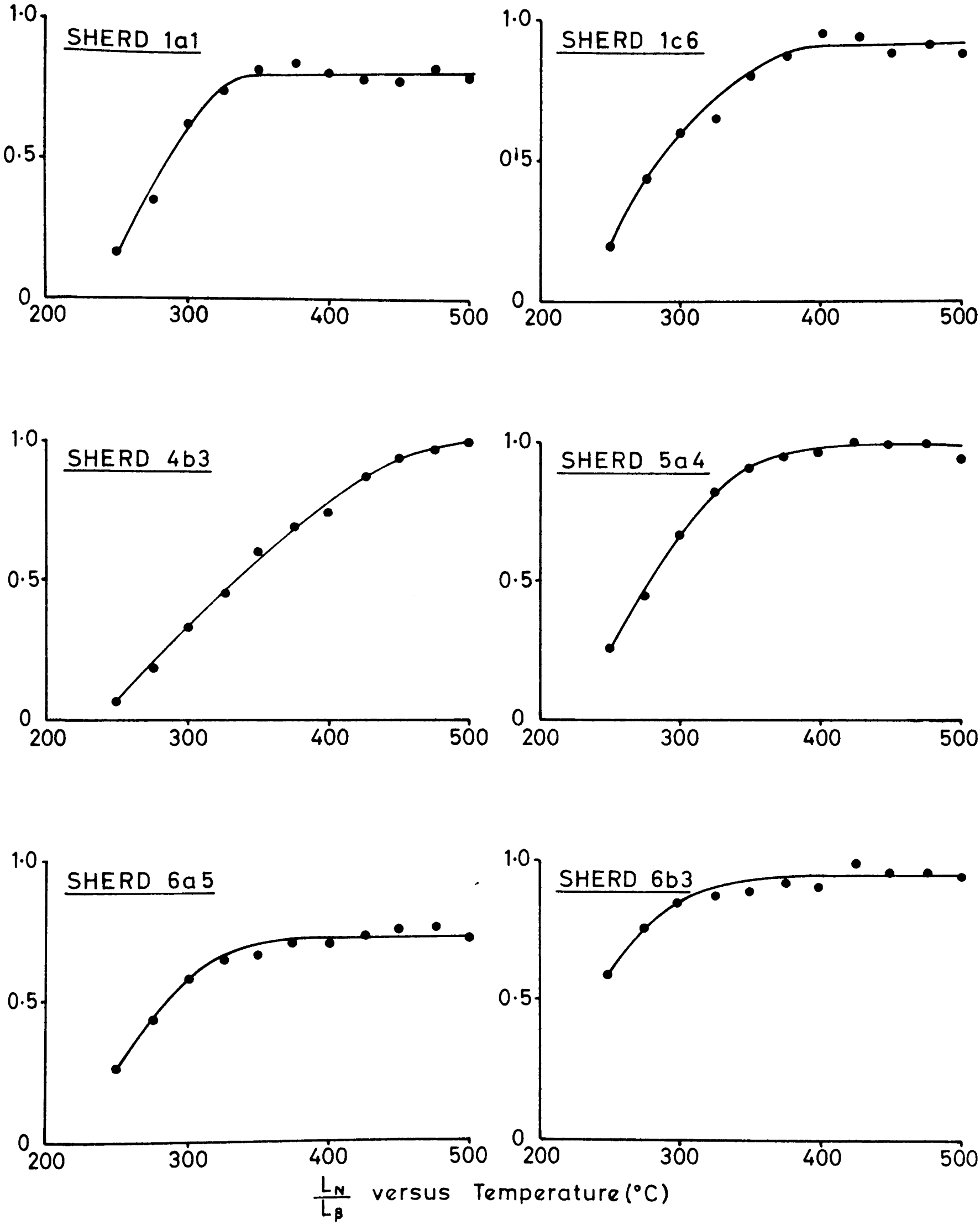

SHERD 1a1
SHERD 1c6
SHERD 4b3
SHERD 5a4
SHERD 6a5
SHERD 6b3
1·0
0·5
0
200
300
400
500
$\frac{L_N}{L_\beta}$ versus Temperature (°C)

Fig 12/1

was constant to within ± 10% throughout the 350-500°C range, indicating that the natural thermoluminescence had not been thermally bleached above 350°C. The result was in agreement with the trap depth measurements and thermal bleaching experiments described in sections 3.2 and 11.1 respectively. An exception was sherd 4b3 for which the ratio, $I_N/L_{1\beta}$, continued to rise throughout the temperature range 350-500°C, suggesting that its natural thermoluminescence had been thermally bleached above 350°C. However the specific thermoluminescence for sherd 4b3 was greater than that for sherd 4b2 which showed no thermal bleaching above 350°C. On the basis of these results, the glow curve areas were measured in the 350-500°C range and these areas were used to calculate the specific thermoluminescence.

12.2.4. Natural radiation dose

The natural radiation dose received by the pottery comes mainly from the presence of small quantities of uranium, thorium and radioactive potassium in the pottery. I am indebted to Mr. S. Fleming for the measurement of the uranium and thorium content and to Miss J. Stern for the measurement of the total potassium content (Appendix 3). In the former case the alpha particle counting technique developed by Reid (1964) was employed while in the latter case X-ray fluorescence analysis was used.

Assuming that all the alpha particles counted are due to the decay of U^{238} and its series and that this series is in equilibrium, Reid (1964) has shown that:

No. of complete U^{238} disintegrations/gm./year = $1.97 \times 10^5 \alpha$ - 12/1

where α = number of alpha counts per 1000 seconds.

Similarly if all the alpha particles counted are due to the decay of Th^{232} and its series:

No. of complete Th^{232} disintegrations/gm./year = $2.21 \times 10^{5}\alpha$ - 12/2

Again assuming that the series are in equilibrium, the total alpha, beta and gamma particle energies (E_α, E_β, and E_γ Mev) associated with each complete disintegration of U^{238} (i.e. $U^{236} \rightarrow Pb^{206}$) and Th^{232} (i.e. $Th^{232} \rightarrow Pb^{208}$) can be calculated. The figures given in Table 12/3 are based on the energies and decay schemes, presented in "Reviews of Modern Physics - Table of Isotopes" (American Physical Society, 1958). It is further assumed that the average beta particle energy equals 1/3 the maximum energy (Loevinger et al., 1956).

Table 12/3

Energies (in Mev.) associated with each complete disintegration

	E_α	E_β	E_γ	Total
U^{238} series	42.84	2.06	1.84	46.74
Th^{232} series	35.93	1.13	2.70	39.76

The effective energy absorbed per gm. per year (R_u) by the pottery, assuming all the alpha particles are due to the U^{238} series is given by (equation 12/1):

$$R_u = 3.15 \times 10^{-3}\alpha\ (kE_\alpha + E_\beta + E_\gamma)_u \text{ rads/year} \qquad - 12/3$$

where k equals the ratio of the susceptibility of the pottery to alpha and beta radiation. The susceptibilities for beta and gamma radiation are assumed to be equal (section 9.2.4). Although only part of the gamma ray

energy is absorbed in the sherd, there will be a corresponding contribution from the radioactive impurities of the soil in which the sherd is buried. In the present work it was assumed that, as far as the gamma ray contribution was concerned, the U^{238} and Th^{232} impurities were equal for the sherd and its environment.

Similarly assuming all the alpha particles are due to the Th^{232} series, the effective energy absorbed per gm. per year (R_T) in the pottery is given by (equation 12/2):

$$R_T = 3.54 \times 10^{-3} \propto (kE_\alpha + E_\beta + E_\gamma)_T \text{ rads/year}$$

The values for R_u and R_T when k equals 1, 0.1 and 0.02 are given in Table 12/4.

Table 12/4

Effective energy absorbed in the pottery (rads/year)

	k = 1	k = 0.1	k = 0.02
R_u	$0.147 \propto$	$0.0258 \propto$	$0.0150 \propto$
R_T	$0.140 \propto$	$0.0261 \propto$	$0.0161 \propto$

The values obtained for the fraction of the alpha counts due to the U^{238} series ranged from 0.25 to 0.98 (Appendix 3) and hence the error introduced by assuming that the alpha activity is due entirely to the U^{238} series will never be more than 6%.

The amount of the radioactive isotope, K^{40}, in the pottery can be calculated from the total potassium content using the values for the isotopic abundance of naturally occurring potassium. K^{40} either decays to stable Ca^{40} with the emission of a 1.3 Mev. beta particle (89%) or produces stable A^{40} by electron capture to an excited state of A^{40} followed by the emission

of a 1.46 Mev. gamma ray (11%). It can be shown (Rankama, 1954) that, if the sherd contains p% of potassium, the energy absorbed per gm. per year (R_k) is 0.113p rads/year. It was again assumed that as far as the gamma ray contribution was concerned, the potassium content of the sherd and its environment were equal.

Spiers (1964) has found that the present day cosmic ray intensity at sea level in England is 0.024 rads/year. On the basis of this figure and assuming that the sherd had been buried at a depth of 5 feet below the surface (Wilson, 1938), the cosmic ray energy absorbed per gm. per year (R_c) was taken to be 0.016 rads/year.

Hence the effective natural radiation dose (R) for the pottery, used in calculating the specific thermoluminescence, is given by:

$$R = R_u + R_k + R_c \qquad 12/4$$

i.e. $R = \left[3.15 \times 10^{-3} \alpha \left(kE_\alpha + E_\beta + E_\gamma\right) + 0.113p + 0.016\right]$ rads/year

where E_α, E_β and E_γ are the total alpha, beta and gamma particle energies in Mev. associated with each complete U^{238} disintegration.

12.3. Specific thermoluminescence

The specific thermoluminescence (S) was defined, for this third age determination programme, as

$$S = \frac{L_N t_1}{L_{1\beta} R} \qquad 12/5$$

The results presented in section 9.2.2. suggested that k, the relative susceptibility of the pottery for alpha particles with respect to that for beta particles, was of the order of 0.1. Therefore R was calculated using

this value (equation 12/4) and the resulting plot of S versus the aregaeological age was compared with those obtained using values for k of 1 and 0.02. Table 12/5 contains the values for L_N, $L_{1\beta}/t_1$, $L_{2\beta}/t_2$, R and S when k equals 1, 0.1 and 0.02 and where S has been calculated using the susceptibility, $L_{1\beta}/t_1$.

Two measurements of the ratio $L_N/L_{1\beta}$ were made for 24 sherds and the mean value was used in calculating S. The difference (Δ e), observed between the two measurements, varied from 0.5 to 15% of the mean value (e). From these figures, a mean percentage error ($\mathcal{E}$) for the value of the ratio, $L_N/L_{1\beta}$, was calculated where $\mathcal{E}$ is given by:

$$\mathcal{E} = \pm \left[\frac{\sum (\Delta e/e)^2}{24} \right]^{1/2} \times 100 = \pm 7.2\%$$

The experimental error associated with the determination of the natural radiation dose is approximately ± 5% and hence the percentage error for the values of the specific thermoluminescence is approximately ± 9%. For k = 1, the spread in the values for the specific thermoluminescence, for a group of sherds with the same archaeological age, is greater than the experimental error in all cases. However for k = 0.1 and k=0.02, the spread in the values of S for groups 1d and 4 b fall within the experimental error.

Fig. 12/2, 3 and 4 show the date graphs for k equal to 1, 0.1 and 0.02, plotted using the mean values of the specific thermoluminescence ($\bar{S}$) obtained for each group (Table 12/6). From Table 12/6 it can be seen that the use of k = 0.1, instead of k = 1, decreases the percentage error in the mean value of the specific thermoluminescence for three groups (1c, 1d and 4b), increases it for three groups 1a, 5 and 6b/c) while for group 6a it is

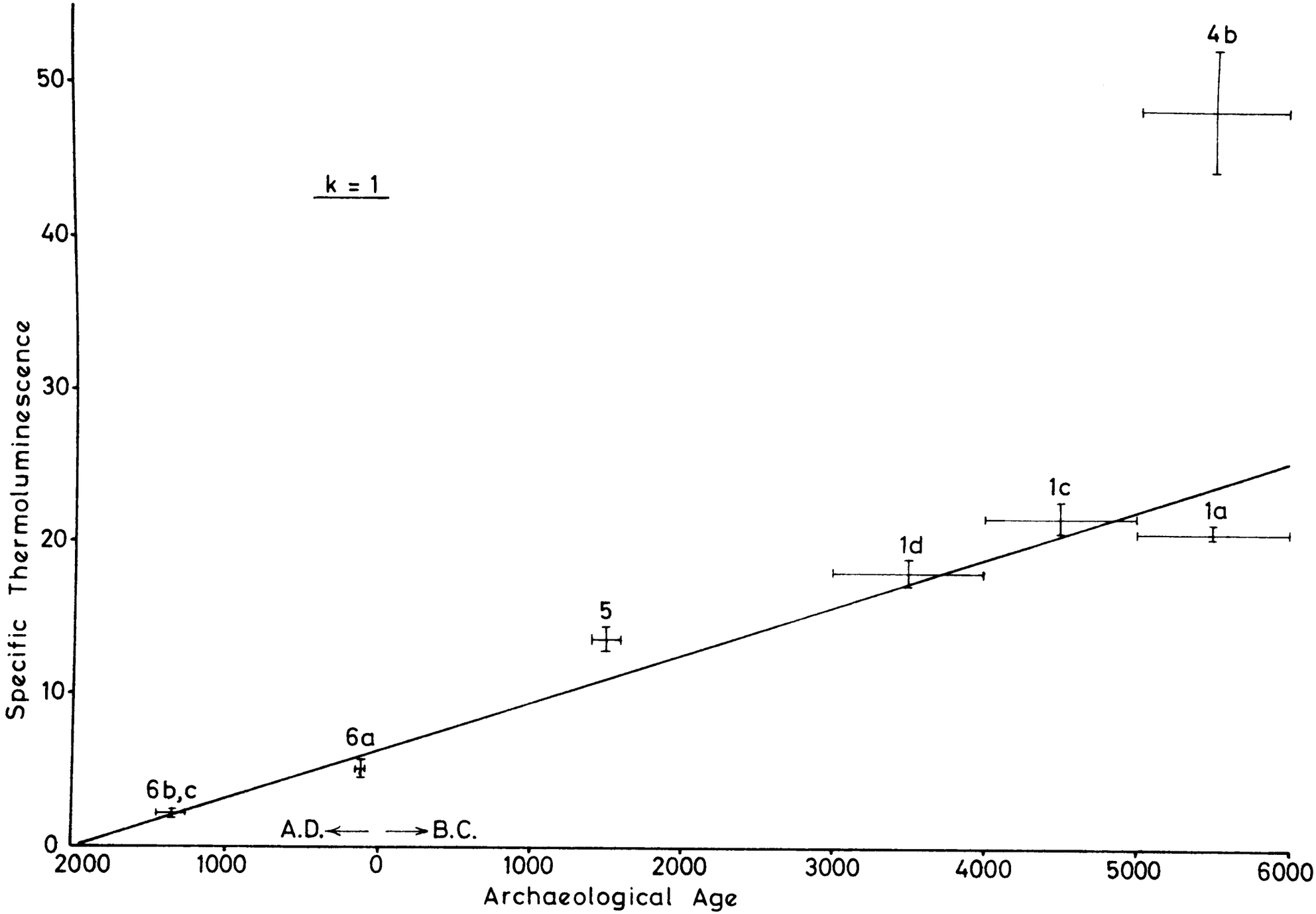

k = 1
Specific Thermoluminescence
Archaeological Age
A.D.
B.C.
0
10
20
30
40
50
2000
1000
0
1000
2000
3000
4000
5000
6000
4b
1c
1a
1d
5
6a
6b,c

Fig 12/2

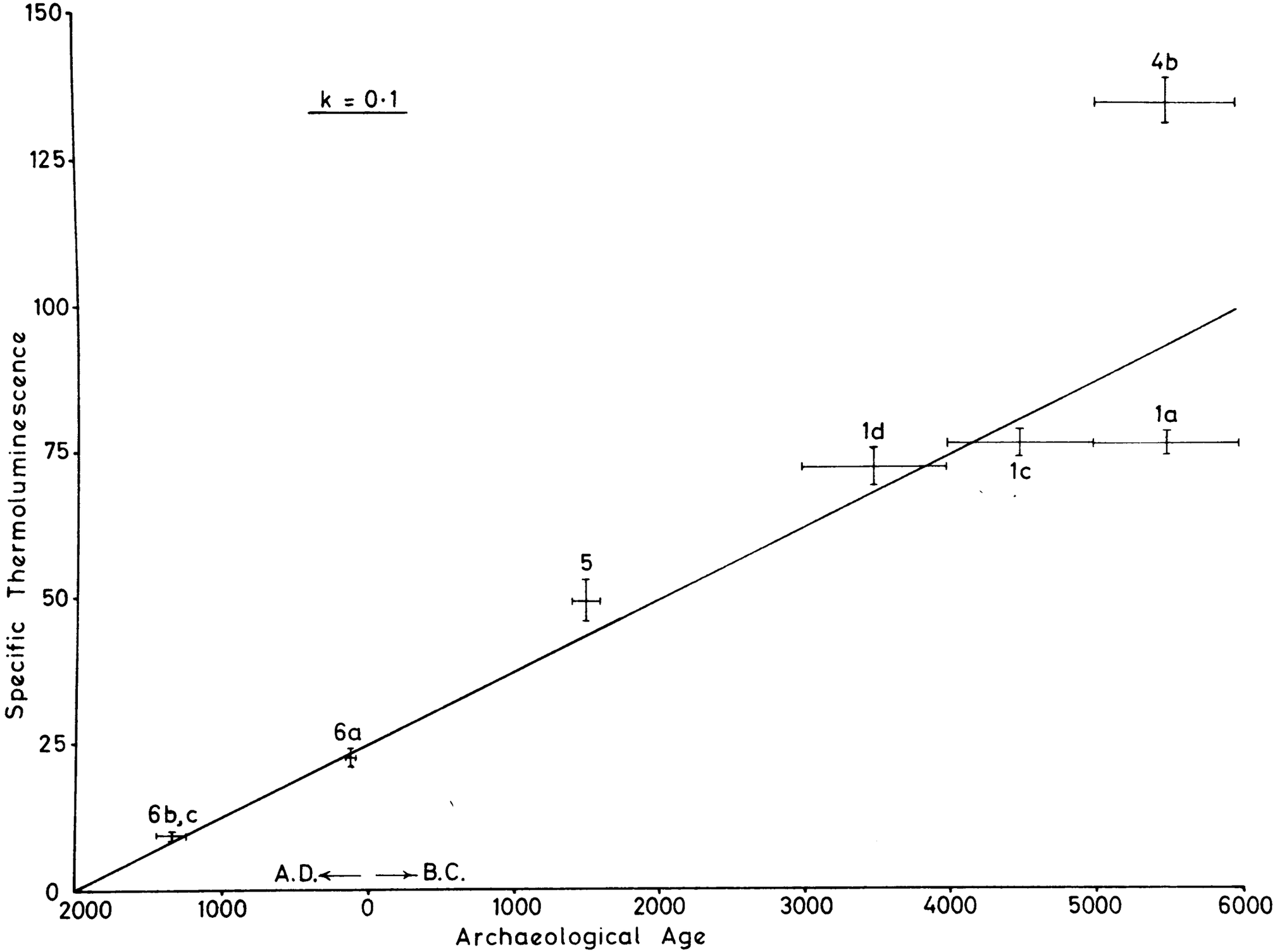

k = 0·1
4b
1a
1d
1c
5
6a
6b,c
A.D. ← → B.C.
Specific Thermoluminescence
Archaeological Age
150
125
100
75
50
25
0
2000
1000
0
1000
2000
3000
4000
5000
6000

Fig 12/3

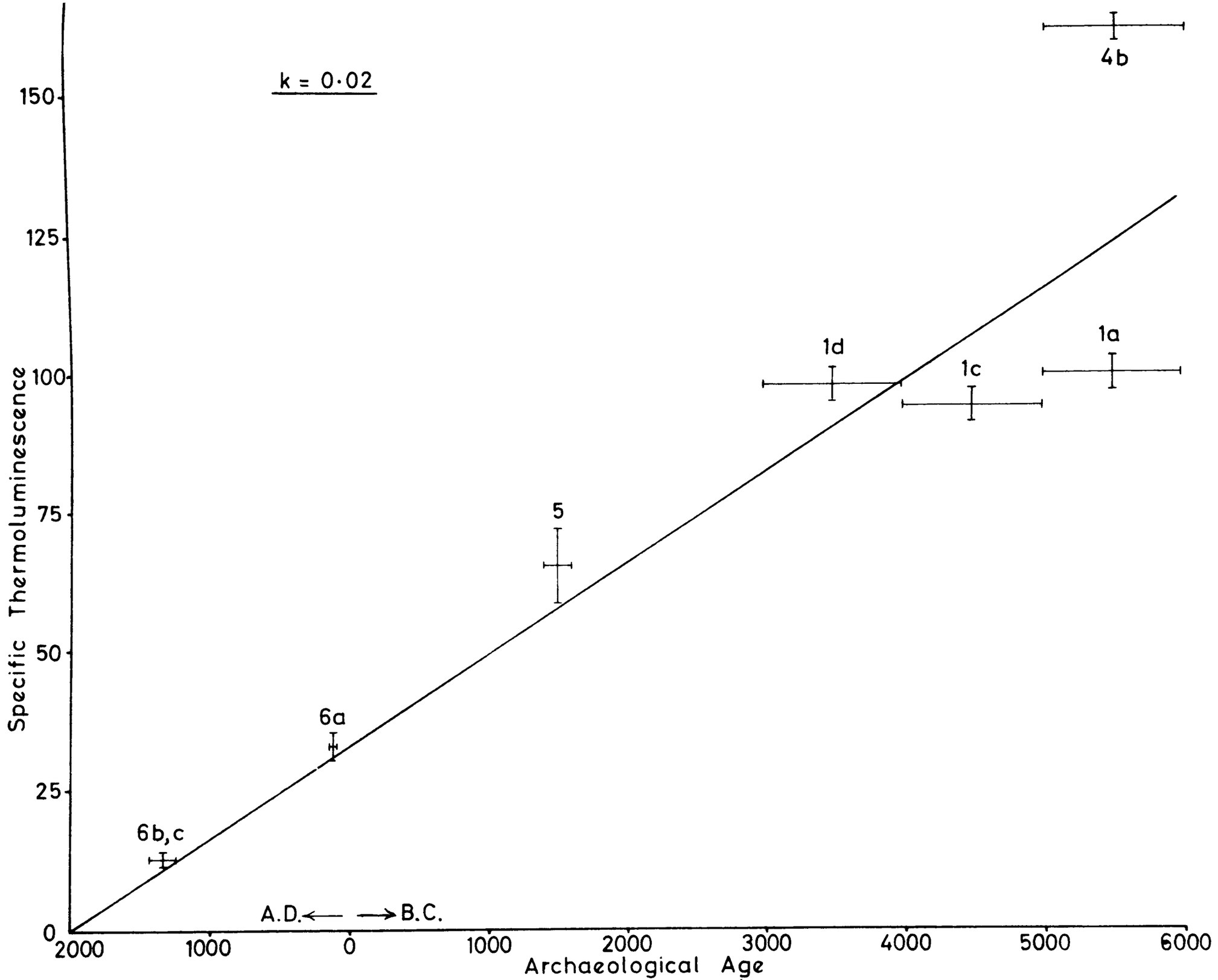

k = 0·02
4b
1d
1c
1a
5
6a
6b,c
Specific Thermoluminescence
0
25
50
75
100
125
150
A.D. ← → B.C.
2000
1000
0
1000
2000
3000
4000
5000
6000
Archaeological Age

Fig 12/4

unchanged. The most spectacular improvement occurs for group 4b. The use of k = 0.02 produces a further decrease for only two groups (1d and 4b).

Assuming that the specific thermoluminescence was zero for a modern sherd, the slope (x) of the date graph, i.e. $\frac{\bar{S}}{\text{archaeological age}}$, was calculated for each group of sherds. Using these values a weighted mean slope ($\bar{x}$) was determined from the relationship:

$$\bar{x} = \frac{\sum x/a^2}{\sum 1/a^2}$$

where a = standard error in the slope for each group.

The standard error for the weighted mean ($\bar{a}$) was calculated from the relationship:

$$\bar{a} = \frac{\sum (x - \bar{x})^2/a^2}{(n-1)\sum 1/a^2}$$

where n = number of groups.

In addition a further error for the weighted mean ($\bar{a}'$) of the form:

$$\bar{a}' = \frac{\sum (x - \bar{x})^2}{n^2}$$

was calculated since this provided a measure of the expected error in the archaeological age determined for a further group of sherds, using the above date graphs.

The values for the weighted mean slope, together with the errors ($\bar{a}$ and $\bar{a}'$) are given in Table 12/7.

Table 12/5

Age determination results

Sherd	L_N	$L_{1\beta}/t_1$	$L_{2\beta}/t_2$	R (rads/yr.) k = 1	R (rads/yr.) k = 0.1	R (rads/yr.) k = 0.02	Specific thermoluminescence k = 1	Specific thermoluminescence k = 0.1	Specific thermoluminescence k = 0.02
1a1	3.6	0.144	0.148	1.297	0.376	0.294	19.4	67.0	85.7
1a2	16.8	0.484	0.547	1.783	0.450	0.331	19.5	77.1	104.8
1a3	15.6	0.495	0.502	1.512	0.409	0.310	20.8	77.0	101.6
1a4	14.3	0.435	0.432	1.505	0.422	0.335	22.3	79.6	103.4
1a5	46.9	1.460	1.465	1.381	0.386	0.297	20.3	72.5	94.3
1a6	28.9	0.722	0.724	1.790	0.480	0.364	22.3	83.3	109.9
1c1	22.5	1.000	1.004	1.096	0.287	0.214	20.5	78.4	105.1
1c2	20.8	0.734	0.818	1.077	0.370	0.307	26.3	76.5	92.2
1c3	8.98	0.339	0.315	1.384	0.417	0.331	19.1	63.5	80.1
1c4	19.0	0.714	0.666	1.116	0.334	0.260	22.7	79.6	102.3
1c5	7.76	0.322	0.348	1.279	0.354	0.271	18.8	68.1	88.9
1c6	8.87	0.386	0.462	0.996	0.304	0.243	23.1	75.6	94.6
1d2	163	5.03	4.98	1.518	0.396	0.296	21.3	81.8	109.4
1d3	13.4	0.590	0.614	1.363	0.331	0.240	16.6	68.6	94.6
1d4	207	6.70	6.80	1.712	0.444	0.331	18.0	69.6	93.3
1d5	17.8	0.674	0.659	1.581	0.384	0.277	16.7	68.7	95.3
4b1	55.1	1.35	1.25	0.714	0.285	0.247	57.3	143.	166
4b2	11.1	0.730	0.895	0.384	0.118	0.094	59.6	129	162
4b3	5.79	0.381	0.400	0.315	0.115	0.097	48.2	132	158

Table 12/5 (cont.)

Sherd	LN	$L_{1\beta}/t_1$	$L_{2\beta}/t_2$	R (rads/yr.)			Specific thermoluminescence		
				k = 1	k = 0.1	k = 0.02	k = 1	k = 0.1	k = 0.02
5a1	74.5	12.02	11.12	0.488	0.101	0.069	12.7	61.4	89.8
5a2	70.3	10.19	10.49	0.593	0.129	0.088	11.6	53.5	78.4
5a3	51.0	8.50	7.85	0.436	0.113	0.084	13.8	53.1	71.4
5a4	87.0	10.74	11.60	0.497	0.156	0.126	16.3	51.9	64.3
5b1	90.3	13.48	13.48	0.416	0.165	0.143	16.1	40.6	46.8
5c1	6.26	1.74	1.96	0.301	0.103	0.083	11.9	34.9	42.3
6a1	6.50	0.283	0.369	3.558	0.843	0.601	6.46	27.3	38.3
6a2	2.56	0.168	0.183	3.102	0.735	0.524	4.90	20.7	29.0
6a3	18.2	1.11	1.12	4.321	0.935	0.633	3.80	17.5	25.9
6a4	2.34	0.134	0.159	3.618	0.877	0.633	4.75	19.6	27.2
6a5	22.5	0.961	1.11	4.329	0.959	0.659	5.40	24.4	35.5
6a6	3.90	0.187	0.196	4.130	0.834	0.540	5.04	24.9	41.3
6b1	17.4	1.95	2.32	3.630	0.819	0.568	2.45	10.9	15.7
6b2	15.2	1.95	2.20	4.053	0.902	0.621	1.92	8.6	12.6
6b3	19.3	3.06	3.06	3.488	0.858	0.623	1.81	7.3	10.1
6c1	11.0	1.36	1.59	2.935	0.705	0.506	2.76	11.5	16.0
6c2	12.0	1.76	1.87	3.580	0.901	0.662	1.90	7.5	10.3

Table 12/6

Mean values for specific thermoluminescence

Group	Age (years B.P)	Specific thermoluminescence ($\bar{s}$) k = 1	k = 0.1	k = 0.02
1a	7500 ± 500	20.8 ± 0.5(2.4%)	76.1 ± 2.1(2.7%)	99.9 ± 3.2(3.2%)
1c	6500 ± 500	21.8 ± 1.1(5.0%)	76.3 ± 2.4(3.1%)	93.9 ± 3.4(3.6%)
1d	5500 ± 500	18.1 ± 0.9(5.0%)	72.2 ± 2.8(3.9%)	98.1 ± 3.3(3.4%)
4b	7500 ± 500	48.3 ± 4.1(8.5%)	134 ± 3 (2.2%)	162 ± 2 (1.2%)
5a, b, c	3500 ± 100	13.7 ± 0.8(5.8%)	49.2 ± 3.6(7.3%)	65.5 ± 6.7(10.2%)
6a	1800 ± 10	5.06 ± 0.32(6.3%)	22.4 ± 1.4(6.3%)	32.9 ± 2.4(7.3%)
6b, c	600 ± 100	2.17 ± 0.17(7.8%)	9.2 ± 0.8(8.7%)	12.9 ± 1.1(8.7%)

Table 12/7

Weighted mean slope for date graphs

k	$\bar{x}$	$\bar{a}$	$\bar{a}'$
0.02	0.0165	± 0.0012 (7.2%)	± 0.0013 (7.9%)
0.1	0.0124	± 0.0009 (7.2%)	± 0.0010 (8.0%)
1	0.00319	± 0.00026 (8.2%)	± 0.00049 (15.4%)

These results show that, when the small susceptibility for the alpha particles is taken into account (k = 0.1), the standard error ($\bar{a}$) for the weighted mean slope is improved slightly while the expected error ($\bar{a}'$), associated with the determination of the archaeological age, is improved by a factor of approximately two. This improvement is principally due to the reduction in the deviation of group 4b from the weighted mean slope when k = 0.1.

12.3.1 Absolute age

The surface dose rate for the 5 mc. (Sr^{90} + Yr^{90}) beta source is, according to the manufacturers (Radiochemical Centre, Amersham), 1.78 ± 0.36 rads/sec. and the dose rate at the surface of the sample is approximately 1.07 ± 0.21 rads/sec. (section 9.2.1). Using this figure the absolute age (A), as defined by the specific thermoluminescence, was calculated for an archaeological age of 8000 B.P. from the weighted mean slopes for k equal to 1, 0.1 and 0.02.

k = 1	A = 1640 ± 350 B.P.
k = 0.1	A = 6370 ± 1330 B.P.
k = 0.02	A = 8470 ± 1770 B.P.

As observed for the second age determination programme, if the susceptibility for alpha radiation is assumed to be equal to that for beta radiation (k = 1), then the value obtained for the absolute age is too low by a factor of between 4 and 6. However when a correction is made for the low alpha particle susceptibility, reasonable agreement between the archaeological age and the absolute age, calculated from the specific thermoluminescence, is obtained.

12.4 Conclusions

The results presented in section 12.3 confirm that the specific thermoluminescence is dependent on the age of the sherd; the weighted mean slope obtained from the seven groups having a standard error of less than 8%.

The improvements observed in the deviation of the points from the weighted mean slope and the agreement obtained between the archaeological age and the absolute age, calculated from the specific thermoluminescence,

justifies the use of the low value for the alpha particle susceptibility ($k = 0.1$) inferred from the Ra^{224} results (section 9.2.3).

The alpha particles from the radioactive impurities will, because of their short range, only fill traps in the immediate vicinity of the uranium and thorium inclusions and the susceptibility of the sherd in these regions may be very different from the average value for the whole sherd, measured using the (Sr^{90} + Yr^{90}) beta source. However the fact that the alpha particle susceptibility is small compared to the susceptibility for beta and gamma radiation means that the alpha particles do not dominate the effective natural radiation dose (R). Therefore the possible non-uniform distribution of uranium and thorium does not necessarily invalidate age determination measurements.

Hence thermoluminescence measurements, based on the number of traps filled since the pottery was fired, provides an essentially valid method of determining the age of archaeological ceramics. However the method has not yet reached the stage when these results can be used to provide reliable ages for the archaeologist since the following major sources of error still remain:

1) the non-linearity of the beta particle rate curves means that the values for the age, obtained by the above procedure, are likely to be too low and the correction factor will vary from sherd to sherd.

2) the value used for the relative susceptibility of the alpha and beta particles was only approximate and no account was taken of its variation from sherd to sherd.

3) it was assumed that as far as the gamma ray, and to a lesser extent the beta particle, contribution to the natural radiation dose was concerned, the uranium, thorium and potassium content of the environment in which the sherd had been buried was the same as that of the sherd itself. The extremely low intrinsic radioactivity of the sherds in groups 4b and 5 could account for the high values obtained for the specific thermoluminescence, since the soil in which these sherds were buried did not necessarily have such a low level of radioactivity.

4) it was assumed that no additional material leached into the sherd during its burial period.

Considering these possible errors in the results presented in section 12.3, the agreement obtained between the archaeological age and the specific thermoluminescence is remarkable.

In order to increase the accuracy of the age determination measurements the following improvements are envisaged:

1) measurement of the radioactivity of the soil in which the sherd is buried. This will provide a more accurate value for the natural radiation dose.

2) measurement of the relative alpha and beta particle susceptibility using either powder with a grain size less than 20 microns or a polished thin section of the sherd.

However even when these improvements are incorporated into the measuring technique, the problem of the non-linearity of the beta particle rate curves still remains. At present, there seems to be no obvious way of emptying

all the traps, filled by the natural radiation dose, without changing the luminescence efficiency of the material (section 5.2). Therefore this non-linearity presents an apparently insuperable barrier to accurate age determination measurements. Furthermore the possible effects of material, leached into the sherd during its burial period, are as yet unknown.

Therefore in conclusion it can be said that, although the specific thermoluminescence of the sherd is certainly age dependent, the ultimate accuracy anticipated for this method of age determination is unlikely to be better than ± 10% and in some cases the error could be even greater. Consequently the method does not compare favourably with radiocarbon dating for which the error quoted for a 8000 year old sample is normally between ± 100 and ± 200 years.

However the errors quoted for radiocarbon dates do not necessarily make allowance for possible contamination of the sample and in addition uncertainties still remain as far as the absolute age provided by radiocarbon measurements is concerned. Therefore further work on the thermoluminescent method of age determination could provide a valuable check to the radiocarbon results particularly for the prehistoric periods.

APPENDIX I

ACTIVITY OF ALPHA SOURCES

I am indebted to Dr. M. J. Aitken for the measurement of the activity of the Po^{210} alpha sources used in this work. The values for the number and energy of the alpha particles reaching the pottery sample using a nominally 4 mc. Po^{210} source are given in Table 4/2. The relative activity of the sources, as measured on 8th January, 1965, are presented below together with the nominal activity in millicuries, based on the figures quoted by the manufacturers (Radiochemical Centre, Amersham).

Activity of Po^{210} sources

Nominal activity (mc.)	Relative activity (nominal)	Relative activity (measured)
4.0	1	1
2.0	0.50	0.55 ± 0.04
1.4	0.35	0.36 ± 0.03
0.9	0.23	0.25 ± 0.05

For the 4 mc. source, the number of alpha particles reaching the surface of the pottery was estimated as 3.1×10^7 per sec. whereas the total number of disintegrations, based on the nominal activity of the source, was 14.8×10^7 per sec.

APPENDIX 2

ARCHAEOLOGICAL NOTES

Groups 1a, 1c and 1d

From the Neolithic mound at Knossos, Crete, excavated in 1958-60 by Professor J. D. Evans (1964). The archaeological context of the sherds used is as follows:

1a1	Early Neolithic I	:	Stratum VI
1a2	" " "	:	" VI
1a3	" " "	:	" VI
1a4	" " "	:	" V
1a5	" " "	:	" VI
1a6	" " "	:	" VII
1c1-6	Middle Neolithic	:	Stratum III
1d2-5	Late Neolithic	:	Stratum II

Radiocarbon dates, obtained for samples taken from the base and top of the Early Neolithic I levels, were 6100 ± 180 B.C. and 5050 ± 180 B.C. respectively (Radiocarbon, 5, 104, BM124 & BM126).

The archaeological dates, suggested by the excavator on the basis of comparable archaeological material found at other Neolithic sites in the Mediterranean area, were 4500 ± 500 B.C. and 3500 ± 500 B.C. for the Middle and Late Neolithic groups respectively.

Group 4b

From the excavations at Ras Shamra, Syria, directed by Professor C. F. A. Schaeffer (1962). The archaeological content of the sherds was Middle Neolithic, level VB.

Radiocarbon dates obtained for samples taken from the Neolithic levels

were 5736 ± 112 B.C. and 5234 ± 84 B.C. (Radiocarbon, 5, 82-83, P458 and P457).

Group 5

From the Bronze Age cemetry at Stephania, Cyprus, excavated in 1951 by Dr. J. B. Hennessy (1963). The sherds used came from the dromos (5a1 - 4 and 5c1) and the chamber (5b1) of Tomb 5 which dated from the Late Cypriot Bronze Age (1A).

The date of 1500 ± 50 B.C., suggested by the excavator, was based on the fact that comparable pottery was found in Egypt, associated with the XVIII Dynasty.

Groups 6a, 6b and 6c

From the 1963 excavations at Lezoux, France, directed by Professor S. S. Frere and Mr. B. R. Hartley.

Group 6a came from a Roman rubbish pit and was dated to the Hadrianic period (117 - 138 A.D.) on the basis of the decoration and potters' stamps on the Samian pottery found. 6a1 - 4 were Samian sherds while 6a5 - 6 were sherds of coarse pottery.

Groups 6b and 6c came from the interior of a Mediaeval house and the date suggested by the excavator was 1350 ± 100 A.D.

APPENDIX 3

RADIOACTIVE IMPURITIES IN THE POTTERY

I am indebted to Mr. S. Fleming for the measurement of the alpha activity of the pottery and to Miss J. Stern for the measurement of the total potassium content. The number of alpha counts per 1000 seconds, the fraction of these counts due to the U^{238} series and the percentage of potassium are listed below. The accuracy of the measurement of the potassium content was ± 5%.

Sherd	Alpha counts per Ks.	Fraction of counts from U^{238} series	Percentage of potassium
1a1	7.60 ± 0.21	-	1.45
1a2	11.00 ± 0.29	-	1.33
1a3	9.10 ± 0.20	0.71	1.40
1a4	8.94 ± 0.29	0.66	1.55
1a5	8.21 ± 0.40	0.64	1.40
1a6	10.80 ± 0.27	0.81	1.65
1c1	6.80 ± 0.21	-	0.85
1c2	5.84 ± 0.23	0.77	1.80
1c3	7.98 ± 0.28	0.60	1.73
1c4	6.88 ± 0.22	0.74	1.25
1c5	7.63 ± 0.34	0.70	1.25
1c6	5.71 ± 0.28	0.65	1.25
1d2	9.26 ± 0.32	0.67	1.25
1d3	8.51 ± 0.36	0.60	0.85
1d4	10.46 ± 0.38	0.50	1.40
1d5	9.88 ± 0.39	0.56	1.00
4b1	3.54 ± 0.12	0.98	1.58
4b2	2.20 ± 0.10	-	0.40
4b3	1.65 ± 0.10	0.77	0.50

Sherd	Alpha counts per Ks.	Fraction of counts from U^{238} series	Percentage of potassium
5a1	2.90 ± 0.18	0.25	0.10
5a2	3.82 ± 0.15	0.59	0.13
5a3	2.67 ± 0.14	0.52	0.25
5a4	2.81 ± 0.14	0.55	0.60
5b1	2.07 ± 0.22	0.52	0.85
5c1	1.63 ± 0.17	0.77	0.40
6a1	22.4 ± 0.52	0.80	2.20
6a2	19.5 ± 0.46	0.83	1.90
6a3	27.9 ± 0.60	0.64	1.75
6a4	22.6 ± 0.49	0.60	2.46
6a5	27.8 ± 0.45	-	2.00
6a6	27.2 ± 0.47	0.75	1.03
6b1	23.2 ± 0.56	0.62	1.80
6b2	26.0 ± 0.44	-	1.90
6b3	21.7 ± 0.36	0.70	2.48
6c1	18.4 ± 0.30	0.55	1.90
6c2	22.1 ± 0.31	0.68	2.78

ACKNOWLEDGEMENTS

I am extremely grateful to Dr. M. J. Aitken for his constant encouragement and advice and also for reading this manuscript. Thanks are extended to Mrs. J. Reid and Mr. S. Fleming for their helpful collaboration and also to Mr. M. Goves and Mr. D. Seeley for their technical assistance.

I am indebted to Dr. R. Oliver for carrying out the irradiations with the Co^{60} source at the Churchill Hospital, Oxford, to Mrs. A. Millett for the spectrographic analyses, to Professor G. F. J. Garlick for the electron spin resonance measurements and to the following archaeologists for providing the pottery sherds used in this work:
Dr. H. W. Catling, Professor J. D. Evans, Professor S. S. Frere, Mr. B. R. Hartley, Dr. J. B. Hennessy, Mr. P. R. S. Moorey and Professor C. F. A. Schaeffer.

Helpful discussions were held with Dr. C. G. Clayton, Dr. N. Grogler, Professor F. G. Houtermans, Professor E. W. J. Mitchell, Professor E. Tongiorgi and Professor E. J. Zeller.

I am most grateful to Dr. E. T. Hall for the use of his laboratory. Financial assistance from D.S.I.R. and Major H. W. Hall is gratefully acknowledged.

REFERENCES

Aitken, M. J. (1961) : Physics and Archaeology, 121-55 (Interscience).

Aitken, M. J., Tite, M.S. and Reid, J. (1963) : Archaeometry, 6, 65-75.

Aitken, M. J., Tite, M. S. and Reid, J. (1964) : Nature, 202, 1032-3.

Amelinckx, S. (1962) : Radiation Damage in Solids (Proc. Int. School of Physics, Enrico Fermi), 422-517.

Appleton, G. J. and Krishmoorthy, P. N. (1960) : Safe Handling of Radio-isotopes, 48-53 and 100-111 (I.A.E.A., Vienna).

Arnold, G. W. (1960) : J. Phys. Chem. Solids, 13, 306-320.

Attix, F. H., Nash, A. E. and Schulman, J. H. (1964) : Report of NRL Progress - Problem Notes, 33-35.

Billington, D. S. and Crawford, J. H. (1961) : Radiation Damage in Solids (O.U.P.).

Bonfiglioli, G., Brovetto, P. and Cortese, C. (1959) : Phys. Rev., 114, 951-60.

Bowen, E. J. (1946) : Chemical Aspects of Light, 267-75 (O.U.P.).

Brattain, W. H. and Peterson, G. L. (1950) : Phys. Rev., 80, 846-50.

Braner, A. A. and Halperin, A. (1957) : Phys. Rev., 108, 932-6.

Braner, A. A. and Israeli, M. (1963) : Phys. Rev., 132, 2501-5.

Cameron, J. R., Daniels, F., Johnson, N. M. and Kenney, G. M. (1961) : Science, 134, 333-4.

Cohen, S. and Priqueler, M. (1963) : Comp. Rend., 257, 1469-72.

Daniels, F., Boyd, C. A. and Saunders, D. F. (1953) : Science, 117, 343-9.

Debenedetti, A. (1958) : Il Nuov. Cim., 7, 251-4.

Dienes, G. J. and Vineyard, G. H. (1957) : Radiation Effects in Solids (Interscience).

Ditchburn, R. W., Mitchell, E. W. J., Paige, E. J. S., Custers, J. F. H., Dyer, H.B. and Clark, C. D. (1954) : Defects in Crystalline Solids, Report of Bristol Conference, 92-107 (Phys. Soc.).

Evans, J. D. (1964) : Bull. Inst. Archaeology, London, 4, 34-60.

Forman, G. (1951) : J. Opt. Soc. Amer., 41, 377-80.

Freeman, I. L. (1958) : Trans. Brit. Cer. Soc., 57, 316-39.

Garlick, G. F. J. (1949) : Luminescent Materials, 35-9 (O.U.P.).

Garlick, G. F. J. (1964) : Private communication.

Glasson, J. L. (1922) : Phil. Mag., xliii, 477.

Griffiths, J. H. E., Owen, J. and Ward, I. M. (1954) : Defects in Crystalline Solids, Report of Bristol Conference, 81-7 (Phys. Soc.).

Grogler, N. and Stauffer, H. (1959) : Helv. Phys. Acta, 32, 129-34 and 284-6.

Gross, G., Stranski, I. N. and Wolff, G. (1955) : Z. Elecktrochem., 59, 346-50.

Halperin, A., Braner, A. A. and Alexander, E. (1957) : Phys. Rev. 108, 928-31.

Halperin, A., and Schlesinger, M. (1959) : Phys. Rev., 113, 762-6.

Halperin, A. and Braner, A. A. (1960) : Phys. Rev., 117, 408-15.

Halperin, A., Braner, A. A., Ben Zvi, A. and Kristianpoller, N. (1960) : Phys. Rev., 117, 416-22.

Hennessy, J. B. (1962) : Stephania (Bernard Quaritch Ltd.).

Hennig, G. R. and Hove, J. E. (1956) : Proc. Int. Conf. Peaceful Uses of At. Energy, 7, 666-75. (U.N.).

Holland, H. D. (1954) : Nuclear Geology (Ed. Faul, H.), 175-80 (Wiley).

Holland, H. D. and Gottfried, D. (1955) : Acta Crystal., 8, 291-300.

Houtermans, F. G., Jager, E., Schon, M. and Stauffer, H. (1957) : Ann. d. Physik, 20, 283-92.

Houtermans, F. G., Gregler, M. and Stauffer, H. (1960) : Helv. Phys. Acta, 33, 595-6.

Johnson, N. M. and Daniels, F. (1961) : J. Chem. Phys., 34, 1434-9.

Johnson, N. M. (1963) : J. Geol., 71, 596-616.

Joly, J. (1923) : Proc. Roy. Soc., A102, 682-705.

Kennedy, G. and Knopff, L. (1960) : Archaeology, 13, 147-8.

Kobayashi, K. (1957) : Phys. Rev., 107, 41-3.

Levy, P.W. (1961) : Phys. Rev., 123, 1226-33.

Levy, P. W. (1964) : Symposium on the Chemical and Physical Effects of High-Energy Radiation on Inorganic Solids, 3-19 (Amer. Soc. for Testing and Materials).

Libby, W. F. (1952) : Radiocarbon Dating (Univ. Chicago Press).

Lloyd, R. A. (1964) : Unpublished D. Phil. thesis (Oxford University).

Loevinger, R., Japha, E.M. and Brownell, G. L. (1956) : Radiation Dosimetry (Ed. Hine, G. J.), 694-754 (Academic Press).

Medlin, W. L. (1959) : J. Chem. Phys., 30, 451-8.

Medlin, W. L. (1963) : J. Chem. Phys., 38, 1132-43.

Medlin, W. L. (1963) : J. Opt. Soc. Amer., 53, 1276-85.

Mitchell, E. W. J. and Paige, E. G. S. (1956) : Phil. Mag., 1, 1085-115.

Moorehead, F. F. and Daniels, F. (1957) : J. Chem. Phys., 57, 1318-24.

Mott, N. F. and Gurney, R. W. (1953) : Electronic Processes in Ionic Crystals, 64-108 (O.U.P.).

O'Brien, M. C. M. (1955) : Proc. Roy. Soc., A231, 404-14.

Oldenburg, H. (1705) : Phil. Trans. Abrdg., 3, 345.

Paige, E. G. S. (1957) : Phil. Mag., 2, 864-76.

Primak, W., Fuchs, L. H. and Day, P. P. (1956) : Phys. Rev., 103, 1184-92.

Primak, W. (1958) : Phys. Rev., 110, 1240-54.

Randall, J. T. and Wilkins, M. H. F. (1945) : Proc. Roy. Soc., A184, 366-89.

Rankama, K. (1954) : Isotope Geology, 304-7 (Pergamon Press).

Reid, J. (1964) : Unpublished B. Sc. thesis (Oxford University).

Richards, E. E. (1959) : Archaeometry, 2, 23-31.

Richardson, H. M. (1961) : X-ray Identification and Crystal Structure of Clay Minerals (Ed. Brown, G.), 132-42 (Min. Soc., London).

Sabels, B. E. (1962), : Symp. on Radioactive Dating, Athens, 87-104, (I.A.E.A., Vienna).

Schaeffer, C. F. A. (1962) : Ugaritica IV, 283.

Schulman, J. H. and Compton, W. D. (1962) : Color Centres in Solids, 79-84 (Pergamon Press).

Seitz, F. (1949) : Disc. Far. Soc., 5, 271-82.

Seitz, F. (1954) : Rev. Mod. Phys., 26, 80-3.

Spiers, F. W. (1964) : The Natural Radiation Environment (Ed. Adams, J. A. S.) 885-905 (Rice University).

Thomas, B. and Houston, E. (1964) : Brit. J. Applied Phys., 15, 953-8.

Tite, M. S. and Waine, J. (1962) : Archaeometry, 5, 53-79.

Titley, S. R. and Damon, P. E. (1962) : J. Geophys. Res., 67, 4491-5.

Turner, R. C., Radley, J. M. and Mayneord, W. V. (1958) : Brit. J. Rad., 31, 397

Varley, J. H. O. (1954) : J. Nucl. Energy, 1, 130-43.

Weeks, R. A. (1956) : J. Applied Phys., 27, 1376-81.

Wick, F. G. (1939) : J. Opt. Soc. Amer., 29, 407-12.

Wilson, V. C. (1938) : Phys. Rev., 53, 337-43.

Wittels, M. C. (1957) : Phil. Mag., 2, 1445-61.

Zeller, E. J. (1954) : Nuclear Geology (Ed. Faul, H.), 180-8 (Wiley).

Zeller, E. J. Wray, J. L. and Daniels, F. (1957) : Bull. Amer. Ass. Pet. Geol., 41, 121-9.

Zeller, E. J. and Ronca, L. B. (1962) : Symp. on Radioactive Dating, Athens, 73-85 (I.A.E.A., Vienna).